Protocols for Collecting and Using Traffic Data in Bridge Design

AUTHORS

Michel Ghosn; Bala Sivakumar; Fred Moses; Transportation Research Board

BUY THIS BOOK

FIND RELATED TITLES

NCHRP REPORT 683

Protocols for Collecting and Using Traffic Data in Bridge Design

Bala Sivakumar
HNTB CORPORATION
New York, NY

Michel Ghosn
New York, NY

Fred Moses
Pittsburgh, PA

TranSystems Corporation
Kansas City, MO

TRANSPORTATION RESEARCH BOARD

NATIONAL COOPERATIVE HIGHWAY RESEARCH PROGRAM

Systematic, well-designed research provides the most effective approach to the solution of many problems facing highway administrators and engineers. Often, highway problems are of local interest and can best be studied by highway departments individually or in cooperation with their state universities and others. However, the accelerating growth of highway transportation develops increasingly complex problems of wide interest to highway authorities. These problems are best studied through a coordinated program of cooperative research.

In recognition of these needs, the highway administrators of the American Association of State Highway and Transportation Officials initiated in 1962 an objective national highway research program employing modern scientific techniques. This program is supported on a continuing basis by funds from participating member states of the Association and it receives the full cooperation and support of the Federal Highway Administration, United States Department of Transportation.

The Transportation Research Board of the National Academies was requested by the Association to administer the research program because of the Board's recognized objectivity and understanding of modern research practices. The Board is uniquely suited for this purpose as it maintains an extensive committee structure from which authorities on any highway transportation subject may be drawn; it possesses avenues of communications and cooperation with federal, state and local governmental agencies, universities, and industry; its relationship to the National Research Council is an insurance of objectivity; it maintains a full-time research correlation staff of specialists in highway transportation matters to bring the findings of research directly to those who are in a position to use them.

The program is developed on the basis of research needs identified by chief administrators of the highway and transportation departments and by committees of AASHTO. Each year, specific areas of research needs to be included in the program are proposed to the National Research Council and the Board by the American Association of State Highway and Transportation Officials. Research projects to fulfill these needs are defined by the Board, and qualified research agencies are selected from those that have submitted proposals. Administration and surveillance of research contracts are the responsibilities of the National Research Council and the Transportation Research Board.

The needs for highway research are many, and the National Cooperative Highway Research Program can make significant contributions to the solution of highway transportation problems of mutual concern to many responsible groups. The program, however, is intended to complement rather than to substitute for or duplicate other highway research programs.

NOTICE

The project that is the subject of this report was a part of the National Cooperative Highway Research Program, conducted by the Transportation Research Board with the approval of the Governing Board of the National Research Council.

The members of the technical panel selected to monitor this project and to review this report were chosen for their special competencies and with regard for appropriate balance. The report was reviewed by the technical panel and accepted for publication according to procedures established and overseen by the Transportation Research Board and approved by the Governing Board of the National Research Council.

The opinions and conclusions expressed or implied in this report are those of the researchers who performed the research and are not necessarily those of the Transportation Research Board, the National Research Council, or the program sponsors.

The Transportation Research Board of the National Academies, the National Research Council, and the sponsors of the National Cooperative Highway Research Program do not endorse products or manufacturers. Trade or manufacturers' names appear herein solely because they are considered essential to the object of the report.

THE NATIONAL ACADEMIES
Advisers to the Nation on Science, Engineering, and Medicine

The **National Academy of Sciences** is a private, nonprofit, self-perpetuating society of distinguished scholars engaged in scientific and engineering research, dedicated to the furtherance of science and technology and to their use for the general welfare. On the authority of the charter granted to it by the Congress in 1863, the Academy has a mandate that requires it to advise the federal government on scientific and technical matters. Dr. Ralph J. Cicerone is president of the National Academy of Sciences.

The **National Academy of Engineering** was established in 1964, under the charter of the National Academy of Sciences, as a parallel organization of outstanding engineers. It is autonomous in its administration and in the selection of its members, sharing with the National Academy of Sciences the responsibility for advising the federal government. The National Academy of Engineering also sponsors engineering programs aimed at meeting national needs, encourages education and research, and recognizes the superior achievements of engineers. Dr. Charles M. Vest is president of the National Academy of Engineering.

The **Institute of Medicine** was established in 1970 by the National Academy of Sciences to secure the services of eminent members of appropriate professions in the examination of policy matters pertaining to the health of the public. The Institute acts under the responsibility given to the National Academy of Sciences by its congressional charter to be an adviser to the federal government and, on its own initiative, to identify issues of medical care, research, and education. Dr. Harvey V. Fineberg is president of the Institute of Medicine.

The **National Research Council** was organized by the National Academy of Sciences in 1916 to associate the broad community of science and technology with the Academy's purposes of furthering knowledge and advising the federal government. Functioning in accordance with general policies determined by the Academy, the Council has become the principal operating agency of both the National Academy of Sciences and the National Academy of Engineering in providing services to the government, the public, and the scientific and engineering communities. The Council is administered jointly by both Academies and the Institute of Medicine. Dr. Ralph J. Cicerone and Dr. Charles M. Vest are chair and vice chair, respectively, of the National Research Council.

The **Transportation Research Board** is one of six major divisions of the National Research Council. The mission of the Transportation Research Board is to provide leadership in transportation innovation and progress through research and information exchange, conducted within a setting that is objective, interdisciplinary, and multimodal. The Board's varied activities annually engage about 7,000 engineers, scientists, and other transportation researchers and practitioners from the public and private sectors and academia, all of whom contribute their expertise in the public interest. The program is supported by state transportation departments, federal agencies including the component administrations of the U.S. Department of Transportation, and other organizations and individuals interested in the development of transportation. **www.TRB.org**

www.national-academies.org

FOREWORD

By Waseem Dekelbab
Staff Officer
Transportation Research Board

This report provides a set of protocols and methodologies for using available recent truck traffic data to develop and calibrate vehicular loads for LRFD superstructure design, fatigue design, deck design, and design for overload permits. The protocols are geared to address the collection, processing, and use of national weigh-in-motion (WIM) data. The report also gives practical examples of implementing these protocols with recent national WIM data drawn from states/sites around the country with different traffic exposures, load spectra, and truck configurations. The material in this report will be of immediate interest to bridge engineers. This report replaces *NCHRP Web-Only Document 135*.

A new vehicular live-load model was developed for the AASHTO LRFD Bridge Design Specifications because the HS20 truck from AASHTO's Standard Specifications for Highway Bridges did not accurately represent service-level truck traffic. The HL93, a combination of the HS20 truck and lane loads, was developed using 1975 truck data from the Ontario Ministry of Transportation to project a 75-year live-load occurrence. Because truck traffic volume and weight have increased and truck configurations have become more complex, the Ontario data do not represent present traffic loadings. Other design live loads were based on past practice and did not consider actual or projected truck traffic. Although the quality and quantity of traffic data have improved in recent years, this information has not been used to update the bridge design loads. Methods of using enhanced traffic data for bridge design needed to be developed.

Under NCHRP Project 12-76 the research team had developed and demonstrated the application of protocols for collecting and processing traffic data to calibrate national bridge live-load models. Additionally, under NCHRP 12-76(01) the research team conducted sensitivity studies and developed key recommendations on sorting of trucks into Strength I and Strength II limit states.

Appendices A through F from the research agency's final report are not published herein but are available on the TRB website (Go to http://trb.org/Publications/Public/PubsNCHRP ProjectReports.aspx and look for NCHRP Report 683). These appendices are titled as follows.

- Appendix A—Survey Questionnaires & Responses
- Appendix B—Main Features of Selected Studies
- Appendix C—National WIM Data Analyses
- Appendix D—Potential Processes to Develop and Calibrate Vehicular Design Loads
- Appendix E—Implementation of WIM Error Filtering Algorithm
- Appendix F—Truck Sorting Strategies & Influence on "r" Values

C O N T E N T S

Note: Many of the photographs, figures, and tables in this report have been converted from color to grayscale for printing. The electronic version of the report (posted on the Web at www.trb.org) retains the color versions.

S U M M A R Y

Protocols for Collecting and Using Traffic Data in Bridge Design

   This report documents and presents the results of a study to develop a set of protocols and methodologies for using available recent truck traffic data to develop and calibrate live-load models for LRFD bridge design. The HL93, a combination of the HS20 truck and lane loads, was developed using 1975 truck data from the Ontario Ministry of Transportation to project a 75-year live-load occurrence. Because truck traffic volume and weight have increased and truck configurations have become more complex, the 1975 Ontario data do not represent present U.S. traffic loadings. The goal of this project, therefore, was to develop a set of protocols and methodologies for using available recent truck traffic data collected at different U.S. sites and recommend a step-by-step procedure that can be followed to obtain live-load models for LRFD bridge design. The protocols are geared to address the collection, processing and use of national weigh-in-motion (WIM) data to develop and calibrate vehicular loads for LRFD superstructure design, fatigue design, deck design, and design for overload permits. These protocols, comprised of 13 steps with detailed instructions on their application, are appropriate for national use or use with data specific to a state or local jurisdiction where the truck weight regulations and/or traffic conditions may be significantly different from national standards. The study also gives practical examples of implementing these protocols with recent national WIM data drawn from states/sites around the country with different traffic exposures, load spectra, and truck configurations.

   The project team recommends that truck traffic data should be collected through WIM systems that can simultaneously collect headway information as well as truck weights, axle weights, and axle configurations while remaining hidden from view and unnoticed by truck drivers. Truck data surveys collected at truck weigh stations and publicized locations are not accurate, because they are normally avoided by illegal overweight vehicles that could control the maximum loads applied on bridge structures. The selection of WIM sites should focus on sites where the owners maintain a quality assurance program that regularly checks the data for quality. WIM devices used for collecting data for live-load modeling should be required to meet performance specifications for data accuracy and reliability. A year's worth of recent continuous data is generally recommended for live-load modeling. Quality information is just as important as the quantity of data collected. It is far better to collect limited amounts of well-calibrated data than to collect large amounts of data from poorly calibrated scales. Even small errors in vehicle weight measurements caused by poorly calibrated sensors could result in significant errors in measured loads.

   High-speed WIM is prone to various errors. Such errors need to be recognized and considered in the data review process to edit out unreliable data and unlikely trucks, and to ensure that only quality data are made part of the load modeling process. It is also important to recognize that unusual data are not all bad data. The WIM data should therefore be scrubbed to include only the data that meet the quality checks. Error filtering procedures provided in

these protocols should be applied for screening the WIM data prior to use in the live-load modeling and calibration processes.

In many spans, the maximum lifetime truck-loading event is the result of more than one vehicle on the bridge at a time. Refined time stamps are critical to the accuracy of multiple presence (MP) statistics for various truck loading cases, including: single, following, side-by-side, and staggered. Many modern WIM data loggers currently in use in the United States have the capability to record and report sufficiently accurate truck arrival times for estimating multiple presence probabilities. Studies also have shown that multiple presence statistics are mostly transportable from site to site with similar truck traffic volumes and traffic flow. Load effects for single-lane and two-lane loadings may be obtained directly from the WIM data when accurate time arrival stamps are collected. Generalized MP statistics may be used for simulation of maximum load effects where accurate truck arrival time stamps are not available. Trucks arriving at a bridge span are grouped into bins by travel lane and run through moment and shear influence lines with their actual relative positions. The resulting load effects are normalized by dividing by the corresponding load effects for HL93. Legal loads and routine permits are grouped under Strength I. Heavy special permits are grouped under Strength II.

There are several possible methods available to calculate the maximum load effect L_{max} for a bridge design period (75 years) from truck WIM data collected over a shorter period of time (1 year). The one implemented in these protocols is based on the assumption that the tail end of the histogram of the maximum load effect over a given return period approaches a Gumbel distribution as the return period increases. The method assumes that the WIM data are assembled over a sufficiently long period of time, preferably a year, to ensure that the data are representative of the tail end of the truck weight histograms and to factor in seasonal variations and other fluctuations in the traffic pattern. Sensitivity analyses have shown that the most important parameters for load modeling are those that describe the shape of the tail end of the truck load effects histogram. The protocols therefore recommend that a year's worth of recent continuous data at each site be collected for use in live-load modeling.

Various levels of complexity are available for utilizing the truck weight and traffic data to calibrate live-load models for bridge design. A simplified calibration approach (Method I) is first proposed that focuses on the maximum live-load variable, L_{max}, for updating the live-load factor for current traffic conditions, in a manner consistent with the LRFD calibration. The ratio, r, for one lane and for two lanes, is used to adjust the LRFD design live-load factor. The ratio, r, is defined as follows:

$$r_1 = \frac{L_{max} \text{ from WIM data projections for one lane}}{L_{max} \text{ used in existing LRFD calibration for one lane}}$$

$$r_2 = \frac{L_{max} \text{ from WIM data projections for two lanes}}{L_{max} \text{ used in existing LRFD calibration for two lanes}}$$

NCHRP Report 368 (Nowak 1999), the LRFD calibration report, provides mean maximum moments and shears for 75 years for simple and continuous spans. An increase in maximum expected live-load based on current WIM data can be compensated in design by raising the live-load factor in a corresponding manner. This simple procedure assumes that the present LRFD calibration and safety indices are adequate for the load data and site-to-site scatter or variability statistics for the WIM data is consistent with values assumed in the LRFD calibration.

When implementing the draft protocols using recent WIM data from various states, it became evident that this procedure, while simple to understand and use, had certain limitations when

applied to statewide WIM data. Using a single maximum or characteristic value for L_{max} for a state would be acceptable if the scatter or variability in L_{max} from site to site for the state was equal to or less than the COV assumed in the LRFD calibration. If the variability in the WIM data is much greater than that assumed in the calibration, then the entire LRFD calibration to achieve the target 3.5 reliability index may no longer be valid for that state and a simple adjustment of the live-load factor as given above should not be done. The site-to-site scatter in the L_{max} values obtained from recent WIM data showed significant variability from span to span, state to state, and between one-lane and two-lane load effects. Therefore, a second, more robust reliability-based approach (Method II) is also presented that considers both the recent load data and the site-to-site variations in WIM data in the calibration of live loads for bridge design.

The draft recommended protocols were implemented using recent traffic data (either 2005 or 2006) from 26 WIM sites in five states (California, Texas, Florida, Indiana, and Mississippi) across the country. The states and WIM sites were chosen to capture a variety of geographic locations and functional classes, from urban interstates, rural interstates, and state routes. An aim of this task was to give practical examples of using these protocols with national WIM data drawn from sites around the country with different traffic exposures, load spectra, and truck configurations. Adjustments and enhancements were made to the protocol steps based on the experience gained from this demonstration task.

Both calibration methods indicate that the lifetime maximum loading for the one-lane loaded case will govern over the maximum loading for a two-lane loaded case. This could be attributable to the increasing presence of heavy exclusion vehicles and/or routine permits in the traffic stream. The load limit enforcement environment in a state will also have a more discernible influence on the maximum single-lane loading than the maximum two-lane loading, which results from the presence of two side-by-side trucks. Additionally, with long-term WIM data with accurate truck arrival time stamps currently available, the projections of L_{max} for two-lane events as undertaken in this study are based on actual side-by-side events rather than on simulations using conservative assumed side-by-side multiple-presence probabilities as done during the AASHTO LRFD code calibration. The WIM data collected as part of this study show that the actual percentage of side-by-side multiple truck event cases is significantly lower than assumed by the AASHTO LRFD code writers who had to develop their models based on a limited set of multiple presence data. Knowing the truck weight distribution in each lane allowed the determination of the actual relationship between the truck weights in the main traffic lane (drive lane) and adjacent lanes, and the determination if there is a correlation between the truck properties. This study seems to indicate that there is some negative correlation between the weights of side-by-side trucks. This means that when a heavy truck is in one lane, the other lane's truck is expected to be lighter. Here again, the conservative assumptions used during the LRFD calibration were not adequately supported by field measurements.

The LRFD did not specifically address deck components in the calibration. The proposed approach to calibration of deck design loads is to assume the present LRFD safety targets are adequate for the strength design of decks and establish new nominal loads for axles based on recent WIM data. The LRFD live-load factors will remain unchanged, but the axle loads and axle types will be updated to be representative of current traffic data.

Updating the LRFD fatigue load model using recent WIM data is described in the protocols. Damage accumulation laws such as Miner's rule can be used to estimate the fatigue damage for the whole design period for the truck population at a site. Based upon the results of the WIM study, changes may be proposed to the LRFD fatigue truck model, its axle configuration, and/or its effective weight.

Additional studies on truck sorting strategies were performed under NCHRP 12-76(01) to further investigate the truck sorting methodology and the sensitivity of r values to how the trucks are sorted into Strength I. These studies developed more detailed recommendations for grouping

trucks into Strength I and II. Using a state's permit and weight regulations to group trucks into Strength I and Strength II was determined to be the most precise and rational approach when using national WIM data.

The protocols and methodologies recommended in this report can be followed to obtain live-load models for bridge design using available truck traffic data collected at different U.S. WIM sites. The models will be applicable for ultimate capacity and cyclic fatigue for main members and for bridge decks. The project was not intended to assemble sufficient data to permit recommendations about revisions to the AASHTO HL93 design load.

CHAPTER 1

Background

Problem Statement and Research Objective

A new vehicular live-load model was developed for the *AASHTO LRFD Bridge Design Specifications* (AASHTO 1994) because the HS20 truck from the Standard Specifications for Highway Bridges did not accurately represent service-level truck traffic. The HL93, a combination of the HS20 truck and lane loads, was developed using 1975 truck data from the Ontario Ministry of Transportation to project a 75-year live-load occurrence. Because truck traffic volume and weight have increased and truck configurations have become more complex, the 1975 Ontario data do not represent present U.S. traffic loadings. Other design live loads were based on past practice and did not consider actual or projected truck traffic and may not be consistent with the LRFD philosophy.

The present HL93 load model and, in fact, the calibration of the AASHTO LRFD specifications, is based on the top 20% of trucks in an Ontario truck weight database assembled in 1975 from a single site over only a 2-week period. It reflects truck configurations and weights taken in the mid-1970s, which primarily consisted of five-axle semi trailer trucks. In the past 30 years, truck traffic has seen significant increases in volume and weight.

Updating bridge live-load models needs representative samples of unbiased truck weight data that meet accepted quality standards. One method that has been developed over the last three decades to capture truck loads in an undetected manner and obtain a true, unbiased representation of actual highway loads is known as weigh-in-motion, or WIM, technology. Although the quality and quantity of traffic data has improved in recent years, it has not been used to update the bridge design loads. In addition to information on truck weights and configurations, the design live load is highly influenced by the simultaneous presence of multiple trucks on the bridge. Such information, usually assembled from headway data, traditionally has not been collected in a manner suitable for the development of design live loads.

The goal of this project is to develop a set of protocols and methodologies for using available truck traffic data collected at different U.S. sites and recommend a step-by-step procedure that can be followed to obtain live-load models for bridge design. The models will be applicable for the design of bridge members, for both ultimate capacity and cyclic fatigue. The models will be applicable for both main structural members as well as the design of bridge decks.

Scope of Study

The original Ontario weight data from one static scale contained 10,000 truck events (2-week sample), which is a relatively small sample. More important for highway truck weight forecasting than the small sample size are the considerable site-to-site, seasonal, and other time variations in the truck weight description. These variations are not modeled in a single realization of data from one site. Heavy trucks may have avoided the static weigh station, and the degree to which this avoidance occurred in the recorded sample is also unknown. The Ontario site was assumed to have a high average daily truck traffic (ADTT) of 5,000. With data from only one site, the influence of volume on traffic loading is also unknown.

In the LRFD development, it was seen that for two-lane bridges, loading events consisting of two side-by-side trucks govern the maximum load effect. It was calculated that the maximum load effect is equivalent to the effect of a side-by-side occurrence where each truck is about 85% of the mean maximum 75-year truck. A truck having 85% of the weight of the 75-year truck also closely corresponds to the maximum 2-month truck. The calibration of the HL93 load model used the following assumptions for side-by-side vehicle crossings (Nowak 1999):

- The total ADTT is assumed to be 5,000 trucks/day.
- One out of every five trucks is a heavy truck.
- One out of every 15 heavy truck crossings occurs with two trucks side by side.

- Of these multiple truck events on the span, one out of 30 occurrences has completely correlated weights.
- Using the product of 1/15 and 1/30 means that approximately 1/450 crossings of a heavy truck occurs with two identical heavy vehicles alongside each other.
- No field data on multiple presence probabilities and truck weight correlation were provided in the LRFD calibration report. Available literature and published reports show that there is little field data to support these assumptions.
- No data on site-to-site variations were provided.
- There was no determination of the extent to which overloaded trucks may have bypassed the static weighing operations.

This project will aim to overcome the above-stated limitations in the previous load modeling study and determine the data required for establishing a representative live-load model.

The first condition that any set of traffic data should meet before being used for the development of load models is the elimination of bias. Truck data surveys collected at truck weigh stations and publicized locations are not accurate because, normally, they are avoided by illegal overweight vehicles that could control the maximum loads applied on bridge structures. Furthermore, an important parameter that controls the load imposed on the structure is related to the number of simultaneous vehicles on the bridge, which is determined through data on truck headways under operating conditions. Accurate headway information cannot be obtained from fixed weigh-stations or from truck data collected at highway bypasses. For these reasons it is determined that truck traffic data should be collected through WIM systems that simultaneously can collect headway information as well as truck weights, axle weights, and axle configurations while remaining hidden from view and unnoticed by truck drivers. Simultaneous data on headways and weights is necessary to determine possible correlations between truck positions or the lanes they occupy and their weights or other characteristics such as truck type, size, and numbers of axles. The 1/15 multiple presence assumption was made because of the lack of sufficient real data at the time of the LRFD calibration. Fortunately, the data needed for multiple presence estimates is presently available and already contained in the raw data files captured by many WIM data loggers.

The quality and quantity of WIM data have greatly improved in recent years. Due to the development of various WIM technologies, unbiased truckloads are now being collected at normal highway speeds, in large quantity, and without the truck driver's knowledge. The more advanced load modeling processes will require a more complete set of input data as discussed herein. The maximum lifetime loading requires as an input the percentage of trucks that cross the bridge side by side and the lane-by-lane distribution of truck weights.

Assuming that the trucks in each lane have identical distribution, as in past simplified approaches, can introduce unnecessary conservatism. Using WIM data could easily improve past estimates or assumptions of various load uncertainties. Some of these uncertainties are now elaborated as follows:

1. Knowing the truck weight distribution in each lane, including mean, coefficient of variation (COV), and distribution type can improve the input parameters needed for the load modeling process.
2. Estimation of expected maximum loading may require different distributions such as an extremal probability distribution derived from the WIM truckload histograms, rather than the normal distribution.
3. Site-to-site variability of truckloads should be incorporated. LRFD used data from only one site in Ontario.
4. Using unbiased data is very important for the estimation of the maximum load. The data used for the LRFD calibration were obtained using a static scale operated by the Canadian province, and some trucks with excessive overloads may have deliberately bypassed the scales. The data must also not be biased by the presence of weight enforcement activity in the vicinity of the data collection site.
5. With additional WIM data, improved estimates of the tail of the probability distribution of the maximum lifetime effect can be made using extremal distributions and other advanced reliability tools. Determining the probability distribution of the maximum effect is needed for the calibration of the live-load factors. The WIM data must also be separated out—WIM measurement scatter from the actual truck weight scatter.
6. Developing and calibrating bridge live-load models requires large amounts of quality WIM data. High-speed WIM is prone to various errors, which need to be recognized and scrubbed/filtered out in the data review process.
7. A major advance in recent WIM operations is their ability to collect improved headway data for trucks. Clearly the headway assumptions used during the LRFD calibration were not based on actual measurements of multiple presence. Field measurements of truck arrival data to a 0.01-second resolution performed in this project and in NCHRP 12-63 consistently showed much lower side-by-side cases than those assumed in the LRFD. These new multiple presence values can be easily incorporated in a simulation model or a simplified model for estimating the maximum lifetime loading.
8. The data must adequately represent daily and seasonal variations in the truck traffic. Hence, it should be collected for a period of 1 year or at random intervals over extended periods of time.
9. The relationship between the truck weights in the main traffic lane (drive lane) and adjacent lanes must be estab-

lished to determine whether passing trucks' characteristics are similar to those in the main traffic lane and if there is a correlation between the truck properties. Here again, the assumptions used during the LRFD calibration were not adequately supported by field measurements. The availability of the current WIM data along with headway information and lane of occupancy will allow us to determine the level of correlation (if any) between the trucks in each lane. The relationship between truck traffic patterns and headways should be related to ADTT. Specifically, data should be collected to determine how the number of side-by-side events varies with ADTT.

The goal of this project is to develop a set of protocols and methodologies for using available current truck traffic data collected at different U.S. sites and recommend a step-by-step procedure that can be followed to obtain live-load models for bridge design. The protocols are geared to address the collection, processing, and use of national WIM data to develop and calibrate vehicular loads for LRFD superstructure design, fatigue design, deck design, and design for overload permits. Various levels of complexity are available for utilizing truck weight and traffic data to calibrate live-load models for bridge design. A simplified calibration approach that focuses on the maximum live-load variable, L_{max}, for updating the load factor and a more robust reliability-based approach that considers the site-to-site variations in WIM data in the calibration of live loads are proposed.

The study also gives practical examples of implementing these protocols with recent national WIM data drawn from states/sites around the country with different traffic exposures, load spectra, and truck configurations. This will give a good cross-section of WIM data for illustrative purposes. This task also allowed the updating and/or refinement of the protocols based on its applicability to WIM databases of varying quality and data standards currently being collected by the states. This report discusses the results of the demonstration studies in detail.

Introduction

This report, prepared in accordance with Task 9 requirements for this project, documents the findings of Tasks 1 through 8. It contains four chapters and six appendices (the appendices are not printed herein but can be found at www.TRB.org). Chapter 1 gives a review of the problem statement, the research objective, and scope of study. Chapter 2 describes the research tasks, findings of the literature search and survey of states, a state-of-the-art summary, and the process to develop and calibrate bridge design live-load models. Chapter 3 provides the draft recommended protocols for using traffic data in bridge design and the results of the demonstration of the draft protocols using national WIM data. Chapter 4 contains the conclusions and recommendations for future research.

Appendix A includes the results of the demonstration of the draft protocols performed in Task 8 using recent national WIM data from five states. Appendix B summarizes the main features of technical publications most relevant to this project that were compiled during the literature search. Appendix C contains the questionnaires used in the surveys and tabulated responses. Appendix D summarizes the findings of Task 2, which investigated potential processes for developing live-load models for bridge design. Appendix E illustrates an implementation of the error filtering algorithm described in the protocols, using recent WIM data. Appendix F discusses the results of truck sorting methods for grouping trucks into Strength I and Strength II, and their influence on "r" values.

CHAPTER 2

Research Approach

Research Tasks

The research effort was organized according to the following nine tasks:

- Task 1. Review relevant practice, data, existing specifications, and research findings from both foreign and domestic sources on the collection and analysis of truck weight data with particular emphasis on evaluating the stresses and deformations induced in highway bridges. This information shall be assembled from both technical literature and unpublished experiences. Information on the quantity and quality of existing WIM data from studies on or near U.S. Interstate bridges is of particular interest.
- Task 2. Describe existing and potential processes to develop and calibrate vehicular loads for superstructure design, fatigue design, deck design, and overload permitting.
- Task 3. Develop the vehicular traffic data requirements (type, quantity, and quality) for each of the processes identified in Task 2. The data requirements should be validated by a sensitivity analysis of each data element.
- Task 4. Assess the statistical adequacy of existing traffic data to meet the requirements developed in Task 3. Recommend means to eliminate any inadequacies.
- Task 5. Using the information from Tasks 1 through 4, recommend candidate protocols for collecting and processing traffic data to calibrate national bridge live-load models. The protocols should include guidance on selecting default values for use when the traffic data do not meet the requirements developed in Task 3. Prepare an updated, detailed work plan for developing and demonstrating the application of the protocols.
- Task 6. Submit an interim report within 6 months of the contract start that documents the results of Tasks 1 through 5 and includes the updated and expanded work plan for developing and demonstrating the protocols for collecting

and processing traffic data. The contractor will be expected to meet with NCHRP approximately 1 month later. Work may not proceed on subsequent tasks without NCHRP approval of the work plan.
- Task 7. Develop the protocols in accordance with the approved work plan.
- Task 8. Demonstrate the application of the protocols using existing national data to develop and calibrate vehicular loads for superstructure design, fatigue design, deck design, and overload permitting.
- Task 9. Submit a final report that documents the entire research effort.

Overview of Data Collection and Review

The first step in the live-load model development process was to assemble and review recent developments and relevant information on practice, specifications, bridge live-load models, WIM systems, WIM data, and studies of truck weights. A purpose of this task was to understand the state of the art and the practice of collecting and utilizing traffic data in bridge design in the United States and in other countries. It included a survey of U.S. state highway agencies. A search of published technical literature in the United States and other countries was conducted for information applicable to this research.

Survey

A survey questionnaire was e-mailed to the traffic monitoring divisions of all state DOTs. The purpose of this questionnaire was to obtain detailed information and document practices on issues central to this research, such as types of WIM equipment in use in each state and the locations of WIM sites, WIM equipment calibration procedures, and the

types of traffic data being collected and how they are being used. A copy of the survey questionnaire is contained in Appendix C. The questionnaire consisted of the following five sections:

- Section 1—Weigh-in-Motion (WIM) Program
- Section 2—WIM Sites
- Section 3—WIM Data
- Section 4—WIM Data Validation and WIM System Calibration
- Section 5—WIM Data Analysis and Applications

Completed questionnaires were received from the following 27 states: Alaska, Arkansas, California, Connecticut, Florida, Georgia, Hawaii, Idaho, Indiana, Iowa, Kansas, Louisiana, Michigan, Minnesota, Mississippi, Missouri, Nevada, New Jersey, New Mexico, New York, North Dakota, Ohio, Oregon, South Dakota, Virginia, Washington, Wyoming. It is believed that states with significant WIM programs have responded to the questionnaire.

State-of-the-Practice Summary

State DOT Survey

Tabulated responses to all survey questions are contained in Appendix C. Responses to certain key questions are presented in Tables 1 through 4.

The responding states have maintained a WIM program over the past 3 to 32 years. The number of high-speed WIM sites varied from 3 to 137, distributed among Interstate and non-Interstate routes. Most states also indicated that they can provide a whole year's worth of WIM data for statistical analyses. This will be an important consideration in the selection of WIM sites for load modeling data because it incorporates any seasonal variability in the traffic data. The types of sensors used at each WIM site, date installed, date last calibrated, number of traffic lanes, and the number of WIM lanes are given in Appendix C. These details were valuable when selecting WIM sites for demonstrating the use of the protocols in this project in Task 8.

There is great variability in the truck arrival time data recorded by the various systems. The range is from 0.01 second

Table 1. WIM program details.

State DOT	WIM Program?	How Long has the WIM Program been in Operation?	Total Number of High-Speed WIM Sites	Number of WIM Sites on Interstates	Do you have WIM Data Available for a Whole Year?
Alaska	Yes	10+ years	7	4	Yes
Arkansas	No				Yes
California	Yes	15 years	137	58	Yes
Connecticut	Yes	9 years	36 bi-directional +4 LTPP	21 bi-directional +2 LTPP	Yes
Florida	Yes	32 years	40	14	Yes
Georgia	Yes	10 years	90	30	No
Hawaii	Yes	18 years	7	2	Yes
Idaho	Yes	12 years	16	6	Yes. Lots of available WIM data.
Indiana	Yes	15 years	52	24	Yes
Iowa	Yes	15 years	28	9	Yes
Kansas	Yes	14 years	9 perm 70 portable	3 perm 25 portable	Yes
Louisiana	Yes	7 years	3	3	No
Michigan	Yes	14 years	41	21	Yes
Minnesota	Yes	22 years	6	2	Yes
Mississippi	Yes	14 years	15	7	Yes
Missouri	Yes	10 years	13	7	Yes
Nevada	Yes	20 years	4	4	Yes
New Jersey	Yes	13 years	64	14	Yes
New Mexico	Yes	17 years	18	7	Yes
New York	Yes	10+ years	21	11	Yes
North Dakota	Yes	3 years	12	4	Yes. Possibly.
Ohio	Yes	15 years	44	21	Yes
Oregon	Yes	8 years	22	18	Yes. In a text format.
South Dakota	Yes	15 years	14	6	Yes
Virginia	Yes		3	2	Yes
Washington	Yes	16 years	37	10	Yes
Wyoming	Yes	8 years	5	3	Yes

Table 2. Accuracy of truck arrival time stamps.

Question 3.4. What is the accuracy of truck arrival time stamps reported in the data set (1 sec, 0.01 sec, etc.)? Are time stamps available for more than one lane at a site? What is the highest resolution possible for truck arrival times? Please explain.	
State DOT	**Time Stamp Accuracy**
Alaska	The accuracy of the truck time arrival is .01 for all lanes of data. The time stamp is on each vehicle record (PVR). This was an Alaska requirement to ensure that duplicate records were not loaded to the database. This is the highest resolution possible for truck arrival times.
California	0.01 sec. Yes.
Connecticut	Truck arrival time stamps are reported for each lane at a site and are recorded by 1 second. The IRD software shows the data time stamp recorded to one-hundredth of a second (0.01) in the individual vehicle viewing software. Additional work would be needed to determine the resolution of the data that is reported in the output file formats.
Florida	Times are recorded to the nearest full second, for all lanes.
Georgia	Accurate to the .01 second and we weigh in one lane of the roadway. At 10 locations we collect truck traffic in the two outside lanes.
Hawaii	Time stamps are not checked for minute/second accuracy. We check them for date accuracy, and we check the WIM system clock at least once per month. Observed accuracy for those can range from within 1-2 seconds to 1-2 minutes.
Idaho	ECM WIM system equipment has a time resolution of one-tenth of a second. The IRD/Diamond WIM systems have a "scientific" mode setting which allows for data collection with a time stamp of one hundred of a second.
Indiana	The timestamps for the vehicle records are to the 1/100 of a second. The ASCII report, however, will alone show the timestamp to the nearest second. This is a shortcoming that has been identified and will be corrected in future versions of the software.
Iowa	They are stored by the hour. We can view the info in real time to the second and can be viewed for all lanes at the site.
Kansas	Accuracy varies because the on-site clock is not externally synchronized. Precision of the arrival time is 1 second, which is the finest resolution available from the equipment. Time stamps are available for each truck, regardless of lane.
Michigan	The time stamp is down to the second for each lane of travel. So we have the hour, minute, and second the vehicle started to cross the sensor.
Minnesota	Whole second
Mississippi	We store the data on an hourly basis in the cardw, but the img file has a time stamp associated with each vehicle. We collect WIM data on all lanes at a permanent site.
Missouri	Year, month, day, hour
Nevada	We have never had the need to investigate this but from my experience it is within a second
New Jersey	Truck arrival time stamps using the "View Vehicle" menu of the IRD office software shows a time stamp of up to 0.01 of a second; processed weight data from the W-record cards only up to one minute.
New Mexico	Hourly, for all lanes.
New York	All lanes are monitored and trucks are time stamped to 0.01 seconds.
North Dakota	1 second resolution—yes, time stamps available on all lanes at all times
Ohio	Mettler-Toledo's time stamp is now sub second at .01 sec. The TMG does not have this resolution and needs to be changed. The time stamp is on each vehicle so it would be by lane. Peek or Pat/IRD do not provide time stamps to the .01 second level.
Oregon	Time stamp accuracy is within .01 seconds. Time stamps are available for each lane in multi-lane systems.
South Dakota	Unknown on accuracy of arrival time and are by lane
Virginia	Time stamps are to the nearest second, and are available for all lanes
Washington	12:00:00:00
Wyoming	Time stamps are to the second and are by lane.

to the hour. The fact that many systems record time stamps to 0.01 second accuracy indicates that there is sufficient availability of refined time stamps for estimating multiple-presence probabilities for truck crossings as discussed in the following chapter.

The responses show that many states have traffic data of similar quality for a number of years at the same site that may be helpful in estimating trends in truck loadings. It is also interesting to note that of the 27 responding states only California and Oregon have begun using WIM data for bridge design applications. These initiatives appear to be in the early states of implementation.

WIM data quality testing and validation is important to ensure that only quality data are made part of the load modeling process. Although WIM systems can provide massive amounts of valuable data in a relatively efficient manner, the data must be checked for accuracy. This accuracy check is a WIM user's quality assurance (QA) program. Most states have implemented QA programs for their WIM systems to check data accuracy. A QA program adds confidence to the validity of the WIM data and alerts the data analyst to problems occurring at the WIM site. The purpose of a QA procedure is to help WIM users check data for accuracy and precision.

Table 3. Multi-year traffic data.

State DOT	Availability of WIM Data for a Number of Years at the Same Site?	Use of WIM Data for Bridge Design Applications?
Alaska	Yes	No
Arkansas		
California	Yes	Yes. Caltrans has started using WIM data for bridge design recently.
Connecticut	No. See answer for previous question.	No. Based loads permitted through the state.
Florida	Yes	No
Georgia	No	No
Hawaii	Yes	No
Idaho	Yes	Yes. We provide some commercial vehicle weight data and reports to our bridge design people.
Indiana	Yes	No. The data is not provided directly to them. However, through Purdue University or our research section they may be utilizing the data.
Iowa	Yes	No
Kansas	Yes	No
Louisiana	No	No
Michigan	Yes	No. Not to my knowledge.
Minnesota	Yes	No
Mississippi	No	No
Missouri	Yes	No
Nevada	Yes	No
New Jersey	Yes	No
New Mexico	Yes	No
New York	Yes	
North Dakota	Yes. Possibly.	No
Ohio	Yes	Yes. Maumee River crossing design & I think for a few other applications a few years back.
Oregon	Yes. From "official" state weigh records. These are available from every weigh station location, not just WIM sites.	Yes—currently the ODOT Bridge Section is conducting an analysis for bridge redesign, and engineering standards.
South Dakota	Yes	Unknown
Virginia	No	No
Washington	Yes	No, at least not to our knowledge
Wyoming	Possibly	Not to my knowledge

Literature Review

An investigation of published technical literature for the monitoring, collection, and analysis of bridge-related WIM data has been performed utilizing transportation organization websites including Transportation Research Information Services (TRIS), National Technical Information Service (NTIS), U.S.DOT, FHWA, and TRB. In addition, transportation engineering websites and databases, and the websites of state departments of transportation and other U.S., Canadian, European, Asian, and Australian transportation institutes, were explored for relevant material regarding the use of WIM data.

This literature search concentrated on the following WIM research topics concerning the use of WIM to:

- Model bridge loads,
- Study the growth or trends in truck weights,
- Study the multiple presence of trucks, and
- Study site-specific bridge loads.

The technical literature search resulted in the compilation of a reference list consisting of approximately 250 abstracts, research papers, journal articles, conference papers, and reports with applicability to the project research.

The collected material was reviewed for pertinence to the areas of research under consideration. The documents determined to be the most relevant were obtained and a scan of the material was performed. Of the examined material, approximately 70 applicable documents were selected for further evaluation and possible summary preparation.

A tabulated summary of approximately 40 documents was prepared from the reviewed material (see Appendix B). Contained in each document summary is a brief study description, the study findings (if any), and recommendations for further research suggested by the authors. A review of the summarized material (Appendix B) reveals that WIM data have been employed in numerous bridge-related applications in North America and abroad.

WIM data have been used to assess current bridge design live loads and to model new design live loads. Several studies

Table 4. WIM data quality assurance.

*Question 4.5 Do you have a Quality Assurance Program in place for your WIM systems to check data accuracy?	
State DOT	**Response**
Alaska	No
Arkansas	NR
California	No
Connecticut	Yes. Through the office checks and the LTPP checks conducted by the FHWA regional contractors.
Delaware	NR
Florida	Yes
Georgia	No
Hawaii	No
Idaho	Yes. This is a daily ongoing part of our WIM maintenance and processing program.
Illinois	NR
Indiana	Yes
Iowa	Yes
Kansas	No
Louisiana	Yes
Michigan	Yes
Minnesota	Yes
Mississippi	Yes
Missouri	Yes
Nevada	Yes
New Jersey	Yes
New Mexico	Yes
New York	Yes
North Dakota	No. Still under development.
Ohio	Yes. TKO
Oregon	Yes. A trouble report system.
South Dakota	Yes
Virginia	Yes
Washington	Yes
Wyoming	Yes

Note: No response (NR).

have found that the current load models were insufficient for the actual loading experienced by the bridge population. WIM data have also been applied to the development of new fatigue models and the assessment of existing models. The results of the investigations reveal that fatigue evaluation is highly site specific and that the actual fatigue damage resulting from the use of WIM data is often underestimated or overestimated by the code-specified fatigue truck.

Truck load growth trends have been assessed utilizing WIM data. For instance, a large-scale California study established that truck volumes have increased over time, however, the gross vehicle weight in the state has remained unchanged. This study also investigated the possibility of applying WIM data that were collected at a bridge site to other nearby bridge locations. The forecasting of truck load spectra as a result of changing truck weight limits also has been investigated by the application of WIM data

The examination of truck multiple presence on bridges has employed WIM data to simulate multi-lane, traffic-critical loading events and extreme load effects. The studies differ in bridge span length and number of lanes investigated, however it was generally noted that as the span length increases, the critical loading event is governed by an increasing num-

ber of trucks. One study indicated that traffic density should be a deciding factor in the development of multiple presence reduction factors.

Numerous studies have investigated WIM-derived site-specific bridge loads for evaluation and design purposes. Generally, it was determined that truck loads are strongly site specific, influenced by factors such as traffic volume, gross vehicle weight, axle weight, local industry, and law enforcement effort, and that current load models for design are often not representative of actual site loading.

WIM Technology

Over the last two decades, highway agencies have recognized the advantages of having automated data collection systems that can provide information on truck weights and truck traffic patterns for economic analysis, traffic management, and various other purposes. The quality and quantity of WIM data has greatly improved in recent years. Due to the development of various WIM technologies, unbiased truckloads are now being collected at normal highway speeds, in large quantity, and without truck driver knowledge. WIM systems that are utilized to provide high-speed weighing of

trucks and other traffic are bending plates, load cells, piezo-electric cables, quartz cables, and bridge WIM systems. One major WIM system vendor alone has approximately 500 permanent WIM sites in operation in 47 states: 246 piezo, 180 bending plate (BP), 42 single load cell (SLC), and 24 Kistler quartz (Table 5). The electronics, software, and storage technologies of WIM data loggers have also advanced in pace with the sensor technology.

Weigh-in-motion equipment currently used in the United States can collect data on truck volumes, axle configurations, truck arrival times, and load spectra. They usually at least classify the vehicles into the 13 FHWA classifications (bins).

The majority of WIM data collection is done with permanently installed weight sensors, although some states may not collect weight data continuously at these sites. Permanent WIM stations provide more extensive datasets at geographically diverse locations over long periods. On a national or regional basis, WIM data is easily obtained from the wide network of permanent sites. If more localized site-specific characteristics are desired, it may be necessary to utilize portable WIM systems for data collection. Portable devices allow flexibility in collecting site-specific traffic data at locations of interest, such as a bridge where significant illegal overloads are suspected.

Table 5. WIM sites and lanes (maintained by one vendor).

State/Province	Piezo Sites	Piezo Lanes	SLC Sites	SLC Lanes	IRD BP Sites	IRD BP Lanes	PAT BP Sites	PAT BP Lanes	Kistler Quartz Sites	Kistler Quartz Lanes
Alabama	11	40								
Alaska	19	48			8	22				
Arizona	5	5					4	8		
Arkansas										
California	16	54			100	345				
Colorado							1	1		
Connecticut	7	38							1	4
DC (Washington)			3	10					1	4
Delaware					1	1				
Florida							13	19		
Georgia										
Hawaii	5	14					2	6		
Idaho	3	12								
Illinois							1	1		
Indiana		20	32	100						
Iowa										
Kansas							2	2		
Kentucky			2	12						
Louisiana							1	1		
Maryland							1	1		
Massachusetts	3	10								
Michigan	1	4			3	14	5	14		
Minnesota	6	12							4	16
Missouri	7	28								
Mississippi							1	4		
Montana										
Nebraska										
Nevada							1	2	6	24
New Hampshire			1	4						
New Jersey	53	131			9	18				
New Mexico					3	12			1	4
New York	20	70								
North Carolina										
North Dakota										
Nova Scotia	8	3								
Ohio	2	2					2	8		
Oklahoma	20	60								
Oregon	10	20	2	6						
Pennsylvania	2	2							10	12
Rhode Island	5	16								
South Dakota					12	34			1	2
Texas					10	40				
Utah	7	36								
Vermont	16	58								
Virginia										
Washington	20	96								
Wisconsin										
Wyoming			2	4						

There are several types of WIM technologies with varying performance and cost considerations (Table 6). Piezoelectric sensor-based systems offer acceptable accuracy (usually ± 15% for gross weights) at such a low cost that their use has become quite widespread for data collection purposes. They can be used as temporary or permanent sites. Strain-based WIM scales and load cell WIM systems provide more accuracy at a higher cost. Strain- and load cell-based systems are used primarily in permanent applications. New WIM technologies continue to be developed and brought to the mar-

ket. Piezoquartz sensors were recently introduced in the United States. They are less sensitive to changes in temperature than the piezo-style sensors, and therefore, are generally more accurate.

Use of In-Service Strain Measurements

Procedures for using in-service peak strain measurements to directly evaluate the safety (using the LRFR method) of existing bridges have been proposed by some researchers. A

Table 6. Sensors commonly used for permanent WIM sites.

Type of Sensor	Strengths	Concerns
Piezoelectric (BL)	Easier, faster installation than many other WIM systems. Generally lower cost than most other WIM sensors. Well supported by industry. Can be used for temporary WIM systems.	Sensitive to temperature change. Accuracy affected by structural response of roadway. Above average maintenance requirement. Requires multiple sensors per lane.
Piezoquartz	Easier, faster installation than many other WIM systems. May be more cost-effective (long term) if sensors prove to be long lived. Very accurate sensor. Sensor is not temperature sensitive. Growing support by industry.	More expensive that other piezo technologies. Requires multiple sensors per lane. Above average maintenance requirement. Sensor longevity data not available. Accuracy affected by structural response of roadway.
Bending Plate	Frame separates sensor from pavement structure. Entire tire fits onto sensor. Moderate sensor cost. Sensor is not temperature sensitive. Extensive industry experience with the technology.	Longer installation time required than piezo systems. Some systems have experienced premature failure, while others have been very long lived.
Load Cell	Entire tire fits onto sensor. Frequently considered the "most accurate" of conventional WIM technologies. Some systems have demonstrated very long lifespans.	Most expensive WIM system. Requires significant construction effort to install. Cost-effective if constructed and maintained for a long lifespan.

considerable part of this effort involves the statistical characterization of the live-load effect using an extreme-value theory. The strains due to ambient traffic are monitored and recorded to represent the distribution of maximum load effects. The maximum load effect distribution is then projected for longer periods, up to 10 years, for determining the maximum expected load effect for evaluation. Because it is based on actual bridge response, it eliminates a substantial part of live-load modeling uncertainties, such as those related to dynamic impact and girder distribution factors. Used in combination with pavement WIM systems, this method has potential applications in other load modeling applications, particularly for fatigue design and assessment. Combining WIM data with bridge response data could significantly reduce uncertainties inherent in high-speed WIM data. One problem involved in such procedures is that the projection is valid for only the stresses at the point where the strain measurements are recorded and the information cannot be generalized for stresses and strain at other locations of the same bridge let alone for application to other bridges. In any case, it is not the aim of this project to develop or recommend new WIM systems. Rather, efforts will concentrate on data now produced by operational WIM networks.

LRFD Fatigue Design

Fatigue criteria for steel bridges are an important consideration for designing for heavy traffic and long expected design lives as well as for assessment of remaining life for existing bridges. As truck weight and volume increase and bridges are maintained in service for increasingly longer periods of time, the fatigue design and assessment issues become even more important.

The present AASHTO fatigue truck, which is based on reliability analyses, was developed by NCHRP Project 12-28 (Moses et al. 1987). The truck traffic load input was taken for some 30 WIM sites in about 8 states collected in the 1980s. For a suite of bridges, each of over 20,000 trucks was used to

calculate the stress ranges and then the fatigue damage averaged according to the fatigue damage law (cubic power). The number of cycles to failure depends on the cube of the stress range and comparison with lab test data for various welded details. A variety of random variables was considered to account for material, analysis, and load uncertainties. This information is used to calibrate the fatigue process to a target β for redundant and non-redundant cases. Moses et al. describes the details of this derivation in *NCHRP Report 299* (1987). The results were incorporated into two AASHTO guide specifications for fatigue design and fatigue evaluation, respectively. Further, the fatigue truck developed for the nominal loading (54-kip, 5-axle truck) in these guide specifications was also incorporated into the AASHTO LRFD specifications and the LRFR manual.

Most of the fatigue damage in a bridge is caused by passages of single trucks across the bridge. The total number of truck passages in the 75-year life of a bridge can exceed 100 million. Static strength design must be based on the most severe load effect expected to occur over the life of the bridge. Fatigue design, on the contrary, should be based on typical conditions that occur, because many repetitions are needed to cause a fatigue failure. (Moses et al. 1987).

The fatigue load specified in the steel structures section of the LRFD specifications also produces a lower calculated stress range than that of the standard specifications. The fatigue provisions of the new specifications are more reflective of the fatigue loads experienced by highway bridges.

In the LRFD, a special vehicle is used for fatigue analysis. It consists of one design truck, as specified above, but with the rear (32-kip) axle spacing fixed at 30.0 ft and without an accompanying uniform load (Figure 1). The fatigue load is used to represent the variety of trucks of different types and weights in actual traffic. For the purposes of fatigue design, a truck is defined as any vehicle with more than either two axles or four wheels. The constant axle spacing approximates that 5-axle semi-trailer trucks do most of the fatigue damage to steel bridges. The specified fatigue loading in LRFD produces
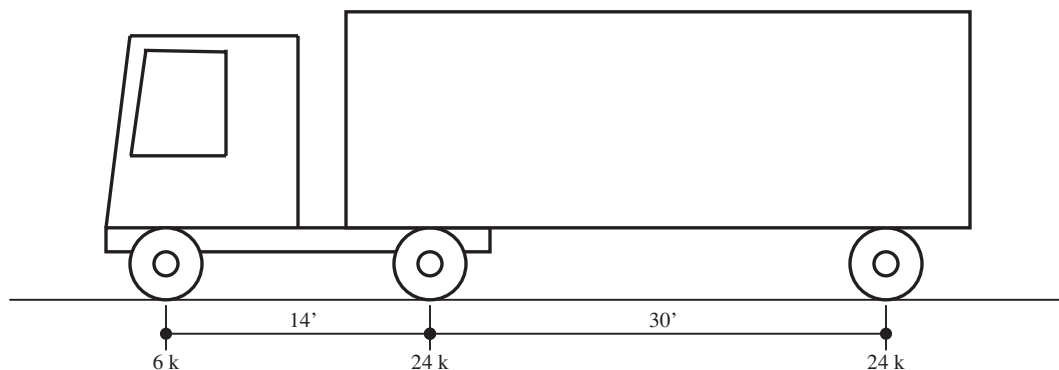

Figure 1. LRFD fatigue truck (includes 0.75 load factor).

a lower calculated stress range than produced by the loadings in the standard specifications. This reduction in calculated stress range is offset by an increase in the number of cycles of loading to be considered in the LRFD specifications. The lower stress range and increased number of cycles are more reflective of the actual conditions experienced by bridges. If the maximum stress a detail experiences in its lifetime is less than the constant amplitude fatigue threshold for that detail, the detail is considered to have infinite fatigue life.

In the FATIGUE load combination given in the LRFD specifications, a load factor of 0.75 is applied to the fatigue load. The factored fatigue load is equivalent to the AASHTO HS15 loading. A revision to Article 3.4.1 was adopted in 2008 to specify two separate fatigue load combinations. For infinite life design under higher traffic volume conditions, the FATIGUE I load combination would be used. In the new FATIGUE I load combination, the stress range caused by the fatigue design truck is multiplied by a load factor of 1.50 (or 2.0 * 0.75). For finite life design under lower traffic volume conditions, the FATIGUE II load combination would be used. The FATIGUE II load combination retains the load factor of 0.75 applied to the stress range caused by the fatigue design truck.

Where the bridge is analyzed using approximate analysis methods, the specified lateral live-load distribution factors for one lane loaded are used in the fatigue check, without the multiple presence factor of 1.2. Where the bridge is analyzed by any refined method, a single fatigue truck is positioned transversely and longitudinally to maximize the stress range at the detail under consideration. A reduced dynamic load allowance of 15% is applied to the fatigue load.

Since fatigue is defined in terms of accumulated stress-range cycles over the anticipated service life of the bridge, the fatigue load should be specified along with the frequency of load occurrence/stress cycles. For the purposes of determining the number of stress cycles per truck passage, LRFD Table 6.6.1.2.5-2 may be used (see Table 7).

The frequency of the fatigue load is taken as the single-lane average daily truck traffic. The number of cycles to be considered is the number of cycles due to trucks actually anticipated to cross the bridge in the most heavily traveled lane over its design life. The frequency of the fatigue load is taken as the single-lane average daily truck traffic ($ADTT_{SL}$). In the absence of better information, the single-lane ADTT shall be taken as follows:

$$ADTT_{SL} = p \times ADTT \tag{1}$$

Where:
$ADTT$ = the number of trucks per day in one direction averaged over the design life
p = fraction of truck traffic in a single lane.

Because of the importance of the lifetime average daily truck volume parameter in fatigue design, the engineer should use whatever site data may be available for making this estimate. It should be made excluding 2-axle trucks consistent with the procedure used in calculating the fatigue truck weight. Traffic volume usually grows at an annual rate of about 2% to 5% until reaching a very high limiting value. It is unrealistic to project traffic growth indefinitely into the future. ADT, including all vehicles, is physically limited to about 20,000 vehicles per day per lane.

AASHTO Fatigue Guide Specifications (1989, 1990)

The *Guide Specifications for Fatigue Design of Steel Bridges* (AASHTO 1989) and the *Guide Specifications for Fatigue Evaluation of Existing Steel Bridges* (AASHTO 1990) specified a 3-axle fatigue tuck having a gross weight of 54 kips to represent the variety of trucks in actual traffic seen in the WIM data collected in the early 1980s. The fatigue truck is similar to the LRFD fatigue load once the loads are scaled down using the 0.75 load factor. One key difference was that the guide specification allowed a variable spacing of 14 ft to 30 ft instead of the standard 30-ft main axle spacing. If used, the reduced axle spacing would have resulted in increased fatigue design stresses.

To recognize the considerable region-to-region and site-to-site differences in truck weight population, alternatives for determining the gross weight of the fatigue truck were permitted. Where the gross-weight histogram for truck traffic (excluding 2-axle trucks) was available, the guide allowed the determination of the gross weight of the fatigue truck from the following:

$$W = \left(\sum f_i W_i^3 \right)^{1/3} \tag{2}$$

Table 7. Stress cycles per truck passage.

Longitudinal Members	Span > 40 ft	Span ≤ 40 ft
Simple span girders	1.0	2.0
Continuous span girders near supports	1.5	2.0
Continuous span girders elsewhere	1.0	2.0
Transverse members	Spacing > 20 ft	Spacing ≤ 20 ft
	1.0	2.0

Where:

f_i = fraction of gross weights within an interval i

W_i = gross weight at mid-width of interval i

The fatigue design was based on the passage of a single fatigue truck across the bridge in the lane under consideration. The net effect of closely spaced trucks was considered to be small for normal traffic conditions (Moses et al. 1987). Therefore, the effect of truck superpositions was neglected for span lengths typically covered by the AASHTO standard specifications. If unusual bunching of trucks is expected at a site, a 15% increase of the fatigue truck weight was specified.

Fatigue Load Research

Research studies have been conducted to establish improved fatigue load models that will cause the same cumulative fatigue damage as the normal truck traffic distribution obtained by WIM measurements in various states. Laman and Nowak (1996) developed a fatigue load model for girder bridges from WIM measurements at five bridge sites in Michigan (Figure 2). Stress cycles also were measured at the midspan of all girders. A new 3-axle fatigue truck was proposed to model vehicles with 3 to 7 axles. The fatigue damage caused by the traffic consisting of 3 to 7 axles is equivalent to the damage caused by an equal number of passes of the 3-axle fatigue truck. A 4-axle fatigue truck was proposed for sites with 10- and 11-axle trucks common in Michigan. The AASHTO fatigue truck was not adequate to model the traffic at these sites. It was found that a high percentage of the fatigue damage was dominated by 10- and 11-axle trucks, although they did not dominate the distribution of truck types. It was found that for these sites,
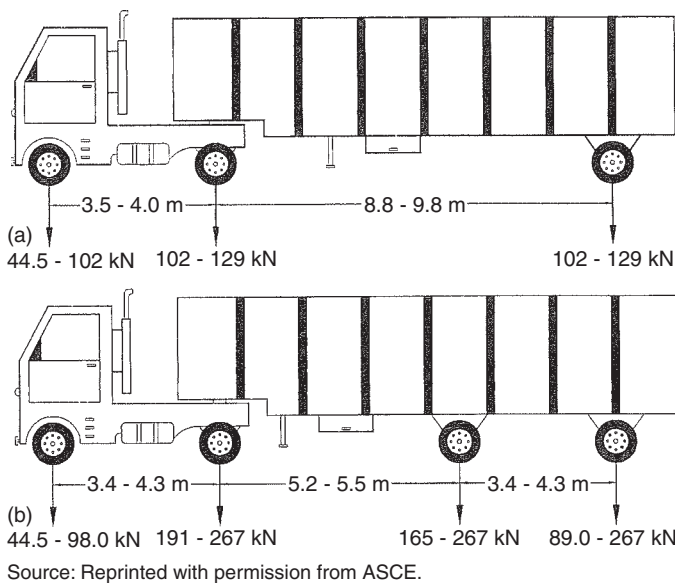
two site-specific fatigue trucks could provide relatively accurate estimates of fatigue damage accumulation over a range of bridge spans. This illustrates that truck load spectra are strongly site specific.

Chotickai and Bowman (2006) developed a new fatigue load model based on WIM data collected from three different sites in Indiana (Figure 3). The recorded truck traffic was passed over simulated bridge spans to investigate moment range responses in simple and continuous span bridges. Based on Miner's hypotheses, fatigue damage accumulations were compared with the damage predicted for the 54-kip AASHTO fatigue truck, a modified AASHTO fatigue truck with an equivalent effective gross weight, and other fatigue truck models. The simulation results indicate that the use of the 54-kip gross weight in an evaluation of bridge structures can result in a considerable overestimation or underestimation of the extent of the actual fatigue damage. It also was shown that the fatigue trucks given by Laman and Nowak (1996) do not provide an accurate estimate of the fatigue damage accumulation for a wide range of span lengths when compared with fatigue damage estimated using the WIM database. Based upon the results of the Indiana WIM study, a new 3-axle fatigue truck and a 4-axle fatigue truck were proposed. The front and rear axle spacing of the new 3-axle fatigue truck are wider than the AASHTO fatigue truck. In addition, a higher percentage of the gross weight is distributed to the front axle compared with the AASHTO fatigue truck. These adjustments were considered to be consistent with statistics of the axle configurations

Source: Reprinted with permission from ASCE.

Figure 2. Fatigue trucks (Laman and Nowak 1996).

Source: Reprinted with permission from ASCE.
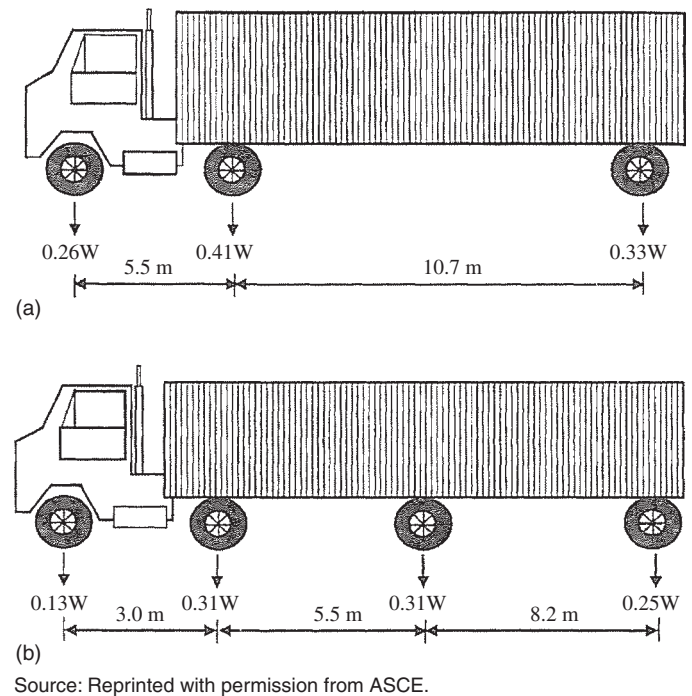
Figure 3. Fatigue trucks (Chotickai and Bowman 2006).

of truck traffic observed. The new 4-axle fatigue truck was most effective when a significant number of 8- to 11-axle trucks pass over a bridge, while the new 3-axle fatigue truck was most effective otherwise.

LRFD Deck Design

In the LRFD specifications, design load for decks and top slabs of culverts using the transverse strip method is the axle load, represented by a 32-kip axle of the design truck or the design tandem consisting of a pair of 25.0-kip axles spaced 4.0 ft apart, whichever creates the most extreme force effect (Figure 4). The two design vehicles should not be considered in the same load case—consider all trucks of one kind, design truck or design tandem (Figure 5), not a mix of the two. The design truck has the same weights and axle spacing as the HS20 load model, which was adopted in 1944 for bridge design, and has been carried over from the standard specifications. Only the truck load is required for decks and not the truck + distributed loads as required for girders.

The slab may be designed by the three following methods: (1.) traditional strip method (2.) empirical design, and (3.) yield-line method. In the traditional strip method, the deck is subdivided into equivalent strips perpendicular to the supporting components. The width of equivalent strips is given in LRFD Table 4.6.2.1.3-1. The strips are analyzed as continuous beams using one or more loaded lanes to determine maximum live-load moments. The empirical design requires that the designer satisfy a few simple rules regarding deck thickness and reinforcement details. An analysis for load effects is not required. Although newer deck design methods were introduced, design load effects on bridge decks have remained essentially the same in the LRFD specifications compared with the requirements of the standard specifications. The live-load modeling in LRFD did not specifically address the increasing load effects on bridge decks from the heavier and more complex axle configurations of current truck traffic.

Figure 5. Typical multi-axle loads.

Axle groups with more than 2 axles are currently not considered for deck design in LRFD. However, LRFD commentary C3.6.1.3.3 states

Individual owners may choose to develop other axle weights and configurations to capture the load effects of the actual loads in their jurisdiction based upon local legal load and permitting policies. Triple-axle configurations of single-unit vehicles have been observed to have load effects in excess of the HL-93 tandem axle load.

Multi-Axle Specialized Hauling Vehicle

To increase load carrying capacity and maximize productivity, in recent years the trucking industry has introduced specialized commercial vehicles with closely spaced multiple axles (Figures 6, 7, and 8). This was the focus of NCHRP Project 12-63 (Sivakumar et al. 2007). States have adopted a variety of short multi-axle vehicles as posting loads in response to

DECK DESIGN – LRFD CODE PROVISIONS

APPROXIMATE STRIP METHOD OF ANALYSIS:

+M = 26.0 + 6.6S

-M = 48.0 + 3.0S

Figure 4. LRFD deck design loads and strip widths.

Figure 6. Concrete ready-mix truck with quad axle.

Figure 7. Multi-axle specialized hauling vehicle (Sivakumar et al. 2007).

Figure 8. Truck with tridem and quad axles.

their potential for overstressing shorter span bridges and bridge decks (Figures 9 and 10). Additionally, short dump trucks are allowed loads of 60K or more in the rear tri-axle group in many states, as seen in Figure 9. Similar exemptions are granted for tandem axles on concrete mixer trucks and other work trucks (>50K allowed on a tandem). Such axle groups usually include lift axles, which are required to be lowered when the truck is loaded, but are not always used in this manner. This further exacerbates the overstress problem on decks and short-span bridges. NCHRP 12-63 has compiled a database of over 70 trucks with complex axle configurations currently in use as legal loads in various states. Many states exempt short hauling vehicles from Federal Formula B and axle weight limits under the grandfathered rights granted when the federal weight laws were first enacted. This information intended for developing new AASHTO load models for evaluation in NCHRP 12-63 can be a valuable resource for developing new axle loads for deck design as the data repre-

sents service loads that the new decks will be subjected to on a routine basis. This has implications for the strength and fatigue design provisions for decks in the current LRFD specifications. Current provisions may be grossly underestimating the maximum and repetitive load effects on bridge decks. Furthermore, the multiple presence probabilities for side-by-side axles could be considerably different than truck multiple presence probabilities for trucks. The former influences deck design, which could be much higher than the side-by-side probabilities for trucks as each truck may have several axle groups that could increase multiple-presence. This issue has not been adequately investigated in past calibrations of the bridge code.

LRFD Overload Design

In addition to routine service loads, bridge owners usually have established procedures that allow the passage of vehicles
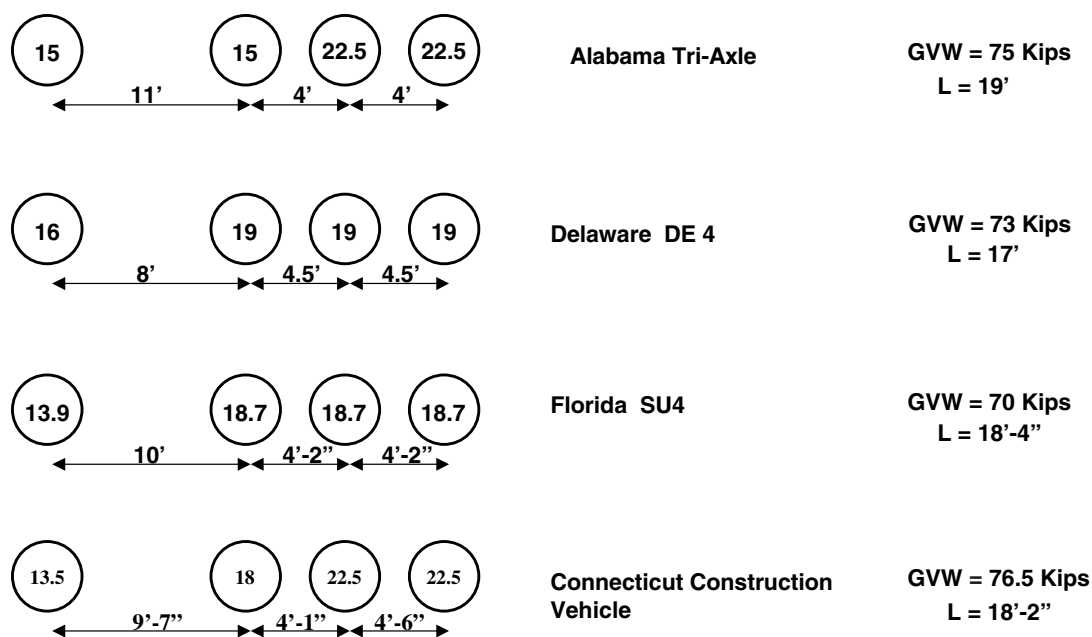
Figure 9. State legal loads that exceed federal weight limits (Sivakumar et al. 2007).
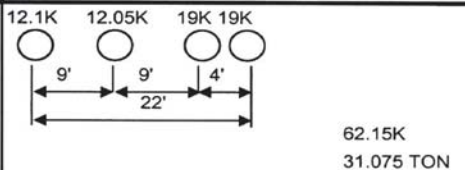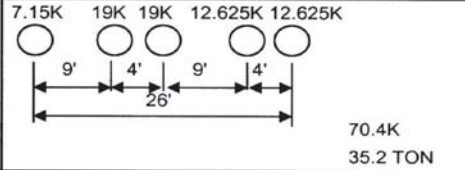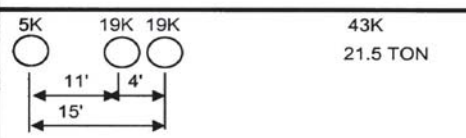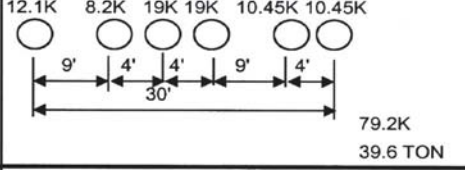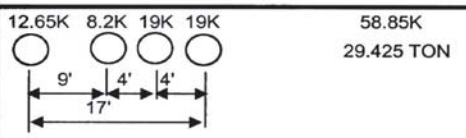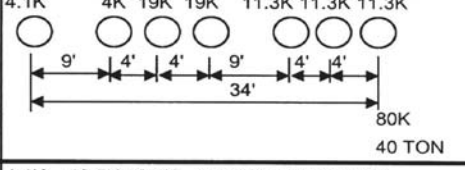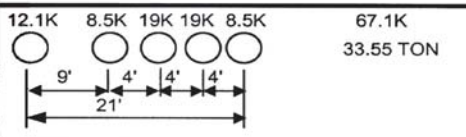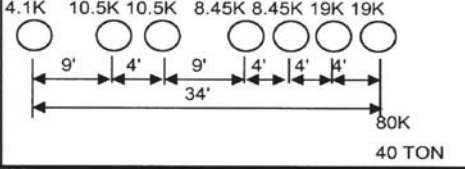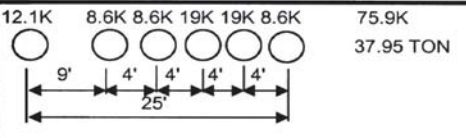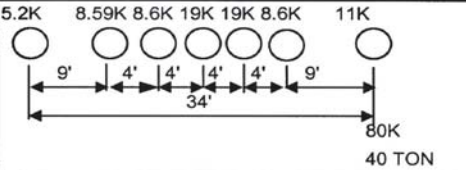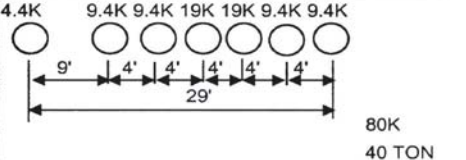
Figure 10. North Carolina legal loads (Sivakumar et al. 2007).

above the legally established weight limitations on the highway system. Depending upon the authorization, these permit vehicles may be allowed to mix with normal traffic or may be required to be escorted in a manner that controls their speed and/or lane position, and the presence of other vehicles on the bridge. The multiple-presence probabilities for permit trucks are significantly different from those used for normal traffic. In the LRFD, the Strength II limit state is specified for checking an owner-specified special design vehicle or permit vehicle during the design process with a reduced load factor of 1.35. No further guidance is given in the LRFD specifica-

tions on how this load factor was derived, the level of safety represented by this limit state, site traffic, or how the load factor might be adjusted when design live-loading characteristics (such as the gross weight of the permit load, likelihood of trucks exceeding the permitted weight, and multiple presence likelihood) differ significantly from the calibration assumptions. These kinds of information need to be obtained locally or regionally through WIM measurements and considered in the Strength II design process since the data used for calibration of national codes are unlikely to be representative of all jurisdictions.

LRFD Superstructure Design

The notional live-load model used in the LRFD specification for the design of bridges, designated HL93, consists of a combination of the

- Design truck or design tandem, and
- Design lane load.

Each design lane under consideration shall be occupied by either the design truck or tandem, coincident with the lane load, where applicable.

The HL93 live-load model was initially developed as a notional representation of shear and moment produced by a group of vehicles routinely permitted on highways of various states under "grandfathered" exclusions to weight laws. The vehicles were based on a 1990 study conducted by TRB that identified 22 representative configurations of vehicles allowed by states as exceptions to weight laws, the smallest and largest of which were a 3-axle, 48-kip single truck, and an 11-axle, 149-kip trailer truck (Kulicki 1994). The notional load model was subsequently compared to the results of truck weight studies, selected WIM data (Ontario), and the 1991 Ontario Highway Bridge Design Code (OHBDC) live-load model. These comparisons showed that the notional load could be scaled by appropriate load factors to be representative of these other load spectra.

Comparisons of moments and shears in simple spans and two-span continuous girders ranging in span from 20 to 150 ft produced by HS20 and the envelope of results produced by the 22 representative exclusion vehicles indicated that the HS20 design loading was not representative of vehicles on U.S. highways. Five candidate notional loads were identified in the live-load development for the AASHTO LRFD specification (Kulicki 1994). Ratios of force effects for each of these live-load models divided by the corresponding force effect from the envelope of exclusion loads indicated that the load model involving a combination of either a pair of 25-kip tandem axles and the uniform load, or the HS20 and the uniform load, seem to produce the best fit to the exclusion vehicles. The tight clustering of force effect ratios for all span lengths, forming bands of data that are essentially horizontal, indicates that the live-load model and load factor can be independent of span length. Thus, the combination of the tandem with uniform load and the HS20 with the uniform load were shown to be an adequate basis for a notional design load in the LRFD specification.

The LRFD specification allows site-specific modifications to the design truck, design tandem, and/or the design lane load under the following conditions:

- The legal load of a given jurisdiction is significantly greater than typical;

- The roadway is expected to carry unusually high percentages of truck traffic;
- Flow control, such as stop sign, traffic signal, or toll booth, causes trucks to collect on certain areas of a bridge; or
- Special industrial loads are common due to the location of the bridge.

The dynamic load model was determined to be a function of three major parameters: road surface roughness, bridge dynamics (frequency of vibration), and vehicle dynamics (suspension system). The actual contribution of road roughness, bridge dynamics, and vehicle dynamics varies from site to site and is difficult to predict. Therefore, the dynamic load allowance in the LRFD was specified as a constant percentage of live load (Nowak 1993b).

Proposed Process to Develop Vehicular Live-Load Models

The design and load capacity evaluation of a bridge member depends on the live-load model and the live-load factor used in the design check equation. The live-load factor $\gamma_L = 1.75$ for Strength I provided in the AASHTO LRFD specifications has been calibrated for use along with the HL93 design load such that bridge members designed with the AASHTO LRFD specifications would achieve a uniform target reliability index $\beta = 3.5$. In actuality, conservative rounding up of the originally calibrated live-load factor indicates that the AASHTO LRFD will produce members with reliability index values higher than 3.5. The reliability index calculations use as input a live-load model that estimates the maximum expected live-load effect on a bridge member. (L_{max} is the expected lifetime maximum load effect on a bridge.) The model includes the mean value of the maximum expected live-load effect along with the standard deviation and the probability distribution type. The live-load model used during the AASHTO LRFD calibration was obtained from a generic set of truck weight and load effect statistics that are presumed to be valid for any typical bridge site in the United States. Because of its generic nature, the live-load model may not represent the actual loading conditions at a particular bridge site or bridges in a state where the truck weights or traffic conditions do not follow the expected typical model. Under these conditions, site-specific or state-specific live-load models may need to be developed based on actual truck weight and traffic data collected at the site or within the state. Several states are currently using WIM systems to collect vast amounts of truck weight and traffic data that can be used to obtain site-specific and state-specific live-load models for bridge design and load capacity evaluation. This would allow individual states to adjust the AASHTO live-load factors to take into consideration the particular truck

traffic conditions throughout a state, a region, or on a particular route.

Task 2 of this research project was focused on existing and potential processes to develop and calibrate vehicular loads for superstructure design, fatigue design, deck design, and overload permitting. The findings are summarized in Appendix D. Several procedures of various levels of complexity exist to estimate the maximum expected load effect on a highway bridge. This section describes the recommended procedure that utilizes site-specific truck weight and traffic data to obtain estimates of the maximum live load for a specified return period. The return period for the design of a new bridge is specified to be 75 years as per the AASHTO LRFD code for Strength I limit state. A 2-year return period has been used for the load capacity evaluation of existing bridges during the calibration of the AASHTO LRFR, and a 1-year period has been proposed for estimating the maximum live-load effect for the AASHTO LRFD Strength II limit state. It should be clearly stated that it is not possible to obtain exact values of the maximum expected 75-year load due to the limitations in the available data. In fact, to obtain accurate results, one would need several cycles of WIM data collected over 75 years for each cycle, which is an impossible task. Even the development of live-load models for 1-year and 2-year return periods would require several cycles of 1-year and 2-year data, which are currently not available due to the relatively recent adoption of WIM technology in the United States. Hence, some form of statistical projection will be needed for any practical load modeling effort as will be described in this section. The approach described in this section uses a normal probability distribution to project the tail end of the collected WIM data histograms. The properties of the normal distribution can then be used to obtain the statistics of the maximum load effects for any return period using extreme value distributions.

This section presents the theoretical background for the proposed procedure for modeling the maximum live-load effect on a highway bridge. The proposed approach for obtaining the live-load model requires as input the WIM data collected at a site after being "scrubbed" and processed to remove data outliers as described in other sections of this report. For state-specific load models, data from several representative sites should be assembled. The statistics of the maximum live-load effects can then be used to adjust the AASHTO live-load factors so that the Strength I and Strength II limit state designs would achieve safety levels similar to those intended by the AASHTO code writers while simultaneously accounting for the state-specific loading conditions.

1. Probability Density Function and Frequency Histogram of Truck Load Effects

For the single-lane loading of short-span bridges, a truck loading event is defined as the occurrence of a single truck on the bridge. For multiple truck presence in multi-lanes, the loading event may consist of two or more trucks simultaneously on the bridge. While all currently used WIM systems are capable of providing axle weights and axle spacings for each truck crossing, only WIM systems capable of taking continuous uninterrupted data at normal highway traffic speeds with accurate time stamps are able to identify multi-lane loading events and provide the axle weights, axle spacings, and relative positions of all the trucks involved in each multi-lane loading event. For the cases when uninterrupted multi-lane data with accurate time stamps are not available, multi-lane loading events can be obtained from simulations based on estimates of the number of side-by-side and information on ADTT data. This could be achieved using an approach that will be described in Chapter 3.

In the first step, using the WIM data files, the shear force or bending moment effect of each truck loading event in the WIM record is calculated by passing the trucks through the proper influence line. For multi-lane loadings, the combined shear force or moment effect from the trucks that are simultaneously on the bridge is obtained. The shear or moment for each truck load event is then normalized by dividing the calculated value by the shear or moment of the HL93 load model.

The shear and moment data for the single-lane loading and the multi-lane loading events are collected into separate percent frequency histograms. Each histogram provides a discretized form of the probability density function (pdf) of the shear or moment effects for the site. The histogram is designated as $H_x(X)$ while the pdf is designated as $f_x(X)$. The relation between $H_x(X)$ and $f_x(X)$ is given by

$$H_x(X) = \int_{X_l}^{X_u} f_x(x)dx \qquad (3)$$

Where:

X_l and X_u give the upper and lower bounds of the bin within which X lies. If the bin size is small, then $f_x(X)$ can be assumed to be constant within the range of X_l to X_u and Equation (3) becomes

$$H_x(X) = f_x(X)\Delta X = f_x(X)(X_u - X_l) \qquad (4)$$

Where:

ΔX is the bin size.

2. Cumulative Distribution Functions and Cumulative Frequency Histograms

Using the histograms and the probability density functions $f_{x1}(\ldots)$, $f_{x2}(\ldots)$, $f_{xs}(\ldots)$, and $f_z(\ldots)$, the cumulative distributions for the shear or moment effects of single or multi-lane

loading events can be obtained. The cumulative distribution is assembled from the pdf using the following equation:

$$F_z(Z) = \int_{-\infty}^{Z} f_z(y)dy \tag{5}$$

In essence, Equation 5 assembles all the bins of the histogram below a certain value Z into a single bin at Z. This is repeated for all possible values of Z. Thus, $F_z(Z)$ will give the probability that a loading event will produce a load effect less than or equal to Z.

3. Cumulative Probability Function for the Maximum Load Effect over a Return Period of Time, t_{return}.

For the AASHTO Strength I limit state, a bridge structure should be designed to withstand the maximum load effect expected over the design life of the bridge. The AASHTO LRFD code specifies a design life of 75 years. The LRFR bridge load rating also requires checking the capacity to resist the maximum load effects for a 2-year return period. The AASHTO LRFD Strength II limit state implicitly assumes a 1-year return period associated with special permit trucks. It is simply impossible to collect enough data to determine the maximum load effect expected over 75 years of loading. Even getting sufficient data for the 1-year and 2-year return periods would require several cycles of 1-year and 2-year data, which are not currently available. Therefore, some form of statistical projection should be performed. The proposed calculation procedure uses the cumulative distribution function for individual loading events and then applies a statistical projection to obtain the information required for a 1-year, 2-year, or 75-year return period.

To find the cumulative distribution for the maximum loading event in a period of time t_{return} one has to start by assuming that N loading events occur during this period of time. These events are designated as $S_1, S_2, \ldots S_N$. The maximum of these N events, called $S_{max,N}$, is defined as

$$S_{max,N} = max(S_1, S_2, \ldots S_N) \tag{6}$$

The study team was interested in finding the cumulative probability distribution of $S_{max,N}$. This cumulative probability distribution, $F_{s\,max\,N}(S)$, gives the probability that $S_{max,N}$ is less than or equal to a value S. If $S_{max,N}$ is less than S, this implies that S_1 is less than S, and S_2 is less than S, ... and S_N is less than S. Hence, assuming that the loading events are independent, the probability that $S_{max,N} \leq S$ can be calculated from

$$F_{s_{max,N}}(S) = F_{s_1}(S) \cdot F_{s_2}(S) \ldots F_{s_N}(S) \tag{7}$$

If $S_1, S_2, \ldots S_N$ are independent random variables that are drawn from the same probability distribution, then

$$F_{s_1}(S) = F_{s_2}(S) = \cdots = F_{s_N}(S) = F_s(S) \tag{8}$$

and Equation 7 reduces to

$$F_{s_{max\,N}}(S) = \lfloor F_s(S) \rfloor^N \tag{9}$$

Note that Equation 9 assumes that the number of events is a known deterministic value. A sensitivity analysis performed as part of this study has however demonstrated that the results of Equation 9 are not highly sensitive to small variations in N as N becomes large.

The application of Equation 9 requires high precision in $F_s(S)$. For example, given 3,000 trucks per day over a 75-year return period, the number of single truck events N would be over 82 million. Thus, to obtain the median value of the maximum event $S_{max\,N}$ corresponding to $F_{s_{max\,N}}(S) = 0.5$ would require $F_s(S)$ to have precision up to the 9th decimal point, which is not possible to obtain without executing some form of statistical projection. To perform the statistical projection, a careful analysis of the tail end of $F_s(S)$ is required.

4. Statistical Fit of Tail End of Probability Distribution of Load Effect of a Single Loading Event

The probability distribution of the single loading event does not follow any known probability distribution type. However, careful observations of the tail ends of the WIM data histograms assembled from several sites indicate that the tail ends match the tail ends of normal probability distributions. For example, Figure 11a shows the plot of the data collected at the I-81 site in Upstate New York on a normal probability scale. A normal probability plot is executed by
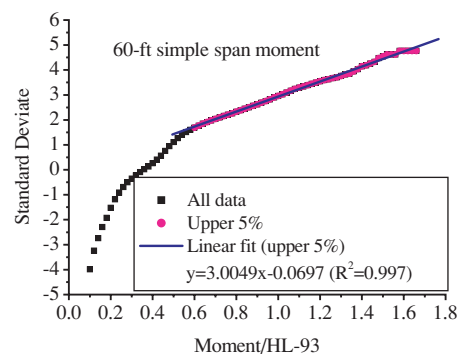
Figure 11a. Normal probability plot for moment effect of trucks in drive lane of I-81 NB.

taking the normal inverse of $F_s(S)$ represented by $\Phi^{-1}[F_s(S)]$ and plotting versus S. The plot would produce a straight line if S follows a normal distribution. In this case, the mean of S would correspond to the abscissa for which $\Phi^{-1}[F_s(S)]$ is zero. The mean plus on standard deviation would correspond to the abscissa for which $\Phi^{-1}[F_s(S)]$ is equal to 1.0.

The plot of the WIM data shows that the data as a whole does not follow a normal distribution as the curve does not follow a straight line. However, the figure shows that the upper 5% of the data does approach a straight line indicating that the tail end of the data resembles the tail end of a hypothetical normal distribution. A linear fit on the normal probability plot of the upper 5% of the data collected at this I-81 site will produce a slope, m, and an intercept, n, which will give the mean of the equivalent normal distribution that best fits the tail end as $\mu_{event} = -n/m$. The standard deviation of the best-fit normal distribution is $\sigma_{event} = 1/m$. For the I-81 data, single truck events give $\mu_{event} = 0.0232$ and $\sigma_{event} = 0.333$. The regression analysis of the upper 5% of the data produces a regression coefficient $R^2 = 0.997$ indicating a good linear fit.

5. Cumulative Distribution of Maximum Load Effect

To verify that the normal fit of the tail end of the data is sufficient to obtain good estimates of the maximum load effect for long return periods, the results of Equation 7 are plotted in Figure 11b for two cases. Case 1 uses as input the cumulative distribution $F_s(S)$ obtained from the WIM data for single

loading events and Case 2 uses the $F_s(S)$ that corresponds to the normal distribution with $\mu_{event} = 0.0232$ and $\sigma_{event} = 0.333$. The application of Equation 7 uses different return periods varying from 1 day to 75 years. The number of events for the I-81 site are obtained as $N_{day} = 3200$ single truck events.

Figure 11b shows good agreement between the projections obtained from the normal fit of the tail and the WIM data for the 1-day, 1-week, and 1-month return periods. The figure also shows that the WIM data are not sufficient to obtain the maximum load effect for return periods greater than 1 month. However, the use of the normal distribution to model the tail end of WIM data would allow for obtaining the maximum load effect distribution for extended return periods.

6. Extreme Value Distribution of Maximum Load Effect

Although the application of Equation 7 can be executed numerically for any parent probability distribution, the fact that the tail end of the WIM data matches that of a normal distribution allows for the application of extreme value theory to obtain the statistics of the maximum load effect in closed form. The approach is based on the following known concept as provided in Ang and Tang (2007), which states "if the parent distribution of the initial variable S has a general normal distribution with mean μ_{event} and standard deviation σ_{event}, then the maximum value after N repetitions approaches asymptotically an Extreme Value Type I (Gumbel) distribution" with a dispersion α_N given by:
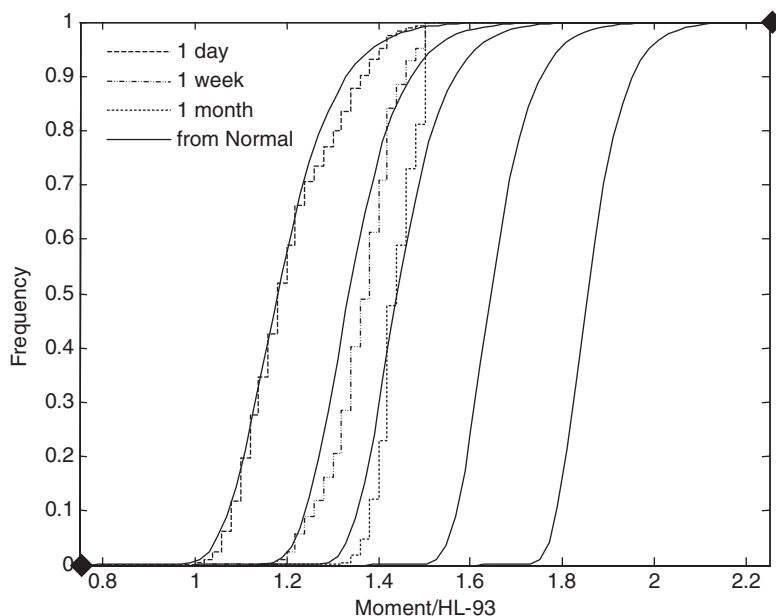
Figure 11b. Cumulative distribution of maximum load effect of single lane events for different return periods.

$$\alpha_N = \frac{\sqrt{2\ln(N)}}{\sigma_{event}} \tag{10}$$

and a most probable value u_N given by:

$$u_N = \mu_{event} + \sigma_{event}\left(\sqrt{2\ln(N)} - \frac{\ln(\ln(N)) + \ln(4\pi)}{2\sqrt{2\ln(N)}}\right) \tag{11}$$

α_N and u_N can be used to find the mean of the maximum load effect, L_{max}, and its standard deviation, σ_{max}, for any return period having N repetitions as

$$\bar{L}_{max} = \mu_{max} = u_N + \frac{0.577216}{\alpha_N} \tag{12}$$

and

$$\alpha_{max} = \frac{\pi}{\sqrt{6}\alpha_N} \tag{13}$$

Monte Carlo Simulation

An alternative to the statistical projections approach consists of using a Monte Carlo simulation to obtain the maximum load effect. In this approach, results of WIM data observed over a short period can be used as a basis for projections over longer periods of time. A Monte Carlo simulation requires the performance of an analysis of a large number of times and then assembling the results of the analysis into a histogram that will describe the scatter in the final results. Each iteration is often referred to as a cycle. The process can be executed for the single lane-loading situation or the side-by-side loading. A step-by-step procedure for Monte Carlo simulation is described in the next chapter in Step 12.3 of the draft protocols.

Monte Carlo simulation will not be accurate for large projection periods because of the limitations in the originally collected data. Also, the Monte Carlo simulation will be extremely slowed down when the number of repetitions K is very high. Furthermore, one should make sure not to exceed the random number generation limits of the software used, otherwise the generated numbers will not be independent and the final results will be erroneous. Hence, statistical projections must be made to estimate the maximum load effects for long return periods. Alternatively, one can use a smoothed tail end of the WIM histogram by fitting the tail with a known probability distribution function (such as the normal distribution) and use that fitted distribution with the Monte Carlo simulation. It should be emphasized however, that the Monte Carlo simulation would still be very inefficient for projections over long return periods.

CHAPTER 3

Findings and Applications

Background to Development of Draft Recommended Protocols

LRFD Background

The HL93 live-load model was initially developed as a notional representation of shears and moments produced by a group of vehicles routinely permitted on highways of various states under "grandfather" exclusions to weight laws. The notional load model was subsequently compared to the results of truck weight studies, selected WIM data (Ontario), and the 1991 OHBDC (Ontario Code) live-load model. These comparisons showed that the notional load could be scaled by appropriate load factors to be representative of these other load spectra.

The calibration of the AASHTO LRFD specifications is based on the top 20% of trucks in an Ontario truck weight database assembled in 1975 from a single site over only a 2-week period. In the past 30 years, truck traffic has seen significant increases in volume and weight.

The goal of this project is to develop a set of protocols and methodologies for using available current truck traffic data collected at different U.S. sites and recommend a step-by-step procedure that can be followed to obtain live-load models for bridge design. The protocols are geared to address the use of national WIM data to develop and calibrate vehicular loads for LRFD superstructure design, fatigue design, deck design, and design for overload permits.

Various levels of complexity are available for utilizing the site-specific truck weight and traffic data to calibrate live-load models for bridge design. A simplified calibration approach is proposed that focuses on the maximum live-load variable, L_{max} for updating the live-load model or the load factor for current traffic conditions, in a manner consistent with the LRFD calibration. A more robust reliability-based approach also is presented to consider the site-to-site variations in WIM data in the calibration of live loads. Some key issues and traffic parameters that influence the estimation of traffic statistics and the maximum load effect are summarized below.

Use of High-Speed WIM Sites

The first condition that any set of traffic data should meet before being used for the development of load models is the elimination of bias. Truck data surveys collected at truck weigh stations and publicized locations are not accurate because they are normally avoided by illegal overweight vehicles that could control the maximum loads applied on bridge structures. Furthermore, an important parameter that controls the load imposed on the structure is related to the number of simultaneous vehicles on the bridge, which is determined through data on truck headways under operating conditions. Accurate headway information cannot be obtained from fixed weigh stations or from truck data collected at highway bypasses. For these reasons, it is determined that truck traffic data should be collected through WIM systems that can collect simultaneously headway information as well as truck weights and axle weights and axle configurations while remaining hidden from view and unnoticed by truck drivers.

WIM Data Quality

WIM data collection should not sacrifice quality for quantity. The selection of WIM system sites should focus on sites where the owners maintain a quality assurance program that regularly checks the data for quality and requires system repair or recalibration when suspect data are identified. Weighing accuracy is sensitive to roadway conditions. Roadway conditions at a WIM site can deteriorate after a system is installed and calibrated. Regular maintenance and recalibrations are essential for reliable WIM system performance. Vehicle dynamics plays a significant role in the force actually applied by any given axle at any given point on the roadway. Site-specific calibration is the only way that the dynamic effects of the

pavement leading to the scale can be accounted for in the WIM scale calibration. The dynamic motion of trucks is also influenced by the vehicle design, gross weight, and suspension systems. The calibration approach should account for the vehicle dynamics and the truck traffic characteristics of each data collection site.

Physical and software-related failures of equipment and transmission failures are common sources of traffic data quality problems. Transmission problems can lead to gaps in the data (i.e., missing data) even though data may be continuously collected in the field. Data quality checks should be implemented to detect and fix "bad data" before processing.

WIM Scale Calibration

Heavy emphasis is placed on the calibration of WIM data collection equipment. Quality information is more important than the quantity of data collected. It is far better to collect small amounts of well-calibrated data than to collect large amounts of data from poorly calibrated scales. Even small errors in vehicle weight measurements caused by poorly calibrated sensors could result in significant errors in measured loads. Key issues concerning the use of WIM equipment are (1.) the calibration of WIM equipment and (2.) the monitoring of the data reported by WIM systems as a means of detecting drift in the calibration of weight sensors. Recommendations for WIM sensor calibration and monitoring of data are given in Appendix 5-A of the Traffic Monitoring Guide (U.S.DOT 2001).

Auto-calibration is the practice by which software calculates and applies an adjustment to the scale calibration factor based on a comparison of the average of a number of measurements of front axle weights against its expected value. There are drawbacks to auto-calibration techniques currently used by some states to offset calibration errors, and it is recommended that direct WIM scale calibration be implemented. Only direct calibration of a WIM scale after it has been installed at a site ensures that it is measuring axle weights correctly. This includes a comparison of static axle weights with axle weights that are estimated from multiple vehicle passes with more than one vehicle. Comparison of static weights and dynamic weights will provide an effective check of system accuracy with regard to sensor errors and errors due to vehicle dynamic effects. For long duration counts, the scale should be calibrated initially, the traffic characteristics at that site should be recorded, and the scale's performance should be monitored over time. The state should also perform additional, periodic, on-site calibration checks (at least two per year). These steps will ensure that the data being collected are accurate and reliable.

WIM data scatter for axles is different from gross weight scatter and is usually much larger. This axle scatter should be assembled separately from the equipment calibration and should be used to modify the measured axle loads.

Filtration of WIM Measurement Errors

Sensitivity analyses have shown that the most important parameters affecting maximum bridge loads are those parameters that describe the shape of the tail end of the truck load effects histogram. Current WIM technology is known to have certain levels of random measurement errors that may affect the accuracy of the load modeling results. These errors are due to the inherent inaccuracies of the WIM system itself, the difference between the dynamic weight measured and the actual static scale weight, as well as the effect of tire pressure, size, and configuration on the WIM results. Hence, it is advisable to use a statistical algorithm to filter out these errors. A standardized approach to executing the error filtering procedure will bring uniformity in the load modeling process that will utilize WIM data from various sites. To execute the filtering process, a calibration of the results of the WIM system should be made by comparing the results of the WIM to those of a static scale. This calibration process should be executed for a whole range of truck and axle weight types and configurations. The ratio of the measured weight to the actual weight (bias) for a large sample of readings is the calibration statistics that should be assembled into a histogram. A procedure for error filtering utilizing the scale calibration data is recommended as part of the load modeling protocols.

Site-to-Site Variability

One of the largest variability in truck traffic is site-to-site variability. Site-to-site variability of truckloads should be incorporated since the calibration of the AASHTO LRFD specifications used data from only one site in Ontario, Canada (U.S. sites were not considered). Dividing truck routes into three functional classifications will allow a systematic assessment of truck load spectra within a state. Each route within a functional classification group is taken to experience truck weights per vehicle type that are similar to those of other routes within that group. The classification groups routes into Interstate and non-Interstate highways. Many states allow heavier loads on non-Interstate routes under grandfather exemptions to weight laws. Interstates are further divided into urban versus rural because many urban areas have been known to experience heavier truck loads and volume due to increased commercial activity, lack of alternate modes of freight movement, and a general lack of truck weight enforcement.

Truck data will be collected from WIM sites on principal arterials. The routes on the principal arterial system are sub-classified as Interstate and other principal arterials (Table 8). Urban and rural areas could have fundamentally different traffic characteristics. Consequently, this workplan provides for separate classification of urban and rural functional systems.

Table 8. Proposed classification scheme for truck weight data collection.

Protocols Functional Class	Description	FHWA Functional Class(es)
A	Rural Interstate Principal Arterial	1
B	Urban Interstate Principal Arterial	11
C	Other Principal Arterial	2, 12, 14

Seasonal Variability in the Traffic Stream

Traffic varies over time. Traffic varies over a number of different time scales, including:

- Time of day,
- Day of week, and
- Season (month) of the year.

Most trucks follow a traditional urban pattern where weekday truck volumes are fairly constant, but on weekends, truck volumes decline considerably. Long-haul trucks are not concerned with the "business day"; they travel equally on all seven days of the week. WIM sites should operate continuously throughout the year to measure temporal changes in the loads carried by trucks. Where possible, more than one site within a functional group should be monitored continuously to provide a more reliable measure of seasonal change. Tracking of seasonal changes in truck traffic is necessary to obtain representative truck weight histograms needed for various analyses.

Directional Variation

Most roads exhibit differences in flow by direction. Truck weights, volumes, and characteristics can also change by direction. One classic example of directional differences in trucks is the movement of loaded trucks in one direction along a road, with a return movement of empty trucks. This is often the case in regions where mineral resources are extracted or near port facilities. Tracking these directional movements is important to obtain the load spectra for bridge load modeling.

Lane-by-Lane Variation

The vast majority of trucks (80% or more) travel in the right (drive) lane. The expected maximum gross vehicle weight (GVW) and, therefore, the expected maximum moments and shears of the trucks in the drive lane are different than those of the trucks in the passing lane. The degree of this difference seems to be dependent on the site and travel direction. The maximum lifetime loading requires as an input the percentage of trucks that cross the bridge side by side and the lane-by-lane distribution of truck weights. Assuming that the trucks in each lane have identical distribution (as in past simplified approaches) can introduce unnecessary conservatism. Using WIM data could easily improve past estimates or assumptions of various load uncertainties for trucks in each lane. Knowing the truck weight distribution in each lane, including mean, COV, and distribution type, can improve the input parameters needed for the load modeling process.

Permit Traffic versus Non-Permit Traffic

In most states permit records are either not specific enough or detailed enough to allow separation of permit loads from non-permit loads in a large WIM database. Routine permits are not route-specific and are allowed unlimited trips. For LRFD bridge design it is not necessary to separate legal loads from routine permits because both are classified as unanalyzed truck loads that should be enveloped by the HL93 design loading. Protocols require that legal loads and routine permits be grouped under Strength I and heavy special permits be grouped under Strength II. The following approach was developed for grouping trucks that would be consistent from site to site:

- Do not attempt to classify trucks as permit or non-permit because customarily the permit records are not reliable enough or readily accessible to do this.
- Group all trucks with six or fewer axles in the Strength I calibration. These vehicles include legal trucks and routine permits or divisible load permits. These vehicles are considered to be enveloped by the HL93 load model.
- Group all trucks with seven or more axles in the Strength II calibration. These vehicles should include the heavy special permit loads, typically in the 150-kip GVW and above category.

For a state that maintains easily accessible permit records with a well established and enforced overweight permits program it would be possible to obtain the records for authorized permits or permit vehicles for a route for a specific data collection period and separate out these heavy vehicles (Strength II) from

the illegal overloads (Strength I), both of which populate the upper tail of the histogram. With many states moving to online and Web-based permits processing, electronic records for permits should become more readily available in the future.

Multiple-Presence Probabilities

In many spans, the maximum lifetime truck-loading event is the result of more than one vehicle on the bridge at a time. An important step in defining nominal design load models is the modeling of multiple-presence probabilities. Many modern WIM data loggers currently in use in the United States have the capability to record and report sufficiently accurate truck arrival times for estimating multiple-presence probabilities. Many traffic counters routinely record data to 1/100 of a second or even a millisecond in their binary files. These time stamps allow the determination of headway separation of trucks in adjacent lanes or in the same lane and the occurrence of simultaneous or near-simultaneous load events in each lane. The sensitivity analysis has demonstrated that small changes in the number of multiple-presence events do not have a significant effect on the estimated maximum load effect over the 75-year design life.

Studies done using New York WIM data during this project show that there is a strong correlation between multiple-presence and ADTT. From Figure 12 it is evident that the number of multiple presences sees a sharp drop-off on days when the ADTT is low (such as weekends). Though not linear, the graph demonstrates that multiple-presence statistics are related to the site traffic conditions. A recent study of truck multiple-presence at 25 sites across New Jersey over a period of 11 years has also provided valuable data on the relationship between truck volume and truck multiple presence (Gindy and Nassif 2006).

Obtaining reliable multiple-presence statistics requires large quantities of continuous WIM data with refined time stamps, which may not be available at every site. The site ADTT could serve as one key variable for establishing a site multiple-presence value. A single WIM site can provide multiple-presence data for varying ADTT values due to daily variation in ADTT.

Multiple-Presence Probabilities for Permit Loads

The multiple-presence probabilities for permit trucks are significantly different from those used for normal traffic. In the LRFD, the Strength II limit state is specified for checking an owner-specified permit vehicle during the design process with a reduced load factor of 1.35. Although no guidance is given in the LRFD specifications on how this load factor was derived, a reduced load factor is considered appropriate due to the reduced likelihood of permit trucks exceeding the authorized
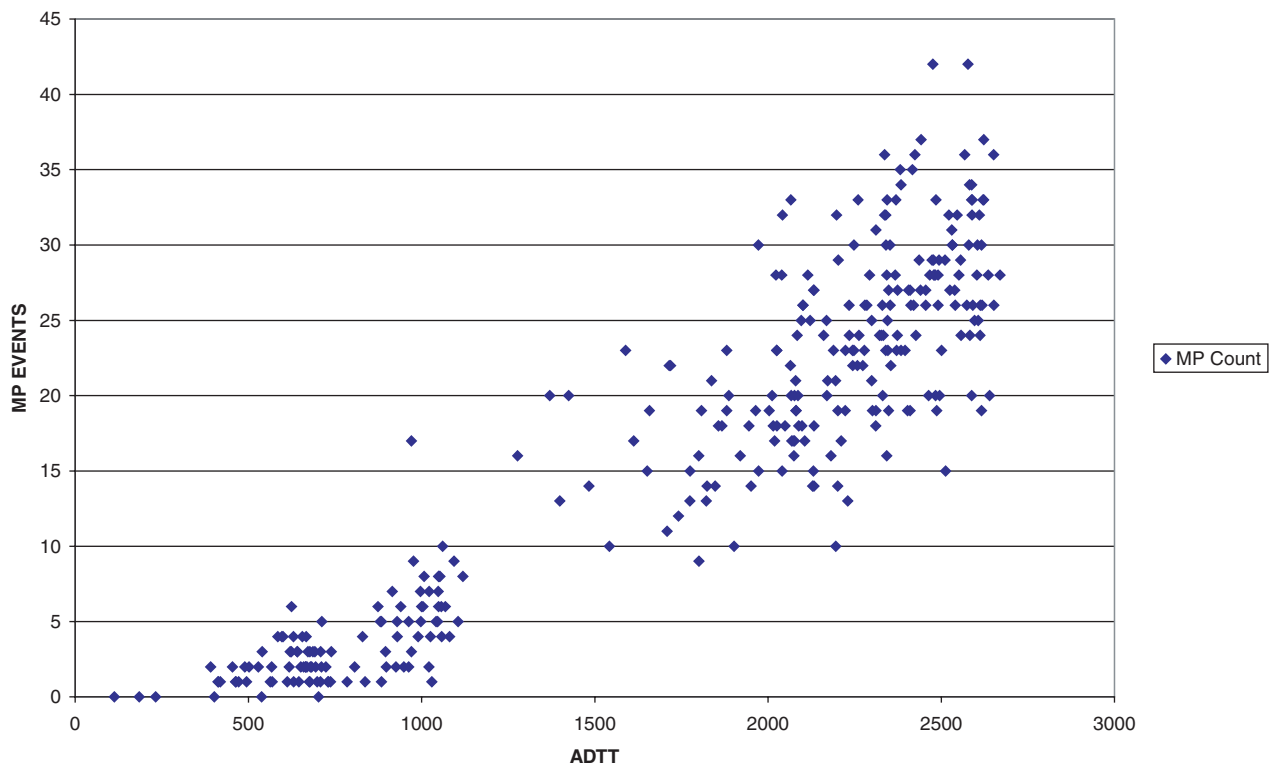
Figure 12. Side-by-side events vs. ADTT—I-81 NB New York.

weight, the reduced multiple-presence likelihood, and the reduced exposure period of 1 year. The permit live-load factors are derived to account for the possibility of simultaneous presence of non-permit heavy trucks on the bridge when the permit vehicle crosses the span. Information on loads and multiple-presence probabilities for permits needs to be obtained locally or regionally through WIM measurements and considered in the Strength II design process since the data used for calibration of national codes are unlikely to be representative of all jurisdictions.

LRFD Fatigue Design

Since fatigue is defined in terms of accumulated stress-range cycles over the anticipated service life of the bridge, fatigue design is based on typical conditions that occur as many cycles are needed to cause a fatigue failure. The present AASHTO fatigue truck, which is based on reliability analyses, was developed using truck traffic load data taken for some 30 WIM sites in about eight states collected in the 1980s. Over 20,000 trucks were used to calculate the stress ranges and then the fatigue damage averaged according to the fatigue damage law (cubic power). The number of cycles to failure was compared with lab test data for various welded details. The fatigue truck developed (54-kip, 5-axle truck) from these studies has been incorporated into the AASHTO LRFD specifications and the AASHTO LRFR manual.

As truck weight and volume increase and bridges are maintained in service for increasingly longer periods of time, the fatigue design and assessment issues become even more important. The AASHTO fatigue load is used to represent the variety of trucks of different types and weights in actual traffic. Applying a single truck model that may not be representative of current traffic as a standard for all fatigue design may be inaccurate or potentially unsafe. Code-based load models based on past WIM data may not adequately represent modern traffic conditions in many jurisdictions.

Draft Recommended Protocols for Using Traffic Data in Bridge Design

Protocols recommended for collecting and using traffic data in bridge design can be categorized into the following steps:

- Step 1: Define WIM data requirements for live-load modeling;
- Step 2: Selection of WIM sites for collecting traffic data for bridge design;
- Step 3: Quantities of WIM data required for load modeling;
- Step 4: WIM calibration and verification tests;
- Step 5: Protocols for data scrubbing, data quality checks, and statistical adequacy of traffic data;

- Step 6: Generalized multiple-presence statistics for trucks as a function of traffic volume;
- Step 7: Protocols for WIM data analysis for one-lane load effects for superstructure design;
- Step 8: Protocols for WIM data analysis for two-lane load effects for superstructure design;
- Step 9: Assemble axle load histograms for deck design;
- Step 10: Filtering of WIM sensor errors/WIM scatter from Measured WIM histograms;
- Step 11: Accumulated fatigue damage and effective gross weight from WIM data;
- Step 12: Lifetime maximum load effect L_{max} for superstructure design; and
- Step 13: Develop and calibrate vehicular load models for bridge design.

The steps to be followed are described in detail in the remainder of this chapter.

Step 1. Define WIM Data Requirements for Live-Load Modeling

An aim of these processes is to capture weight data appropriate for national use or data specific to a state or local jurisdiction where the truck weight regulations and/or traffic conditions may be significantly different from national standards. The objective is to use data from existing WIM sites to develop live-load models for bridge design. The models will be applicable for the strength and fatigue design of bridge members, including bridge decks and design vehicles for overload permitting. The traffic data needs for live-load modeling are summarized as follows.

- Data needed for calibration of superstructure (Strength I) design load models include
  - Lane-by-lane truck type distribution, total weights, and axle weights and spacings with particular emphasis on the tails of the weight histograms;
  - Headways and multi-presence for single, two, or more lanes including side by side, staggered and following trucks, which are of particular interest for multi-span or longer single-span bridges (how headways are affected by truck volumes is important for developing models that take into consideration local or regional traffic patterns); and
  - Calibration statistics for the WIM scale to filter out sensor errors.
- Data needed for overload permitting (Strength II) include
  - State permit policies and routine permit types authorized for a specific route;
  - Where available, record of special permits authorized for a specific route during the data collection period,

including truck descriptions, axle weights, and axle spacings;

– Information on multiple-presence for permit loads—two permit trucks side by side or a permit truck with a non-permit truck; and

– WIM calibration data using overloaded test trucks, if available (if not, utilize same calibration data as for Strength I).

- Data needed for calibration of deck design load models include
  – Common axle configurations and axle weight distributions of legal trucks and permit trucks;
  – Frequencies of occurrences of common axle configurations;
  – Other multi-axle configurations with fixed and variable axles;
  – Headway information for side-by-side effects of axle groups or single axles; and
  – WIM scale calibration statistics for axle loads.

- Data needed for calibration of fatigue load models (FATIGUE) include
  – Truck type distribution, total weights, and axle weights and spacings with emphasis on the most common vehicles rather than on the tails (this is because the fatigue process is due to the accumulation of damage from every truck crossing and is less dependent on the extreme loading events);
  – Frequencies of occurrences of common truck configurations; and
  – WIM scale calibration statistics.

Step 2. Selection of WIM Sites for Collecting Traffic Data for Bridge Design

- Select remote WIM sites away from weigh stations. This is very important for obtaining unbiased data. Traffic monitoring unknown to the truck drivers is key.

- Select sites that do not experience significant breakdowns and provide reliable year-round operation. Select sites that can provide a year's worth of continuous data.

- Select WIM sites that have been recently calibrated and are subject to a regular maintenance and quality assurance program. A review of recent WIM data will indicate if there is an obvious problem with the calibration. Perform a calibration check of the system. Accuracy of the weight data and the time stamps should be verified. Request a manual recalibration using a group of trucks of known weight and configuration if the system does not meet specified tolerances. Calibration data must be available for filtering out measurement errors. The project will recommend data quality requirements for WIM sites used for data collection.

- Select WIM sites with free-flowing traffic, where trucks usually maintain their lanes and travel speed (>10 mph), and that do not experience any significant stop-and-go traffic or traffic backups. The sites should be away from exits, on level grade, with smooth roadway surfaces near the WIM installation. Avoid sites with numerous traffic stoppages.

- Select sites with WIM sensors in right lane and passing lanes, in both directions. Some sites have sensors only in the drive lane.

- The user should have a good understanding of the state's overweight permit policies that apply to the specific routes. It would be difficult to identify continuous or routine permits in the traffic stream in most states. These permits are not route-specific and are allowed unlimited trips within the period of duration for the permit. Special permits that are issued for very heavy loads are subject to restrictions on the route taken and the number of crossings made. Use records of special permits (usually available from the permit office) to identify and remove those vehicles that populate the extreme end of the load data prior to statistical processing of "random" traffic.

- Select sites equipped with current sensor and equipment technologies. Regular maintenance and periodic recalibration of any WIM system is critical for obtaining reliable traffic data. It is also important to filter out WIM data measurement errors so that they do not affect the accuracy of the load modeling results. The calibration of the WIM system will provide information on the calibration factor, ϵ, for use in the filtering process.

- Preferably, the WIM system should be able to capture and record truck arrival times to the nearest 1/100th of a second, or better, to allow the determination of truck headway separations.

In general, the selection of WIM sites for bridge load modeling will depend on the geographic spread of the truck load data represented by the model.

Step 2.1 Sites for National Design Live-Load Modeling

- Study of truck loads can be conveniently handled by dividing the country into five regions as shown in Figure 13 (FHWA 2001).

- Ten states with the highest truck populations are California, Illinois, Texas, Ohio, Florida, Pennsylvania, Oklahoma, New York, North Carolina, and Indiana (Table 9).

- Select one representative state from each region. The state should have a well-established and maintained WIM program that has been in place for a number of years that could provide the data needed for load modeling. The five recommended states, one from each region, are California, Florida, Indiana, New York, and Texas (Table 10).

Figure 13. U.S. regions for truck loads.

- For each representative state, select the sites and routes for WIM data collection based on functional classifications defined in Table 8.

For each functional classification, select two WIM sites, guided by the following considerations, as applicable:

- Heavy freight routes or routes known to have significant permit traffic;

- Bulk cargo shipping routes;
- Logging routes;
- Specialized equipment shipping routes;
- WIM sites near ports, railroad terminals, or other truck origination points;
- WIM sites near industrial facilities or mining operations;
- WIM sites near landfills or waste transfer sites;
- WIM sites near military installations;

Table 9. Candidate states for national data collection for live-load modeling.

State	State Ranking Based on Truck Population	Region (see map, Figure 14)	How Long has the WIM Program been in Operation?	Total Number of High-Speed WIM Sites	Number of WIM Sites on Interstates	WIM Data Available for a Whole Year?
California	1	WE	15 years	137	58	Yes
Florida	5	SA	32 years	40	14	Yes
Indiana	10	NC	15 years	52	24	Yes
Michigan	11	NC	14 years	41	21	Yes
Missouri	15	NC	10 years	13	7	Yes
New Jersey	19	NE	13 years	64	14	Yes
New York	8	NE	10+ years	21	11	Yes
Ohio	4	NC	15 years	44	21	Yes
Oregon	23	WE	8 years	22	18	Yes
Texas	3	SG	21 years	18	6	Yes

Table 10. Recommended states from each of the five regions.

State	State Ranking Based on Truck Population	Region	How Long has the WIM Program been in Operation?	Total Number of High-Speed WIM Sites	Number of WIM Sites on Interstates	WIM Data Available for a Whole Year?
California	1	WE	15 years	137	58	Yes
Florida	5	SA	32 years	40	14	Yes
Indiana	10	NC	15 years	52	24	Yes
New York	8	NE	10+ years	21	11	Yes
Texas	3	SG	21 years	18	6	Yes

Table 11. Sites by functional classification for WIM data collection.

Functional Class	FHWA Functional Classes	Description	WIM Sites
A	1	Rural Interstate Principal Arterial	2
B	11	Urban Interstate Principal Arterial	2
C	2, 12, 14	Other Principal Arterial	2

- WIM sites should preferably be geographically dispersed within a state; and
- WIM sites should preferably have varied truck volumes.

Step 2.2 Sites for State-Specific Design Live-Load Modeling

It is important to recognize that there can be significant variations in traffic conditions within a state that should be accounted for in truck weight studies. For calibrating design load models for a specific state, some broad guidelines may be given as follows:

- Select two sites from each of the three highway functional classes. Where WIM sites exist, verify that WIM data from all major truck routes within a state are included (Table 11).
- Each site in a functional class should preferably be from a different region of the state.
- The guidelines for selecting individual WIM sites should be as discussed above under Step 2.1, Sites for National Design Live-Load Modeling.

Step 2.3 Sites for Design Live-Load Modeling for a Metro Area or Transportation Hub

- For calibrating load models for a city or a transportation hub within a state, select at least six WIM sites from within a 25-mile radius of the city or region. Where WIM sites exist, verify that WIM data from all major truck routes within the area of interest are included.
- The guidelines for selecting individual WIM sites should be as discussed above under Step 2.1.
- Where enough permanent WIM sites are not in operation, temporary WIM sites for short-term data collection may be employed. Data should be collected to capture likely seasonal variability in truck traffic.

Step 2.4 Sites for Route-Specific Design Live-Load Modeling

- For calibrating live-load models for a designated hauling route, select a minimum of three WIM sites on that route or on feeder routes.
- The guidelines for selecting individual WIM sites should be as discussed above in Step 2.1.

- Where enough permanent WIM sites are not in operation, temporary WIM sites for short-term data collection may be employed. Data should be collected to capture likely seasonal variability in truck traffic.

Step 2.5. Sites for Site-Specific Design Live-Load Modeling

- This sub-step would be particularly relevant to major bridge design and/or evaluation.
- For calibrating site-specific load models for a specific bridge, select three WIM sites on that route or feeder routes, preferably within a distance of 25 miles of the bridge.
- If permanent WIM sites are not available, a temporary WIM site may be deployed at the approaches to the bridge. Data should be collected to capture likely seasonal variability in truck traffic. WIM data shall be gathered in both travel directions.

For the purposes of picking WIM data collection sites for the demonstration of the protocols for this project, one site for each functional classification in two states is proposed. In this regard, the resources available on this project were also a consideration.

Step 3. Quantities of WIM Data Required for Load Modeling

Some recommendations for the quantity of WIM data to be collected from each site to capture the variability in traffic loads include the following:

- A year's worth of recent continuous data at each site to observe seasonal changes of vehicle weights and volumes is preferable.
- If continuous data for a year is unavailable, seek a minimum of 1 month of data for each season for each site.
- Use data from all lanes in both directions of travel.

Step 4. WIM Calibration and Verification Tests

To ensure that high-quality data will be collected for use in bridge live-load modeling, all WIM devices used for this purpose should be required to meet performance specifications for data accuracy and reliability. Because collection of accurate

traffic loading rates throughout the year is necessary to provide the load data needed, the WIM systems used in this effort must meet the ASTM criteria all year long. Historically, many WIM systems have had problems accurately weighing vehicles when environmental conditions have changed from those that were present when the equipment was last calibrated. Changes in pavement condition at the scale location are also known to cause problems with WIM system sensor accuracy.

Pavement design procedures compute equivalent single-axle loads (ESALs) from measured axle weights using a mathematical formula developed by AASHTO. The fourth-order relationship in this formula heavily magnifies the effects of poor scale calibration, which can lead to significant errors in determining the load experienced by a pavement and thus computing the expected pavement life. Bridge design, however, is controlled by shear and moment effects that bear a linear relationship to axle loads and axle spacings. Therefore, errors in scale calibration are not magnified to the same extent as in pavement design.

Many states attempt to work around the cost of scale calibration by relying on a variety of auto-calibration techniques provided by WIM equipment vendors. Auto-calibration is the practice by which software calculates and applies an adjustment to the scale calibration factor. This is a common technique utilized on piezo systems to account for changing sensitivity of the scale sensors to changing environmental conditions. It is based on a comparison of the average of a number of measurements of some specific variable against its expected value. Some of these techniques adjust scale-calibration factors to known sensitivities in axle sensors for changing environmental conditions, "known" truck conditions, and equipment limitations. Although these techniques have considerable value, they are only useful after the conditions being monitored at the study site have been confirmed. A state must determine whether the auto-calibration procedure used is based on assumptions that are true for a particular site and whether enough test trucks are crossing the sensor during a given period to allow the calibration technique to function as intended. Auto-calibration may not be particularly suited to low truck volume sites. Field tests to verify that a WIM system is performing within the accuracy required is an important component of data quality assurance for bridge load modeling applications.

Steps to ensure that the data being collected are accurate and reliable follow.

Step 4.1 Initial Calibration

Initial calibration of WIM equipment should follow LTPP calibration procedures or ASTM 1318 standards.

Step 4.2 Periodic Monitoring

Periodic monitoring of the data reported by WIM systems should be performed as a means of detecting drift in the calibration of weight sensors.

Step 4.3 Periodic On-Site Calibration Checks

For long duration counts, the scale should be calibrated initially, the traffic characteristics at that site should be recorded, and the scale's performance should be monitored over time. The state should also perform additional, periodic on-site calibration checks (at least two per year). Only direct calibration of a WIM scale after it has been installed at a site ensures that it is measuring axle weights correctly. This includes a comparison of static axle weights with axle weights that are estimated from multiple vehicle passes with more than one vehicle.

Assemble calibration statistics for a WIM site for filtration of sensor errors during the load modeling process (see Step 11). This calibration process should be executed for a range of truck and axle weight types and configurations operating at normal highway speeds. The ratio of the measured weight to the actual weight for a large sample of readings is the calibration factor that should be assembled into a histogram. WIM data scatter for axles is different from gross weight scatter and is usually much larger. This axle scatter should be assembled separately from the equipment calibration and should be used to modify the measured axle loads.

Step 5. Protocols for Data Scrubbing, Data Quality Checks, and Statistical Adequacy of Traffic Data

Step 5.1 Data Scrubbing

The key to developing and calibrating bridge live-load models is quality of WIM data and not quantity. High-speed WIM is prone to various errors that need to be recognized and considered in the data review process. It is important to review the WIM data to edit out "bad or unreliable data" containing unlikely trucks to ensure that only quality data is made part of the load modeling process. It is also important to recognize that unusual data are not all bad data as truck configurations are becoming increasingly more complex and truck weights are getting heavier. Slow moving traffic (<10 mph) and stop-and-go traffic could cause difficulty in separating vehicles. Two or more trucks may be read as one truck. It is therefore important to check speed data. Trucks with very large axle spacings and excessive total wheelbase may be combining separate trucks. Maximum likely axle spacing must be specified. This could be done by importing the WIM text files into a database. The filters can be used to screen the

database for bad data or unlikely trucks during the data transfer process.

The WIM survey data should be scrubbed to include only the data that meet the quality checks. The following is a filtering protocol that was applied for screening the WIM data used in this project. Truck records that meet the following filters were eliminated:

- Speed <10 mph,
- Speed >100 mph,
- Truck length >120 ft,
- Total number of axles <3,
- Record where the sum of axle spacing is greater than the length of truck,
- GVW <12 kips (and max as required),
- Record where an individual axle is >70 kips,
- Record where the steer axle is >25 kips,
- Record where the steer axle is <6 kips,
- Record where the first axle spacing is <5 ft,
- Record where any axle spacing is <3.4 ft,
- Record where any axle is <2 kips, and
- Record which has GVW +/− sum of the axle weights by more than 10% (this may indicate that the axle records provided may not be complete or accurate).

The data scrubbing rules have been refined and updated as WIM data from typical sites were processed during the course of this study. Adjustments to the data scrubbing rules may need to be made to accommodate differences in traffic characteristics, truck configurations and weight limit compliance from state to state. Some newer trucks with complex axle configurations may need rules specifically tailored to fit their use. The rules do not propose a maximum GVW limit. This ensures that trucks are not excluded just because they are very heavy. The test is to see if a truck configuration is "realistic" based upon an understanding of feasible axle configurations.

Step 5.1.1 Review of Eliminated Suspect Data

Reviewing a sampling of trucks that were eliminated during the data scrubbing process is recommended to check if the process is performing as intended and that real trucks have not been inadvertently removed from the dataset. This is a valuable quality assurance check of the data scrubbing process. Comparing WIM data with permit data or data from any nearby weigh station would provide an additional check. Where feasible, short-duration monitoring of trucks using real-time WIM data could be helpful to verify scale performance and the accuracy of truck classifications. Stopping of trucks for static weighing is not recommended during such monitoring because it may bias the WIM data if the heavy overweight trucks find an alternate route to avoid detection.

Step 5.2 Quality Control Checks for Scrubbed WIM Data

This section describes simple quality checks performed on WIM data to quickly confirm that a properly calibrated data collection device is working as intended. It should not be confused with calibration tests.

Perform the following quality control checks for each WIM site for each lane, for each month of data collection:

1. Check vehicle classification statistics (truck percentages by class) and compare results with historical values or manual counts where available for the site/route. Large deviations from expected values could indicate sensor problems.
2. Produce a GVW histogram of Class 9 trucks (5-axle semi-trailer trucks) using a 4-kip increment. Most sites will have two peaks in the GVW distribution (unloaded peak usually falls between 28 kips and 32 kips; the loaded peak falls somewhere between 72 kips and 80 kips). A shift in the peaks could indicate that the scale calibration may be changing or the scale may be malfunctioning. If both peaks have shifted, the scale is probably out of calibration.
3. Compute the number and percentage of Class 9 trucks over 100 kips. If the percentage of Class 9 trucks over 100 kips is high, the scale calibration may be questionable, unless such readings could be explained by a state's weight and permitting laws or by known movement of heavy commodities on a route. Such readings may indicate operational problems with the sensor.
4. Produce a histogram of steer axle weights for Class 9 trucks. The average front axle weight for Class 9 trucks is fairly constant for most sites. It ranges between 9 kips and 11 kips. Some variations are possible due to truck characteristics and GVW. Significant deviation of steer axle weights is a sign of scale operational problems.
5. Produce a histogram of Class 9 drive tandem axle weights. Compare with mean drive axle weight for Class 9 trucks given in *NCHRP Report 495* (Fu et al. 2003) (estimates wheel weights as a function of truck GVW).
6. Produce a histogram of spacing between front axles and drive tandem axles. Check mean spacing between drive tandem axles. Compare results to historical values available for Class 9 trucks.

Step 5.3 Assess the Statistical Adequacy of Traffic Data

The proposed protocols for calculating the maximum 75-year live-load effect, L_{max}, is based on the WIM truck weight and truck traffic database assembled at various sites within the jurisdiction for which the L_{max} estimates are required. The protocols are based on collecting truck weight and truck traffic

WIM data over a period of a year in order to cover all possible seasonal variations and other short-term fluctuations in truck traffic patterns.

The models used in this study assume that the WIM data is stationary in the sense that the 1-year data is representative of all subsequent years within the 75-year design life of a bridge site. Possible growth in truck weights and traffic intensities must be considered using an economic projection analysis, which is beyond the scope of this study.

Furthermore, the proposed protocols assume that the tail end of the truckload effect histogram for a bridge span follows a normal distribution, the statistical properties of which are obtained from a regression analysis of the upper 5% of the data plotted on a normal probability curve. Normal probability plots of truckload effects obtained from WIM data collected at several different sites have confirmed that the upper 5% of the data approaches a straight line with a regression coefficient R^2 on the order of 0.97 to 0.99 indicating that the normal distribution does reasonably well model the upper tail of the truck load effect histograms. The slope and intercept of the regression fit of the upper tail on the normal probability plot can then be used to find the mean and standard deviation of the normal distribution. However, the values of the slope and intercept depend on the estimates of the frequency of trucks in each bin of the histogram. In particular, the normal probability plot uses the cumulative frequencies as the basis for the calculation of the slope and intercept of the regression line and thus the mean and standard deviation of the equivalent normal distribution. The calculated values for the mean and standard deviation provide "best estimates" of these parameters. However, the process does not provide any information about the accuracy of these estimates except our understanding that these estimates will improve as the sample size increases. In order to provide some quantitative measure of the accuracy of these estimates, it is herein proposed to use statistical confidence intervals. A confidence interval of a parameter defines a range with lower and upper limits within which the true value of the parameter will lie with a prescribed probability. These confidence intervals will reflect the effect of the sample size and the number of samples that are found to lie within a bin of the truck load effect. Obviously the more data is collected, the more confidence the engineer will have in the estimated truck load effect frequencies in each category and the higher will be the accuracy of the calculated mean and standard deviations of the equivalent normal distribution.

Confidence Intervals on the Cumulative Frequencies. Assume that the percent cumulative frequency in a particular bin of the load effect histogram at a given site is given as "p_i" which is calculated as the total number of trucks that produced moments within the bin "i" divided by the total number of trucks, n. It can be proven that statistically speaking, this p_i is

an unbiased estimate of the true value p_i. Thus, according to Ang and Tang (2007), the $(1 - \alpha)$ lower and upper confidence intervals of p_i can be obtained from the following:

$$\text{Lower limit: } p_{i-\alpha/2} = \hat{p}_i + k_{\alpha/2}\sqrt{\frac{\hat{p}_i(1 - \hat{p}_i)}{n}} \tag{14}$$

$$\text{Upper limit: } p_{i-\alpha/2} = \hat{p}_i + k_{(1-\alpha/2)}\sqrt{\frac{\hat{p}_i(1 - \hat{p}_i)}{n}} \tag{15}$$

Where $k_{\alpha/2} = -\Phi^{-1}(1 - \alpha/2)$ and $k_{(1-\alpha/2)} = \Phi^{-1}(1 - \alpha/2)$, $\Phi^{-1}(\ldots)$ is the inverse cumulative function of the normal standard distribution. If the 95% confidence limits are desired, then $1 - \alpha = 95\%$ leading to $k_{\alpha/2} = -1.96$ and $k_{(1-\alpha/2)} = +1.96$.

To get the 95% confidence interval on the projected maximum live-load effect L_{max}, follow Step 12.2.1 but use the upper and lower limits of the cumulative frequency p_i rather than the value obtained directly from the WIM data. The evaluating engineer should decide whether the resulting confidence intervals L_{max} are sufficiently narrow. If the intervals are not adequate, more WIM data should be collected to further narrow the intervals.

Step 6. Generalized Multiple-Presence Statistics for Trucks as a Function of Traffic Volume

In many spans, the maximum lifetime truck-loading event is the result of more than one vehicle on the bridge at a time. Refined time stamps are critical to the accuracy of multiple-presence statistics. Accurate multiple-presence data requires time stamps of truck arrival times to the hundredth of a second. Many states typically report arrival times to the nearest second. A time stamp that records to the nearest second could result in an error of over a truck length for trucks traveling at highway speeds. With time stamps recorded to the nearest hundredth of a second, headway separations will be accurate to within a foot. As noted, multiple-presence statistics need not be developed for each site because there is a correlation between multiple presence and ADTT. There also may be a correlation between multiple presence and the functional class of the highway. Higher multiple-presence probabilities may be more likely at urban WIM sites due to slower traffic speeds and increased congestion.

Multiple-presence statistics are mostly transportable from site to site with similar truck traffic volumes and traffic flow. A single WIM site can provide multiple-presence data for varying ADTT values due to daily variation in ADTT. In this study, few sites with large quantities of continuous WIM data that include refined time stamps to a resolution of 0.01 second or better were investigated. A relationship between multiple

presence and traffic volume was developed to utilize the multiple-presence values from national data to any given site without performing a site-specific analysis. Where accurate time stamps are not available multiple-presence events may be evaluated using multiple-presence statistics from other sites with similar traffic conditions and functional classifications. Multiple-presence statistics are obtained as a function of headway separation for side-by-side and following trucks.

Definitions

- Headway: The distance between front axles of side-by-side trucks.
- Gap: the distance between the rear axle of the first truck and the first axle of the following truck. If the gap exceeds the span length, then there is no multiple-presence on the bridge span.
- Light Volume: ADTT ≤ 1000
- Average Volume: 1000 < ADTT ≤ 2500
- Heavy Volume: 2500 < ADTT ≤ 5000
- Very Heavy Volume: ADTT > 5000

Trucks can occur on a bridge in many different arrangements. Five loading patterns are defined as follows:

- Single: Only one truck is present on the bridge in any lane.
- Following: Two trucks in the same lane, with varying headway distances, with a gap less than the span length.
- Side by Side: Two trucks in adjacent lanes with an overlap of more than one-half the truck length of the first truck.
- Staggered: Two trucks in adjacent lanes with an overlap of less than one-half the truck length of the first truck and a gap less than the span length (Figure 14).
- Multiple: Simultaneous presence of trucks in adjacent lanes and in same lane.

For each WIM site with refined time stamp data, the cumulative frequencies for side-by-side, staggered, and following events are obtained for headway separation from 0 ft to 300 ft in 20-ft increments. Report multiple-presence probabilities for each day for each site as a function of daily truck count and headway separations or gap. For each site, the daily truck count will vary by day of week and by season. The study needs to be repeated for multiple WIM sites in several states with varying ADTTs (including very high ADTT > 5000) and on routes with a variety of functional classes. With a large dataset of multiple-presence statistics as a function of ADTT and highway class, guidelines for appropriate multiple-presence values for systemwide use may be developed.

To calculate and report multiple-presence percentages, use the following procedure:

- For each site, each direction, lump all days with light volume (daily truck counts ≤ 1000) into one bin. Find the average MP for each gap increment.
- For each site, each direction, lump all days with Average volume (daily truck counts > 1000 but ≤ 2500) into one bin. Find the average multiple presence for each gap increment.
- For each site, each direction, lump all days with heavy volume (daily truck counts > 2500 but ≤ 5000) into one bin. Find the average multiple presence for each gap increment.
- For each site, each direction, lump all days with very heavy volume (daily truck counts > 5000) into one bin. Find the average multiple presence for each gap increment.

Tabulate and chart the variation of multiple presence as a function of gap and traffic volume (light, average, heavy, and very heavy).

Multiple-Presence Data from Published Literature (New Jersey WIM Sites). Multiple truck presence statistics based on actual truck load data from New Jersey highways is
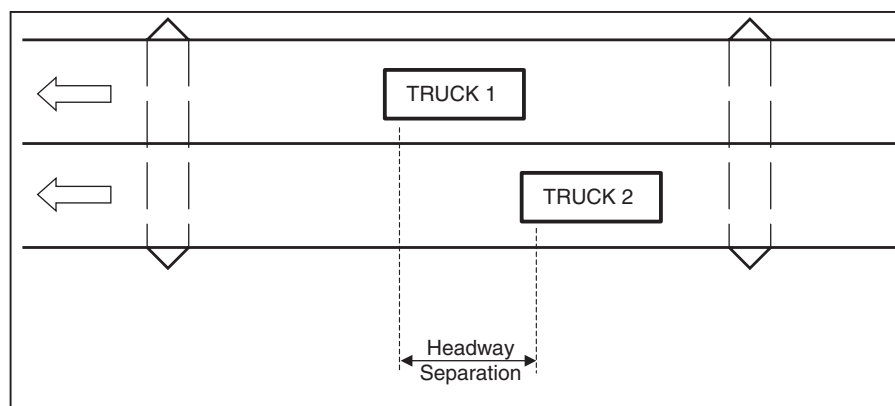
Figure 14. Staggered truck event with overlap less than one-half truck length.

available in the published literature (Gindy and Nassif 2006). The data consist of WIM measurements from various sites located throughout New Jersey and recorded over a 10-year period, between 1993 and 2003 (with some gaps). The database included 25 sites that are geographically dispersed across New Jersey and constitute a variety of functional classes including rural and urban principal and minor arterials. The sites represent a variety of site-specific conditions including truck volume, road and area type, and number of lanes. The study did not include heavy truck traffic sites with ADTT > 5000. Timestamps of truck arrivals to the hundredth of a second were recorded. Statistics for various truck loading cases including single, following, side by side, and staggered are presented (see Figure 15).

Multiple truck presence statistics depend on factors such as truck volume and bridge span length. The position of all trucks in the near vicinity were checked to determine whether multiple trucks simultaneously occur on the bridge The statistics shown in Table 12 for multiple truck occurrences were extracted from Figure 15 for various truck volumes and span lengths. Since the paper did not provide a tabulation of multiple-presence statistics, the values are close approximations scaled from the charts. Use a linear interpolation for other spans.

Multiple-Presence Data from Current Research (New York WIM Sites). By studying the occurrence of multiple trucks within a given headway separation at WIM sites with accurate time stamps, the effects of multiple trucks on a span can be simulated for WIM sites without accurate time stamps. Five WIM sites (10 directional sites) with free-flowing traffic in New York State were studied by the 12-76 research team to determine the maximum multiple-presence probabilities for various truck traffic volumes. The sites chosen were Route 12 eastbound and westbound (WIM Site 2680), a rural state route, I-84 eastbound and westbound (WIM Sites 8280 and 8382), a rural Interstate, I-81 northbound and southbound (WIM Site 9121), a rural Interstate, and Route 17 northbound and southbound (WIM Site 9631), a rural state route. Two WIM sites on urban interstates (I-95 and I-495) were studied, but not included in the results due to frequent traffic congestion, which precludes free-flowing traffic. Daily truck traffic volume was classified as light (less than 1,000 trucks per day), average (more than 1,000 trucks but less than 2,500 trucks per day), heavy (more than 2,500 trucks but less than 5,000 trucks per day), and very heavy (more than 5,000 trucks per day).

When considering multiple trucks on a given span, a multiple-presence event is said to have occurred if the gap
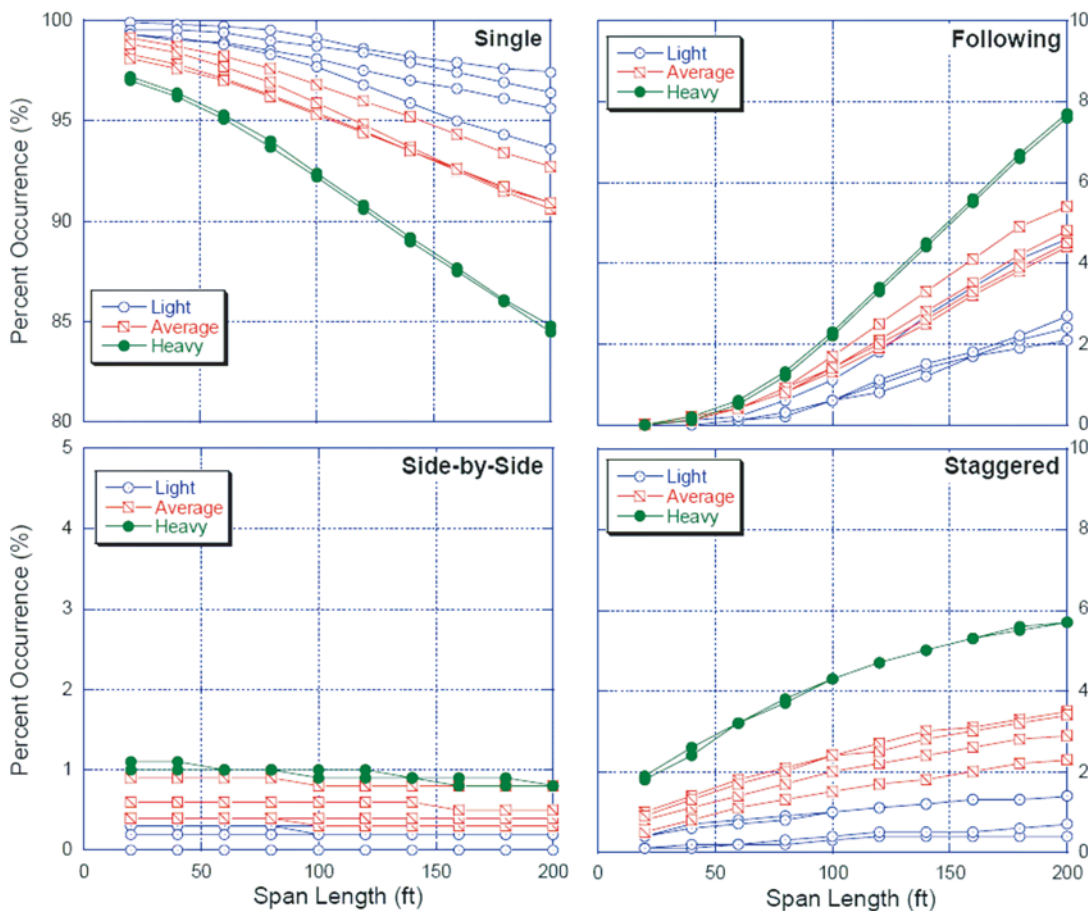
Figure 15. Variation of multiple-presence with span length—NJ WIM sites.

Table 12. Maximum observed multiple-presence probabilities as a function of ADTT and bridge span length—New Jersey sites.

	Maximum Side-by-Side Trucks Percent Probabilities			
	Site Truck Traffic			
Span	Light: ADTT ≤ 1000	Average: 1000 < ADTT ≤ 2500	Heavy: 2500 < ADTT ≤ 5000	Very Heavy ADTT > 5000
All Spans	0.30	0.90	1.00	
	Maximum Staggered Trucks Percent Probabilities			
	Site Truck Traffic			
Span	Light: ADTT ≤ 1000	Average: 1000 < ADTT ≤ 2500	Heavy: 2500 < ADTT ≤ 5000	Very Heavy ADTT > 5000
20	0.40	1.20	1.90	Not Available
40	0.60	1.60	2.30	Not Available
60	0.70	1.80	3.20	Not Available
80	0.80	2.00	3.80	Not Available
100	0.90	2.40	4.20	Not Available
120	1.00	2.60	4.60	Not Available
160	1.20	3.20	5.20	Not Available
200	1.40	3.60	5.90	Not Available
	Maximum Following Trucks Percent Probabilities			
	Site Truck Traffic			
Span	Light: ADTT ≤ 1000	Average: 1000 < ADTT ≤ 2500	Heavy: 2500 < ADTT ≤ 5000	Very Heavy ADTT > 5000
20	0.00	0.00	0.00	Not Available
40	0.00	0.00	0.10	Not Available
60	0.10	0.50	0.60	Not Available
80	0.60	1.00	1.20	Not Available
100	1.20	1.80	2.20	Not Available
120	1.80	2.40	3.40	Not Available
160	3.40	4.00	4.80	Not Available
200	4.40	5.40	7.80	Not Available

between two trucks (i.e., the distance between the last axle of the leading truck and the first axle of the trailing truck) is less than the span length. For instance, two trucks with a headway separation H ≤ 100 ft will be simultaneously on span of length = 100′ − truck length. Multiple-presence probabilities were compiled for two trucks in adjacent lanes side-by-side, two trucks in adjacent lanes staggered, and two trucks in the same lane. For the purpose of simulating a multiple-presence event, only the headway separation (i.e., the distance from the front axle of the lead truck to the front axle of the trailing truck) is important. Multiple-presence probabilities were compiled for headway separations up to 300 ft, in 20-ft increments (Table 13).

For each day that truck data were captured at a WIM site, the number of multiple-presence events that occurred in that day was recorded as a percentage of the total truck count for that day. The average multiple-presence percentage is then calculated for all days with light truck volume, average truck volume, heavy truck volume, and very heavy truck volume, respectively. Each direction of traffic was considered separately. The maximum multiple-presence percentages are summarized in Tables 13 and 14.

Multiple-presence data at New York WIM sites were calculated in NCHRP Project 12-76 using the same approach as the New Jersey statistics, to allow a direct comparison. The findings from the two states for side-by-side and staggered truck occurrences are quite comparable across most span lengths. The New Jersey values for following trucks are generally higher. The New York findings, defined in terms of headway separation intervals (Table 14), will be used in the interim to simulate multiple-presence events for sites where accurate time stamps are not available. This is achieved by categorizing the likelihood of trucks occupying various slots or headway intervals on the bridge either in the adjacent lane or in the same lane.

Step 7. Protocols for WIM Data Analysis for One-Lane Load Effects for Superstructure Design (Single Events and Following Events)

Step 7.1 Load Effects for Single Events for Superstructure Design

- Group data into bins by travel lane. Generate GVW relative and cumulative histograms for all trucks. Use 4-kip bins.
- Run the trucks (FHWA Class 6 and above—three or more axles) through moment and shear influence lines (or structural analysis program) for simple and two-span continuous

Table 13. Maximum observed multiple-presence cumulative probabilities as a function of headway separation and ADTT—NY sites.

Maximum Side-by-Side Truck Multiple Presence Cumulative Probabilities				
	Site Truck Traffic			
Headway H (ft)	Light: ADTT < 1k	Average: 1k < ADTT < 2.5k	Heavy: 2.5k < ADTT < 5k	Very Heavy: ADTT > 5k
H ≤ 20	0.19	0.41	0.61	0.00
H ≤ 40	0.33	0.84	1.27	0.00
H ≤ 60	0.54	1.25	1.95	0.00
H ≤ 80	0.80	1.60	2.57	0.00
H ≤ 100	1.00	2.13	3.33	0.00
H ≤ 120	1.21	2.54	4.14	0.00
H ≤ 140	1.45	2.88	4.80	0.00
H ≤ 160	1.62	3.18	5.41	0.00
H ≤ 180	1.80	3.47	5.97	0.00
H ≤ 200	1.99	3.73	6.49	0.00
H ≤ 220	2.09	3.97	6.97	0.00
H ≤ 240	2.23	4.21	7.42	0.00
H ≤ 260	2.35	4.43	7.85	0.00
H ≤ 280	2.49	4.64	8.26	0.00
H ≤ 300	2.60	4.84	8.66	0.00
Maximum Following Truck Multiple Presence Cumulative Probabilities				
	Site Truck Traffic			
Headway H (ft)	Light: ADTT < 1k	Average: 1k < ADTT < 2.5k	Heavy: 2.5k < ADTT < 5k	Very Heavy: ADTT > 5k
H ≤ 20	0.00	0.00	0.00	0.00
H ≤ 40	0.00	0.00	0.00	0.00
H ≤ 60	0.01	0.00	0.00	0.00
H ≤ 80	0.02	0.00	0.00	0.00
H ≤ 100	0.08	0.04	0.03	0.00
H ≤ 120	0.20	0.19	0.19	0.00
H ≤ 140	0.41	0.52	0.64	0.00
H ≤ 160	0.77	1.09	1.37	0.00
H ≤ 180	1.25	1.76	2.28	0.00
H ≤ 200	1.71	2.51	3.26	0.00
H ≤ 220	2.22	3.19	4.20	0.00
H ≤ 240	2.70	3.86	5.11	0.00
H ≤ 260	3.12	4.51	5.98	0.00
H ≤ 280	3.53	5.11	6.83	0.00
H ≤ 300	3.92	5.70	7.63	0.00

spans. Use span lengths of: 20 ft, 40 ft, 60 ft, 80 ft, 100 ft, 120 ft, 160 ft, and 200 ft.

- Normalize maximum moment and shear values by dividing by the corresponding load effects for HL93. Generate a database table of normalized load effects. Make sure that each record contains GVW, class, number of axles, date, arrival time, and travel lane, in addition to load effects. The date, GVW, and arrival time will serve as a truck record indicator.

Step 7.2 Following Truck Events for Superstructure Design When Accurate Truck Arrival Time Stamps are Available

Load effects for following trucks may be obtained directly from the WIM data where accurate time arrival stamps are collected together with truck weight data. The load effects analysis is performed with the following trucks in their proper relative positions.

Estimate the maximum daily load effects for two random following trucks crossing the bridge as follows:

- Combine the two trucks by superimposing the second truck on the first truck with the axles offset by the measured headway separation.
- Run the combined truck through moment and shear influence lines for simple and two-span continuous spans. Use span lengths of 20 ft, 40 ft, 60 ft, 80 ft, 100 ft, 120 ft, 160 ft, and 200 ft.
- Repeat the process for each following truck event.
- Normalize the results by dividing by the effects of HL93.

Step 7.3 Simulation of Following Truck Events When Accurate Truck Arrival Time Stamps are not Available

Load effects for following trucks may be obtained directly from the WIM data where accurate time arrival stamps are

Table 14. Maximum observed multiple-presence probabilities by headway interval as a function of ADTT—NY sites.

Maximum MP Probabilities based on 5 WIM sites (10 directional sites) in New York State				
Maximum Side-by-Side Truck Multiple Presence Probabilities				
	Site Truck Traffic			
Headway H (ft)	Light: ADTT ≤ 1k	Average: 1k < ADTT ≤ 2.5k	Heavy: 2.5k < ADTT ≤ 5k	Very Heavy: ADTT > 5k
H ≤ 20	0.19	0.41	0.61	0.00
20 < H ≤ 40	0.14	0.43	0.66	0.00
40 < H ≤ 60	0.21	0.41	0.68	0.00
60 < H ≤ 80	0.26	0.35	0.62	0.00
80 < H ≤ 100	0.20	0.53	0.76	0.00
100 < H ≤ 120	0.21	0.41	0.81	0.00
120 < H ≤ 140	0.24	0.34	0.66	0.00
140 < H ≤ 160	0.17	0.30	0.61	0.00
160 < H ≤ 180	0.18	0.29	0.56	0.00
180 < H ≤ 200	0.19	0.26	0.52	0.00
200 < H ≤ 220	0.10	0.24	0.48	0.00
220 < H ≤ 240	0.14	0.24	0.45	0.00
240 < H ≤ 260	0.12	0.22	0.43	0.00
260 < H ≤ 280	0.14	0.21	0.41	0.00
280 < H ≤ 300	0.11	0.20	0.40	0.00
Maximum Following Truck Multiple Presence Probabilities				
	Site Truck Traffic			
Headway H (ft)	Light: ADTT ≤ 1k	Average: 1k < ADTT ≤ 2.5k	Heavy: 2.5k < ADTT ≤ 5k	Very Heavy: ADTT > 5k
H ≤ 20	0.00	0.00	0.00	0.00
20 < H ≤ 40	0.00	0.00	0.00	0.00
40 < H ≤ 60	0.01	0.00	0.00	0.00
60 < H ≤ 80	0.01	0.00	0.00	0.00
80 < H ≤ 100	0.06	0.04	0.03	0.00
100 < H ≤ 120	0.12	0.15	0.16	0.00
120 < H ≤ 140	0.21	0.33	0.45	0.00
140 < H ≤ 160	0.36	0.57	0.73	0.00
160 < H ≤ 180	0.48	0.67	0.91	0.00
180 < H ≤ 200	0.46	0.75	0.98	0.00
200 < H ≤ 220	0.51	0.68	0.94	0.00
220 < H ≤ 240	0.48	0.67	0.91	0.00
240 < H ≤ 260	0.42	0.65	0.87	0.00
260 < H ≤ 280	0.41	0.60	0.85	0.00
280 < H ≤ 300	0.39	0.59	0.80	0.00

collected together with truck weight data. The load effects analysis is performed with the following trucks in their proper relative positions. Where accurate truck arrival time stamps are not available, generalized multiple-presence statistics obtained in Step 6 may be used to simulate following trucks in their likely relative positions as follow:

1. From Step 6, obtain the probabilities for following trucks in the same lane with varying headway separations (given in 20-ft increments) as a function of ADTT in each direction (see Table 14).
2. The number of expected multiple-presence (MP) events in each direction for each headway separation interval, H, can be determined from the following equation:

$$\text{Number of MP Events} = \text{MP Probability} \times \text{AADT}$$

3. Randomly select two trucks from the entire population of trucks in the desired direction. Being that there is no correlation between the truck population and travel lane, any two randomly selected trucks can be considered, regardless of lane, as long as the trucks are traveling in the desired direction.
4. Randomly select a headway separation within the desired headway separation interval.
5. With the randomly selected truck pair separated by the randomly selected headway separation, maximum load effects can be calculated in the same manner as for trucks with accurate time stamps and measured headway separation (Step 7.2).
6. Repeat Steps 3 through 5 for each headway separation interval and each direction of travel until the expected number of multiple-presence events has been generated for each headway separation and each direction of travel.

7. Normalize by dividing the results by the effects of HL93 loading.

Step 7.4 Group Load Effects into Strength I and Strength II (One Lane)

Overloaded trucks seen in the WIM data could be either illegal overloads or authorized permit loads. It should be noted that separating permits from non-permit overloads in the WIM data is only viable where accurate permit records are available. In most jurisdictions only the special permit or single-trip permit moves are tracked in terms of their actual load configurations and travel routes. These heavy loads populate the upper tails of the load spectra and it would be beneficial to know which vehicles are authorized and which are illegal. Separating routine permits may not be possible due to the lack of necessary permit records at the state level and the sheer volume of permits in operation in most states. This is not considered a necessary requirement for live-load modeling since routine permits can be taken as variations of the exclusion loads allowed under state law.

Legal loads, routine permits, and illegal overloads are grouped under Strength I. Heavy special permits are grouped under Strength II. For following events, if one of the trucks is a heavy special permit truck, group that loading event under Strength II.

Step 7.5 Assemble Single-Lane Load Effects Histograms for Strength I and Strength II

- Combine the normalized load responses of single truck events and following truck events into a single histogram for each load effect (M, V) and assemble in narrow bins of 0.02 increments for Strength I and Strength II. These combined histograms will represent the single-lane load effects from a single truck or multiple trucks in the same lane.
- These will constitute the single-lane measured load effects histograms without any filtering for WIM sensor errors (see Step 10).

Step 8. Protocols for WIM Data Analysis for Two-Lane Load Effects for Superstructure Design (Side by Side and Staggered Events)

Step 8.1 Truck Load Effects from Trucks in Adjacent Lanes Using Accurate Truck Arrival Time Stamps to the 1/100th of a Second

- Determine the number of truck multiple-presence (MP) events where trucks are in adjacent lanes in each direction for each day. During an MP event there could be more than one truck in a lane.

- For each MP event, obtain the headway separation between trucks in adjacent lanes and in the same lane using the WIM data.
- For estimating the maximum daily load effects for two random trucks simultaneously crossing the bridge, proceed as follows:
  1. Combine the two trucks by superimposing the second truck in the adjacent lane on the first truck with the axles offset by the headway separation.
  2. Run the combined truck through moment and shear influence lines for simple and two-span continuous spans. Use span lengths of 20 ft, 40 ft, 60 ft, 80 ft, 100 ft, 120 ft, 160 ft, and 200 ft.
  3. Keep track of the normalized M and V.
  4. For each MP event, repeat the process.

Step 8.2 Simulation of Load Effects of Trucks in Adjacent Lanes Using Generalized MP Statistics

1. From Step 6, obtain the probabilities for side-by-side/ staggered trucks in adjacent lanes with varying headway separations (given in 20-ft increments) as a function of ADTT in each direction (see Table 14).
2. The number of expected multiple-presence events in each direction for each headway separation interval, H, can be determined from the equation

Number of MP Events = MP Probability × AADT

3. Randomly select two trucks from the entire population of trucks in the desired direction. Since there is no correlation between the truck population and travel lane, any two randomly selected trucks can be considered, regardless of lane, as long as the trucks are traveling in the desired direction.
4. Randomly select a headway separation within the desired headway separation interval.
5. With the randomly selected truck pair separated by the randomly selected headway separation, maximum load effects can be calculated in the same manner as for trucks with accurate time stamps and measured headway separation (Step 8.1).
6. Repeat Steps 3 through 5 for each headway separation interval and each direction of travel until the expected number of MP events has been generated for each headway separation and each direction of travel.

Step 8.3 Group Load Effects into Strength I and Strength II (Two-Lane)

Overloaded trucks seen in the WIM data could be either illegal overloads or authorized permit loads. It should be noted

that separating permits from non-permit overloads in the WIM data is only viable where accurate permit records are available. In most jurisdictions only the special permit or single-trip permit moves are tracked in terms of their actual load configurations and travel routes. These heavy loads populate the upper tails of the load spectra and it would be beneficial to know which vehicles are authorized and which are illegal. Separating routine permits may not be possible due to the lack of necessary permit records at the state level and the sheer volume of permits in operation in most states. This is not considered a necessary requirement for live-load modeling since routine permits can be taken as variations of the exclusion loads allowed under state law.

Legal loads, routine permits, and illegal overloads are grouped under Strength I. Heavy special permits are grouped under Strength II. For MP events, if one of the trucks is a heavy special permit truck, group that loading event under Strength II.

Step 8.4 Assemble Two-Lane Load Effects Histograms for Strength I and Strength II

- Assemble normalized load effects frequency histograms for two-lane load effects for Strength I and Strength II in narrow bins of 0.02 increments.
- These will constitute the two-lane measured load effects histograms without any filtering for WIM sensor errors (see Step 10).

Step 9. Assemble Axle Load Histograms for Deck Design

Step 9.1 One-Lane Axle Loads for Deck Design

- Separate trucks into Strength I and Strength II groups.
- For each group, generate axle weight relative frequencies histograms for single, tandem, tridem, and quad axle types. Use a 2-kip interval for the bins. Axles spaced at less than 6 ft are to be considered as part of the same axle group.
- This will constitute the measured axle load histogram without any filtering for WIM sensor errors (see Step 10).
- Assuming normal distribution models for axle weight data for the filtered histogram, determine the mean and standard deviation for all axles, top 20% axles, top 5% axles. For each axle type, report the 99th percentile statistic W_{99}.

Step 9.2 Side-by-Side Axle Events for Two Lanes

Multiple-presence studies specifically for axles loads are performed for the two-lane loaded case. There will be a greater probability of side-by-side axle events than side-by-side truck events, because each truck has two or more axles. However, an axle with a headway separation greater than the effective strip width for the slab as defined in the LRFD specifications would not have an influence on the load effect of the axle in the adjacent lane and may be neglected, if using the strip method. With these key differences recognized, the process for MP computations for axle loads will follow an approach similar to that used for truck MP studies.

Determine the number of side-by-side axle events in each direction for the following combinations:

- Single–single,
- Single–tandem,
- Tandem–tandem, and
- Other.

Step 10. Filtering of WIM Sensor Errors/ WIM Scatter from Measured WIM Histograms

The live-load modeling protocols presented in this project rely on the weight histograms and the histograms of the corresponding load effects as collected from WIM stations at various highway sites. Current WIM systems are known to have certain levels of random measurement errors that may affect the accuracy of the load modeling results. This section proposes an approach to filter out WIM measurement errors from the collected WIM data histograms. To execute the filtering process, a calibration of the results of the WIM system should be made by comparing the results of the WIM system to those of a static scale. The calibration process should be repeated several times within the WIM data collection timeframe. The results of this calibration will be the basis for filtering out WIM measurement errors for each WIM data site.

Step 10.1 WIM System Calibration

Typical WIM calibration procedures consist of taking several WIM measurements from representative calibration trucks and comparing the WIM measurements to those obtained from a certified static scale. Traditionally, it has been common to use a single truck for the calibration process, although it would be advisable to use different trucks having different characteristics to ensure that the accuracy of the results remain consistent independent of the truck characteristics. For example, Table 15 gives a summary sheet of the calibration data assembled for the northbound lane of Site No. 7100 on I-87 in New York. The table shows the actual axle weight along with the weights estimated from the piezo-loop WIM system installed at the site. The WIM data were collected for 10 different crossings of the same calibration truck. The truck's speeds were approximately 40 mph. Table 16 shows the ratio of the WIM weight divided by the actual weight for each of the 5 axles for the 10 crossings. The average of the

44

Table 15. Typical WIM calibration results for NY State DOT installations.

	SITE: 7100				LOCATION: I87 Champlain Exit 42 Rt 11 (BIN 1009070) - Acc Rt 9									
	DATE: 5/25/2006													
				Lane: 1 Northbound										
	Sensor configuration Piezo-Loop_Piezo					Contract#/Sales Order								
		Drive			Trailer				60-ft					
	Steer	2nd Axle	3rd Axle	Total	4th Axle	5th Axle	Total	GVW	Moment	Axle 1-2	Axle 2-3	Axle 3-4	Axle 4-5	Length
Actual	12.61	16.10	15.85	31.95	20.28	18.75	39.03	83.58	275.37	12.83	4.50	37.25	4.13	58.71
Pass	1st Axle	2nd Axle	3rd Axle	Total	4th Axle	5th Axle	Total	GVW	Moment	Axle 1-2	Axle 2-3	Axle 3-4	Axle 4-5	Length
1	11.60	17.20	14.20	31.40	21.70	19.30	41.00	84.0	287.2	12.3	4.6	37.3	4.10	58.30
2	11.90	14.10	14.40	28.50	17.90	18.40	36.30	76.7	254.3	12.3	4.6	37.2	4.00	58.10
3	10.20	14.20	15.00	29.20	28.00	19.00	47.00	86.4	332.2	12.8	4.5	37.1	4.00	58.40
4	11.50	15.70	14.30	30.00	21.50	17.60	39.10	80.6	275.2	12.80	4.50	37.20	4.00	58.50
5	12.50	18.20	15.50	33.70	17.00	19.30	36.30	82.5	288.3	12.8	4.5	37.2	4.00	58.50
6	12.70	13.90	15.60	29.50	21.20	19.20	40.40	82.6	283.7	12.8	4.6	37.3	4.00	58.70
7	12.80	19.00	17.00	36.00	18.00	17.50	35.50	84.3	292.8	16.7	4.4	33.2	4.10	58.40
8	11.20	16.20	13.80	30.00	23.10	20.20	43.30	84.5	303.8	12.8	4.6	37.2	4.10	58.70
9	11.80	15.90	14.40	30.30	21.00	19.20	40.20	82.3	281.6	12.8	4.5	37.2	4.10	58.60

Table 16. WIM errors expressed as a ratio of measured values over actual values.

Pass	1st Axle	2nd Axle	3rd Axle	4th Axle	5th Axle	Moment on 60-ft span			
1	0.92	1.07	0.90	1.07	1.03	1.04			
2	0.94	0.88	0.91	0.88	0.98	0.92			
3	0.81	0.88	0.95	1.38	1.01	1.21			
4	0.91	0.98	0.90	1.06	0.94	1.00			
5	0.99	1.13	0.98	0.84	1.03	1.05			
6	1.01	0.86	0.98	1.05	1.02	1.03			
7	1.02	1.18	1.07	0.89	0.93	1.06			
8	0.89	1.01	0.87	1.14	1.08	1.10			
9	0.94	0.99	0.91	1.04	1.02	1.02			
10	0.97	0.86	0.97	0.96	0.97	0.96	**Overall**	**Axle**	**Moment**
Average	0.94	0.98	0.94	1.03	1.00	1.04	Average	0.97	1.04
Stdev	0.062	0.116	0.059	0.157	0.046	0.078	Stdev	0.100	0.078

ratios from all of the 50 measurements is 0.97 with a standard deviation of 10%. The plot of WIM error versus axle weight in Figure 16 demonstrates that the correlation between the bias value and the axle weight is practically negligible. There appears to be a difference in the standard deviations as the axle weights change. However, more data is needed to analyze this trend more accurately. Similarly, it is not clear why the readings for Axles 2 and 3 (or Axles 4 and 5), which respectively have somewhat similar weights, are leading to large differences in their standard deviations.

Axle weight histograms are needed for modeling the live loads for deck design, while the design of main bridge members requires the maximum bending moment and shear force effect. Thus, for main bridge members, it is more important to study the influence of WIM errors on the load effect rather than on the axle weights. Because main member load effects are influenced by the weight and spacing of several axles, some of the axle weight errors will cancel out and thus the overall error may have a lower standard deviation than that for individual axles. For example, for the calibration data of the same I-87 site studied above, the maximum moment effect of the calibration truck for a 60-ft simple span beam would be equal to 275.4 kip-ft, if the actual axle weights and axle spacings were used. The maximum moment effect for the values obtained from the eighth pass would be 303.8 kip-ft. The maximum moments from the 10 different passes are provided in Table 16 showing an overall average error ratio of 1.04 and a standard deviation of 7.8%. These are compared to an average error of 0.97 and a standard deviation of 10% for the axle weights. The information provided in Table 16 can be used to filter out the errors from the axle weight and moment effect histograms as described in the next section.
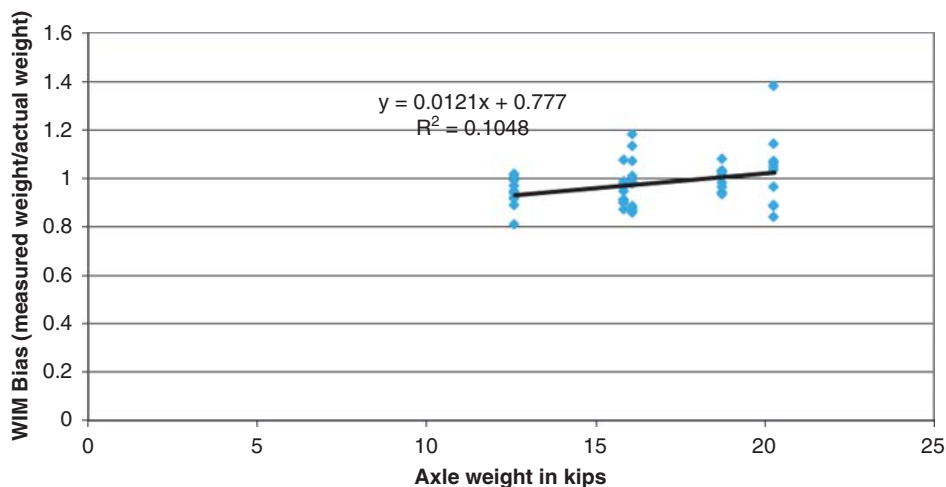
Figure 16. Plot of WIM error ratio versus axle weight for I-84 site.

The variation of the ratio with each truck crossing indicates that the measured axle weight to actual axle weight ratio is a random variable designated as ϵ with a mean value of 0.97 and a standard deviation of 10% for this particular site. Figure 17 shows a plot of the axle error ratio data on a normal probability plot. With only one exception, all of the data lies within the 95% confidence levels, indicating that the data can be reasonably well represented by a normal probability distribution function. This information will be required to execute the WIM error filtration as will be discussed in the next section. In the following, the research team assumed that these results are valid for all of the trucks collected at the WIM sites independent of truck type, vehicle speed, and time at which the WIM measurements were taken. A sensitivity analysis is performed in Appendix E to study how the standard deviation of the error would affect the results.

Step 10.2 WIM Error Filtration Procedure

Assume that the actual weight of an axle, or the actual moment effect of a truck, is denoted by x_r, while the measured value using the WIM system is x_m. Because of WIM system measurement errors, the difference between the measured value and the actual value can be represented by a calibration factor or an error ratio, ϵ. Because the error may depend on various random factors related to the WIM system's characteristics and truck/structure/WIM system dynamic interaction as well as some truck features including tire size and pressure, the calibration factor ϵ is a random variable that relates the measured WIM data results to the "true" weight through the following equation:

$$x_m = x_r \epsilon \tag{16}$$
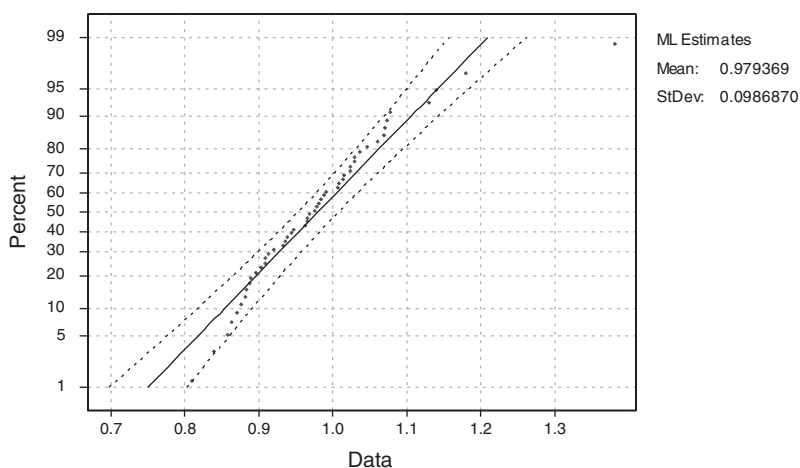
Figure 17. Plot of WIM axle error ratio on normal probability plot.

If the histogram and statistical information for ϵ are obtained from the calibration of the WIM system, these statistics can be used to filter out the errors in the measured raw WIM truck weight histogram collected at a given site. The goal then is to obtain the histogram of x_r given that the measured data give the histogram of x_m and given the statistics of ϵ using the following equation:

$$x_r = \frac{x_m}{\epsilon} \tag{17}$$

Since the error ϵ varies randomly, it will not be possible to obtain x_r for each particular truck. Instead, an algorithm can be developed to obtain a histogram for all of the actual truck weights given the histogram of the measured weights and the probability distribution of the error ratio ϵ.

The WIM data collected at a site will produce a histogram for x_m which can be related to the probability distribution function of x_m represented by $f_{xm}(\ldots)$.

Similarly, the calibration of the WIM system will provide information on the distribution function of ϵ represented by $f_\epsilon(\ldots)$. For example, the WIM calibration of I-84 NB Lane 4 indicates that the error of the WIM system axle weights can be modeled as a normal probability distribution with a probability function $f_\epsilon(\epsilon)$ with mean value $\overline{\epsilon} = 0.97$ and a standard deviation $\sigma_\epsilon = 0.10$.

Since x_r is the ratio of two random variables with known probability distribution functions, the probability distribution function of the actual weight x_r, $f_{xr}(\ldots)$ can be obtained using the following expression (Ang and Tang 2007):

$$f_{x_r}(z) = \int_{-\infty}^{\infty} |y| f_{x_m,\epsilon}(zy, y) dy \tag{18}$$

The analysis of the correlation of the error with the actual magnitude of the axle weight, as illustrated in Figure 16, has shown that they are practically independent (i.e., the percent error does not depend on the magnitude of the actual truck weight). It should be noted, however, that the number of readings is limited to those of a single truck. Actual statistics for ϵ should be obtained from runs of different trucks at normal highway speeds. If one assumes that the measured truck weight x_m and the error ϵ are also independent random variables, then Equation 18 can be expanded as

$$f_{x_r}(z) = \int_{-\infty}^{\infty} |y| f_{x_m}(zy) f_\epsilon(y) dy \tag{19}$$

Step 10.3 WIM Error Filtration Algorithm

The integration of Equation 19 can be executed numerically using a simple algorithm so that the integration is changed into a simple summation and the equation can be represented as

$$f_{x_r}(z) = \sum_{\text{all values of } \epsilon = y} |y| f_{x_m}(zy) f_\epsilon(y) \Delta y \tag{20}$$

Recalling that the probability distribution functions of ϵ, x_r, and x_m are related to the histograms by

$$H_\epsilon(y) = f_\epsilon(y)\Delta y$$
$$H_{x_r}(z) = f_{x_r}(z)\Delta z \tag{21}$$
$$H_{x_m}(zy) = f_{x_m}(zy)\Delta(zy)$$

where $\Delta(\ldots)$ is the bin size for each histogram. If the bin sizes for the histogram of the actual weight x_r and that of the measured weight x_m are taken to be the same, so that $\Delta z = \Delta(zy)$, then Equation 20 can be expressed as

$$f_{x_r}(z)\Delta(z) = \sum_{\text{all values of } \epsilon = y} |y| f_{x_m}(zy)\Delta(z) f_\epsilon(y)\Delta y \tag{22}$$

$$H_{x_r}(z) = \sum_{\text{all values of } \epsilon = y} |y| H_{x_m}(zy) f_\epsilon(y)\Delta y \tag{23}$$

Thus, given the histogram of the measured WIM data, x_m, and the probability distribution of the calibration factor, ϵ, the integration of Equation 19 for all possible values of $x_r = z$ can be executed numerically using software tools.

The protocols for calculating L_{max} should then be executed using the filtered histogram $H_{xr}(z)$.

Implementation of the above WIM Error Filtration Algorithm, based on New York calibration data, is given in Appendix E.

Step 11. Accumulated Fatigue Damage and Effective Gross Weight from WIM Data

WIM data can be used to study the stress range produced by individual trucks on a bridge component. Damage accumulation laws such as Miner's Rule can then be used to estimate the fatigue damage for the whole design period for the expected truck population at a site.

Obtain cumulative fatigue damage from the WIM population and compare to LRFD fatigue truck (Figure 18, 54-kip gross weight) moments for each span. Use span lengths of 20 ft, 40 ft, 60 ft, 80 ft, 100 ft, 120 ft, 160 ft, and 200 ft. Determine fatigue damage adjustment factor K, defined as

$$K \times M_{FT} = \left[\frac{\sum (M_i)^3}{\# \text{Trucks}} \right]^{1/3} \tag{24}$$

$M_{FT} =$ Moment from LRFD fatigue truck, includes 0.75 load factor;
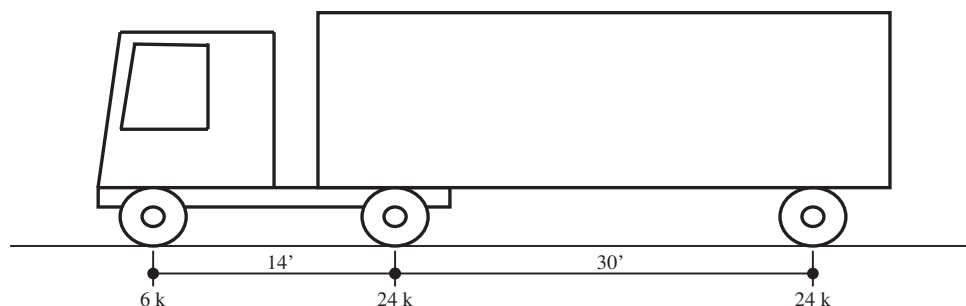
Figure 18. LRFD design fatigue truck (54 kips).

K = Fatigue damage adjustment factor;
M_i = Moment range of trucks measured; and
Trucks = Total number of trucks measured.

Obtain K for each span. For varying spans, determine the effective gross weight for trucks measured at the site using the following equation:

$$W_{eq} = \left(\sum f_i W_i^3\right)^{1/3} \qquad (25)$$

where:

f_i is the fraction of gross weights within interval i and
W_i is the mid-width of interval i.

In this calculation, use trucks only with three or more axles (Class 6 and above).

Step 12. Lifetime Maximum Load Effect L_{max} for Superstructure Design (Strength I)

Step 12.1 Methods for Estimating L_{max}

To check the calibration of load models and/or load factors for a specification, it is necessary to estimate the mean maximum loading or load effect L_{max}. If further calibration of the specification is to be carried out, the corresponding COV also should be found. The estimation of the maximum load effect L_{max} expected over a 75-year bridge design period can be executed through a variety of methods. Simplified analytical methods or simulations may be used to estimate the maximum loading over a longer period, from short-term WIM data. This has to be done from a limited set of data that is collected for truck weights and truck configurations as well as truck traffic headways over relatively short periods of time. These methods can be categorized as

- Convolution or numerical integrations,
- Monte Carlo simulations, and
- Simplified statistical projections.

The models require as input the WIM data collected at a site after being scrubbed for data quality and filtered for WIM errors as described in the previous steps. The design of bridges requires the estimation of the maximum load effect over periods of 75 years. The convolution method uses numerical integrations of the collected WIM data histograms to obtain projections of the expected maximum load effect within a given return period (e.g., 75 years). The WIM data collected cannot reasonably be accurate enough in the tail of the distributions to obtain good estimates of the parameters for such extended return periods. Hence, the only possible means to obtain the parameters of the distributions of the 75-year maximum load effect is by using statistical projections. The probability distribution of the maximum value of a random variable will asymptotically approach an extreme value distribution as the number of repetitions increases. Generally, a Gumbel fit can be executed on the tail of the short-term maximums for statistical projections.

An alternative to the convolution approach consists of using a Monte Carlo simulation to obtain the maximum load effect. The Monte Carlo simulation uses random sampling from the collected data to obtain the maximum load effect. A Monte Carlo simulation requires the performance of an analysis a large number of times and then assembling the results of the analysis into a histogram that will describe the scatter in the final results. Each iteration is often referred to as a cycle. The process can be executed for the single-lane loading situation or the side-by-side loading. The Monte Carlo simulation may be performed to find L_{max} in one of following two ways:

- Use the empirical histogram to find L_{max} by simulation for a short period and then project for a longer period (use an extreme value distribution such as Gumbel distribution). As mentioned earlier, the probability distribution of the maximum value of a normal random variable will asymptotically approach the Gumbel distribution.
- Alternatively, use a smoothed tail end of the WIM histogram by fitting the tail with a known probability distribution

48

function (such as the normal distribution) and use that fitted distribution with the Monte Carlo simulation. This will require a very large number of repetitions.

It should be emphasized however, that the Monte Carlo simulation would be very inefficient for projections over long return periods when the number of repetitions is very high. (Algorithms such as Markov Chain Monte Carlo modeling may allow improved performance in such cases.) Furthermore, one should make sure not to exceed the random number of generation limits of the software used, otherwise the generated numbers will not be independent and the final results will be erroneous.

Simplified statistical projections for estimating the maximum load effect in a given return period can be developed based on the assumption that the tail end of the moment load effect for the original population of trucks as assembled from the WIM data approaches a normal distribution. The method uses the properties of the extreme value distribution. Equations in closed form provide such a projection, requiring much less effort than the convolution approach. The estimation of the maximum load effect for two side-by-side trucks improves as the return period increases. This is again due to the asymptotic nature of the solution, which yields good results only as the number of load repetitions increases and as the sampling is made from the tail end of the raw WIM histogram.

Step 12.2 Procedure for Calculating L_{max} from WIM Data Using an Extreme Value Distribution for the Upper Tail

There are several possible methods available to calculate the maximum load effect for a bridge design period from truck WIM data. The one implemented in these protocols is found to be one of the easiest methods that provide results comparable to many other methods including Monte Carlo simulations. This method is based on the assumption that the tail end of the histogram of the maximum load effect over a given return period approaches a Gumbel distribution as the return period increases. The method assumes that the WIM data are assembled over a sufficiently long period of time to ensure that the data are representative of the tail end of the truck weight histograms and to factor in seasonal variations and other fluctuations in the traffic pattern. The use of WIM data for a whole year will satisfy this requirement. In a separate analysis, this study will investigate how the confidence intervals in the projection results are affected by the number of samples collected and the number of days for which the WIM data are available, especially when only limited data are available at a site.

Sensitivity analyses have shown that the most important parameters for load modeling are those that describe the shape of the tail end of the truck load-effects histogram. Current WIM technology has certain levels of random measurement errors that may affect the accuracy of the load modeling results. To bring uniformity in the load modeling process, a standardized approach to executing the error filtering procedure that utilizes calibration statistics for the WIM scale is described in Step 10. This procedure should be executed on the raw data prior to calculating L_{max}.

Step 12.2.1 Protocols for Calculating Maximum Load Effect L_{max}

The process begins by assembling the WIM truck weight data and load effects for single-lane events and two-lane events and filtering the data for WIM sensor errors.

- Assemble the measured load effects histograms (moment effect or shear force effect) in narrow bins of 0.02 increments.
- Execute a statistical algorithm to filter out WIM scatter/sensor errors from the load effects histograms as described in Step 10.
- Find the cumulative distribution function $F_x(x) =$ cumulative distribution function value for each event x sample by dividing the number of samples in a bin by the total number of samples and adding the value to the value in the previous bin.
- Calculate the standard deviate of the cumulative function for each bin. In MS Excel, this can be achieved by taking NORMSINV(F(x)).
- Take the upper 5% of the values and plot the normal deviate versus X.
- Take the trend line and find the slope, m, and the intercept, n, of the regression line.
- Find the mean of normal that best fits the tail end of the distribution as $\mu_{event} = -n/m$.
- Find the standard deviation of the best fit normal distribution to be $\sigma_{event} = (1-n)/m - \mu_{event}$.
- Take the number of events per day, n_{day}.
- Find, N, the total number of events for the return period of interest. For 75 years, take $N = n_{day} * 365 * 75$.
- The most probable value, u, for the Gumbel distribution that models the maximum value in 75 years L_{max} is given as

$$u_N = \mu_{event} + \sigma_{event} \times \left[\sqrt{2\ln(N)} - \frac{\ln(\ln(N)) + \ln(4\pi)}{2\sqrt{2\ln(N)}} \right] \quad (26)$$

- The dispersion coefficient for the Gumbel distribution that models the maximum load effect L_{max} is given as

$$\alpha_N = \frac{\sqrt{2\ln(N)}}{\sigma_{event}} \quad (27)$$

- The mean value of L_{max} is given as

$$L_{max} = \mu_{max} = u + \frac{0.577216}{\alpha_N} \qquad (28)$$

- Calculate the standard deviation of the Gumbel distribution that best models the maximum daily effect as

$$\sigma_{max} = \frac{\pi}{\sqrt{6}\alpha_N} \qquad (29)$$

Step 12.3 Alternate Method for Calculating Maximum Load Effect L_{max} Using Monte Carlo Simulation

An alternative to the statistical projections approach described in Step 12.2 consists of using a Monte Carlo simulation to obtain the maximum load effect. If there are not enough multiple events recorded in the WIM data, one could utilize simulations to generate MP events that conform to the measured statistical MP probabilities. In this approach, results of WIM data observed over a short period can be used as a basis for projections over longer periods of time. It should be noted that the Monte Carlo method for single-lane events will not be able to give L_{max} for 75 years directly. At best, a 1-week or a 1-month maximum single event could be obtained from a year's worth of WIM data because the Monte Carlo simulation will not go beyond the maximum value measured at the site. A statistical projection technique must then be executed to extend the single event results to 75 years. Alternatively, one can use the fitted normal distribution to represent the tail end of the histogram rather than use the raw data histogram and then the projection is automatically performed by the simulation. The same is not true for the two-lane loading cases because the Monte Carlo procedure will simulate more samples of side-by-side events based on the observed MP probabilities.

A Monte Carlo simulation requires the performance of an analysis a large number of times and then assembling the results of the analysis into a histogram that will describe the scatter in the final results. The process can be executed for the single-lane loading situation or the side-by-side loading. Figure 19 gives a schematic representation of the Monte Carlo simulation, which follows the procedure described in the following steps:

1. Assemble the data representing the filtered load effects for the trucks in the drive lane into a histogram labeled Bin I.
2. Assemble the data representing the filtered load effects for the trucks in the passing lane into a histogram labeled Bin II.
3. Assemble the corresponding cumulative frequency curves for the two histograms.
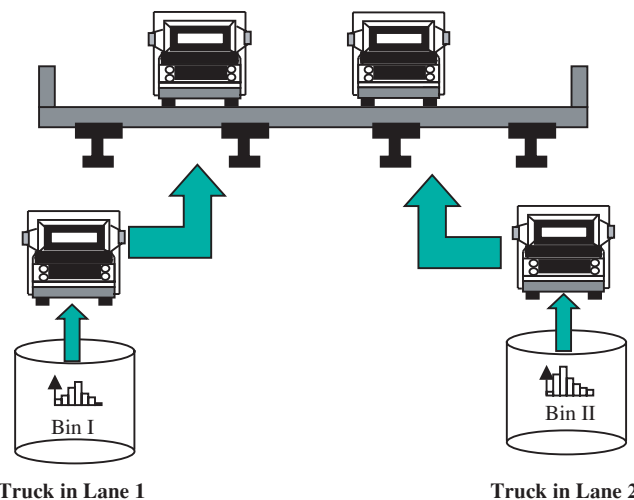
Figure 19. Schematic illustration of Monte Carlo simulation procedure.

4. Determine a main return period, t_{return}, for which the expected maximum moment is desired. For example, a 1-week, 1-month, 2-year, or 75-year period may be selected. However, as noted earlier, it is unlikely that the sample size of the available WIM data will be sufficiently large to obtain results for the large return periods. Hence, it is expected that the process will be applicable for only short periods (e.g., a 1-week or 1-month period), the results of which can then be projected for longer periods using the extreme value projection. Alternatively, one can use the fitted normal distribution to represent the tail end of the histogram rather than use the raw data histogram and then the projection is automatically performed by the simulation.
5. Use a uniform distribution random generator to produce a pseudo random number varying between 0 and 1. Such random generator routines are provided in all general-purpose computer software and programming tools (such as Excel, MATLAB).
6. The pseudo-random number of Step 5 will serve to select a single value from Bin I representing the load effect of a truck arriving in the drive lane. The selection of the moment effect is executed by assuming that the pseudo-random number generated (call it ran_{1i}) represents the cumulative frequency of the moment for this truck. Thus, to find the value of the moment, X_{1i}, the cumulative distribution function needs to be inverted so that $X_{1i} = F_{x1}^{-1}(ran_{1i})$ where $F_{x1}^{-1}(\ldots)$ is the inverse of the cumulative function for the effect of the trucks in the drive lane (Figure 20).
7. For estimating the maximum load effect for the trucks crossing the bridge in the drive lane, follow Sub-Steps A through E, otherwise skip this step and go to Step 8.
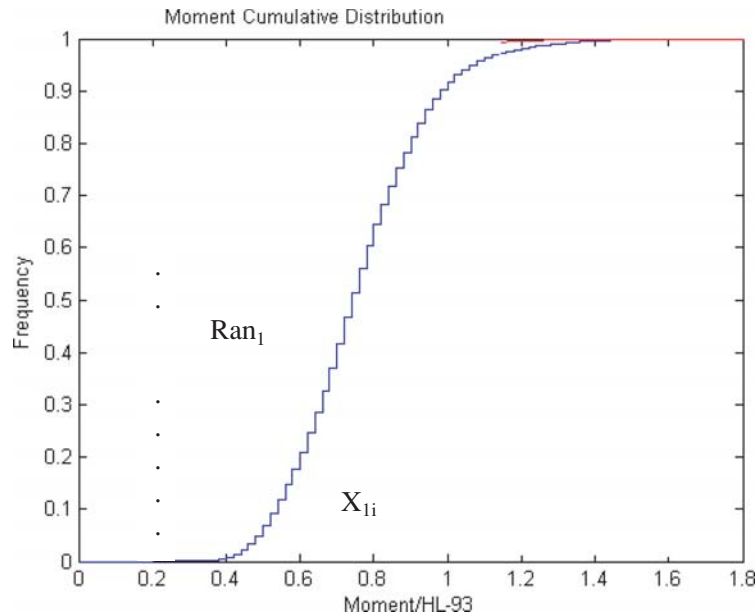
Figure 20. Schematic illustration of the random generation of a sample X_{1i}.

A. Find the number of loading events in the drive lane, K_1, corresponding to the pre-selected return period t_{return}.

B. Repeat Steps 5 through 6 K_1 times to generate K_1 samples for the moments in the drive lane in the period t_{return}.

C. Compare the K_1 values and choose the largest one of these. This will give you one estimate of the maximum expected value in t_{return}, which is designated as $X_{1mx\,K1}$.

D. Repeat Sub-Steps A through C for several cycles to generate several estimates of the maximum value $X_{1mx\,K1}$.

E. Assemble the values collected in Step D in a histogram. Also, find their average value and standard deviations.

8. For estimating the maximum response for two side-by-side trucks, do the following:

- Repeat Sub-Steps 5 and 6 by generating a pseudo number ran$_{2i}$, which represents the cumulative frequency of the moment for trucks in the passing lane. Find the value of the moment, X_{2i}, by inverting the cumulative frequency, $F_{x2}(...)$, for the load effects of the truck in the passing lane so that $X_{2i} = F_{x2}^{-1}(ran_{2i})$.

- Assuming that the maximum effect of the truck in the drive lane occurs at the same time as the maximum effect of the truck in the passing lane, add the moment effects of these two trucks to produce the moment effect of a single side-by-side event $X_{si} = X_{1i} + X_{2i}$.

- Repeat the process K_s times where K_s = number of side-by-side events expected in the basic return period t_{return}.

- Compare all the K_s moment effects $X_{s1} \ldots X_{sKs}$ and take the maximum value out of these K_s values. This will produce a single estimate of the maximum response corresponding to the basic return $X_{s\,max\,Ks}$.

- Repeat the whole simulation process m cycles to get m estimates of $X_{s\,max\,Ks}$.

- Obtain the histogram of the m estimates of $X_{s\,max\,Ks}$ and calculate the average value and standard deviation.

Step 13. Develop and Calibrate Vehicular Load Models for Bridge Design

Step 13.1 Superstructure Design Live-Load Calibration (Strength I)

There are two calibration methods, as follows, that can be applied to calibrate a new live-load model based on recent changes in truck weights:

- Method I: The first approach, which is relatively simple, is to focus on the mean or expected maximum live-load variable, L_{max}. That is, assume that the present LRFD calibration and safety indices are adequate for the strength and load data then available, but update the load model or the load factor for current traffic conditions in a manner consistent with the LRFD calibration approach. One key assumption in this regard is that the site-to-site variability in L_{max} as measured by the COV (COV = STDEV/Mean) is the same as that used during the AASHTO LRFD calibration. In the AASHTO LRFD calibration, the overall live-load COV was taken as 20%.

- Method II: If the variability in the WIM data is much greater than that assumed in the calibration, then the entire LRFD

calibration to achieve the target 3.5 reliability index may no longer be valid for that state and a simple adjustment of the live-load factor as given above should not be done. The second approach, which is more robust, is to perform a reliability analysis using the new statistical data for live loads and determine the live-load factors needed to achieve the same reliability target adopted in the LRFD calibration.

Method I: Simplified Adjustment of Strength I Live-Load Factor

The process adjusts the loading model and/or the corresponding live-load factor by the following ratio:

$$r_1 = \frac{L_{max} \text{ from WIM data projections for one-lane}}{L_{max} \text{ used in existing LRFD calibration for one-lane}} \tag{30}$$

$$r_2 = \frac{L_{max} \text{ from WIM data projections for two-lanes}}{L_{max} \text{ used in existing LRFD calibration for two-lanes}} \tag{31}$$

An increase in maximum expected live load based on current WIM data can be compensated in design by raising the live-load factor in a corresponding manner. The basic steps are summarized as follows:

A. Obtain quality WIM data from a variety of jurisdictions and traffic conditions and compute the expected lifetime maximum load, L_{max}, for each data set for one-lane and two-lane loadings.
B. Compare L_{max} for a suite of bridges to this expected 75-year maximum load for a similar suite of bridges given by *NCHRP Report 368* (Nowak 1999).
C. Compute the average ratio, r (L_{max} WIM data, divided by L_{max} Ontario data) for one lane and for two lanes. Compute also the corresponding COV for all sites examined.
D. Adjust the design requirements by modifying the live-load factor by the average ratio, r, as given above. If r is relatively

uniform over the suite of bridges used to fix L_{max} then the HL93 model can be maintained without adjustment. It is relatively easy to modify the live-load factor γ_L but this cannot be done unless it applies to every span.

L_{max} Used in Existing LRFD Calibration

NCHRP Report 368 (Nowak 1999) provides mean maximum moments and shears for various periods of time from 1 day to 75 years for simple span moments, shears, and negative moments for continuous spans. Span lengths range from 10 ft to 200 ft (Table 17). Continuous spans are composed of two equal spans. Continuous span positive moments and shears at the center pier have not been provided in the report. The maximum one-lane load effect is caused either by a single truck or two or more trucks (with the weight smaller than that of the single truck) following behind each other. There was little data to verify statistical parameters for multiple presence. The maximum values of moments and shears were calculated by simulations. For two-lane moments and shears, simulations indicated that the load case with two fully correlated side-by-side trucks will govern, with each truck equal to the maximum 2-month truck. The ratio of the mean maximum 75-year moment (or shear) and a mean 2-month moment (or shear) is about 0.85 for all spans.

Based on the above simple method, an increase in the maximum expected 75-year live-load as estimated from current WIM data can be accounted for in the design equation by raising the live-load factor in proportion to the ratio of the estimated live-load projection from WIM data to the value used during the calibration of the AASHTO LRFD specifications.

Method II: Reliability Analysis and Adjustment of Strength I Live-Load Factor

The simplified approach in Method I focuses on the maximum live-load variable, L_{max}, assuming that the overall LRFD calibration, multiple-presence factors, and target reliability indices are adequate. Hence, the approach only updates the load

Table 17. L_{max} used in existing LRFD calibration.

Span (Ft)	75-Year Lmax					
	Simple Span Moment		Simple Span Shear		Negative moment	
	One-Lane	Two-Lane	One-Lane	Two-Lane	One-Lane	Two-Lane
20	1.30	2.12	1.23	2.12	1.27	2.28
40	1.35	2.34	1.23	2.18	1.30	2.40
60	1.32	2.30	1.23	2.22	1.25	2.30
80	1.32	2.28	1.27	2.26	1.21	2.24
100	1.31	2.26	1.28	2.28	1.20	2.22
120	1.29	2.24	1.22	2.20	1.20	2.22
160	1.24	2.18	1.20	2.14	1.20	2.22
200	1.23	2.16	1.17	2.08	1.20	2.22

52

factors to better represent current truck traffic conditions. One key assumption in this regard is that the site-to-site variability in L_{max} as measured by the COV (COV = STDEV/Mean) is the same as that used during the AASHTO LRFD calibration. In the AASHTO LRFD calibration, the overall live-load COV was taken as 20%. This 20% includes site-to-site variability, uncertainties in estimating the load distribution factors, uncertainties in estimating the dynamic allowance factor, and uncertainties in estimating L_{max} due to the randomness of the parameter and the limitations in the data.

When implementing the draft protocols using recent WIM data in Task 8 from various states, it became evident that this procedure, although simple to understand and use, had certain limitations when applied to statewide WIM data. Using a single maximum or characteristic value for L_{max} for a state would be acceptable if the scatter or variability in L_{max} from site to site for the state was equal to (or less than, to be conservative) the COV assumed in the LRFD calibration. If the variability in the WIM data is much greater than that assumed in the calibration, then the entire LRFD calibration to achieve the target 3.5 reliability index may no longer be valid for that state and a simple adjustment of the live-load factor as given above should not be done. The site-to-site scatter in the L_{max} values obtained from recent WIM data showed significant variability from span to span, state to state, and between one-lane and two-lane load effects as given in Table 18 for a sample set of states. For example, the data from Florida show a COV for the moments of simple span bridges under one-lane loadings that varies from 32.5% for the 20-ft simple spans to 22.3% for the 200-ft simple spans. These COVs for site to site must be augmented by the COVs for the other variables that control the maximum load including within site variability,

the effect of the dynamic allowance factor, load distribution factor, and WIM data sample size, leading to much higher overall COV for the live load than the 20% used during the AASHTO LRFD calibration. For the same maximum moment of simple span bridges under one-lane loading, the site-to-site variability for the data collected in California shows a COV that ranges between 19.3% for the 20-ft simple span bridges down to 5.9% for the 200-ft simple span bridges.

Overall, the results of Table 18 indicate that the Florida sites evidenced the highest variability in L_{max}, whereas California data was a lot more uniform. As shown by the data in Table 18, the site-to-site COV statistics alone for FL are greater than the overall live-load COV used in the LRFD calibration. On the other hand, the site-to-site COV statistics for California are lower. It should also be noted that the one-lane COVs for Florida are higher than the two-lane COV, whereas in California the two-lane event has a higher site-to-site variability.

The maximum L_{max} values, site-to-site variability in L_{max}, as well as the variability in one-lane vs. two-lane events are influenced by several factors that appear to be state specific. These factors include

1. The presence of exclusion vehicles that are state legal loads—these heavy hauling vehicles usually operate mostly on state truck routes. There is likely to be a greater variation in truck weights on different routes in states with exclusion vehicles such as Florida. These heavy exclusion vehicles (and routine permits) may also be resulting in high L_{max} values for the one-lane loaded case. It should be noted that all trucks with six or fewer axles were grouped in the Strength I calibration. This group included legal loads, exclusion loads, and illegal overloads as well as routine permits.

Table 18. Site-to-site variability in L_{max} measured by coefficient of variation (COV).

State		Event Type	SPAN (ft)							
			20	40	60	80	100	120	160	200
	M-simple	1-Lane								
FL		COV	0.325	0.307	0.278	0.276	0.270	0.260	0.238	0.223
IN		COV	0.185	0.137	0.122	0.135	0.147	0.142	0.122	0.132
CA		COV	0.193	0.104	0.045	0.054	0.061	0.062	0.058	0.059
	M-simple	2-Lane								
FL		COV	0.201	0.187	0.213	0.213	0.207	0.207	0.206	0.212
IN		COV	0.150	0.139	0.132	0.125	0.116	0.113	0.116	0.119
CA		COV	0.112	0.125	0.136	0.146	0.133	0.126	0.121	0.113
	V-simple	1-Lane								
FL		COV	0.340	0.299	0.289	0.279	0.248	0.241	0.224	0.214
IN		COV	0.188	0.129	0.108	0.113	0.105	0.103	0.115	0.131
CA		COV	0.143	0.087	0.056	0.047	0.049	0.049	0.058	0.056
	V-simple	2-Lane								
FL		COV	0.203	0.204	0.205	0.183	0.174	0.175	0.180	0.189
IN		COV	0.140	0.119	0.122	0.133	0.134	0.136	0.135	0.140
CA		COV	0.109	0.127	0.137	0.120	0.113	0.112	0.107	0.109

2. The load limit enforcement environment in a state will have an influence on the level of illegal overloading. For instance, California is known to have an effective truck weight monitoring (and enforcement) operation that effectively utilizes the network of WIM systems throughout the state.
3. Site-to-site variability in truck weight data is also impacted by the quality and reliability of WIM data collected at the remote WIM sites. WIM data quality is highly dependent on the WIM quality assurance programs implemented by the state DOTs. Quality assurance programs must regularly check data for quality and require system repair or recalibration when suspect data is identified. Weighing accuracy is also sensitive to roadway conditions. Less variability in traffic data is expected when all WIM systems are maintained to the same standard of performance and data accuracy.

To incorporate the site-to-site statistical variations in WIM data collected in a given state, a reliability-based approach to adjusting the live-load factors is proposed as described in this report.

Reliability-Based Adjustment of Live-Load Factors

AASHTO LRFD Background. The calculation of the L_{max} values is meant for use to adjust the live-load factors in the LRFD design check equations. Since L_{max} is a random variable with high levels of uncertainties including site-to-site variability, the most appropriate procedure for adjusting the live-load factor is by applying the principles of structural reliability. A reliability-based procedure for adjusting the live-load factors would explicitly account for the variations in the L_{max} values as well as the other variables that control the loading of a bridge member and its capacity to resist the applied loads.

The variability in the L_{max} values is due to the random nature of L_{max} including the projection to the 75-year design life, the limitation in the data sample size collected within each site, and site-to-site variability. For developing a new design code, the L_{max} values for a wide range of nationally representative sites should be used as input. For adjusting the live-load factors to reflect state-specific truck weights and truck traffic patterns, L_{max} values obtained from a representative sample of sites within the state should be used. This section illustrates how the reliability-based adjustment of the live-load factor can be executed given a set of L_{max} values obtained from WIM data.

The LRFD design equation takes the form

$$\phi R_n \geq \gamma_{DW} D_W + \gamma_{DC} D_C + \gamma_L L_n \tag{32}$$

Where ϕ and γ are the resistance and load factors, R_n is the nominal resistance, D_W is the dead load effect for wearing surface, D_C is the dead load effect for the components and attachments and L_n is the live-load effect of the HL93 load including dynamic allowance and load distribution factor. According to the LRFD specifications $\phi = 1.0$ for the bending moment capacities of steel and prestressed concrete members, $\gamma_{DW} = 1.50$, $\gamma_{DC} = 1.25$. The current live-load factor is given as $\gamma_L = 1.75$. The dynamic allowance factor is 1.33 times the truck moment effect and the load distribution factor is calculated as a function of span length and beam spacing for different numbers of loaded lanes. If the WIM data in a particular state show large differences from the standard generic data used during the calibration of the AASHTO LRFD equations, it may be necessary to adjust the LRFD live-load factor to maintain the same safety levels. The adjustment requires the modeling of the live-load effects and the other random variables that control the safety of bridge members.

Modeling of Live-Load Effect on a Single Beam. For bending of typical prestressed concrete and steel girder bridges loaded by one lane of traffic, the load distribution factor equation is given as (AASHTO 2007) follows:

$$D.F. = 0.06 + \left(\frac{S}{14}\right)^{0.4} \left(\frac{S}{L}\right)^{0.3} \left(\frac{K_g}{12Lt_s^3}\right)^{0.1} \tag{33}$$

Where S is the beam spacing, L is the span length, t_s is the deck thickness, and K_g is a beam stiffness parameter. Note that Equation 33 already includes a multiple-presence factor m = 1.2, which accounts for the higher probability of having one heavy truck in one lane as compared to the probability of having two side-by-side heavy trucks in two adjacent lanes.

For two lanes loaded, the load distribution factor equation for bending becomes (AASHTO 2007)

$$D.F. = 0.075 + \left(\frac{S}{9.5}\right)^{0.6} \left(\frac{S}{L}\right)^{0.2} \left(\frac{K_g}{12Lt_s^3}\right)^{0.1} \tag{34}$$

Observing that the L_{max} values are for the normalized total static load effects on a bridge and observing that the D.F. of Equation 33 for a single lane already includes a multiple-presence factor m = 1.2, the final mean value for maximum load effect on a single beam can be calculated for one lane and two lanes loaded as follows:

For one lane

$$\overline{LL} = L_{max\,beam} = L_{max} \times HL_{93} \times IM \times D.F./1.2$$

For two lanes

$$\overline{LL} = L_{max\,beam} = L_{max} \times HL_{93} \times IM \times D.F./2 \tag{35}$$

Dividing D.F. of one lane by 1.2 is done to remove the multiple-presence factor, while dividing the D.F. of two lanes by 2 is done to account for the fact that the L_{max} values for two lanes calculated in this report are normalized by dividing by the effect of one lane of HL93 loading.

The COV of the maximum beam live-load effect should account for the site-to-site variability represented by $V_{site-to-site}$, the variability within a site represented by $V_{projection}$, the uncertainty associated with the limited WIM data sample size represented by V_{data}, the variability in the dynamic amplification factor, V_{IM} and the variability in the load distribution factor V_{DF}. The final COV for the applied live-load effect on a single beam can be obtained from

$$V_{LL} = \sqrt{V_{site-to-site}^2 + V_{projection}^2 + V_{data}^2 + V_{IM}^2 + V_{DF}^2} \qquad (36)$$

$V_{site-to-site}$ is obtained by comparing the L_{max} values from different WIM sites within the state. An analysis of the results of L_{max} projections shows that the uncertainties within a site are associated with a COV on the order of $V_{projection} = 3.5\%$ for the projection of the one-lane maximum effect and a COV of $V_{projection} = 5\%$ for the two side-by-side trucks' load effect. Additional uncertainties are associated with L_{max} due to the limited number of data points used in the projections and the confidence levels associated with the number of sample points. Using the +/−95% confidence limits, it is estimated that the COV associated with the use of 1 year's worth of WIM data is on the order of $V_{data} = 2\%$ for the one-lane case and about $V_{data} = 3\%$ for the two-lane case. Nowak (1999) also observed that the dynamic amplification factors augmented the L_{max} load effect by an average of 13% for one lane of traffic and by 9% for side-by-side trucks. The dynamic amplification also resulted in a COV of $V_{IM} = 9\%$ on the one-lane load effect and $V_{IM} = 5.5\%$ on the two-lane effect. In previous studies on live-load modeling, Ghosn and Moses (1985) included the uncertainties in estimating the lane distribution factor, which was associated with a COV equal to $V_{DF} = 8\%$ based on field measurements on typical steel and prestressed concrete bridges.

Modeling of Other Random Variables. In addition to the live loads, the random variables that control the safety of a bridge member include the actual resistance and the applied dead loads. Nowak (1999) provided models to represent the mean values and the COVs or standard deviations of these random variables that can be summarized as follows for the dead loads:

$$\overline{D_{C1}} = 1.03\, D_{C1} \qquad V_{DC1} = 8\%$$

$$\overline{D_{C2}} = 1.05\, D_{C2} \qquad V_{DC2} = 10\%$$

$$\overline{D_W} = 1.0\, D_W \qquad V_{DW} = 25\% \qquad (37)$$

For the bending moment resistance the mean and COV are given as

$$\overline{R} = 1.12\, R_n \qquad V_R = 10\% \qquad \text{for composite beams}$$

$$\overline{R} = 1.05\, R_n \qquad V_R = 7.5\% \qquad \text{for prestressed concrete beams} \qquad (38)$$

Calculation of Reliability Index and Adjustment of Live-Load Factor. In the LRFD specifications, safety is measured using the reliability index, β, which accounts for the uncertainties in estimating the effects of the applied loads and the resistance of bridge members. The reliability index, β, is related to the probability of failure, P_f, by

$$\beta = \Phi^{-1}(-P_f) \qquad (39)$$

Where $\Phi^{-1}(\ )$ is the inverse of the cumulative normal distribution function. If all the random variables representing the resistance, dead load, and live load follow Gaussian (normal) probability distributions, the reliability index, β, can be calculated as follows:

$$\beta = \frac{\overline{R} - \overline{DL} - \overline{LL}}{\sqrt{\sigma_R^2 + \sigma_{DL}^2 + \sigma_{LL}^2}} \qquad (40)$$

Where the mean of the total dead load is given by

$$\overline{DL} = \overline{D}_{c1} + \overline{D}_{c2} + \overline{D}_w, \qquad (41)$$

the COV of the total dead load is

$$\sigma_{DL} = \sqrt{\sigma_{DC1}^2 + \sigma_{DC2}^2 + \sigma_{DW}^2} \qquad (42)$$

and the standard deviations are obtained as

$$\sigma_R = \overline{R} \times V_R$$

$$\sigma_{DL} = \overline{DL} \times V_{DL}$$

$$\sigma_{LL} = \overline{LL} \times V_{LL} \qquad (43)$$

The AASHTO LRFD was calibrated so that all bridge members designed using the specified load and resistance factors produce a uniform level of risk expressed in terms of a reliability index β equal to a preset target value β_{target}. The AASHTO LRFD calibration was based on a standard set of L_{max} values and live-load standard deviations. If the L_{max} values or their COVs within a state are different than those used during the AASHTO LRFD calibration it may be necessary to adjust the live-load factors in order to maintain the same β_{target}. The adjustment of the live-load factors requires the calculation of the reliability index for different values of the live-load

factor γ_L and adopting the γ_L that produces reliability index values as close to the target as possible for all material types, spans, and geometric configurations.

During the calibration of the AASHTO LRFD, Nowak (1999) assumed that the resistance is Lognormal while the combined effect of the dead and live loads is normal. The reliability index calculations were then executed using a first-order reliability method (FORM) algorithm instead of using Equation 40. However, in order to illustrate the procedure and keep the calculations as simple as possible, it is herein assumed that all the random variables representing the resistance, dead load, and live load follow Gaussian (normal) probability distributions. In such a case, the reliability index, β, can be directly calculated from Equation 40. Note that the data and models used by Nowak (1999) led to a target reliability index $\beta_{target} = 3.5$.

Method II Reliability-Based Adjustment Procedure for Live-Load Factors

1. Assemble a set of representative bridge samples for the state comprising steel and concrete bridges of different span lengths, number of beams, and beam spacing.
2. Assume a value for γ_L.
3. Choose one bridge from the representative sample of bridges.
4. Find the nominal dead loads of components and wearing surface: D_{C1}, D_{C2}, and D_W.
5. Find the nominal live-load effect for the HL93 loading.
6. Apply the new value of γ_L into Equation 32 to obtain the required nominal resistance value R_n.
7. Find the mean resistance $\overline{R}$ using Equation 38.
8. Find the COV V_R also using Equation 38.
9. Find the mean dead load effects using Equation 37.
10. Find the COV for the dead loads using Equation 37 and find the standard deviations $\sigma_{DC1} = V_{DC1}\overline{DC_1}$ $\sigma_{DC2} = V_{DC2}\overline{DC_2}$ $\sigma_{DW} = V_{DW}\overline{DW}$
11. Use the protocols for the WIM data analysis to get L_{max} for 75 years for one-lane loadings and two-lane loadings for several sites within the state.
12. Take the average L_{max} and find $V_{site-to-site}$ COV for one-lane loading and two-lane loading for site-to-site variability.
13. Find the mean value of the live-load effect for one lane and two lanes using Equation 35.
14. Find the COV of the live-load effect for one-lane loading and two-lane loading using Equation 36.

The proposed adjustment of the live-load factor is based on the following assumptions:

- The target reliability index $\beta_{target} = 3.50$ is a satisfactory target and does not need to be modified. This target was estab-

lished by the AASHTO LRFD code writers based on the generic live-load data available at the time. Future research could lead to selecting a different target.
- Although the changes in γ_L would lead to different bridge member capacities R_n, it is assumed that these changes would not lead to changes in the dead loads applied on the bridge members.
- Equation 40 is based on the assumption that the resistance, dead load effects, and live-load effects follow normal (Gaussian) probability functions. Otherwise one should use a first-order reliability method (FORM) algorithm as described by Nowak (1999).
- The models used to obtain the statistical data on the mean values and COVs of the moment and shear capacity of steel composite and prestressed concrete members, as well as the dynamic amplification factors and load distribution factors used during the AASHTO LRFD calibration, are still valid.
- The goal of the calibration is to adjust the live-load factor only so that the representative sample of bridges would, on average, match the target reliability index. In general, the target reliability index should be matched as closely as possible for all representative span lengths and bridge configurations. However, this may not be always possible by changing the live-load factor only.

Step 13.2 Deck Design Load Calibration (Strength I)

The database upon which the present AASHTO LRFD deck provisions were fixed is less defined for bending and shear in longitudinal members. LRFD design loads for decks represented by a 32-kip axle or a pair of 25-kip axles (Figure 21) were not based on the Ontario WIM data. The design truck has the same weights and axle spacing as the HS20 load model, which was adopted in 1944 for bridge design, and has been carried over from the standard specifications. WIM data were not used to validate these axle load models during LRFD development. *NCHRP Report 368* (Nowak 1999) on LRFD calibration is focused on bridge loads for superstructure design and does not specifically address calibration of load models for deck design, fatigue design, or overload permitting.

DECK DESIGN – LRFD CODE PROVISIONS
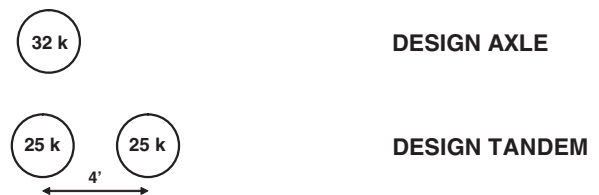
Figure 21. LRFD deck design loads.
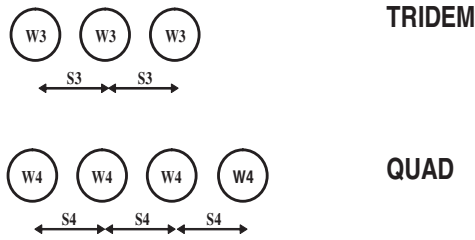
Figure 22. Common axle group loads.

Axle groups with more than two axles (Figure 22) are currently not considered for deck design in the LRFD. However, LRFD commentary C3.6.1.3.3 states the following:

> Individual owners may choose to develop other axle weights and configurations to capture the load effects of the actual loads in their jurisdiction based upon local legal load and permitting policies. Triple-axle configurations of single-unit vehicles have been observed to have load effects in excess of the HL-93 tandem-axle load.

A relevant issue that is beyond the scope of this project is the conservative nature of the present checking rules on the resistance side. The simple strip flexural model is conservative with respect to the true capacity of a deck that actually fails in a punching shear mode. Introducing an accurate strength model would require a change in nominal strength formulas as well as the calibrated factors, which require research beyond the current scope. Resistance factors vary with design methods and are not constant.

Rigorous calibration of load and resistance factors for deck design requires the availability of statistical data beyond live loads. The LRFD did not specifically address deck components in the calibration. It is important to note that there are no β calculations or database of loads/load effects used for the calibration of decks in the LRFD available for use in this project.

One reasonable approach to calibration of deck design loads is to assume the present LRFD safety targets are adequate for the strength design of decks and establish new nominal loads for axles based on recent WIM data. The LRFD live-load factors will remain unchanged, but the axle loads and axle types will be updated to be representative of current traffic data. For instance, tri-axles and quad-axles that are currently not included in the LRFD loadings may need to be considered.

Axle weight statistics from WIM data will first be assembled. The measured axle weights should be adjusted for WIM scatter and measurement errors as detailed in Step 10. This procedure will be repeated for multiple WIM sites to determine the governing nominal loads, taken as follows:

- For single axles, 32 kips or the 99th percentile statistic W_{99}, whichever is higher;
- For tandem axles, 50 kips (2×25 kips) or the 99th percentile statistic W_{99}, whichever is higher;
- For tridem axles, the 99th percentile statistic W_{99}; and
- For quad axles, the 99th percentile statistic W_{99}.

The nominal axle loads derived using WIM data are used instead of the code specified values, where the W_{99} statistic is higher than the code values. W_{99} represents an axle load with a 1% probability of exceedance in a year. This approach provides realistic axle loads for deck design based on current WIM data while keeping all other factors (load factor, deck dynamic load allowance) unchanged (Table 19). It also allows the introduction of three- and four-axle configurations for deck design in a consistent manner. WIM data will also be applied to define nominal axle spacings for the multi-axle groups.

Step 13.3 Repetitive Live-Load Calibration (FATIGUE)

The LRFD fatigue truck configuration will be checked and updated to ensure that it produces fatigue damage similar to that obtained from actual trucks from the traffic data for typical bridge configurations and fatigue details. Adjustments to the fatigue load model could include changes to

- Effective gross weight and
- Axle configuration and axle loads.

Fatigue adjustment factor K for each span using site WIM data could provide the basis for calibrating fatigue design load models, as follows:

1. Use LRFD fatigue truck if K values are uniform and equal to 1.0.
2. LRFD fatigue truck should be modified using the effective gross weight if K values are uniform but not equal to 1.0.

Table 19. Deck design load calibration using WIM.

AXLE TYPE	DESIGN AXLE LOAD	AXLE SPACING	LOAD FACTOR
Single	W_{99} not less than 32 K	N/A	1.75
Tandem	W_{99} not less than 50 K	4 ft	1.75
Tridem	W_{99} from WIM	4 ft	1.75
Quad	W_{99} from WIM	4 ft	1.75

3. Recommend site-specific fatigue trucks if K varies from 1.0 for varying spans.

Step 13.4 Superstructure Design Overload Calibration (Strength II)

Live-Load Modeling for Strength II

The AASHTO LRFD Strength II limit state is used when checking the safety of bridge members under the effect of owner-specified special design vehicles or evaluation permit vehicles. The return period implicit in Strength II is equal to 1 year. To develop appropriate live-load factors for the AASHTO LRFD Strength II limit state, the following three loading scenarios must be considered:

- Case I: permit vehicle alone;
- Case II: permit vehicle alongside another permit; and
- Case IIII: permit vehicle alongside random vehicle.

Case I is exclusively used if the permit vehicle is escorted and traffic is controlled such that no other heavy vehicle is allowed to cross the bridge when the permit is on. Otherwise, Case I should be compared to Cases II and III and the most critical case would govern. Case II may control the loading if a high number of permits are allowed over a certain route or are allowed to travel freely within a jurisdiction. Case III may control depending on the relative weights of the permit as compared to the heavy legal and illegal vehicles that normally cross the bridge.

Case I: Permit Vehicle Alone. In this case, assume that the axle weights and axle configuration of the permit truck are perfectly known so that the total maximum static live-load effect on the bridge of the permit truck, designated by P, is a deterministic value. However, this does not imply that the total live-load effect on a bridge member is deterministic due to the uncertainties in estimating the dynamic effect represented by the dynamic amplification factor, IM, and the uncertainties in the structural analysis process that allocates the fraction of the total load to the most critical member. For multi-girder bridges, the structural analysis is represented by the load distribution factor, D.F. The equations for the D.F. of multi-girder bridges loaded by a single lane given in the AASHTO LRFD specifications already include a multiple-presence factor m = 1.2. Therefore, the expression for the maximum load effect on the most critical beam when a single vehicle is on the bridge can be calculated from

For Case I $\quad \overline{LL} = L_{\text{max beam}} = P \times IM \times D.F./1.2$ (44)

Nowak (1999) observed that the dynamic amplification factor augments the load effect by an average of 13% for one lane of

traffic. Assuming that the weight and axle configuration of the permit vehicle are exactly known, the COVs of the maximum beam live-load effect are obtained from the COV of IM and the COV of DF as follows:

$$V_{LL} = \sqrt{V_{IM}^2 + V_{DF}^2}$$ (45)

Using the data for V_{IM} and V_{DF} for one lane proposed by Nowak (1999) and Ghosn and Moses (1985), for the loading of a single permit vehicle, the live-load COV becomes $V_{LL} = \sqrt{(9\%)^2 + (8\%)^2} = 12\%$.

Case II: Two Permits Side by Side. In this case, assume that the axle weights and axle configurations of the two permit trucks are the same and are perfectly known so that the total maximum static live-load effect on the bridge is a deterministic value equal to 2P. However, this does not imply that the total live-load effect on a bridge member is deterministic due to the uncertainties in estimating the dynamic effect represented by the dynamic amplification factor, IM, and the uncertainties in the structural analysis process that allocates the fraction of the total load to the most critical member. The structural analysis is represented by the load distribution factor, D.F. The equations for the D.F. of multi-girder bridges loaded in two lanes given in the AASHTO LRFD specifications assume that the two lanes are loaded by the same vehicle and give the load on the most critical beam as a function of the load in one of the lanes. Thus, the live-load effect on one member can be given as:

For Case II $\quad \overline{\overline{LL}} = L_{\text{max beam}} = P \times IM \times D.F.$ (46)

According to Nowak (1999), the dynamic amplification factor augments the load effect by an average of 9% for side-by-side trucks. The dynamic amplification also results in a COV of $V_{IM} = 5.5\%$ on the two-lane effect. Also assume that the same COV for the lane distribution factor $V_{DF} = 8\%$ obtained by Moses and Ghosn (1986) from field measurements on typical steel and prestressed concrete bridges is still valid. Therefore, for the loading of a single permit vehicle, the live-load COV becomes $\overline{\overline{LL}} = \sqrt{(5.5\%)^2 + (8\%)^2} = 9.71\%$.

The reliability index conditional on the arrival of two side-by-side permits on the bridge can then be calculated using Equation 40 where $\overline{R}$ is the mean resistance when the bridge member is designed for two side-by-side permits and $\overline{\overline{LL}}$ is the live-load effect on the beam due to two side-by-side permits.

The reliability index calculated from Equation 40 in this case is conditional on having two side-by-side trucks. The probability that a bridge member would fail given that two permit vehicles are side by side can be calculated from the inverse of

Equation 39. However, the final unconditional probability of failure will depend on the conditional probability given two side-by-side events and the probability of having a situation with side-by-side permits. Thus

$$P_f = P_{f/\text{side-by-side events}} \times P_{\text{side-by-side}}$$ (47)

The probability of having two-side-by-side permits depends on the number of permit trucks expected to cross the bridge within the return period within which the permits are granted. The percentage of these permits that will be side by side is related to the total number of permit crossings. Tables relating the percentage of side-by-side events, $P_{\text{side-by-side}}$, as a function of the number of truck crossings can be obtained from the WIM data. The final unconditional reliability index is then obtained by inserting the results of Equation 47 into Equation 39.

Case III: Permit Truck Alongside a Random Truck. For Case III, the maximum live-load effect is due to the permit truck alongside the maximum truck expected to occur simultaneously in the other lane. The maximum total load effect depends on the number of side-by-side events expected within the return period.

To determine the number of side-by-side permit-random truck events that would occur within a 1-year period, assume that N_P gives the number of permit truck crossings expected in a return period T. The final number of random trucks alongside a permit will be

$$N_R = P_{\text{side-by-side}} \times N_P$$ (48)

Where $P_{\text{side-by-side}}$ is the percentage of side-by-side events that depend on the ADTT and N_p is the number of permits within the return period of interest.

The maximum live-load effect is obtained from

$$\overline{LL} = \left(P \times DF_P + L_{\max N_R} \times DF_R\right)IM$$ (49)

Where P is the load effect of the permit truck, DF_P is the distribution factor for the load P, $L_{\max N_R}$ is the maximum load effect of random trucks for N_R events which correspond to the 1-year return period applicable for the Strength II case, DF_R is the distribution factor for the random load, and IM is the impact factor for side-by-side events. The problem in this case is that the DF tables provided in the AASHTO LRFD for two lanes assume that the two side-by-side trucks are of equal weight, which is clearly not the case. Following the AASHTO LRFD approach for permit trucks alongside random trucks, Moses (2001) suggested that DF_P be obtained from the AASHTO LRFD tables for single lane while DF_R be obtained from the difference between the DF of two lanes and that of a single lane.

The coefficient of variation for $L_{\max N_R} \times DF_R$ is estimated as:

$$V_{L\max *} = \sqrt{V_{\text{site-to-site}}^2 + V_{\text{projection}}^2 + V_{\text{data}}^2 + V_{DF}^2}$$ (50)

Where all of the values are taken for the single-lane case.

Assuming the effect of the permit load is deterministic, the coefficient of variation for $P \times DF_P$ is estimated as follows

$$V_{P*} = 8\%$$ (51)

which is the COV for the load distribution factor, DF_P. Hence, the standard deviation of LL without the impact factor is

$$\sigma_{LL*} = \sqrt{\left(V_{P*} \times P \times DF_P\right)^2 + \left(V_{L\max *} \times L_{\max N_R} \times DF_R\right)^2}$$ (52)

and the COV for the live-load effect on the critical beam including the effect of the impact factor is given by

$$V_{LL} = \sqrt{\left(\frac{\sigma_{LL*}}{LL*}\right)^2 + V_{IM}^2}$$ (53)

where $LL* = (P \times DF_P + L_{\max N_R} \times DF_R)$ is the static live-load effect on the most critical bridge member.

The mean live load obtained from Equation 49 and the COV obtained from Equation 53 are then used to find the reliability index from Equation 40.

The calibration of the appropriate live-load factor would consist of finding the γ_L that will lead to reliability index values equal to the target value for Cases I, II, and III.

Method II: Reliability-Based Adjustment Procedure for Overload Live-Load Factors

1. Assemble a set of representative bridge samples for the state comprising steel and concrete bridges of different span lengths, number of beams, and beam spacing.
2. Determine the permit vehicle configuration.
3. Assume a value for γ_L.
4. Choose one bridge from the representative sample of bridges.
5. Find the nominal dead loads of components and wearing surface: D_{C1}, D_{C2}, and D_W.
6. Find the nominal live-load effect, P, for the permit vehicle.
7. Apply the new value of γ_L into Equation 32 to obtain the required nominal resistance value R_n.
8. Find the mean resistance $\overline{R}$ using Equation 38.
9. Find the COV V_R also using Equation 38.
10. Find the mean dead load effects using Equation 37,
11. Find the COV of the dead loads from Equation 37 and find the standard deviations $\sigma_{DC1} = V_{DC1}\overline{DC_1}$ $\sigma_{DC2} = V_{DC2}\overline{DC_2}$ $\sigma_{DW} = V_{DW}\overline{DW}$

12. Use the protocols for the WIM data analysis to get $L_{\max N_R}$ for one-lane loadings for a 1-year return period.
13. Calculate $\overline{LL}$ for Case I, Case II, and Case III from Equations 44, 46, and 49.
14. Find the COV for LL for each case using Equations 45 or 53.
15. Find the standard deviations using Equations 42 and 43.
16. Apply the mean and standard deviation values of loads and resistance into Equation 40 to calculate the reliability index, β, for the bridge configuration selected in Step 4 for each of the three cases.
    - For Cases I and III the reliability index is obtained from Equation 40 directly.
    - For Case II, the conditional reliability index, β_{cond} is obtained from Equation 40. The final unconditional reliability index, β, is obtained from $\beta = \Phi^{-1}(-P_f)$ where P_f is obtained from Equation 47 and $P_{f/\text{side-by-side}} = \Phi(-\beta_{cond})$ where Φ is the standard normal cumulative distribution function.
17. Go to Step 4 to select another bridge and repeat Steps 4 to 16 until you exhaust all of the bridges in the representative sample.
18. Find the average β_{ave} of each load case for the representative sample of bridges.
19. If $\beta_{ave} = \beta_{target} = 3.50$, stop. Otherwise, go to Step 3 and start the process over.
20. Determine the value of γ_L that leads to $\beta_{ave} = \beta_{target} = 3.50$ for each of the three cases.

Demonstration of Recommended Protocols Using National WIM Data

In this chapter, draft protocols including step-by-step procedures for collecting and using traffic data in bridge design were developed. They are geared to address the use of national WIM data to develop and calibrate vehicular loads for LRFD superstructure design, fatigue design, deck design, and design for overload permits.

The aim of this section is to give practical examples of using these protocols with national WIM data drawn from sites around the country with different traffic exposures, load spectra, and truck configurations. This will give a good cross-section of WIM data for illustrative purposes. This step will allow the updating and/or refinement of the protocols based on its applicability to WIM databases of varying quality and data standards currently being collected by the states. This section of the report discusses the results of the demonstration studies in more detail.

Selection of Sites for National WIM Data Collection

The protocols established in this chapter were implemented using recent traffic data (either 2005 or 2006) from 26 WIM

sites (47 directional sites) in five states across the country (Table 20). The sites were chosen to capture a variety of geographic locations and functional classes, including urban interstates, rural interstates, and state routes.

Requests for WIM data needed for the studies were sent out to certain selected states based on the national survey findings. The requirements for selection of WIM sites were for WIM data for a whole year (2006 or 2005) from the following highway functional classifications:

- Two WIM sites on rural interstates,
- Two WIM sites on urban interstates, and
- Two WIM sites on principal arterials (non-interstate routes).

Table 20. WIM sites studied in Task 8.

State	Site ID	Route	Dir	# Truck Records	ADTT
CA	0001	Lodi	E/N	1537613	5058
CA	0001	Lodi	W/S	1470924	4839
CA	0003	Antelope	E	719834	2790
CA	0004	Antelope	W	806122	3149
CA	0059	LA710	S	4243780	11627
CA	0060	LA710	N	3806748	11432
CA	0072	Bowman	E/N	310596	2318
CA	0072	Bowman	W/S	289319	2159
FL	9916	US-29	N	175905	498
FL	9919	I-95	N	939637	2708
FL	9919	I-95	S	875766	2524
FL	9926	I-75	N	1096076	4136
FL	9926	I-75	S	1032680	3897
FL	9927	SR-546	E	204549	567
FL	9927	SR-546	W	168114	466
FL	9936	I-10	E	700774	1980
FL	9936	I-10	W	723512	2044
IN	9511	I-65	N	2119022	5919
IN	9511	I-65	S	2068073	5777
IN	9512	I-74	E	931971	2596
IN	9512	I-74	W	1003443	2795
IN	9532	US-31	N	224506	629
IN	9532	US-31	S	229532	643
IN	9534	I-65	N	2128577	5929
IN	9534	I-65	S	2162874	6025
IN	9544	I-80/I-94	E	3786127	11235
IN	9544	I-80/I-94	W	4032537	11966
IN	9552	US-50	E	95900	278
IN	9552	US-50	W	102212	296
MS	2606	I-55	N	564393	1622
MS	2606	I-55	S	604919	1733
MS	3015	I-10	E	750814	2248
MS	3015	I-10	W	667560	1999
MS	4506	I-55	N	530517	2002
MS	4506	I-55	S	477931	1804
MS	6104	US-49	N	462301	1288
MS	6104	US-49	S	498054	1387
MS	7900	US-61	N	69996	220
MS	7900	US-61	S	68198	216
TX	0506	US-287	E/N	559663	1701
TX	0506	US-287	W/S	520092	1581
TX	0516	I-35	E/N	717666	2384
TX	0516	I-35	W/S	707744	2449
TX	0523	US-281	E/N	430227	1429
TX	0523	US-281	W/S	394804	1312
TX	0526	I-20	E/N	1330799	4070
TX	0526	I-20	W/S	1174954	3593

Table 21 lists the sites studied along with their respective ADTTs. For consistency, lanes one and two are eastbound or northbound lanes; lanes three and four are westbound or southbound lanes.

Data Filtering and Quality Control (Protocol Steps 5.1 and 5.2)

The same data scrubbing criteria established in Steps 5.1 and 5.2 were employed. That is, truck records that met any one of the following criteria were eliminated as unlikely or unwanted trucks for the purposes of this study. The following filtering protocol was applied for screening the WIM data used in this project. Truck records that met the following filters were eliminated:

- Speed < 10 mph
- Speed > 100 mph
- Truck length > 120 ft
- Total number of axles > 12
- Total number of axles < 3
- Record where the sum of axle spacing is greater than the length of truck
- GVW < 12 kips
- Record where an individual axle > 70 kips
- Record where the steer axle > 25 kips
- Record where the steer axle < 6 kips
- Record where the first axle spacing < 5 ft
- Record where any axle spacing < 3.4 ft
- Record where any axle < 2 kips
- Record which has GVW +/− sum of the axle weights by more than 10%

The two most common criteria used to eliminate records were "number of axles < 3" (2-axle light vehicles) and "steer axle < 6 kips." Typically, one of these two criteria was responsible for 75% to 90% of all scrubbed records at a given WIM site. Furthermore, the gross vehicle weight of these trucks tends to be low. Therefore, their removal from the study has very little effect on the analysis, which tends to concentrate on the upper tail of the data. Table 21 shows the number of trucks, as well as the percentage of the total truck population, eliminated from each WIM site for meeting one or more of the above criteria. Also shown is the mean gross vehicle weight, in kips, of all of the eliminated trucks.

The scrubbed WIM data were passed through various quality control checks. The quality control checks established in Step 5.2 were employed for each WIM site studied. The quality control checks look specifically at Class 9 trucks (5-axle semi-trailer trucks). Since Class 9 trucks are so prevalent in the population and their configurations are well defined, deviations from their expected characteristics can be noted and corrective measures taken.

Table 21. Trucks eliminated by data filtering.

State	Site	Number	%	GVW
CA	0001	1671347	35.7	12.0
CA	0003	643461	47.2	11.2
CA	0004	771032	48.9	11.4
CA	0059	1242393	22.6	14.3
CA	0060	1366271	26.4	14.8
CA	0072	407724	40.5	10.9
FL	9916	533513	73.0	16.5
FL	9919	457426	20.1	22.5
FL	9926	1752902	45.2	13.7
FL	9927	276965	42.6	16.5
FL	9936	330745	18.8	26.3
IN	9511	984044	19.0	14.6
IN	9512	421592	17.9	13.2
IN	9532	839445	64.9	10.9
IN	9534	1952426	31.3	10.9
IN	9544	1855062	19.2	12.9
IN	9552	162192	45.0	11.0
MS	2606	380794	24.6	27.8
MS	3015	1712866	53.4	25.9
MS	4506	458419	31.3	19.1
MS	6104	488899	33.7	24.3
MS	7900	86777	38.6	13.6
TX	0506	584553	35.1	10.9
TX	0516	881932	38.2	9.6
TX	0523	465556	36.1	10.7
TX	0526	1261244	33.5	11.4

The quality control checks are described as follows:

1. Percentage of trucks by class. Class 9 trucks should be the most prevalent truck class in the population.
2. Class 9 truck GVW histogram. The characteristic bi-modal shape of the GVW histogram should show an "unloaded" peak between 28 kips and 32 kips, and a "loaded" peak between 72 kips and 80 kips.
3. Overweight Class 9 trucks. The percentage of Class 9 trucks over 100 kips should be small.
4. Class 9 truck steer axle weight histogram. The weight of the front axle of Class 9 trucks should be between 9 kips and 11 kips. There should not be a significant deviation from this range.
5. Class 9 drive tandem weight histogram. The weight of the drive tandem should not deviate significantly from the estimated values given in *NCHRP Report 495* (Fu et al. 2003).
6. Class 9 axle spacing histogram. The spacing between the steer axle and the drive tandem axle as well as the spacing between the drive tandem axles should be fairly consistent.

The traffic in each lane at a WIM site is recorded by its own sensor. If a sensor malfunctions or begins to lose its calibration it will manifest itself in one or more of the results of the quality control checks. By segregating the data of these quality control checks by lane and by month, deviations from the normal,

expected values can be more easily identified and isolated. If a sensor appears to be malfunctioning or providing less reliable data, then the data collected by the offending sensor is eliminated from the population.

Of all the sites studied, only two required additional data scrubbing due to non-conformance during the quality control checks. At WIM Site 3015 in Mississippi, all data from Lane 3 during the months of January through June were eliminated. This accounted for 74,351 trucks, or 5.0% of the filtered truck data. At WIM Site 9916 in Florida, all data from Lane 1 during the month of January were eliminated. This accounted for 14,521 trucks, or 7.6% of the filtered truck data.

After this second round of data scrubbing due to sensor issues, all remaining data was considered reliable and ready for processing.

Truck Multiple-Presence (Protocol Step 6)

Accurate multiple-presence data requires time stamps of truck arrival times to the hundredth of a second. The research team requested this time stamp resolution, but the WIM data records were mostly to a second accuracy. Multiple-presence statistics need not be developed for each site. Multiple-presence statistics are mostly transportable from site to site with similar truck traffic volumes and traffic flow. A relationship between multiple presence and ADTT was developed in this study, which could be applied to any given site without performing a site-specific analysis (see Step 7).

WIM Data Analysis for One-Lane Loading (Step 7)

Grouping Trucks into Strength I. Protocols developed in Step 7 require that legal loads, illegal overloads, and routine permits be grouped under Strength I and heavy special permits be grouped under Strength II. The following approach to sorting trucks in the WIM databases was used initially:

- Do not attempt to classify New York trucks as permit or non-permit based on permit records when using large-scale WIM databases. The permit data are unreliable, incomplete, or not easily accessed to allow this to be achieved.
- Group all trucks with six or fewer axles in the Strength I calibration. These vehicles include legal trucks, illegal overloads, and routine permits. These vehicles are considered to be enveloped by the HL93 load model.
- Group all trucks with seven or more axles in the Strength II calibration. These vehicles should include the heavy special permit loads, typically in the 150-kip GVW and above category. An analysis of WIM data from several states indicates a big drop-off in truck population for vehicles with seven or greater axles. Only a very small percentage of trucks belong to this permit group.

This simple approach to separating trucks into Strength I and Strength II was considered reasonable. There are other approaches with varying degrees of complexity that may also provide a satisfactory way to achieve the same objective and may even provide better accuracy in some cases. Under the initial 12-76 study, the demonstration of the protocols was based only on the above noted sorting methodology. A follow-on study, NCHRP 12-76 (01), to investigate the sensitivity of "r" values to truck sorting strategies was conducted by the NCHRP 12-76 research team from 2009 to 2010. The results of this study and key recommendations on sorting of trucks into Strength I and Strength II limit states are presented at the end of this chapter.

Gross Vehicle Weight Histograms (Step 7.1)

Gross vehicle weight (GVW) histograms were generated by direction of travel for each WIM site. Figure 23 shows, as a sample, the GVW histogram for WIM Site 9926 in Florida (I-75). Appendix C contains the GVW histograms for all other WIM sites studied in this task.
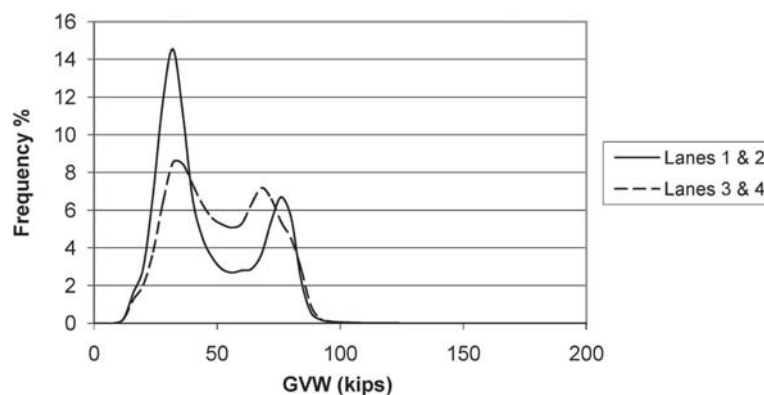
Figure 23. GVW histogram (WIM Site 9926 in Florida).
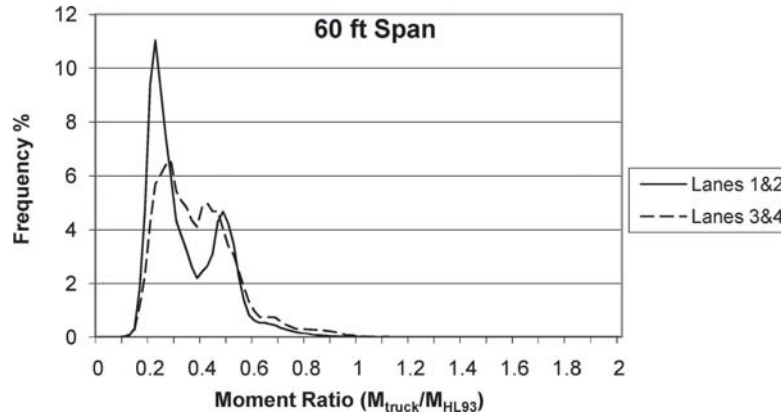
Figure 24. Single truck simple-span moment histogram (WIM Site 9926 in Florida).

The bi-modal shape of this histogram is typical of GVW histograms with the first major peak representing unloaded or lightly loaded trucks and the second major peak representing trucks loaded near the legal limit of 80 kips.

One-Lane Load Effects (Step 7.1)

The load effects of each truck individually were calculated for eight span lengths from 20 ft to 200 ft for both simple spans and two-span continuous spans. The load effects calculated were maximum mid-span moment for a simple span, shear at a support for a simple span, maximum positive moment for a two-span continuous span, maximum negative moment for a two-span continuous span, and shear at the center support of a two-span continuous span. All load effects were normalized to those of HL93 loading. Figure 24 shows, as a sample, the single truck maximum mid-span moment histogram for a simple 60-ft span for WIM Site 9926 in Florida (I-75). Similarly, Figure 25 shows the single truck maximum shear histogram

for a simple 60-ft span for WIM Site 9926. Appendix C contains the moment histograms for all other WIM sites studied in this task.

As would be expected, the general shape of these histograms is similar to that of the GVW histogram; that is, bi-modal with the first major peak representing unloaded or lightly loaded trucks and the second major peak representing trucks loaded near the legal limit.

WIM Data Analysis for Two-Lane Loading (Step 8)

Simulation of Truck Events using Generalized Multiple-Presence Statistics (Step 8.2)

All of the New York WIM sites studied captured accurate time stamps with each truck record. This allowed for the analysis of two trucks existing simultaneously on a span. Additional data also were available from several WIM sites in New Jersey.
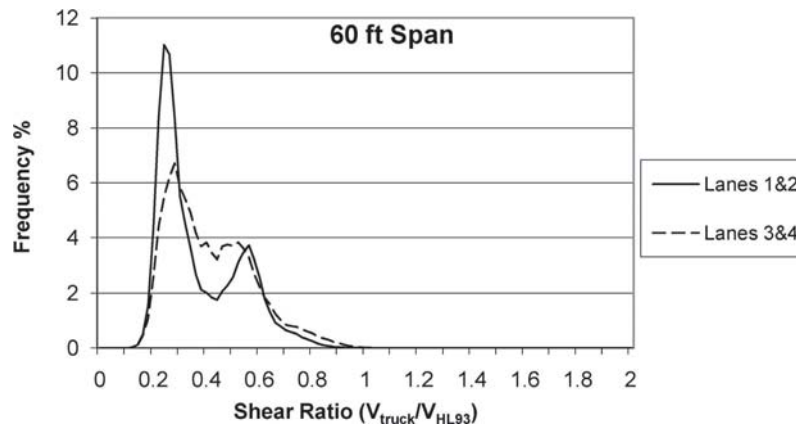
Figure 25. Single truck simple-span shear histogram (WIM Site 9926 in Florida).

Table 22. Multiple-presence probabilities.

	Multiple Presence Probabilities (%)							
	Two-Lane Events (Side-by-Side)				One-Lane Events (Following)			
Headway	Site Truck Traffic (ADTT)**				Site Truck Traffic (ADTT)**			
(ft)	Light	Average	Heavy	Very Heavy	Light	Average	Heavy	Very Heavy
0 to 20	0.19	0.41	0.61	0.60	0.00	0.00	0.00	0.00
20 to 40	0.14	0.43	0.66	0.63	0.00	0.00	0.00	0.00
40 to 60	0.21	0.41	0.68	0.66	0.01	0.00	0.00	0.01
60 to 80	0.26	0.35	0.62	0.64	0.01	0.00	0.00	0.09
80 to 100	0.20	0.53	0.76	0.74	0.06	0.04	0.03	0.49
100 to 120	0.21	0.41	0.81	0.64	0.12	0.15	0.16	1.81
120 to 140	0.24	0.34	0.66	0.61	0.21	0.33	0.45	3.04
140 to 160	0.17	0.30	0.61	0.56	0.36	0.57	0.73	3.29
160 to 180	0.18	0.29	0.56	0.53	0.48	0.67	0.91	3.03
180 to 200	0.19	0.26	0.52	0.50	0.46	0.75	0.98	2.74
200 to 220	0.10	0.24	0.48	0.48	0.51	0.68	0.94	2.52
220 to 240	0.14	0.24	0.45	0.43	0.48	0.67	0.91	2.28
240 to 260	0.12	0.22	0.43	0.41	0.42	0.65	0.87	2.18
260 to 280	0.14	0.21	0.41	0.39	0.41	0.60	0.85	1.98
280 to 300	0.11	0.20	0.40	0.36	0.39	0.59	0.80	1.87

** Light: ADTT $\leq$ 1000
  Average: 1000 < ADTT $\leq$ 2500
  Heavy: 2500 < ADTT $\leq$ 5000
  Very Heavy: ADTT > 5000

None of the WIM sites included reported time stamps with sufficient precision (to the nearest 1/100th of a second) to accurately model the relative positions of two trucks on a span. However, the probabilities of two trucks existing within various headway separations were determined. These probabilities, shown in Table 22, were used to simulate the simultaneous presence of two trucks on a span.

Note that the very heavy ADTT multiple presence was based only on one site in New York City and has some anomalies that should be addressed by additional studies at other U.S. sites. Based on a WIM site's ADTT and the multiple-presence probabilities established as shown in Table 23, the number of expected multiple-presence events for the given WIM site were determined. For each expected multiple-presence event,

two trucks traveling in the desired direction were chosen at random from the entire population of trucks traveling in that direction and positioned to achieve the required headway separation. The load effects of the simulated multiple-presence events were calculated as for the single truck events.

For the purpose of design, in consideration of distribution factors, load effects were segregated into one-lane and two-lane; one-lane load effects are those due to a single truck as well as two trucks in the same lane, while two-lane load effects are those due to two trucks in adjacent lanes. Figure 26 shows, as a sample, the one-lane and two-lane moment histograms for a 60-ft simple span for lanes one and two of WIM Site 9926 in Florida (I-75). Figures 27 and 28 are similar, but show the histograms for simple-span shear and negative moment,
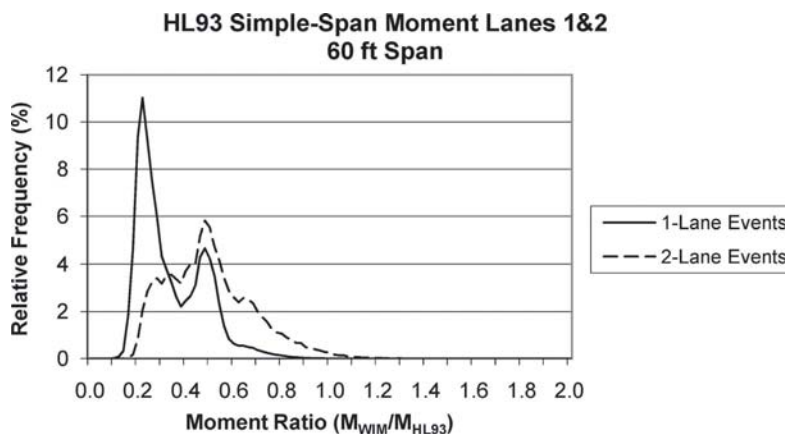
Figure 26. Simple-span moment histogram (WIM Site 9926 in Florida).

HL93 Simple-Span Shear Lanes 1&2 60 ft Span
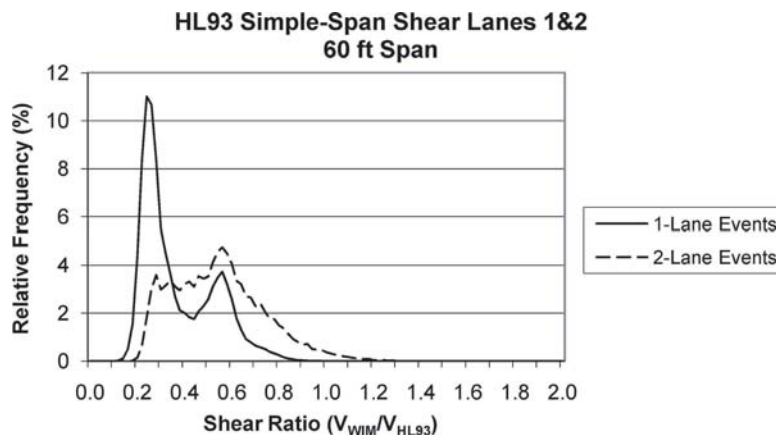
Figure 27. Simple-span shear histogram (WIM Site 9926 in Florida).

respectively. Appendix C contains the load effect histograms for all other WIM sites studied in this task.

Since it is unlikely that two trucks traveling in the same lane will be separated by less than 60 ft, the load effects histograms for the one-lane events are very similar to the single-truck load effects histograms; that is, they display the typical bi-modal shape. The same cannot be said of the two-lane events. Here, the distinction between unloaded trucks and loaded trucks is blended, resulting in a unimodal distribution.

Accumulated Fatigue Damage and Effective Gross Weight (Step 11)

Damage accumulation laws such as Miner's Rule can then be used to estimate the fatigue damage for the whole design period for the expected truck population at a site. For varying spans, the effective gross weight for trucks measured at the site was determined using the following equation:

$$W_{eq} = \left(\sum_i f_i W_i^3 \right)^{1/3} \tag{54}$$

where:

f_i is the fraction of gross weights within interval i, and
W_i is the mid-width of interval i.

In this calculation, use trucks only with three or more axles (Class 6 and above). The LRFD fatigue truck has a 54-kip effective gross weight. Table 23 shows the effective gross weights calculated for the various WIM sites.

Accumulated fatigue damage was studied, as in Step 11, by calculating the fatigue adjustment factor, K. The fatigue adjustment factor K was calculated relative to three reference trucks—the LRFD fatigue truck, the modified LRFD fatigue truck, and the site-specific fatigue truck.

$$K \times M_{FT} = \left[\frac{\sum (M_i)^3}{\# \text{Trucks}} \right]^{1/3} \tag{55}$$

HL93 Negative Moment Lanes 1&2 60 ft Span
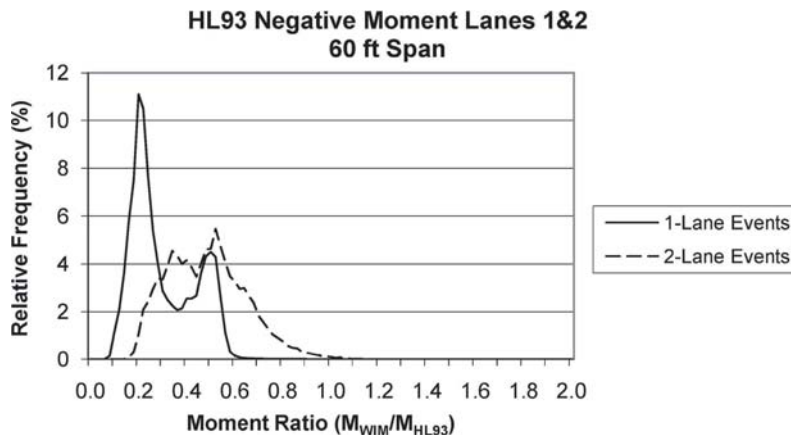
Figure 28. Two-span continuous negative moment histogram (WIM Site 9926 in Florida).

Table 23. Effective gross vehicle weight for all WIM sites studied in Task 8.

State	Site ID	Route	Dir	W_{eff}
CA	0001	Lodi	E/N	61.5
CA	0001	Lodi	W/S	60.3
CA	0003	Antelope	E	56.3
CA	0004	Antelope	W	56.4
CA	0059	LA710	S	45.8
CA	0060	LA710	N	54.4
CA	0072	Bowman	E/N	56.0
CA	0072	Bowman	W/S	57.2
FL	9916	US-29	N	56.1
FL	9919	I-95	N	49.3
FL	9919	I-95	S	50.0
FL	9926	I-75	N	56.2
FL	9926	I-75	S	59.6
FL	9927	SR-546	E	52.9
FL	9927	SR-546	W	47.2
FL	9936	I-10	E	73.9
FL	9936	I-10	W	50.2
IN	9511	I-65	N	51.4
IN	9511	I-65	S	47.4
IN	9512	I-74	E	64.5
IN	9512	I-74	W	65.1
IN	9532	US-31	N	47.4
IN	9532	US-31	S	50.7
IN	9534	I-65	N	49.0
IN	9534	I-65	S	51.6
IN	9544	I-80/I-94	E	53.5
IN	9544	I-80/I-94	W	50.1
IN	9552	US-50	E	55.7
IN	9552	US-50	W	46.3
MS	2606	I-55	N	73.7
MS	2606	I-55	S	66.0
MS	3015	I-10	E	56.9
MS	3015	I-10	W	61.7
MS	4506	I-55	N	67.1
MS	4506	I-55	S	56.9
MS	6104	US-49	N	65.5
MS	6104	US-49	S	66.0
MS	7900	US-61	N	58.9
MS	7900	US-61	S	60.7
TX	0506		E/N	63.1
TX	0506		W/S	62.7
TX	0516		E/N	55.6
TX	0516		W/S	58.4
TX	0523		E/N	60.9
TX	0523		W/S	62.2
TX	0526		E/N	60.8
TX	0526		W/S	61.9

The modified LRFD fatigue truck has the same number of axles, the same axle spacing, and the same axle weight distribution as the LRFD fatigue truck, but a GVW equal to the effective gross weight of the truck population at the WIM site. For the site-specific fatigue truck, the most common axle spacings and axle weight distributions were determined for the 5-axle trucks (the most common truck type) and used to define an equivalent 3-axle fatigue truck. That is, the drive tandem axles were combined into an equivalent single axle (with an axle weight equal to the combined weight of the tandem, located mid-way between the two tandem axles), and the trailer tandem axles were combined into an equivalent single axle. This is a slight adjustment to the definition of the site-specific fatigue truck used. The effective gross weight of the truck population was still used for the GVW of this fatigue truck. Table 24 shows the effective gross vehicle weight, in kips, used in calculating K for each directional WIM site studied in this task.

The most common axle configuration of the five-axle trucks was gathered from histograms of axle weights and axle spacing for each WIM site. This information was used to define a site-specific fatigue truck for each site. Figure 29 shows, as a sample, the typical configuration of 5-axle trucks and the equivalent 3-axle fatigue truck derived from it for WIM Site 9926 in Florida (I-75). Table 24 shows, as a sample, the values of the fatigue adjustment factor, K, for the northbound lanes of WIM Site 9926. Appendix C contains the fatigue adjustment factor values for all other WIM sites studied in this task.

The more closely the reference truck represents the actual truck traffic at a site, the closer the value of the fatigue adjustment factor is to unity. Values of K greater than 1.0 indicate that the reference truck underestimates the accumulated fatigue damage of the traffic, while values of K less than 1.0 indicate that the reference truck overestimates the accumulated fatigue damage. As would be expected, the site-specific fatigue truck most closely represents the entire truck population in regard to accumulated fatigue damage.

0.214 W   0.213 W   0.204 W   0.187 W   0.182 W

16.5 ft   4 ft   31.5 ft   4 ft

Typical 5-Axle Truck Configuration

0.21 W   0.42 W   0.37 W

18.5 ft   35.5 ft

Site-Specific Fatigue Truck Configuration
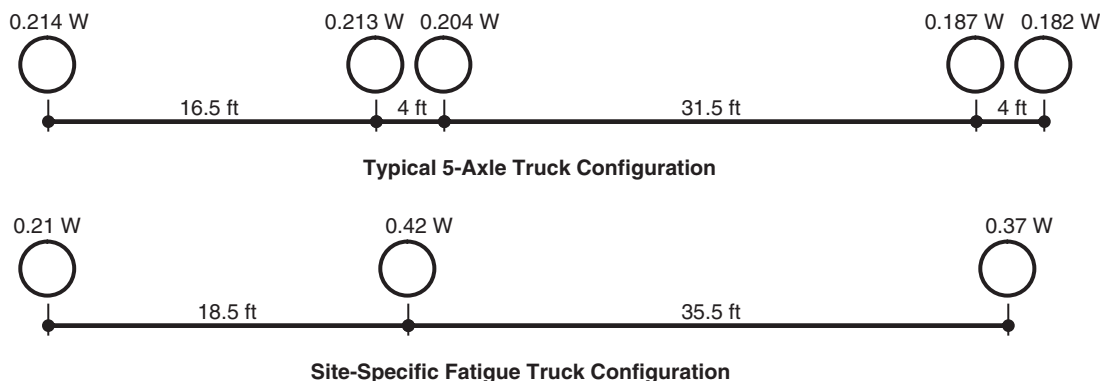
Figure 29. Site-specific truck configurations (WIM Site 9926 in Florida on I-75.)

Table 24. Fatigue adjustment factor, K (WIM Site 9926 in Florida on I-75).

Lanes 1 and 2

LRFD Fatigue Truck		GVW =		54 kips					
Axle Weight:		Steer =		6 kips	Drive =		24 kips	Trailer =	24 kips
Axle Spacing:					14 ft			30 ft	
Span (ft)	20	40	60	80	100	120	160	200	
K (simple)	0.8965	0.9933	1.0718	0.9749	0.9846	0.9944	1.0069	1.0142	
K (pos.)	0.875	0.9761	0.9988	0.967	0.9789	0.9885	1.0014	1.0094	
K (neg.)	1.1614	0.9462	1.0834	1.0868	0.9887	1.0004	1.0175	1.0257	

Modified LRFD Fatigue Truck		GVW =		56.203 kips	(effective gross weight)				
Axle Weight:		Steer =		6.245 kips	Drive =		24.979 kips	Trailer =	24.979 kips
Axle Spacing:					14 ft			30 ft	
Span (ft)	20	40	60	80	100	120	160	200	
K (simple)	0.8613	0.9544	1.0298	0.9367	0.946	0.9554	0.9675	0.9745	
K (pos.)	0.8407	0.9378	0.9596	0.9291	0.9406	0.9498	0.9622	0.9698	
K (neg.)	1.1158	0.9091	1.0409	1.0442	0.95	0.9612	0.9777	0.9855	

Site-Specific Fatigue Truck		GVW =		56.203 kips	(effective gross weight)				
Axle Weight:		Steer =		11.803 kips	Drive =		23.605 kips	Trailer =	20.795 kips
Axle Spacing:					18.5 ft			35.5 ft	
Span (ft)	20	40	60	80	100	120	160	200	
K (simple)	0.9115	1.0464	1.0364	1.0236	1.0072	1.0028	1.0002	0.9995	
K (pos.)	0.8896	1.0024	1.0203	1.0128	1.0051	1.0021	1	0.9994	
K (neg.)	0.9749	1.0111	0.9887	1.0052	1.029	1.0147	1.0073	1.0045	

Lanes 3 and 4

LRFD Fatigue Truck		GVW =		54 kips					
Axle Weight:		Steer =		6 kips	Drive =		24 kips	Trailer =	24 kips
Axle Spacing:					14 ft			30 ft	
Span (ft)	20	40	60	80	100	120	160	200	
K (simple)	0.9928	1.1091	1.1941	1.0721	1.0701	1.0739	1.0804	1.0848	
K (pos.)	0.9649	1.0879	1.1129	1.0638	1.0657	1.0695	1.0763	1.0811	
K (neg.)	1.2809	1.0062	1.149	1.1622	1.0599	1.0688	1.0831	1.0901	

Modified LRFD Fatigue Truck		GVW =		59.573 kips	(effective gross weight)				
Axle Weight:		Steer =		6.619 kips	Drive =		26.477 kips	Trailer =	26.477 kips
Axle Spacing:					14 ft			30 ft	
Span (ft)	20	40	60	80	100	120	160	200	
K (simple)	0.8999	1.0054	1.0824	0.9718	0.97	0.9734	0.9794	0.9833	
K (pos.)	0.8746	0.9861	1.0088	0.9643	0.966	0.9695	0.9756	0.9799	
K (neg.)	1.1611	0.9121	1.0415	1.0535	0.9607	0.9688	0.9818	0.9881	

Site-Specific Fatigue Truck		GVW =		59.573 kips	(effective gross weight)				
Axle Weight:		Steer =		12.51 kips	Drive =		25.021 kips	Trailer =	22.042 kips
Axle Spacing:					18.5 ft			35.5 ft	
Span (ft)	20	40	60	80	100	120	160	200	
K (simple)	0.9523	1.1023	1.0894	1.0619	1.0327	1.0217	1.0125	1.0086	
K (pos.)	0.9255	1.0541	1.0726	1.0512	1.0323	1.0229	1.014	1.0099	
K (neg.)	1.0144	1.0143	0.9893	1.0142	1.0406	1.0228	1.0115	1.0071	

Lifetime Maximum Load Effect L_{max} for Strength I (Step 12.2)

Statistical projections with a Gumbel distribution fit to the upper tail of the load effects histograms were used to determine the lifetime maximum load effects, L_{max}, for Strength I superstructure design. L_{max} was calculated for all 5 load effects, 8 span lengths, and 47 directional WIM sites, and segregated by one-lane and two-lane events.

The results of the calculation of L_{max} based on the data assembled from several WIM sites are provided in Tables 25 through 29 for different span lengths. The results show a slight decrease in the value of L_{max} with span length. The average value of L_{max} tends to be more closely related to its minimum value than to its maximum value, indicating a bias to less heavily loaded spans. Where the information is available, the 75-year L_{max} values used in the LRFD calibration also are shown. With the exception of negative moment in a two-span continuous span, the L_{max} values used in the LRFD calibration are unconservative, being less than the maximum values observed in this study. The degree to which these values are unconservative is more pronounced in the one-lane events where the L_{max} values used in the LRFD calibration are less than the average values observed

Table 25. Maximum L$_{max}$ values for California.

Load Effect		20	40	60	80	100	120	160	200
					Span (ft)				
M-simple	1-Lane	1.989	1.635	1.413	1.392	1.351	1.311	1.227	1.168
	2-Lane	1.955	1.823	1.844	1.891	1.859	1.783	1.676	1.544
V-simple	1-Lane	1.861	1.526	1.483	1.427	1.391	1.349	1.258	1.175
	2-Lane	1.930	1.843	1.904	1.870	1.842	1.796	1.662	1.549
M-positive	1-Lane	1.861	1.526	1.483	1.427	1.391	1.349	1.258	1.175
	2-Lane	1.867	1.859	1.859	1.894	1.854	1.806	1.697	1.564
M-negative	1-Lane	1.599	1.557	1.364	1.346	1.250	1.078	0.939	0.846
	2-Lane	2.017	2.013	1.446	1.086	1.020	0.973	0.895	0.812
V-center	1-Lane	1.752	1.508	1.506	1.439	1.344	1.208	1.020	0.915
	2-Lane	1.906	1.846	1.896	1.848	1.757	1.520	1.356	1.200

Table 26. Maximum L$_{max}$ values for Florida.

Maximum L$_{max}$ Values of 9 Directional WIM Sites in Florida

Load Effect		20	40	60	80	100	120	160	200
M-simple	1-Lane	2.860	2.571	2.234	2.240	2.178	2.112	1.939	1.800
	2-Lane	2.511	2.478	2.471	2.451	2.405	2.365	2.244	2.141
V-simple	1-Lane	2.955	2.515	2.456	2.395	2.290	2.193	2.008	1.854
	2-Lane	2.444	2.467	2.493	2.380	2.297	2.273	2.199	2.101
M-positive	1-Lane	2.880	2.586	2.273	2.230	2.220	2.145	2.003	1.829
	2-Lane	2.407	2.423	2.496	2.497	2.429	2.361	2.260	2.151
M-negative	1-Lane	2.640	2.336	1.807	1.582	1.396	1.195	1.025	0.958
	2-Lane	2.480	2.577	1.814	1.615	1.489	1.361	1.279	1.128
V-center	1-Lane	2.851	2.436	2.404	2.306	2.204	1.903	1.588	1.421
	2-Lane	2.506	2.270	2.288	2.371	2.280	2.074	1.821	1.649

Table 27. Maximum L$_{max}$ values for Indiana.

Maximum L$_{max}$ Values of 12 Directional WIM Sites in Indiana

Load Effect		20	40	60	80	100	120	160	200
M-simple	1-Lane	2.302	2.207	1.932	1.896	1.859	1.806	1.702	1.636
	2-Lane	2.219	1.958	1.814	1.765	1.706	1.749	1.740	1.669
V-simple	1-Lane	2.422	2.079	1.899	1.883	1.839	1.789	1.687	1.618
	2-Lane	2.134	1.820	1.885	2.019	2.057	2.034	1.914	1.798
M-positive	1-Lane	2.352	2.175	1.961	1.891	1.858	1.807	1.736	1.636
	2-Lane	2.278	1.952	1.800	1.735	1.739	1.768	1.742	1.672
M-negative	1-Lane	1.861	1.917	1.608	1.505	1.302	1.153	1.009	0.939
	2-Lane	1.841	2.335	1.853	1.324	1.076	1.073	1.017	0.934
V-center	1-Lane	2.392	2.024	1.831	1.810	1.764	1.581	1.395	1.302
	2-Lane	2.100	1.791	1.837	1.971	1.991	1.799	1.555	1.416

Table 28. Maximum L$_{max}$ values for Mississippi.

Maximum L$_{max}$ Values of 10 Directional WIM Sites in Mississippi

Load Effect		20	40	60	80	100	120	160	200
M-simple	1-Lane	1.687	1.679	1.666	1.674	1.678	1.796	1.989	2.010
	2-Lane	2.255	2.156	1.930	1.935	2.025	2.031	1.954	1.856
V-simple	1-Lane	1.683	1.689	1.790	1.781	1.957	2.083	2.158	2.133
	2-Lane	2.309	2.135	2.054	2.097	2.104	2.093	1.981	1.861
M-positive	1-Lane	1.618	1.659	1.660	1.646	1.626	1.791	1.955	2.012
	2-Lane	2.237	2.182	1.979	1.989	2.034	2.035	1.973	1.873
M-negative	1-Lane	1.905	1.816	2.164	1.972	1.733	1.466	1.240	1.186
	2-Lane	2.059	2.490	1.911	1.353	1.228	1.193	1.118	1.015
V-center	1-Lane	1.711	1.702	1.853	1.839	1.940	1.920	1.824	1.764
	2-Lane	2.260	2.086	2.054	2.069	2.071	1.864	1.635	1.467

Table 29. Maximum L_{max} values for Texas.

Maximum L_{max} Values of 8 Directional WIM Sites in Texas									
Load Effect		Span (ft)							
		20	40	60	80	100	120	160	200
M-simple	1-Lane	1.718	1.844	1.793	1.647	1.524	1.463	1.313	1.190
	2-Lane	1.966	1.763	1.598	1.557	1.600	1.611	1.559	1.462
V-simple	1-Lane	1.742	1.694	1.648	1.578	1.515	1.454	1.345	1.260
	2-Lane	1.996	1.655	1.706	1.776	1.785	1.759	1.666	1.554
M-positive	1-Lane	1.688	1.741	1.798	1.674	1.570	1.479	1.331	1.233
	2-Lane	1.937	1.698	1.579	1.561	1.609	1.612	1.575	1.490
M-negative	1-Lane	1.642	1.605	1.206	0.864	0.941	0.966	0.906	0.850
	2-Lane	1.567	2.028	1.536	1.098	0.978	0.993	0.952	0.838
V-center	1-Lane	1.666	1.706	1.670	1.569	1.447	1.242	1.057	0.966
	2-Lane	1.951	1.605	1.682	1.732	1.733	1.560	1.356	1.224

in this study. Appendix B contains the L_{max} results for all the WIM sites studied in this task.

Table 25 through Table 29 show, for each state studied in this task respectively, the maximum values of L_{max} calculated for each load effect and span length. (The maximum value shown in a cell in the table is the maximum for all WIM sites in that state.) Although in many cases the maximum L_{max} value for a two-lane event is larger than that of the equivalent one-lane event, this is not a generality that holds true for all load effects, all span lengths, or even all states. It is, however, evident that the truck traffic is state-dependent, resulting in a broad range of L_{max} values among the states.

Table 30 shows the 75-year L_{max} values used in the LRFD calibration. Here the L_{max} values remain fairly constant with span length and even with load effect. One apparent trend is for the L_{max} value of the two-lane event to be nearly 2×0.85 that of the equivalent one-lane event.

Discussion and Analysis of L_{max} Results

- The ratio of two-lane L_{max} divided by one-lane L_{max} is reasonably constant for shear and moments within a range of 1.05 to 1.13 (Figure 30).
- The ratio of $L_{max\ 2\text{-lane}}/L_{max\ 1\text{-lane}}$ for moments and shear of simple spans is relatively small, compared with the LRFD calibration data. This would indicate that in many cases the

single event may govern design load effects. This would also depend on the LRFD live-load distribution factors for one- and two-lane loaded conditions.

- Average L_{max} seems to decrease with span length (Figure 31) indicating that HL93 loading is not entirely consistent with current truck weight data.
- The spread in L_{max} is very high with a coefficient of variation (COV) 0.36 to 0.24 with a tendency to go lower with span length. This COV expresses the site-to-site variability. Also, the COV accounts for the extreme distribution property (obtained from the projections protocols). The one-lane COV is lower and decreases faster with span length than the two-lane COV.
- There seems to be no correlation between L_{max} and ADTT. R^2 is approximately zero for all the cases (Figures 32 through 36).

Calibrate Vehicular Load Factors for Bridge Design Strength I (Step 13.1)

Method I

An increase in maximum expected live load based on current WIM data can be compensated in design by raising the live-load factor in a corresponding manner. The calibration process adjusts the corresponding live-load factor by the ratios r_1 and r_2 of Equations 30 and 31, as shown in Equation 56.

Table 30. Seventy-five-year L_{max} values used in LRFD calibration.

75-year L_{max} Values Used in LRFD Calibration									
Load Effect		Span (ft)							
		20	40	60	80	100	120	160	200
M-simple	1-Lane	1.300	1.350	1.320	1.320	1.310	1.290	1.240	1.230
	2-Lane	2.120	2.340	2.300	2.280	2.260	2.240	2.180	2.160
V-simple	1-Lane	1.230	1.230	1.230	1.270	1.280	1.220	1.200	1.170
	2-Lane	2.120	2.180	2.220	2.260	2.280	2.200	2.140	2.080
M-negative	1-Lane	1.270	1.300	1.250	1.210	1.200	1.200	1.200	1.200
	2-Lane	2.280	2.400	2.300	2.240	2.220	2.220	2.220	2.220
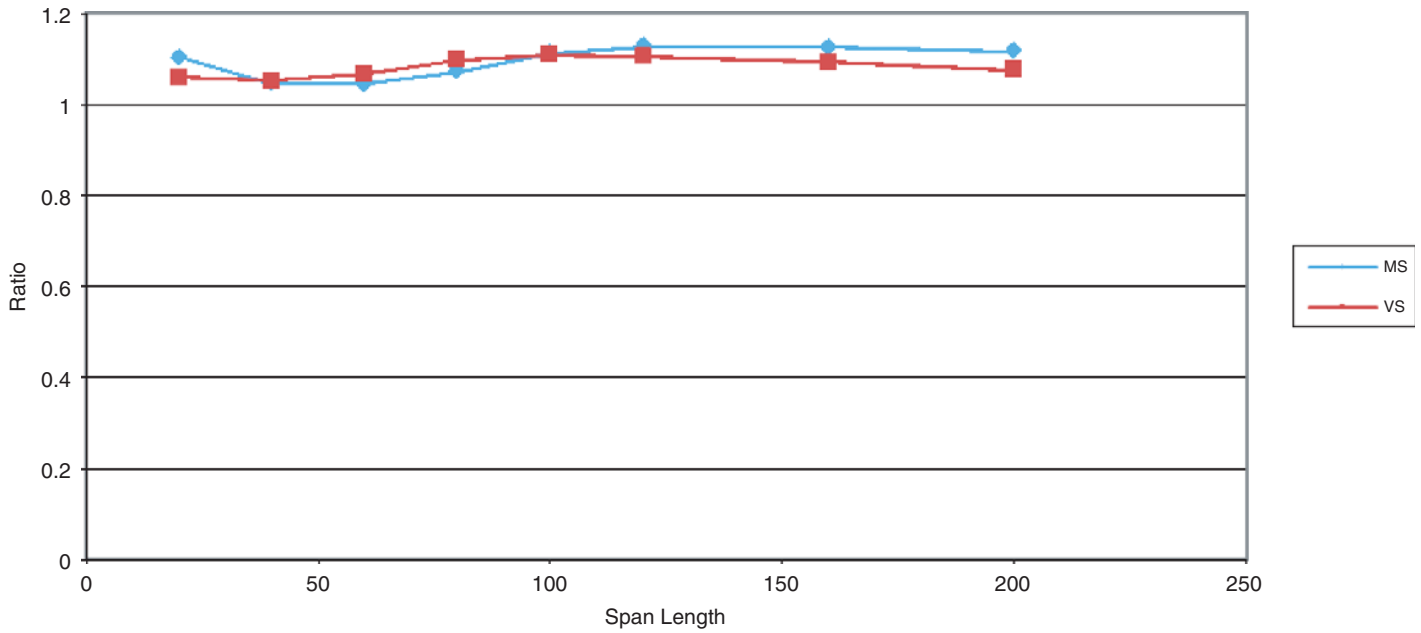
Figure 30. L_{max} for 2-lane/L_{max} for one-lane for moments and shear of simple spans.
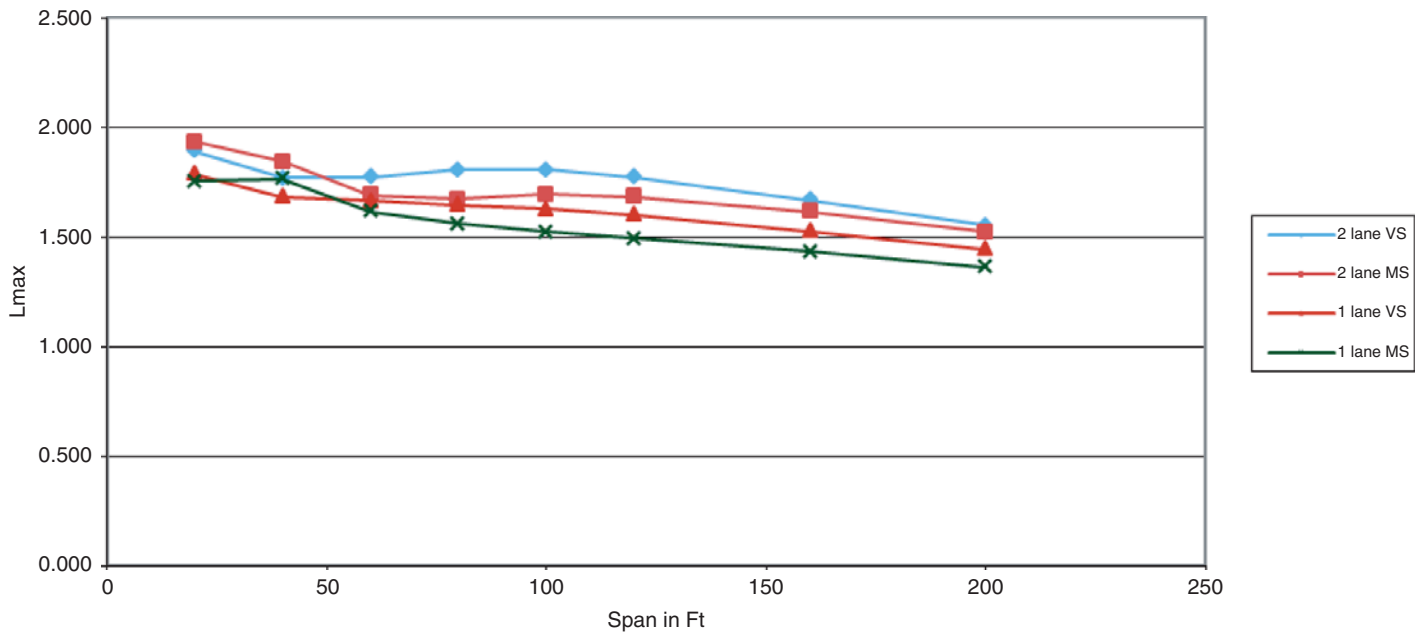
Figure 31. Average L_{max} vs. span length.
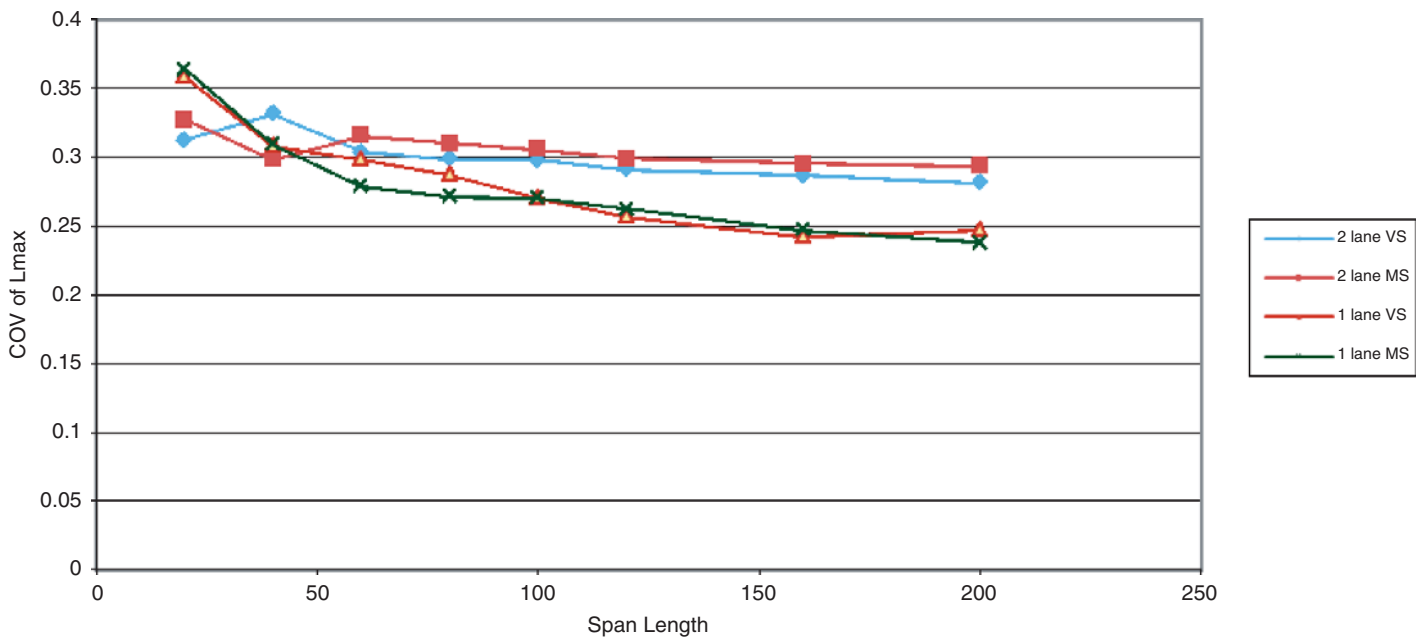
Figure 32. COV of L_{max} vs. span length.
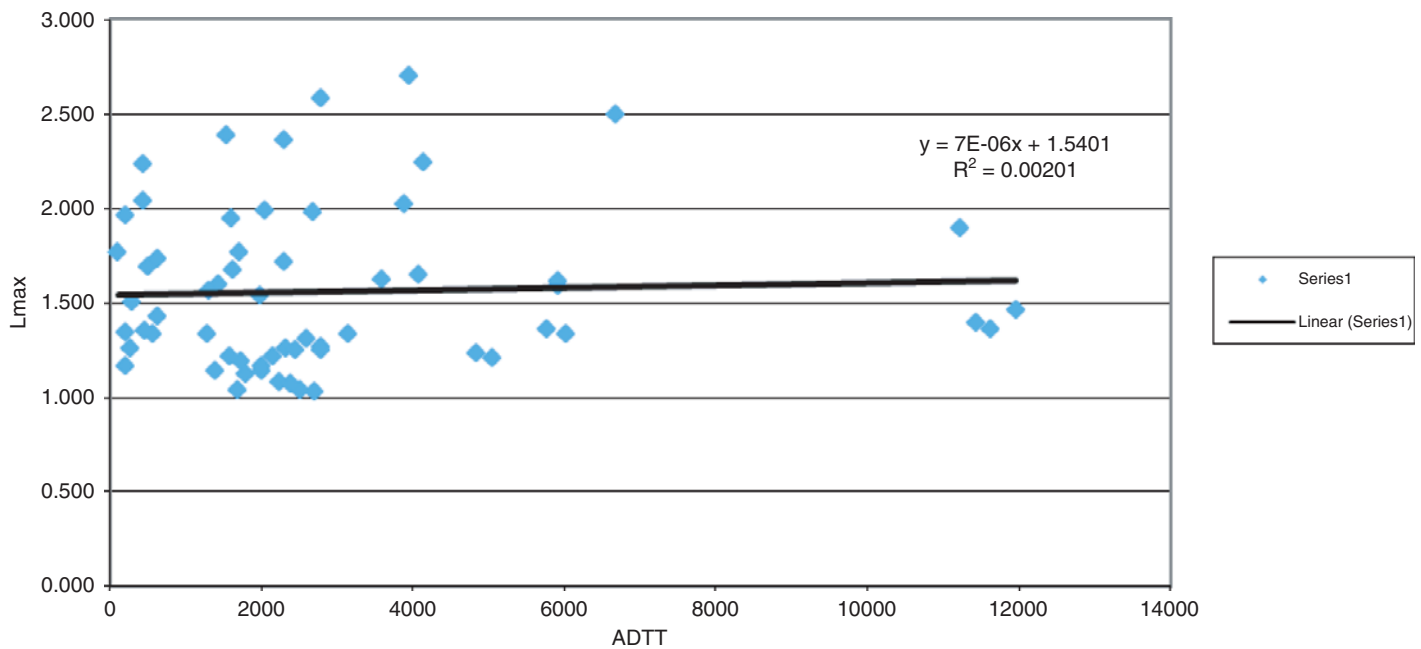
Figure 33. L_{max} vs. ADTT for one-lane simple span moment.
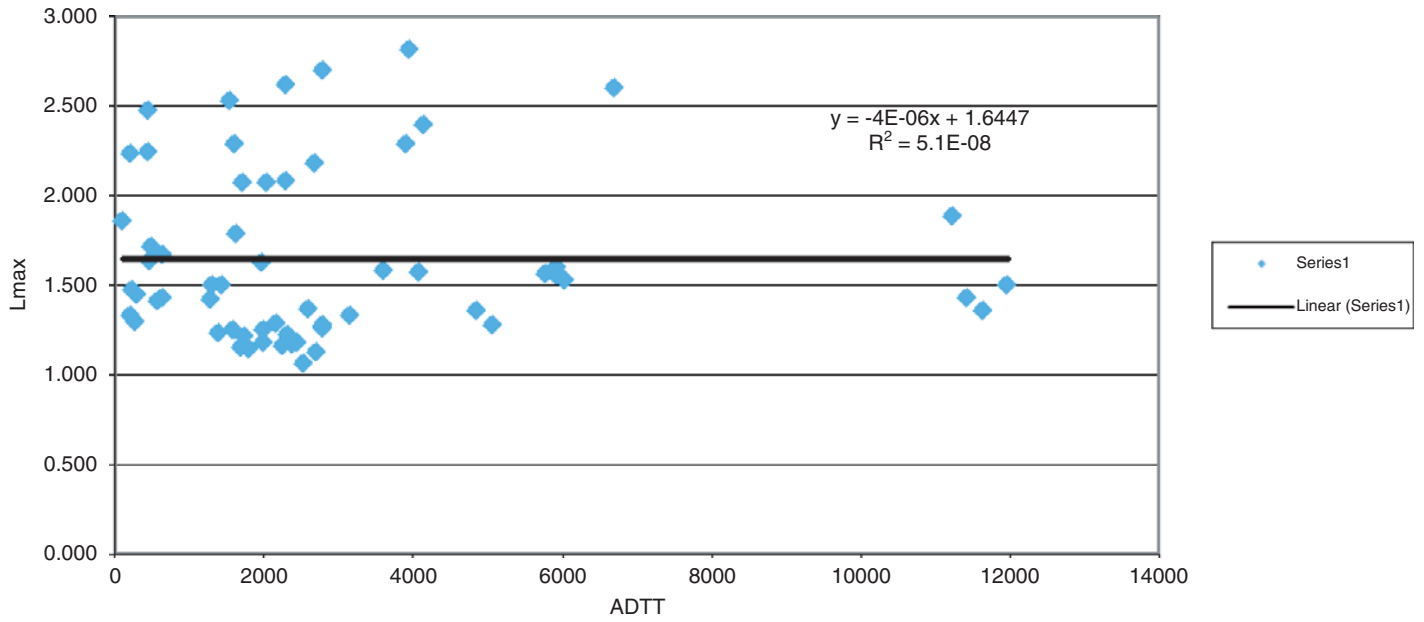
Figure 34. L_{max} **vs. ADTT for one-lane simple span shear.**
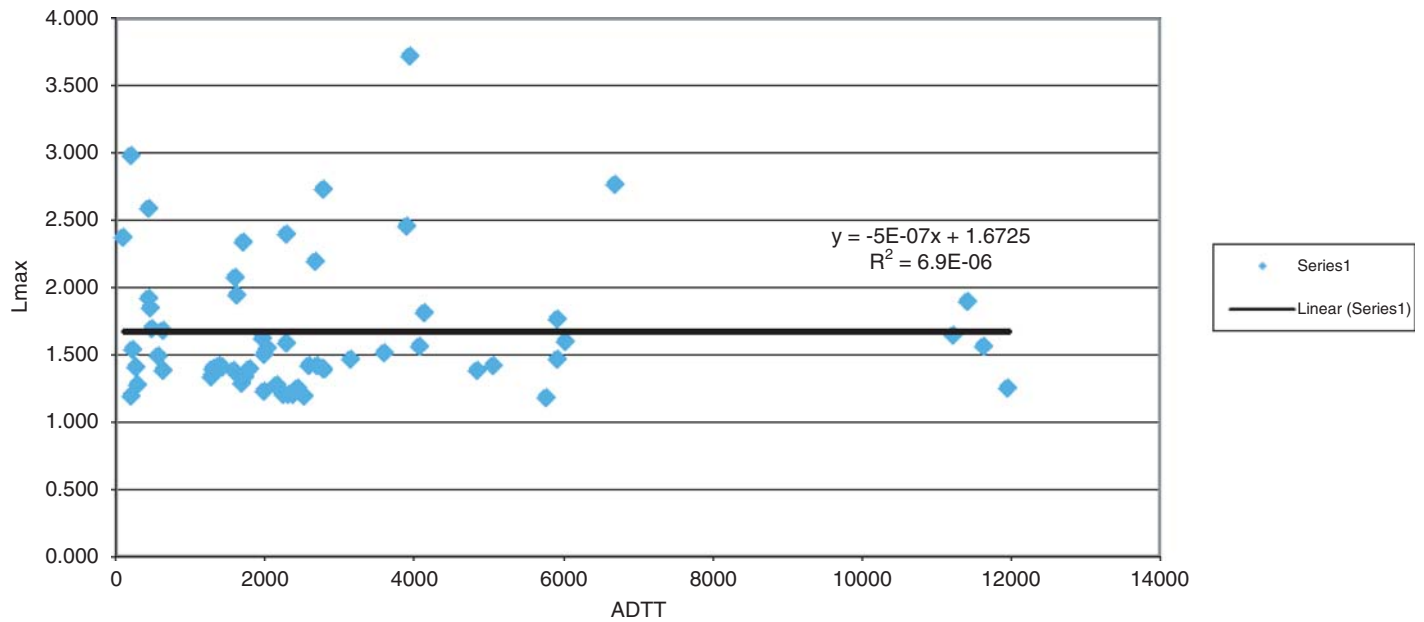
Figure 35. L_{max} **vs. ADTT for two-lane simple span moment.**
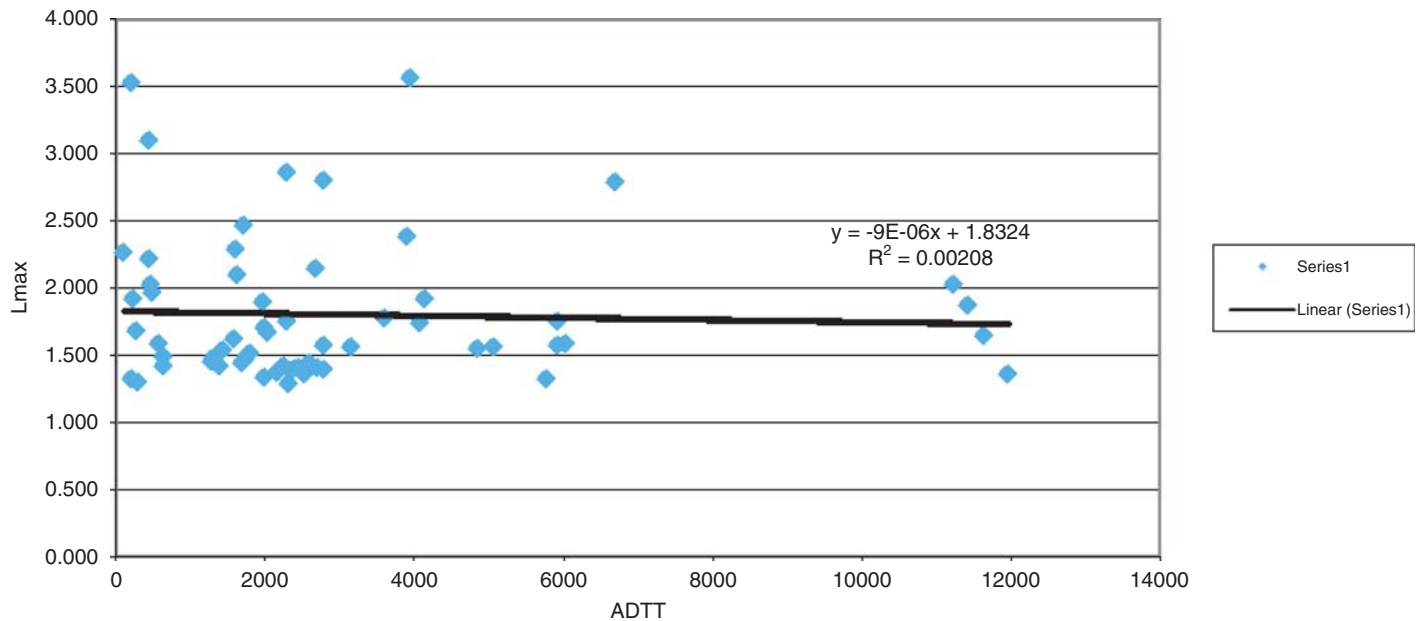
Figure 36. L_{max} vs. ADTT for two-lane simple span shear.

$$\gamma_{L,StrengthI} = 1.75 \times r_{StrengthI} \qquad (56)$$

The value r is taken to be the ratio of the L_{max} value as calculated from WIM data to the L_{max} value used in the LRFD calibration. It can be used to determine the effectiveness of HL93 for lifetime maximum loading. One key assumption with regard to this simplified procedure for adjusting live-load factors is that the site-to-site variability in L_{max} as measured by the COV is the same as that used during the AASHTO LRFD

calibration. In the AASHTO LRFD calibration, the overall live-load COV was taken as 20%.

Table 31 through Table 35 show, for each state studied in this task respectively, the maximum values of r calculated for each load effect and span length.

Summary of Method I Results. As with L_{max}, the value of r is state dependent. Unlike L_{max}, however, there is a significant—and consistent—difference between the r-values for one-lane

Table 31. Maximum r values for California.

Maximum r Values of 8 Directional WIM Sites in California									
		Span (ft)							
Load Effect		20	40	60	80	100	120	160	200
M-simple	1-Lane	1.530	1.211	1.070	1.055	1.031	1.016	0.990	0.950
	2-Lane	0.922	0.779	0.802	0.829	0.823	0.796	0.769	0.715
V-simple	1-Lane	1.513	1.241	1.206	1.124	1.087	1.106	1.048	1.004
	2-Lane	0.910	0.845	0.858	0.827	0.808	0.816	0.777	0.745
M-negative	1-Lane	1.259	1.198	1.091	1.112	1.042	0.898	0.783	0.705
	2-Lane	0.885	0.839	0.629	0.485	0.459	0.438	0.403	0.366

Table 32. Maximum r values for Florida.

Maximum r Values of 9 Directional WIM Sites in Florida									
		Span (ft)							
Load Effect		20	40	60	80	100	120	160	200
M-simple	1-Lane	2.200	1.904	1.692	1.697	1.663	1.637	1.564	1.463
	2-Lane	1.184	1.059	1.074	1.075	1.064	1.056	1.029	0.991
V-simple	1-Lane	2.402	2.045	1.997	1.886	1.789	1.798	1.673	1.585
	2-Lane	1.153	1.132	1.123	1.053	1.007	1.033	1.028	1.010
M-negative	1-Lane	2.079	1.797	1.446	1.307	1.163	0.996	0.854	0.798
	2-Lane	1.088	1.074	0.789	0.721	0.671	0.613	0.576	0.508

Table 33. Maximum r values for Indiana.

Maximum r Values of 12 Directional WIM Sites in Indiana									
Load Effect		Span (ft)							
		20	40	60	80	100	120	160	200
M-simple	1-Lane	1.771	1.635	1.464	1.436	1.419	1.400	1.373	1.330
	2-Lane	1.047	0.837	0.789	0.774	0.755	0.781	0.798	0.773
V-simple	1-Lane	1.969	1.690	1.544	1.483	1.437	1.466	1.406	1.383
	2-Lane	1.007	0.835	0.849	0.893	0.902	0.925	0.894	0.864
M-negative	1-Lane	1.465	1.475	1.286	1.244	1.085	0.961	0.841	0.783
	2-Lane	0.807	0.973	0.806	0.591	0.485	0.483	0.458	0.421

Table 34. Maximum r values for Mississippi.

Maximum r Values of 10 Directional WIM Sites in Mississippi									
Load Effect		Span (ft)							
		20	40	60	80	100	120	160	200
M-simple	1-Lane	1.298	1.244	1.262	1.268	1.281	1.392	1.604	1.634
	2-Lane	1.064	0.921	0.839	0.849	0.896	0.907	0.896	0.859
V-simple	1-Lane	1.368	1.373	1.455	1.402	1.529	1.707	1.798	1.823
	2-Lane	1.089	0.979	0.925	0.928	0.923	0.951	0.926	0.895
M-negative	1-Lane	1.500	1.397	1.731	1.630	1.444	1.222	1.033	0.988
	2-Lane	0.903	1.038	0.831	0.604	0.553	0.537	0.504	0.457

Table 35. Maximum r values for Texas.

Maximum r Values of 8 Directional WIM Sites in Texas									
Load Effect		Span (ft)							
		20	40	60	80	100	120	160	200
M-simple	1-Lane	1.322	1.366	1.358	1.248	1.163	1.134	1.059	0.967
	2-Lane	0.927	0.753	0.695	0.683	0.708	0.719	0.715	0.677
V-simple	1-Lane	1.416	1.377	1.340	1.243	1.184	1.192	1.121	1.077
	2-Lane	0.942	0.759	0.768	0.786	0.783	0.800	0.779	0.747
M-negative	1-Lane	1.293	1.235	0.965	0.714	0.784	0.805	0.755	0.708
	2-Lane	0.687	0.845	0.668	0.490	0.441	0.447	0.429	0.377

events and two-lane events. The r-values for one-lane events are significantly greater than those for two-lane events. Whereas the maximum r-values for two-lane events exceed 1.0 in some cases, its maximum value among all WIM sites is 1.184. This indicates that the HL93 loading defined in the LRFD specification is fairly adequate in modeling the lifetime maximum loading on a span with two lanes loaded. For one-lane events, the maximum r-values are often greater than 1.5 with a maximum value among all WIM sites of 2.402. This indicates that the HL93 loading defined in the LRFD specification underestimates the lifetime maximum loading on a span with only one lane loaded. It should be noted that HL93 load effects are being compared with routine truck traffic at a site, defined as all trucks with six or fewer axles that will include legal loads, illegal overloads, and routine permits. These unanalyzed routine permits are a form of exclusion traffic for a particular state and should be enveloped by the HL93 design live-load model. This simplified procedure for adjusting live-load factors assumes that the site-to-site variability in L_{max} is within the AASHTO LRFD calibration limits. This needs to be verified as a precondition for the use of Method I.

Adjustment of Live-Load Factors Using Method II

An example illustrating the application of the protocols for adjusting the load factors for Strength I using the reliability-based approach is presented. The illustration is provided for a set of bridges varying in span length between 60 ft to 200 ft with beam spacing varying between 4 ft and 12 ft. Composite steel and prestressed concrete simple span bridges are selected.

The procedure follows the protocols provided in Step 13.1, Method II, using the equations of Chapter 2, and the results are given in Tables 40 through 45. For example, using the data provided by Nowak (1999) for a typical 60-ft simple span composite steel bridge with beams at 4-ft spacing, the wearing surface dead load is estimated to be $D_W = 49$ kip-ft (referred to as D_3 in Tables 36 and 37), the other dead loads are combined into $D_C = 284$ kip-ft (with $D_{C1}=39$ kip-ft for factory-made members, referred to as D_1 in Tables 36 and 37, and $D_{C2} = 245$ kip-ft for cast in place members referred to as D_2 in Tables 36 and 37).

Assuming that $\left(\dfrac{K_g}{12Lt_s^3}\right) = 1.0$ as suggested by the AASHTO LRFD (2007) for the cases when the detailed design is not

Table 36. Calculation of nominal resistance, R_n, using current LRFD for a sample of typical composite steel bridges.

Composite steel		Dead Loads			HL-93		Required Nominal Resist.	
Span	Spacing	D1	D2	D3	Truck load	lane load	two lanes	one lane
ft	ft	kip-ft	kip-ft	kip-ft	kip-ft	kip-ft	kip-ft	kip-ft
60	4	39	245	49	805	288	1430.07	1210.44
60	6	48	335	73	805	288	1905.25	1580.00
60	8	70	414	97	805	288	2362.18	1931.67
60	10	84	521	122	805	288	2831.06	2295.99
60	12	103	639	146	805	288	3307.38	2668.51

Composite steel			Dead Loads		HL-93		Required Nominal Resist.	
Span	Spacing	D1	D2	D3	Truck load	lane load	one lane	two lanes
ft	ft	kip-ft	kip-ft	kip-ft	kip-ft	kip-ft	kip-ft	kip-ft
120	4	502	981	194	1882	1152	4552.49	3925.44
120	6	607	1341	292	1882	1152	6019.48	5112.16
120	8	650	1656	389	1882	1152	7302.59	6119.07
120	10	681	2083	486	1882	1152	8676.66	7220.72
120	12	773	2556	583	1882	1152	10158.57	8433.60

Composite steel			Dead Loads		HL-93		Required Nominal Resist.	
Span	Spacing	D1	D2	D3	Truck load	lane load	one lane	two lanes
ft	ft	kip-ft	kip-ft	kip-ft	kip-ft	kip-ft	kip-ft	kip-ft
200	4	2780	2725	540	3320	3200	12317.82	10987.92
200	6	3303	3725	810	3320	3200	16016.30	14116.20
200	8	3790	4600	1080	3320	3200	19422.06	16963.58
200	10	4190	5788	1350	3320	3200	23046.27	20039.36
200	12	4875	7100	1620	3320	3200	27132.98	23586.16

Table 37. Calculation of nominal resistance, R_n, using current LRFD for a sample of typical prestressed concrete bridges.

Prestressed Concrete			Dead Loads		HL-93		Required Nominal Resist.	
Span	Spacing	D1	D2	D3	Truck load	lane load	two lanes	one lane
ft	ft	kip-ft	kip-ft	kip-ft	kip-ft	kip-ft	kip-ft	kip-ft
60	4	262	245	49	805	288	1708.82	1489.19
60	6	262	335	73	805	288	2172.75	1847.50
60	8	262	414	97	805	288	2602.18	2171.67
60	10	262	521	122	805	288	3053.56	2518.49
60	12	262	639	146	805	288	3506.13	2867.26

Prestressed Concrete			Dead Loads		HL-93		Required Nominal Resist.	
Span	Spacing	D1	D2	D3	Truck load	lane load	one lane	two lanes
ft	ft	kip-ft	kip-ft	kip-ft	kip-ft	kip-ft	kip-ft	kip-ft
120	4	1899	981	194	1882	1152	6298.74	5671.69
120	6	1899	1341	292	1882	1152	7634.48	6727.16
120	8	1899	1656	389	1882	1152	8863.84	7680.32
120	10	1899	2083	486	1882	1152	10199.16	8743.22
120	12	1899	2556	583	1882	1152	11566.07	9841.10

Prestressed Concrete			Dead Loads		HL-93		Required Nominal Resist.	
Span	Spacing	D1	D2	D3	Truck load	lane load	one lane	two lanes
ft	ft	kip-ft	kip-ft	kip-ft	kip-ft	kip-ft	kip-ft	kip-ft
200	4	5650	2725	540	3320	3200	15905.32	14575.42
200	6	5650	3725	810	3320	3200	18950.05	17049.95
200	8	5650	4600	1080	3320	3200	21747.06	19288.58
200	10	5650	5788	1350	3320	3200	24871.27	21864.36
200	12	5650	7100	1620	3320	3200	28101.73	24554.91

Table 38. L_{max} values for one lane for the moment effect of simple-span beams.

				1-Lane Event Lmax for Simple Span Moment								Max
				Span Length (ft)								
State	Site ID	Direction	ADTT	20	40	60	80	100	120	160	200	Value
CA	0001	E/N	5058	1.370	1.278	1.239	1.206	1.173	1.164	1.137	1.086	1.370
CA	0001	W/S	4839	1.400	1.354	1.305	1.237	1.174	1.161	1.124	1.069	1.400
CA	0003	E	2790	1.190	1.216	1.293	1.268	1.219	1.191	1.149	1.106	1.293
CA	0004	W	3149	1.365	1.354	1.382	1.337	1.253	1.189	1.114	1.051	1.382
CA	0059	S	11627	1.340	1.291	1.368	1.358	1.338	1.293	1.212	1.127	1.368
CA	0060	N	11432	1.989	1.635	1.413	1.392	1.351	1.311	1.227	1.168	1.989
CA	0072	E/N	2318	1.138	1.228	1.297	1.255	1.221	1.140	1.052	1.003	1.297
CA	0072	W/S	2159	1.217	1.227	1.272	1.213	1.149	1.094	1.046	0.976	1.272
			Min Value	1.138	1.216	1.239	1.206	1.149	1.094	1.046	0.976	
			Avg Value	1.376	1.323	1.321	1.283	1.235	1.193	1.132	1.073	
			Max Value	1.989	1.635	1.413	1.392	1.351	1.311	1.227	1.168	
			stand. Dev.	0.266	0.137	0.060	0.070	0.076	0.074	0.065	0.063	0.101
			COV	0.193	0.104	0.045	0.054	0.061	0.062	0.058	0.059	0.057

available, Equation 34 will yield a distribution factor D.F. = 0.42 for two lanes loaded and Equation 33 gives D.F. = 0.33 for one lane loaded. Given that the AASHTO HL93 lane load moment for a 60-ft simple span is 288 kip-ft and the HL93 truck load is 805 kip-ft, and applying the dynamic allowance factor IM = 1.33 on the truck load, Equation 32 would lead to a nominal required resistance for a single beam R_n=1430 kip-ft for the two-lane case and R_n=1210 kip-ft for the one lane case. Since in this case the R_n value for two lanes is higher than that obtained for one-lane loading, the two-lane case governs the design.

Similar calculations can be executed to find the required nominal bending moment capacity of steel and prestressed concrete bridges having different span lengths and beam spacings. For example, Tables 36 and 37 show the nominal bending moment resistances obtained using Equation 32 with the AASHTO LRFD-specified live-load factor γ_L = 1.75 for a sample of simple-span bridge configurations. The configurations selected and the corresponding values for the dead weights are adopted from the report of the AASHTO LRFD calibration study (Nowak 1999).

Live-Load Effect Modeling

The work performed as part of NCHRP 12-76 consisted of collecting WIM truck traffic data on a variety of sites within the United States and using these data to project for the maximum expected live-load effects, L_{max}, over the 75-year design life of a new bridge. For example, Table 38 provides a set of L_{max} values obtained for the maximum bending moments of 60-ft, 120-ft, and 200-ft simple-span bridges from eight sites in California. The L_{max} values were calculated for one lane of traffic and two lanes of traffic, and they are normalized with respect to the effect of one lane of HL93 loading. For example, the results of Table 38 for the 60-ft span show that, on average, the 75-year maximum load effect will be equal to 1.321 times the static load effect of the HL93 design load. The values vary from site to site, showing a standard deviation for site-to-site variability of 0.060 or as expressed in terms of a coefficient of variation $V_{site-to-site}$ = 4.5%. Table 39 gives the calculated L_{max} values for the same sites for the cases when two lanes are loaded simultaneously. Note that the 60-ft span for the two-lane L_{max} is, on average, equal to 1.44 times the effect of one lane of

Table 39. L_{max} values for two lanes for the moment effect of simple-span beams.

				2-Lane Event Lmax for Simple Span Moment								Max
				Span Length (ft)								
State	Site ID	Direction	ADTT	20	40	60	80	100	120	160	200	Value
CA	0001	E/N	5058	1.663	1.706	1.515	1.412	1.456	1.450	1.386	1.299	1.706
CA	0001	W/S	4839	1.592	1.475	1.324	1.382	1.445	1.460	1.410	1.341	1.592
CA	0003	E	2790	1.447	1.421	1.429	1.392	1.374	1.332	1.281	1.213	1.447
CA	0004	W	3149	1.575	1.441	1.440	1.460	1.515	1.529	1.479	1.388	1.575
CA	0059	S	11627	1.678	1.665	1.490	1.553	1.562	1.578	1.506	1.419	1.678
CA	0060	N	11432	1.955	1.823	1.844	1.891	1.859	1.783	1.676	1.544	1.955
CA	0072	E/N	2318	1.368	1.235	1.172	1.199	1.224	1.233	1.177	1.122	1.368
CA	0072	W/S	2159	1.499	1.428	1.335	1.265	1.286	1.247	1.198	1.125	1.499
			Min Value	1.368	1.235	1.172	1.199	1.224	1.233	1.177	1.122	
			Avg Value	1.597	1.524	1.444	1.444	1.465	1.452	1.389	1.306	
			Max Value	1.955	1.823	1.844	1.891	1.859	1.783	1.676	1.544	
			stand. Dev.	0.179	0.191	0.196	0.211	0.195	0.183	0.168	0.148	
			COV	0.112	0.125	0.136	0.146	0.133	0.126	0.121	0.113	0.127

76

HL93 with a site-to-site variability expressed through a COV, $V_{site-to-site} = 13.6\%$. The higher COV for the two-lane effects is partially due to the differences in the number of two-lane events collected at each site over the 1-year WIM data collection period as compared to the number of data samples collected for single-truck events in the main traffic lane. Other factors that influence the differences in the COVs include the ADTT at the sites, the frequency of heavy legal and overloaded vehicles (illegal, exclusion, or permit) in the truck traffic stream, and the probability of having two lanes loaded by such vehicles.

In addition to the site-to-site variability, the uncertainties associated with the estimated values for L_{max} include the uncertainties within a site due to the random nature of L_{max} and the fact that the WIM data histograms do not necessarily include all of the extreme load events that may occur within the 75-year design period of the bridge. An analysis of the results of the projections shows that the uncertainties within a site are associated with a COV on L_{max} on the order of $V_{projection} = 3.5\%$ for the projection of the one-lane maximum effect and a COV of $V_{projection} = 5\%$ for the two side-by-side load effect. $V_{projection}$ was obtained from the analysis of the WIM data described in the draft protocols, by taking the ratio of the standard deviation σ_{max} obtained from Equation 29 divided by the mean $L_{max} = \mu_{max} = $ of Equation 28.

Additional uncertainties are associated with L_{max} due to the limited number of data points used in the projections and the confidence levels associated with the number of sample points. Using the +/−95% confidence limits, it is estimated that the COV is on the order of $V_{data} = 2\%$ for the one-lane case and about $V_{data} = 3\%$ for the two-lane case. V_{data} is an estimate obtained from the upper and lower 95% confidence intervals calculated as presented earlier in Step 5.3, Assess the Statistical Adequacy of Traffic Data. The research team took the upper and lower 95% values and assumed that they fall within +/− 1.96 standard deviations from the mean. So, by dividing the difference between the mean value and the upper and lower 95% values by 1.96 estimates of the standard deviation were obtained that, when divided by the mean value, gave estimates of the COV. For example, the upper and lower 95% limits for the WIM data collected at the I-81 site in New York State for L_{max} of the one lane loading for the moment at the midpoint of a 60-ft simple span are 1.964 and 1.839. The mean L_{max} for the one lane loading case is obtained as 1.906. Thus, one estimate of the standard deviation is obtained as $(1.906 − 1.839)/1.96 = 0.034$. The estimate of the COV, V_{data}, becomes $0.034/1.906 = 0.018$ or about 1.8%. Another estimate is obtained as $(1.964 − 1.906)/1.96/1.906 = 1.6\%$. The final V_{data} used is rounded up to 2%. Similarly for the two-lane loading, the mean is $L_{max} = 3.276$, the lower 95% limit is 3.058, and the upper 95% limit is 3.462. One estimate for the standard deviation is $(3.276 − 3.058)/1.96 = 0.111$ and the estimate for the COV is $0.111/3.276 = 3.40\%$. Another estimate is obtained as $(3.462 − 3.276)/1.96/$

$3.276 = 2.90\%$ and the final V_{data} used is 3%. Strictly speaking, the approach followed for finding V_{data} is not exact, but the V_{data} calculated gives some measure of the uncertainty related to the size of the data sample.

Nowak (1999) also observed that the dynamic amplification factors augmented the L_{max} load effect by an average of 13% for one lane of traffic and by 9% for side-by-side trucks. The dynamic amplification also resulted in a COV of $V_{IM} = 9\%$ on the one-lane load effect and $V_{IM} = 5.5\%$ on the two-lane effect. In previous studies on live-load modeling, Ghosn and Moses (1985) included the uncertainties in estimating the lane distribution factor, which was associated with a COV equal to $V_{DF} = 8\%$ based on field measurements on typical steel and prestressed concrete bridges. This information is used in Equations 35 and 36 to find the mean value of the live load and the COV.

For example, the application of Equation 35 for the average load effect on a 60-ft simple-span bridge from the California sites with beams at 4 ft would lead to the following:

For one lane:

$$\overline{LL} = L_{max\ bean} \times HL_{93} = 1.32 \times (288 + 805) \times 1.13 \times 0.33/1.2$$
$$= 448 \text{ kip-ft}$$

For two lanes:

$$\overline{LL} = L_{max\ bean} \times HL_{93} = 1.44 \times (288 + 805) \times 1.09 \times 0.42/2$$
$$= 360 \text{ kip-ft}$$

For the one-lane case, $L_{max} = 1.32$ is obtained from Table 38 as the average value for the California sites for 60-ft spans. $L_{max} = 1.44$ for two lanes is obtained from Table 39 as the average value for the 60-ft spans from all of the sites.

Note that the mean live-load effect for the one-lane case is higher than that of the two-lane case. This is due to the fact that the number of side-by-side events is generally low compared to the number of single-lane events, thus the projection to the 75-year maximum for one lane of traffic would lead to the possibility of having a very heavy single truck load (1.32 times the effect of the HL93 load) as compared to having two very heavy side-by-side trucks, the maximum for each one being on the order of 0.72 (1.44/2) times the effect of the HL93 live load. Also, the load distribution factor D.F. indicates that the effect of a single truck would more likely load a single beam by 27% of the weight of one truck (D.F. = 0.33/1.2 = 0.27) as compared to the weights of two trucks side-by-side, which would be more evenly spread over all the beams of the bridge such that the most loaded beam would carry 21% of the lane load (D.F = 0.42/2 = 0.21). Furthermore, the dynamic amplification peaks of two trucks are not likely to coincide due to the different natural frequencies, which would lead to a lower

overall dynamic allowance factor for the two-lane case (1.09) as compared to the one-lane case (1.13). Note that in these calculations and following the procedure of Nowak (1999), it has been assumed that the load distribution factors provided by AASHTO LRFD are the expected (mean) values. It should also be mentioned that the data for the dynamic allowance and for the load distribution factors as used by Nowak (1999) are based on very limited data and much more research is needed on these topics to study how these factors change from site to site and how they relate to the truck weights and traffic data. However, these issues are beyond the scope of this study and in this case, this study uses the same data applied during the AASHTO LRFD calibration.

The application of Equation 36 for the 60-ft L_{max} yields the following:

For two lanes:

$$V_{LL} = \sqrt{(13.5\%)^2 + (5\%)^2 + (3\%)^2 + (5.5\%)^2 + (8\%)^2} = 18\%$$

For one lane:

$$V_{LL} = \sqrt{(4.5\%)^2 + (3.5\%)^2 + (2\%)^2 + (9\%)^2 + (8\%)^2} = 13\%$$

$V_{site-to-site}$ values of 4.5% and 13.5% for one-lane and two-lane cases are respectively obtained from Tables 39 and 40 for the 60-ft spans. The standard deviation for the two-lane case becomes $\sigma_{LL} = V_{LL} * \overline{LL} = 65$ kip-ft and for the one-lane case it is $\sigma_{LL} = 58$ kip-ft.

Thus, the COV of the two-lane effect for the California sites is comparable to the V_{LL}=19% to 20% obtained by Ghosn and Moses (1985) and subsequently used by Nowak (1999) during the calibration of the AASHTO LRFD specifications. Note that the COV for the single-lane effect is lower than that of the two-lane effect, indicating that the estimation of the maximum load effect for one lane is associated with lower levels of uncertainty. The difference in the two V_{LL} COVs is primarily due to the site-to-site variability, which is much higher for the two-lane loading as compared to that for the one-lane loading.

Modeling of Other Random Variables

The application of Equations 37 and 38 for the beams of the 60-ft composite steel bridge at 4-ft spacing will yield mean dead loads as follows:

$$\overline{D_{C1}} = 40 \text{ kip-ft}, \overline{D_{C2}} = 257 \text{ kip-ft and } \overline{D_W} = 49 \text{ kip-ft.}$$

The standard deviations are $\sigma_{DC1} = 3.2$ kip-ft, $\sigma_{DC2} = 25.7$ kip-ft, and $\sigma_{DW} = 12.3$ kip-ft. The mean of the total dead load be-

comes $\overline{DL} = 346$ kip-ft and, using the square root of the sum of the square, the standard deviation for the total dead load is $\sigma_{DL} = 29$ kip-ft. The mean nominal resistance is as follows:

For a two-lane bridge: $\overline{R} = 1602$ kip-ft and

For a one-lane bridge: $\overline{R} = 1355$ kip-ft.

The standard deviation for the resistance for the two-lane bridge is $\sigma_R = 160$ kip-ft and for the one-lane bridge, $\sigma_R = 136$ kip-ft. For the maximum moment of the sample of simple-span bridges studied in this report, Equations 37 and 38 will yield the mean and standard deviation values provided in Tables 36 and 37 for the bending moment of simple-span composite steel and prestressed concrete bridges.

Calculation of Reliability Index and Calibration of Live-Load Factor

The adjustment of the live-load factors requires the calculation of the reliability index for different values of the live-load factor γ_L. The γ_L that produces reliability index values as close to the target as possible for all material types, spans, and geometric configurations will be adopted as the final γ_L. Using $\gamma_L = 1.75$ for the one-lane 60-ft bridge with beams at 4-ft spacing, the reliability index is calculated from Equation 40 as

One lane: $\quad \beta = \dfrac{1355 - 346 - 448}{\sqrt{136^2 + 29_L^2 + 58_L^2}} = 3.72$

For the two-lane 60-ft bridge with beams at 4-ft spacing, the reliability index is calculated as

Two lanes: $\quad \beta = \dfrac{1602 - 346 - 360}{\sqrt{160^2 + 29^2 + 65^2}} = 5.12$

The results for this example indicate that, based on the WIM data collected at the California sites, the use of the AASHTO LRFD strength design equation with a live-load factor $\gamma_L = 1.75$ and the HL93 loading leads to a reliability index of $\beta = 3.72$ for the 75-year design life of a 60-ft simple-span steel bridge with beams at 4-ft spacing. In this case, the one-lane load governs the safety of the bridge beams, producing a reliability index value of $\beta = 3.72$, which is higher than the target $\beta = 3.50$ set during the calibration of the AASHTO LRFD specifications. It should be emphasized that the target $\beta = 3.50$ was set during the AASHTO LRFD code calibration based on the observation made at the time that, under the generic live-loading data, typical bridge configurations that were designed to satisfy the AASHTO LRFD specifications produced an average reliability index $\beta = 3.50$. Thus, the new LRFD code was developed in order for new designs to match this $\beta = 3.50$ as closely as possible for all bridge spans, configurations, and material types.

The two-lane loading leads to a much higher reliability index value of $\beta = 5.12$. This indicates that for the two-lane case, the AASHTO LRFD is conservative.

It is noted that for the sake of simplicity this report assumed that the resistance, dead load and live load follow normal (Gaussian) distributions. The work of Nowak (1999) assumed that the resistance is lognormal while the combination of all the loads is normal. A preliminary sensitivity analysis was performed indicating that the normal model produces lower reliability index values than the lognormal model. The calculation of the reliability index can be executed using Monte Carlo simulations (or other simulation techniques) if the probability distributions of all of the random variables are available. Previous sensitivity analyses performed by this research team have demonstrated that the calibration of LRFD design equations is not sensitive to the probability distribution type used as long as the new equations are designed to match an average reliability index calculated using the same models and probability distributions (Ghosn and Moses 1985, 1986).

California Data. Tables 40 and 41 show the reliability index values obtained for the maximum bending moment of a sample of simple-span steel composite and prestressed bridge configurations. The results show that for the California truck traffic conditions, the reliability index for one lane is on the average equal to $\beta = 3.55$ which is close to the target $\beta = 3.50$. For two lanes of truck traffic, the average reliability index is $\beta = 4.63$. This indicates that for the two-lane loading of California bridges, the current AASHTO LRFD is conservative producing higher reliability index values than the target $\beta = 3.50$ set by the AASHTO LRFD code writers. The range of the β's however is large varying between a $\beta = 5.32$ for short span prestressed concrete bridges with closely spaced beams to $\beta = 4.0$ for long span prestressed concrete bridges with closely spaced beams. The fact that the loading of the short-span bridges is dominated by the live loads while the long span bridges' loading is dominated by the dead load indicates that for California bridges, the HL93 nominal design live load is conservative.

If one wishes to reduce the reliability index for the two-lane cases and achieve an average reliability index for the two-lane cases equal to the target β=3.50, then a live-load factor $\gamma_L = 1.20$ should be used. This would mean that the HL93 loading should be associated with a multiple lane reduction factor of 1.46 (1.75/1.20) when checking the design for two lanes of traffic. Alternatively, for the California WIM data, one could keep the current AASHTO LRFD live-load factor $\gamma_L = 1.75$ and accept the fact that the design will yield the target reliability index for one lane of traffic with the understanding that the design would be conservative for multiple lanes.

The adjusted $\gamma_L = 1.20$ for the two-lane loading conditions is obtained by trial and error using the steps provided in 13.1,

Method II. These steps are based on having established a representative sample of bridge configurations that represent the most common bridge spans, types, and configurations in the state and having predetermined an appropriate reliability index target β_{target}, that bridges evaluated using the adjusted live-load factor should meet.

In usual reliability-based adjustments of design and evaluation equations, the reliability index after adjusting the live-load factor should match the target reliability, β_{target}, as closely as possible for all representative span ranges, bridge types, loading cases, etc. Given the large spread in the calculated reliability index values observed in Tables 40 and 41, this may not be possible to achieve by only adjusting the live-load factor. Furthermore, the sample of bridges selected for analysis may not actually be representative of the California bridges. However, to illustrate the process, the steps provided in 13.1 outline a reliability-based live-load adjustment procedure that assumes that the target reliability index has already been established as $\beta_{target} = 3.5$ for the sample of bridges analyzed in the previous section, and the goal of the trial and error analysis process is to adjust the live-load factor γ_L so that the average reliability index of the bridges analyzed after adjusting the live-load factor will produce the target index.

Florida Data. The results presented above for the California WIM data may not be consistent with the data from other states or jurisdictions. The differences are mainly due to the legal truck weight limits or exemptions and the permit overload frequencies and weight regulations that may vary from state to state. For example, if the L_{max} values generated from the Florida WIM data sites are used as input for the live-load modeling, the reliability index values shown in Tables 42 and 43 are obtained. These tables show that the reliability index for one lane of loading drops to an average of $\beta = 2.58$. The two-lane L_{max} would lead to an average reliability index $\beta = 3.96$. The latter value is still higher than the target $\beta = 3.50$ while the one-lane reliability is lower than the target. It is noted that the Florida data shows high variations from the results of different sites leading to a high COV for L_{max} and subsequently lower reliability index values than those observed from the California data. It is noted that if the live-load factor is raised to $\gamma_L = 2.37$ the reliability indexes for the Florida sites would increase to $\beta = 3.50$ for the one-lane cases, and $\beta = 4.95$ for the two-lane cases, bringing the reliability indexes more in line with the California results.

Indiana Data. Using the L_{max} values generated from the Indiana WIM data sites, the reliability index values shown in Tables 44 and 45 are obtained. These tables show that the reliability index for one lane of loading is, on average, equal to $\beta = 3.16$ for one-lane loading. The two-lane L_{max} would lead to an average reliability index of $\beta = 4.71$. The latter value is higher than the target $\beta = 3.5$ while the one-lane reliability is

Table 40. Reliability index calculation for bending moment of simple span composite steel bridges based on California WIM data.

Span	Spacing	Ave. Res. 1	Av. Res. 2	σ Res. 1	σ Res. 2	Mean DL	σ DL	Mean LL 1	Mean LL 2	σ LL 1	σ LL 2	beta 1-lane	beta 2-lane
60	4	1356	1602	136	160	346	28	447	362	60	64	3.73	5.11
60	6	1770	2134	177	213	474	38	567	476	76	84	3.71	5.09
60	8	2163	2646	216	265	604	48	675	583	91	103	3.69	5.07
60	10	2572	3171	257	317	756	61	776	684	105	121	3.66	5.02
60	12	2989	3704	299	370	923	74	870	782	117	138	3.63	4.97
120	4	4396	5099	440	510	1741	117	949	904	134	153	3.60	4.50
120	6	5726	6742	573	674	2325	160	1193	1181	169	200	3.57	4.49
120	8	6853	8179	685	818	2797	199	1414	1440	200	244	3.57	4.50
120	10	8087	9718	809	972	3375	247	1618	1686	229	286	3.53	4.47
120	12	9446	11378	945	1138	4063	301	1811	1923	256	326	3.49	4.42
200	4	12306	13796	1231	1380	6265	377	1630	1611	228	258	3.38	4.07
200	6	15810	17938	1581	1794	8123	500	2035	2095	285	335	3.36	4.08
200	8	18999	21753	1900	2175	9814	614	2401	2547	336	408	3.35	4.09
200	10	22444	25812	2244	2581	11743	749	2740	2977	384	476	3.32	4.06
200	12	26416	30389	2642	3039	14096	906	3059	3390	428	542	3.28	4.01

Table 41. Reliability index calculation for bending moment of simple span prestressed concrete bridges based on California WIM data.

Span	Spacing	Ave. Res. 1	Av. Res. 2	σ Res. 1	σ Res. 2	Mean DL	σ DL	Mean LL 1	Mean LL 2	σ LL 1	σ LL 2	beta 1-lane	beta 2-lane
60	4	1564	1794	125	144	576	34	447	362	60	64	3.78	5.32
60	6	1940	2281	155	183	695	44	567	476	76	84	3.80	5.40
60	8	2280	2732	182	219	802	52	675	583	91	103	3.82	5.45
60	10	2644	3206	212	256	939	64	776	684	105	121	3.80	5.45
60	12	3011	3681	241	295	1087	77	870	782	117	138	3.78	5.43
120	4	5955	6614	476	529	3180	187	949	904	134	153	3.45	4.35
120	6	7064	8016	565	641	3656	215	1193	1181	169	200	3.53	4.51
120	8	8064	9307	645	745	4084	245	1414	1440	200	244	3.57	4.61
120	10	9180	10709	734	857	4629	285	1618	1686	229	286	3.58	4.64
120	12	10333	12144	827	972	5223	331	1811	1923	256	326	3.56	4.64
200	4	15304	16701	1224	1336	9221	545	1630	1611	228	258	3.28	4.00
200	6	17902	19898	1432	1592	10541	620	2035	2095	285	335	3.36	4.17
200	8	20253	22834	1620	1827	11730	699	2401	2547	336	408	3.41	4.28
200	10	22958	26115	1837	2089	13247	808	2740	2977	384	476	3.41	4.32
200	12	25783	29507	2063	2361	14895	934	3059	3390	428	542	3.40	4.32

Table 42. Reliability index calculation for bending moment of simple span composite steel bridges based on Florida WIM data.

Span	Spacing	Ave. Res. 1	Av. Res. 2	σ Res. 1	σ Res. 2	Mean DL	σ DL	Mean LL 1	Mean LL 2	σ LL 1	σ LL 2	beta 1-lane	beta 2-lane
60	4	1356	1602	136	160	346	28	566	425	151	134	2.25	4.02
60	6	1770	2134	177	213	474	38	718	558	192	177	2.27	4.02
60	8	2163	2646	216	265	604	48	855	683	229	216	2.30	4.02
60	10	2572	3171	257	317	756	61	982	802	263	254	2.32	4.01
60	12	2989	3704	299	370	923	74	1102	916	295	290	2.34	3.99
120	4	4396	5099	440	510	1741	117	1201	1036	315	269	2.69	4.01
120	6	5726	6742	573	674	2325	160	1510	1354	397	351	2.71	4.00
120	8	6853	8179	685	818	2797	199	1789	1651	470	429	2.71	4.01
120	10	8087	9718	809	972	3375	247	2048	1934	538	502	2.72	3.99
120	12	9446	11378	945	1138	4063	301	2292	2205	602	572	2.72	3.96
200	4	12306	13796	1231	1380	6265	377	2120	1851	565	498	2.82	3.78
200	6	15810	17938	1581	1794	8123	500	2648	2407	706	648	2.83	3.79
200	8	18999	21753	1900	2175	9814	614	3123	2926	833	788	2.83	3.79
200	10	22444	25812	2244	2581	11743	749	3565	3420	950	921	2.83	3.78
200	12	26416	30389	2642	3039	14096	906	3980	3894	1061	1049	2.82	3.74

Table 43. Reliability index calculation for bending moment of simple span prestressed concrete bridges based on Florida WIM data.

Span	Spacing	Ave. Res. 1	Av. Res. 2	σ Res. 1	σ Res. 2	Mean DL	σ DL	Mean LL 1	Mean LL 2	σ LL 1	σ LL 2	beta 1-lane	beta 2-lane
60	4	1564	1794	125	144	576	34	1201	1036	151	134	2.21	4.07
60	6	1940	2281	155	183	695	44	1510	1354	192	177	2.20	4.09
60	8	2280	2732	182	219	802	52	1789	1651	229	216	2.19	4.10
60	10	2644	3206	212	256	939	64	2048	1934	263	254	2.20	4.10
60	12	3011	3681	241	295	1087	77	2292	2205	295	290	2.21	4.09
120	4	5955	6614	476	529	3180	187	2120	1851	315	269	2.67	3.91
120	6	7064	8016	565	641	3656	215	2648	2407	397	351	2.68	4.01
120	8	8064	9307	645	745	4084	245	3123	2926	470	429	2.69	4.07
120	10	9180	10709	734	857	4629	285	3565	3420	538	502	2.69	4.09
120	12	10333	12144	827	972	5223	331	3980	3894	602	572	2.68	4.09
200	4	15304	16701	1224	1336	9221	545	1630	1611	565	498	2.75	3.71
200	6	17902	19898	1432	1592	10541	620	2035	2095	706	648	2.79	3.84
200	8	20253	22834	1620	1827	11730	699	2401	2547	833	788	2.80	3.92
200	10	22958	26115	1837	2089	13247	808	2740	2977	950	921	2.80	3.94
200	12	25783	29507	2063	2361	14895	934	3059	3390	1061	1049	2.80	3.94

Table 44. Reliability index calculation for bending moment of simple span composite steel bridges based on Indiana WIM data.

Span	Spacing	Ave. Res. 1	Av. Res. 2	σ Res. 1	σ Res. 2	Mean DL	σ DL	Mean LL 1	Mean LL 2	σ LL 1	σ LL 2	beta 1-lane	beta 2-lane
60	4	1356	1602	136	160	346	28	508	376	62	50	3.31	5.17
60	6	1770	2134	177	213	474	38	644	495	79	65	3.30	5.14
60	8	2163	2646	216	265	604	48	767	606	94	80	3.29	5.12
60	10	2572	3171	257	317	756	61	881	711	107	94	3.28	5.07
60	12	2989	3704	299	370	923	74	988	812	121	107	3.26	5.01
120	4	4396	5099	440	510	1741	117	1137	888	162	100	3.15	4.64
120	6	5726	6742	573	674	2325	160	1430	1161	203	131	3.14	4.62
120	8	6853	8179	685	818	2797	199	1695	1415	241	160	3.14	4.63
120	10	8087	9718	809	972	3375	247	1940	1657	275	187	3.12	4.59
120	12	9446	11378	945	1138	4063	301	2170	1890	308	214	3.09	4.54
200	4	12306	13796	1231	1380	6265	377	1999	1598	264	190	3.08	4.11
200	6	15810	17938	1581	1794	8123	500	2496	2078	329	247	3.07	4.12
200	8	18999	21753	1900	2175	9814	614	2944	2526	389	301	3.07	4.13
200	10	22444	25812	2244	2581	11743	749	3360	2952	444	351	3.05	4.10
200	12	26416	30389	2642	3039	14096	906	3752	3362	495	400	3.02	4.05

Table 45. Reliability index calculation for bending moment of simple span prestressed concrete bridges based on Indiana WIM data.

Span	Spacing	Ave. Res. 1	Av. Res. 2	σ Res. 1	σ Res. 2	Mean DL	σ DL	Mean LL 1	Mean LL 2	σ LL 1	σ LL 2	beta 1-lane	beta 2-lane
60	4	1564	1794	125	144	576	34	508	376	62	50	3.34	5.40
60	6	1940	2281	155	183	695	44	644	495	79	65	3.35	5.50
60	8	2280	2732	182	219	802	52	767	606	94	80	3.36	5.55
60	10	2644	3206	212	256	939	64	881	711	107	94	3.36	5.55
60	12	3011	3681	241	295	1087	77	988	812	121	107	3.34	5.53
120	4	5955	6614	476	529	3180	187	1137	888	162	100	3.05	4.46
120	6	7064	8016	565	641	3656	215	1430	1161	203	131	3.10	4.64
120	8	8064	9307	645	745	4084	245	1695	1415	241	160	3.13	4.76
120	10	9180	10709	734	857	4629	285	1940	1657	275	187	3.13	4.80
120	12	10333	12144	827	972	5223	331	2170	1890	308	214	3.12	4.80
200	4	15304	16701	1224	1336	9221	545	1999	1598	264	190	2.99	4.04
200	6	17902	19898	1432	1592	10541	620	2496	2078	329	247	3.05	4.22
200	8	20253	22834	1620	1827	11730	699	2944	2526	389	301	3.09	4.34
200	10	22958	26115	1837	2089	13247	808	3360	2952	444	351	3.09	4.37
200	12	25783	29507	2063	2361	14895	934	3752	3362	495	400	3.08	4.38
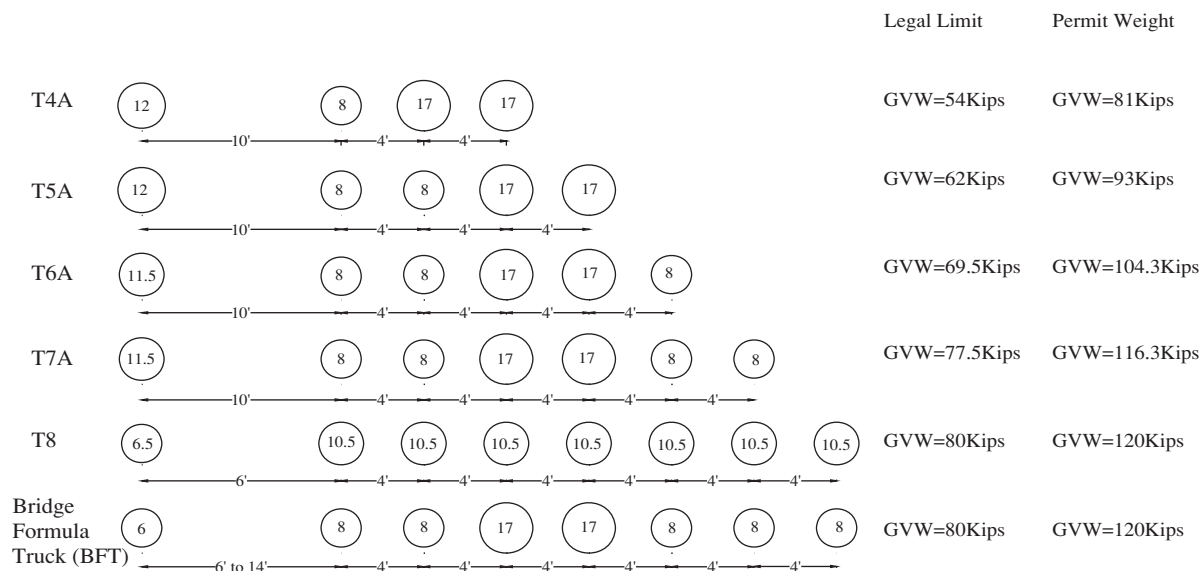
Figure 37. Examples of permit truck configurations.

slightly lower than the target. The Indiana data show a site-to-site variability in COVs on the order of 11% to 15% for both one-lane and two-lane loadings. This is compared to the California data that show low site-to-site variability in the one-lane loading cases (typically less than 10% for spans greater than 40 ft) and the Florida data that show high COVs for both the one-lane and two-lane cases (typically greater than 20%).

Summary. Using a single maximum or characteristic value for L_{max} for a state would be acceptable if the scatter or variability in L_{max} from site-to-site for the state was equal to (or less than, to be conservative) the COV assumed in the LRFD calibration. If the variability in the WIM data is much greater than that assumed in the calibration, then the entire LRFD calibration to achieve the target 3.5 reliability index may no longer be valid for that state and a simple adjustment of the live-load factor as given in the Method I, Step 13.1 protocols, should not be done. This example presented a reliability-based procedure to adjust the live-load factors based on the L_{max} values assembled for each state. The results show that the average reliability index values vary considerably from state to state as a function of the average L_{max} values, the live-load case that governs, and the site-to-site variability expressed in terms of the COV of L_{max}. Also, the results reflect that current WIM data indicate that one-lane loadings are often dominating

the safety of bridge members due to the lower number of side-by-side events and the lower load effects produced by these events when compared to the data used during the calibration of the AASHTO LRFD. The Method II procedure outlined provides a more robust method for updating live-load factors for LRFD design using recent WIM data.

Calibrate Overload Load Factors for Strength II (Step 13.4)

Reliability Analysis and Adjustment of Live-Load Factor for Case I—Permit Vehicle Alone

To execute the reliability calculations, the research team used a set of typical permit vehicle configurations as shown in Figure 37. These configurations are for typical special hauling vehicles (SHV) and are adopted from the work performed for NCHRP 12-63 (Sivakumar et al. 2007). The weights of these SHVs are increased by 150% from the legal limits to be considered as special permit loads. For 60-ft, 120-ft, and 200-ft simple spans, these hypothetical permit vehicles produce the maximum moments of Table 46.

The nominal resistance that would be required for a set of multi-beam simple-span steel bridges can be calculated by applying Equation 32 with $\gamma_D = 1.25$ for component dead

Table 46. Moment effect for a set of permit trucks.

| Span length | Moments in kip-ft | | | | | |
	T4A	T5A	T6A	T7A	T8	BFT
60 ft	1016	1116	1240	1346	1336	1405
120 ft	2230	2508	2802	3090	3134	3205
200 ft	3850	4366	4887	5415	5534	5604

Table 47. Nominal resistance for beams of simple-span bridges under a single permit.

Composite steel		Dead weight effect (kip-ft)			R_N Nominal resistance (kip-ft)					
Span (ft)	Space (ft)	DC_1	DC_2	D_W	T4A	T5A	T6A	T7A	T8	BFT
60	4	39	245	49	928	978	1038	1091	1086	1120
60	6	48	335	73	1222	1285	1362	1428	1422	1465
60	8	70	414	97	1506	1580	1672	1751	1743	1795
60	10	84	521	122	1806	1892	1998	2089	2080	2139
60	12	103	639	146	2119	2215	2334	2436	2426	2492
120	4	502	981	194	3074	3190	3312	3432	3450	3480
120	6	607	1341	292	4041	4187	4341	4491	4515	4552
120	8	650	1656	389	4850	5023	5205	5384	5411	5455
120	10	681	2083	486	5768	5966	6175	6379	6411	6461
120	12	773	2556	583	6808	7029	7263	7492	7527	7583
200	4	2780	2725	540	9116	9307	9500	9695	9740	9765
200	6	3303	3725	810	11779	12018	12259	12502	12558	12590
200	8	3790	4600	1080	14206	14488	14772	15060	15125	15163
200	10	4190	5788	1350	16893	17214	17538	17867	17941	17984
200	12	4875	7100	1620	20073	20432	20794	21160	21243	21292

weights and $\gamma_D = 1.50$ for the wearing surface. In Equation 32, the effect of the permit trucks is multiplied by a load factor $\gamma_L = 1.35$ after applying the D.F. of Equation 33 and the impact factor specified in the AASHTO LRFD as IM = 1.33. The required nominal resistance values for the cases considered in this example are provided in Table 47. In these calculations the research team assumed that the dead loads of the components remain essentially unchanged when the applied live loads are changed. The application of Equation 40 leads to the reliability index values provided in Table 48.

The results of Table 48 illustrate the following points:

- For a given span length and beam spacing, the different vehicle configurations produce little change in the reliability index. The largest difference in β is on the order of 0.11 when the range is between $\beta = 3.22$ to $\beta = 3.33$ for the 60-ft span with beams at 12 ft.

- Increasing the beam spacing leads to slightly lower reliability index values.
- Increasing span length leads to lower reliability index values.
- The average reliability index for the span lengths and beam spacings considered is on the order of $\beta_{ave} = 3.07$ with a minimum value of $\beta = 2.74$ and a maximum value of $\beta = 3.40$.
- Using a live-load factor $\gamma_L = 1.35$ for Strength II produces an average reliability index of $\beta_{ave} = 3.07$ for a single permit on the bridge. This average value is lower than the $\beta_{target} = 3.50$ used for the calibration of the AASHTO LRFD equations. If an average reliability $\beta_{ave} = 3.50$ is desired for the bridge configurations considered in this example, then a $\gamma_L = 1.62$ should be used when considering the case of a permit load alone on the bridge. The $\gamma_L = 1.62$ is obtained using a trial-and-error procedure. The process is repeated until a $\beta_{ave} = 3.5$ is obtained.
- An average reliability index $\beta_{ave} = 2.5$ was used for the calibration of the operating rating live-load factor in the LRFR

Table 48. Reliability index for a single permit with $\gamma_L = 1.35$.

Composite steel		Reliability index, β					
Span (ft)	Space (ft)	T4A	T5A	T6A	T7A	T8	BFT
60	4	3.31	3.34	3.37	3.39	3.39	3.40
60	6	3.30	3.33	3.36	3.38	3.38	3.39
60	8	3.28	3.31	3.34	3.37	3.37	3.38
60	10	3.25	3.29	3.32	3.34	3.34	3.36
60	12	3.22	3.26	3.29	3.32	3.31	3.33
120	4	3.01	3.05	3.08	3.12	3.12	3.13
120	6	2.99	3.03	3.07	3.10	3.11	3.11
120	8	2.99	3.03	3.07	3.10	3.10	3.11
120	10	2.96	3.00	3.04	3.07	3.08	3.09
120	12	2.93	2.97	3.01	3.04	3.05	3.06
200	4	2.78	2.81	2.84	2.86	2.87	2.87
200	6	2.77	2.80	2.83	2.86	2.87	2.87
200	8	2.78	2.81	2.83	2.86	2.87	2.87
200	10	2.76	2.79	2.82	2.84	2.85	2.85
200	12	2.74	2.77	2.80	2.82	2.83	2.83

code. If an average reliability $\beta_{ave} = 2.5$ is desired for the bridge configurations considered in this example, then a $\gamma_L = 1.04$ should be used when considering the case of a permit load alone on the bridge.

Reliability Analysis and Adjustment of Live-Load Factor for Case II—Two Permits Side by Side

In this case, assume that the axle weights and axle configurations of the two permit trucks are the same and are perfectly known so that the total maximum static live-load effect on the bridge, L_{max}, is a deterministic value. However, this does not imply that the total live-load effect on a bridge member is deterministic due to the uncertainties in estimating the dynamic effect represented by the dynamic amplification factor, IM, and the uncertainties in the structural analysis process that allocates the fraction of the total load to the most critical member. The structural analysis is represented by the load distribution factor, D.F. The equations for the D.F. of multi-girder bridges loaded in two lanes given in the AASHTO LRFD specifications assume that the two lanes are loaded by the same vehicle and give the load on the most critical beam as a function of the load in one of the lanes. Thus, the live-load effect on one member can be given from Equation 46. According to Nowak (1999), the dynamic amplification factor augments the load effect by an average of 9% for side-by-side trucks. The dynamic amplification also resulted in a COV of $V_{IM} = 5.5\%$ on the two-lane effect. Also assume that the same COV for the lane distribution factor $V_{DF} = 8\%$, obtained by Ghosn and Moses (1986) from field measurements on typical steel and prestressed concrete bridges, is still valid. Therefore, for the loading of a single permit vehicle, the live-load COV becomes

$$V_{LL} = \sqrt{(5.5\%)^2 + (8\%)^2} = 9.71\%$$

The reliability index, conditional on the arrival of two side-by-side permits on the bridge, can then be calculated using Equation 40 where $\overline{R}$ is the mean resistance when the bridge member is designed for two side-by-side permits and $\overline{LL}$ is the live-load effect on the beam due to two side-by-side permits.

The reliability index calculated from Equation 40 in this case is conditional on having two side-by-side trucks. The probability that a bridge member would fail given that two permit vehicles are side by side can be calculated from $P_{f/side-by-side} = \Phi(-\beta_{cond})$. However, the final unconditional probability of failure will depend on the conditional probability given two side-by-side events and the probability of having a situation with side-by-side permits as shown in Equation 47. The probability of having two side-by-side permits depends on the number of permit trucks expected to cross the bridge within the return period within which the permits are granted. In this example, assume that all of the permits will likely cross the same bridges so that the number of permits crossing a certain bridge within a 1-year period is equal to the number of permits granted. The percentage of these permits that will be side by side is related to the total number of crossings as provided in Table 49. For example, assuming that the number of permit-vehicles expected on a bridge during the return period when the permits are in effect will be on the order of 1,000 vehicles then, according to Table 49, the probability of having side-by-side events is 0.54% (= 0.19 + 0.14 + 0.21). This value is obtained by conservatively assuming that trucks within a headway distance H < 60 ft are actually side by side.

Table 49. Multiple-presence probabilities for side-by-side events as a function of headway distance.

Maximum MP Probabilities based on 5 WIM sites (10 directional sites) in New York State				
	Maximum Side-by-Side Truck Multiple Presence Probabilities			
	Site Truck Traffic			
Headway H (ft)	Light: ADTT ≤ 1k	Average: 1k < ADTT ≤ 2.5k	Heavy: 2.5k < ADTT ≤ 5k	Very Heavy: ADTT > 5k
H < 20	0.19	0.41	0.61	0.00
20 < H ≤ 40	0.14	0.43	0.66	0.00
40 < H ≤ 60	0.21	0.41	0.68	0.00
60 < H < 80	0.26	0.35	0.62	0.00
80 < H ≤ 100	0.20	0.53	0.76	0.00
100 < H ≤ 120	0.21	0.41	0.81	0.00
120 < H ≤ 140	0.24	0.34	0.66	0.00
140 < H ≤ 160	0.17	0.30	0.61	0.00
160 < H < 180	0.18	0.29	0.56	0.00
180 < H ≤ 200	0.19	0.26	0.52	0.00
200 < H ≤ 220	0.10	0.24	0.48	0.00
220 < H < 240	0.14	0.24	0.45	0.00
240 < H ≤ 260	0.12	0.22	0.43	0.00
260 < H < 280	0.14	0.21	0.41	0.00
280 < H ≤ 300	0.11	0.20	0.40	0.00

Table 50. Conditional Reliability Index for Case II.

Composite steel		Conditional Reliability index, β					
Span (ft)	space (ft)	T4A	T5A	T6A	T7A	T8	BFT
60	4	3.65	3.69	3.72	3.74	3.74	3.76
60	6	3.64	3.68	3.71	3.74	3.73	3.75
60	8	3.64	3.67	3.70	3.73	3.73	3.74
60	10	3.61	3.65	3.68	3.71	3.71	3.72
60	12	3.59	3.62	3.66	3.69	3.68	3.70
120	4	3.29	3.34	3.39	3.43	3.44	3.45
120	6	3.29	3.34	3.39	3.43	3.43	3.44
120	8	3.29	3.35	3.39	3.44	3.44	3.45
120	10	3.27	3.33	3.38	3.42	3.42	3.43
120	12	3.25	3.30	3.35	3.39	3.40	3.41
200	4	2.97	3.02	3.06	3.10	3.11	3.12
200	6	2.98	3.03	3.07	3.11	3.12	3.13
200	8	2.99	3.04	3.08	3.12	3.13	3.13
200	10	2.98	3.02	3.07	3.11	3.12	3.12
200	12	2.96	3.00	3.04	3.08	3.09	3.10

To execute the reliability calculations, a set of typical permit vehicle configurations is used, as shown in Figure 37. These configurations were adopted from the work performed for NCHRP 12-63 (Sivakumar et al. 2007) and multiplying the legal weights of each SHV by 150%. For 60-ft, 120-ft, and 200-ft simple spans, these vehicles produce maximum moments as shown in Table 47.

The nominal resistance that would be required for a set of multi-beam simple-span steel bridges can be calculated by applying Equation 32 with $\gamma_D = 1.25$ for component dead weights and $\gamma_D = 1.50$ for the wearing surface. In Equation 32, the effect of the permit trucks is multiplied by a load factor of $\gamma_L = 1.35$ after applying the D.F. of Equation 34 and the impact factor specified in the AASHTO LRFD as IM = 1.33. These calculations assume that the dead loads of the components remain essentially unchanged when the applied live loads are changed. The conditional reliability index is given in Table 50. Equation 46 is then used to find the unconditional probability of failure that is then inverted using Equation 39 to find the unconditional reliability index β. The final (unconditional) reliability index values are provided in Table 51 for the bridge configurations analyzed in this example.

The results of Tables 50 and 51 illustrate the following points:

- For a given span length and beam spacing, the different vehicle configurations produce little change in the reliability index. The largest difference in the unconditional β is on the order of 0.12 for the 120-ft span bridges.
- Increasing the beam spacing leads to small changes of less than 0.06 in the reliability index values.
- Increasing the span length leads to lower reliability index values.
- The average unconditional reliability index for the span lengths and beam spacings considered is on the order of $\beta_{ave} = 4.62$ with a minimum value of $\beta = 4.30$ and a maximum value $\beta = 4.91$
- The higher reliability index obtained for the two side-by-side permits as compared to the single permit is primarily due to

Table 51. Final (Unconditional) Reliability Index for Case II.

Composite steel		Reliability index, β					
Span (ft)	space (ft)	T4A	T5A	T6A	T7A	T8	BFT
60	4	4.83	4.85	4.88	4.90	4.89	4.91
60	6	4.82	4.84	4.87	4.89	4.89	4.90
60	8	4.81	4.84	4.86	4.88	4.88	4.89
60	10	4.79	4.82	4.85	4.87	4.87	4.88
60	12	4.77	4.80	4.83	4.85	4.85	4.86
120	4	4.55	4.59	4.62	4.66	4.66	4.67
120	6	4.55	4.58	4.62	4.65	4.66	4.66
120	8	4.55	4.59	4.63	4.66	4.66	4.67
120	10	4.54	4.58	4.61	4.65	4.65	4.66
120	12	4.52	4.55	4.59	4.62	4.63	4.64
200	4	4.32	4.35	4.38	4.41	4.42	4.42
200	6	4.32	4.35	4.39	4.42	4.42	4.43
200	8	4.33	4.36	4.39	4.42	4.43	4.43
200	10	4.32	4.35	4.38	4.41	4.42	4.42
200	12	4.30	4.34	4.37	4.40	4.40	4.41

the low probability of having side-by-side events. If one looks at the conditional reliability index, then the average $\beta_{conditional} = 3.38$ is closer to, but still higher than, the $\beta_{ave} = 3.07$ obtained for a single permit truck. In this case, the still higher conditional reliability index value is partially due to the lower mean impact factor ($\overline{IM} = 1.09$ versus 1.13) and the lower corresponding COV ($V_{IM} = 5.5\%$ versus 9%) for side-by-side events, which are justified by the low likelihood of having the peaks of the dynamic oscillations of the two side-by-side vehicles occur simultaneously.

Reliability Analysis and Adjustment of Live-Load Factor for Case III—Permit Truck Alongside a Random Truck

For Case III, the maximum live-load effect is due to the permit truck alongside the maximum truck expected to occur simultaneously in the other lane. The maximum total load effect depends on the number of side-by-side events expected within the return period.

To determine the number of side-by-side permit-random truck events that would occur within a 1-year period, assume that the number of side-by-side events involving one random truck is obtained from Table 43 based on the ADTT. For example, assume that N_P gives the number of permit truck crossings expected in a return period T. The average number of random trucks in 1 day is given by the ADTT. For ADTT between 1,000 and 2,500 trucks per day, the percentage of side-by-side events involving a random truck (assumed to be those within a headway H≤60 ft) is taken from Table 43 to be 1.25% (= 0.41% + 0.43% + 0.41%). Thus, within a 1-year return period, there will be $4.56 \times ADTT$ (= $1.25\% \times 365 \times ADTT$) random trucks alongside another truck. Assuming that there will be 1,000 permits on this route within this 1-year period, the percentage of permits in the total truck population will be

$2.74/\text{ADTT}\left(= \dfrac{1000}{\text{ADTT} \times 365}\right)$. This indicates that the num-

ber of random trucks alongside a permit truck will be, on average, $N_R = 12.5$ (=4.56×2.74) events within a 1-year return period. The maximum live-load effect expected within this 1-year period will be due to the heaviest of these 12.5 random trucks combined with the effect of the permit. Table 52 gives the L_{maxNR} values for the maximum moment effect on simple spans obtained for the maximum of 12.5 events for single lanes for WIM data collected at six California sites. These are obtained by applying the protocols Step 12.2.1 with $N = N_r = 12.5$ in Equations 26 and 27. The values in Table 52 are normalized as a function of the effect of the HL93 vehicle.

The maximum live-load effect is obtained from Equation 49 where P is the load effect of the permit truck, DF_P is the distribution factor for the load P, L_{maxNR} is the maximum load effect of random trucks for N_R events, DF_R is the distribution

Table 52. L_{max} values for the maximum moment effect on simple spans obtained for the maximum of 12.5 events for single lanes.

Site	L_{maxN_R} for N_R=12.5 events		
	60-ft	120-ft	200-ft
Lodi 1	0.67	0.70	0.67
Lodi 2	0.69	0.71	0.63
Antelope 1	0.67	0.66	0.59
Antelope 2	0.72	0.70	0.62
LA 710 1	0.70	0.68	0.63
LA 710 2	0.74	0.71	0.66
Bowman 1	0.64	0.62	0.56
Bowman 2	0.63	0.64	0.58
Average	0.68	0.68	0.62
Std. Dev.	0.04	0.03	0.04

factor for the random load, and IM is the impact factor for side-by-side events. The coefficient of variation for $L_{maxN_R} \times DF_R$ is estimated using Equation 50 as follows:

$$V_{Lmax^*} = \sqrt{(5.6\%)^2 + (3.5\%)^2 + (2\%)^2 + (8\%)^2} = 10.6\%$$

where:

  5.6% is the COV for site-to-site variability,
  3.5% is due to randomness in the WIM data,
  2% is due to the limitation in the WIM sample size, and
  8% is due to the uncertainties in estimating DF_R.

Assuming the effect of the permit load is deterministic, the coefficient of variation for $PxDF_P$ is estimated as $V_{P^*} = 8\%$, which is the COV for the load distribution factor, DF_P. Hence, the standard deviation of LL without the impact factor is obtained using Equation 52 as follows:

$$\sigma_{LL^*} = \sqrt{(8\% \times P \times DF_P)^2 + (10.6\% \times L_{\max N_R} \times DF_R)^2}$$

The COV for the live-load effect on the critical beam including the effect of the impact IM is given by Equation 53.

The live-load mean obtained from Equation 49 and the COV obtained from Equation 53 are then used to find the reliability index from Equation 40. In these example calculations, the same bridge configurations used for Case II are assumed and the nominal R_n values are obtained from two side-by-side permit loads as traditionally done. The reliability calculations produce the results shown in Table 53.

The results in Table 53 show a large range for β varying between 2.93 and 4.51 with an average $\beta = 3.72$. To reduce the average to $\beta_{target} = 3.5$, the live-load factor would need to be reduced from $\gamma_L = 1.35$ to 1.25.

Table 53. Reliability Index for Case III.

Composite steel		Reliability index, β					
Span (ft)	space (ft)	T4A	T5A	T6A	T7A	T8	BFT
60	4	4.03	4.16	4.30	4.41	4.40	4.47
60	6	4.04	4.17	4.32	4.44	4.43	4.49
60	8	4.04	4.18	4.33	4.45	4.44	4.51
60	10	4.01	4.16	4.32	4.43	4.42	4.49
60	12	3.98	4.13	4.29	4.41	4.40	4.47
120	4	3.37	3.52	3.67	3.80	3.82	3.85
120	6	3.37	3.53	3.68	3.81	3.83	3.86
120	8	3.38	3.54	3.70	3.84	3.86	3.89
120	10	3.36	3.52	3.68	3.82	3.84	3.87
120	12	3.33	3.49	3.65	3.79	3.81	3.84
200	4	2.95	3.07	3.18	3.28	3.30	3.31
200	6	2.96	3.08	3.19	3.30	3.32	3.33
200	8	2.97	3.09	3.20	3.31	3.34	3.35
200	10	2.95	3.08	3.19	3.30	3.32	3.34
200	12	2.93	3.05	3.16	3.27	3.30	3.31

Summary. The reliability analysis executed in this report for the limit state of Strength II with a live-load factor $\gamma_L=1.35$ shows large variations in the reliability index depending on whether the permit load crosses the bridge with no other trucks alongside of it, the permit is alongside another permit, or the permit is alongside a random truck. When the permit crossing is controlled such that no other trucks are alongside, the average reliability index for the span lengths and beam spacings considered in this report is on the order of $\beta_{ave} = 3.07$. The average reliability index for two permits side by side is on the order of $\beta_{ave} = 4.62$. The results for a permit alongside a random truck is, on average, $\beta = 3.72$. A high average reliability index for two side-by-side permits is due to the low probability of the occurrence of such cases. If the number of permits is such that the chances of their side-by-side occurrences is close to 100%, then the average reliability index becomes $\beta = 3.38$ which is lower than the random-permit reliability index of 3.72. In this latter case, the reliability index $\beta = 3.38$ is lower than the 3.72 because in the random-permit case it is unlikely that the random truck will be as heavy as the permit truck.

Adjustments to the live-load factor $\gamma_L = 1.35$ can be made to match a target reliability index. It should be noted that the determination of the target reliability index and the sample of bridge configurations for which the adjustment of the live-load factor need to be made should be based on the experience of bridge owners with the performance of the bridges in their jurisdiction. The calculations performed as part of this report assume that the resistance, dead loads, and live loads follow normal (Gaussian) probability distributions. This assumption was made to illustrate the procedure and can be adjusted as more information on these variables is assembled from ongoing and recent research studies.

Axle Loads for Deck Design from WIM Data (Step 9)

Axle Group Weight (Steps 9.1 and 9.2)

One-lane (single truck) and two-lane (side-by-side trucks) axle events were analyzed for the purpose of calibrating deck design loads. For the one-lane events, single, tandem, tridem, and quad axle groups were considered. For the two-lane events, single-single, single-tandem, and tandem-tandem axle group combinations were considered. All other axle group combinations were consolidated into one group. Single axles and tandem axles are, by far, the most common axle groups.

Figure 38 shows, as a sample, the one-lane axle group weight histograms for WIM Site 9926 in Florida (I-75). Table 54 shows summary statistics for the data. Figure 39 shows the two-lane axle group weight histograms for the same site and Table 55 shows summary statistics for these data. In addition to the mean and standard deviation of the entire population, top 20% of the population, and top 5% of the population, the 99th percentile is shown. This upper extreme is taken in this project as the maximum anticipated load for design. Table 56 shows the 99th percentile of the one-lane axle group weights for all the WIM sites studied in this task. Table 57 shows the 99th percentile of the two-lane axle group weights for all the WIM sites studied in this task. As expected, the combined load of the two-lane events is less than sum of the constituent one-lane events, indicating that the heaviest axle loads are not, necessarily, involved in side-by-side events. Appendix C contains axle group weight histograms for all other WIM sites studied in this task.

Rigorous calibration of load and resistance factors for deck design requires the availability of statistical data beyond live loads. LRFD did not specifically address deck components in the calibration. In the protocols developed in this study, the nominal axle loads derived using WIM data are used instead
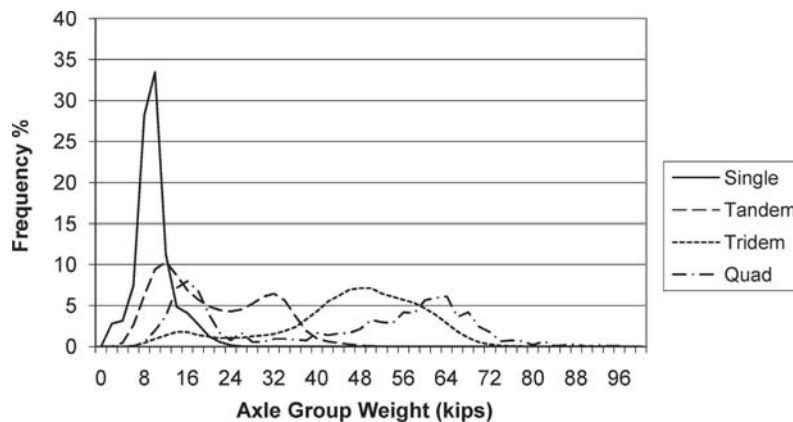
Figure 38. One-lane axle group weight histogram (WIM Site 9926 in Florida).

of the code specified values, where the W_{99} statistic is higher than the code values. All other factors are kept unchanged (load factor, deck dynamic load allowance). The governing nominal axle loads for LRFD deck design are taken as follows:

- For single axles, 32-kip load given in LRFD or the 99th percentile statistic W_{99}, whichever is higher;
- For tandem axles, 50 kips (2×25 kips given in LRFD) or the 99th percentile statistic W_{99}, whichever is higher;
- For tridem axles, the 99th percentile statistic W_{99}; and
- For quad axles, the 99th percentile statistic W_{99}.

The 99th percentile axle weights are as given in the tables for each axle type at each WIM site.

Additional Studies on Truck Sorting Strategies—NCHRP 12-76 (01)

The original NCHRP 12-76 study addressed the issue of separating traffic data into Strength I and Strength II limit states by recommending that all uncontrolled traffic that con-

stitutes normal traffic or service loads at a site be grouped into Strength I and all controlled or analyzed overload permits be grouped into Strength II. NCHRP 12-76 protocols for classifying trucks into Strength I and Strength II limit states may be summarized as follows:

1. All legal trucks, illegal overloads and un-analyzed permits (all routine permits) were grouped into Strength I because they were considered to represent normal service traffic at bridge sites.
2. All controlled or analyzed overload permits were grouped into Strength II.
3. Due to the difficulty in separating permit vs. non-permit traffic using permit records, it was decided to group all trucks with six or fewer axles in the Strength I calibration.

The high r values (r is defined as L_{max} WIM data/L_{max} LRFD calibration data) obtained for Strength I in the NCHRP 12-76 study for one-lane loaded conditions may have been influenced by the truck sorting methodology (based on number of axles) used in the study. This additional study was conducted to further investigate the truck sorting methodology and the sensitivity of r values to how the trucks are sorted into Strength I. The two-lane loaded condition is governed by the presence of two heavy trucks side by side and is less sensitive to the weight and configuration of an individual truck than it is for the one-lane loaded condition. That is, truck sorting into Strength I and Strength II is more of a factor for the single-lane loading.

Issues investigated in this phase of the research are as follows:

1. Strategies for sorting trucks into non permit (state legal loads and illegal loads), routine or annual permits, and special permits (superloads);
2. Strategies for grouping the various trucks defined in Step 1 into Strength I and Strength II for design load calibration; and

Table 54. One-lane axle group weight statistics (WIM Site 9926 in Florida).

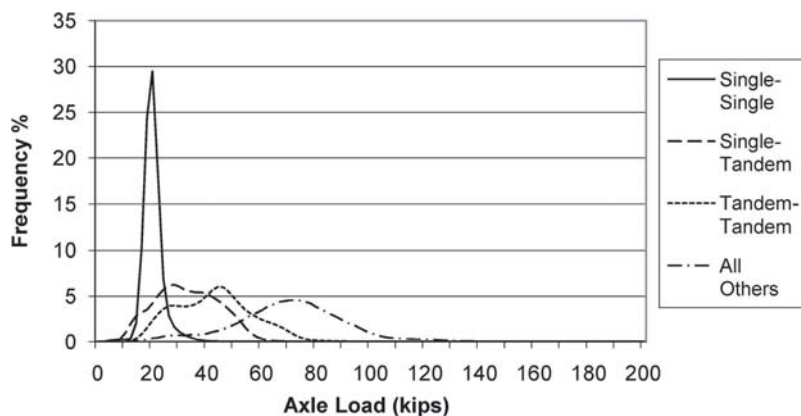| Statistics	Single	Tandem	Tridem	Quad
Axle Count	2986536	3293111	94115	1077
Mean All Axles	10.831	21.773	46.649	43.899
Std Dev All Axles	3.494	9.847	13.955	22.070
COV All Axles	0.323	0.452	0.299	0.503
Mean Top 20% Axles	16.039	36.285	63.111	70.777
Std Dev Top 20% Axles	2.932	3.763	3.976	6.282
COV Top 20% Axles	0.183	0.104	0.063	0.089
Mean Top 5% Axles	20.152	41.357	68.343	79.444
Std Dev Top 5% Axles	2.008	3.913	3.817	6.380
COV Top 5% Axles	0.100	0.095	0.056	0.080
99th Percentile	20	42	68	82

Figure 39. Two-lane axle group weight histogram (WIM Site 9926 in Florida).

Table 55. Two-lane axle group weight statistics (WIM Site 9926 in Florida).

Statistics	Single-Single	Single-Tandem	Tandem-Tandem	All Others
Event Count	13124	29735	16306	1801
Mean All Events	21.585	32.535	43.445	63.314
Std Dev All Events	4.994	10.486	14.111	17.759
COV All Events	0.231	0.322	0.325	0.280
Mean Top 20% Events	29.141	47.916	64.044	87.483
Std Dev Top 20% Events	3.345	4.509	6.522	8.462
COV Top 20% Events	0.115	0.094	0.102	0.097
Mean Top 5% Events	33.655	54.181	72.988	99.089
Std Dev Top 5% Events	3.003	4.094	5.088	7.489
COV Top 5% Events	0.089	0.076	0.070	0.076
99th Percentile	34	54	74	102

Table 56. One-lane axle group weight (99th percentile).

State	Site ID	Route	Single	Tandem	Tridem	Quad
CA	0001	Lodi	18	36	50	40
CA	0003	Antelope	16	32	52	62
CA	0004	Antelope	18	34	56	64
CA	0059	LA 710	16	34	46	54
CA	0060	LA 710	18	36	46	60
CA	0072	Bowman	16	32	50	54
FL	9916	US-29	20	46	78	88
FL	9919	I-95	14	32	50	62
FL	9926	I-75	20	42	68	82
FL	9927	SR-546	18	38	58	64
FL	9936	I-10	22	44	74	94
IN	9511	I-65	14	30	52	62
IN	9512	I-74	18	38	58	68
IN	9532	US-31	16	34	58	72
IN	9534	I-65	16	34	56	66
IN	9544	I-80/I-94	16	34	54	64
IN	9552	US-50	16	34	56	62
MS	2606	I-55	20	48	76	78
MS	3015	I-10	16	36	52	68
MS	4506	I-55	18	40	60	78
MS	6104	US-49	16	36	52	74
MS	7900	US-61	16	40	56	78
TX	0506		18	36	56	--
TX	0516		18	36	56	--
TX	0523		18	36	62	--
TX	0526		18	36	60	--

Table 57. Two-lane axle group weight (99th percentile).

State	Site ID	Route	Single-Single	Single-Tandem	Tandem-Tandem	Other
CA	0001	Lodi	34	50	66	76
CA	0003	Antelope	30	46	62	82
CA	0004	Antelope	32	48	64	78
CA	0059	LA710	26	44	62	72
CA	0060	LA710	30	48	66	74
CA	0072	Bowman	30	46	62	80
FL	9916	US-29	36	60	78	90
FL	9919	I-95	26	42	58	74
FL	9926	I-75	32	58	74	120
FL	9927	SR-546	30	50	70	76
FL	9936	I-10	38	60	84	106
IN	9511	I-65	26	40	54	78
IN	9512	I-74	34	52	72	90
IN	9532	US-31	28	46	64	84
IN	9534	I-65	28	44	58	86
IN	9544	I-80/I-94	28	46	60	80
IN	9552	US-50	28	46	64	70
MS	2606	I-55	36	62	86	92
MS	3015	I-10	28	46	66	78
MS	4506	I-55	34	54	72	84
MS	6104	US-49	32	50	68	90
MS	7900	US-61	32	52	68	76
TX	0506		32	50	68	84
TX	0516		30	48	66	82
TX	0523		30	50	70	96
TX	0526		32	50	68	96

3. The influence of the various truck sorting strategies on r values.

Truck Definitions

To further refine the truck sorting criteria, the following truck definitions were utilized based on state vehicle weight and permit regulations:

- State highway agencies have established processes for permitting overweight non-divisible loads on state highways. Some states also have "grandfather rights" to authorize permits for divisible loads that exceed 80,000 lbs. A "divisible load" is any vehicle or combination of vehicles transporting cargo of legal dimensions that can be separated into units of legal weight without affecting the physical integrity of the load. Examples of divisible loads include: aggregate (sand, top soil, gravel, stone), logs, scrap metal, fuel, milk, trash/refuse/garbage, etc.
- State legal trucks are trucks that meet state vehicle weight regulations for legal loads. Typically specified are axle weight limits or single and axle groups, gross weight limit, and requirements for axle configuration and spacing based on Federal Bridge Formula B.
- Annual (or blanket) overweight permits are usually valid for unlimited trips within a state over a period of time, not to exceed 1 year, for vehicles of a given configuration within specified gross and axle weight limits.
- Trip (or superload) overweight permits are usually valid for a single trip only, a limited number of trips, a vehicle of specified configuration, axle weights, and gross weight. Special permit vehicles are usually heavier than those vehicles issued annual permits.
- Illegal trucks do not meet state vehicle weight regulations for legal loads or for permit loads.

Sorting Variations

Variation P12: All vehicles in Strength I.
The sorting variations investigated in this study can be placed into the following groups:

- **Group I: Sorting based on number of axles**
  - Baseline: Strength I = 6 axles or less (same as NCHRP 12-76 protocols)
  - Variation P1: Strength I = 7 axles or less
  - Variation P2: Strength I = 8 axles or less
  - Variation P3: Strength I = 5 axles or less
- **Group II: Sorting based on GVW**
  - Variation P4: Strength I = GVW ≤ 84
  - Variation P5: Strength I = GVW ≤ 100
  - Variation P6: Strength I = GVW ≤ 120
  - Variation P7: Strength I = GVW ≤ 150

- **Group III: Sorting based on state permit regulations**
  - Variation P8: Strength I = state legal trucks only
  - Variation P9: Strength I = state legal trucks, annual (routine) permits
  - Variation P10: Strength I = state legal trucks, illegal trucks
  - Variation P11: Strength I = state legal trucks, illegal trucks, annual permits (only trip permits in Strength II)
- **Group IV: Non Sorted**

NCHRP 12-76 protocols for classifying trucks into Strength I and Strength II limit states (defined as the baseline case in this study) included all legal trucks, illegal overloads, and un-analyzed permits (all routine permits) into Strength I; trip permits were grouped into Strength II as shown in Table 58. Sorting Variation P11 is aimed at achieving the same classification of trucks into Strength I and Strength II, but using the state's permit regulations as the criteria, not the number of axles. Both the baseline case and Sorting Variation 11 have the same objective but take different approaches to sorting trucks into Strength I and Strength II.

WIM Sites for Testing Sorting Variations

This phase of the NCHRP 12-76 study considered three WIM sites each from Indiana, California, and Florida that were taken from the original NCHRP 12-76 research for studying how changing the definition of classification of loads into Strengths I and II changes the results of the study (especially in terms of the r value, which is a measure of how each site compares to the HL93 design basis). As shown in Table 59, the states and sites were chosen to capture a variety of geographic locations and functional classes.

Truck Sorting Strategies Based on State Permit Regulations

The previously noted sorting strategies were implemented using permit rules and recent WIM data. For each state with the selected WIM sites (Indiana, California, and Florida), the permit variations were customized to incorporate state-specific vehicle weight laws and permit regulations as described below.

Indiana Permit Regulations. Indiana generally uses the federal definition of overweight vehicles. The following is from the *Indiana Oversize/Overweight Vehicle Permitting Handbook* (Indiana ND):

Once your load is non-divisible, you must determine if your truck and load are over the legal dimensions and/or legal weight for Indiana. To travel legally on any Indiana roads, you cannot exceed the following weights:

80,000 lbs gross vehicle weight; or
12,000 lbs on the steering axle; or

Table 58. Sorting variations used for including trucks into Strength I/Strength II.

Sorting Variation	Strength I	Strength II	Comment
Baseline	Trucks with 6 or fewer axles	Trucks with 7 or more axles	Same as NCHRP 12-76 protocols. Provides a basis for comparison.
12	All trucks		Provides a basis for comparison and for sensitivity studies.
Generalized Sorting Methods Applicable to All States			
1	Trucks with 7 or fewer axles	Trucks with 8 or more axles	
2	Trucks with 8 or fewer axles	Trucks with 9 or more axles	
3	Trucks with 5 or fewer axles	Trucks with 6 or more axles	
4		GVW > 84 kips	Includes a 5% scale allowance over 80 kips.
5		GVW > 100 kips	
6		GVW > 120 kips	
7		GVW > 150 kips	
State-Specific Sorting Methods Based on State Weight Regulations and Permit Rules			
8	State Legal Trucks	Illegal Trucks Annual (Routine) Permits Trip Permits	Only State legal trucks in Strength I.
9	State Legal Trucks Annual (Routine) Permits	Illegal Trucks Trip Permits	Only used for comparison purposes.
10	State Legal Trucks Illegal Trucks	Annual (Routine) Permits Trip Permits	All valid permit trucks grouped in Strength II.
11	State Legal Trucks Illegal Trucks Annual (Routine) Permits	Trip Permits	Truck sorting goal intended in 12-76 protocols. Useful to compare with baseline case.

Table 59. WIM sites used in the current research.

State	Site ID	Route	Direction	No. of Truck Records	ADTT
IN	9512	I-74	E	931971	2596
IN	9512	I-74	W	1003443	2795
IN	9532	US-31	N	224506	629
IN	9532	US-31	S	229532	643
IN	9544	I-80/I-94	E	3786127	11235
IN	9544	I-80/I-94	W	4032537	11966
CA	0003	Antelope	E	719834	2790
CA	0059	LA710	S	4243780	11627
CA	0072	Bowman	E/N	310596	2318
CA	0072	Bowman	W/S	289319	2159
FL	9919	I-95	N	939637	2708
FL	9919	I-95	S	875766	2524
FL	9926	I-75	N	1096076	4136
FL	9926	I-75	S	1032680	3897
FL	9936	I-10	E	700774	1980
FL	9936	I-10	W	723512	2044

20,000 lbs on a single axle; or

34,000 lbs on a tandem axle; or

800 lbs per inch of rim width and subject to the above axle weights.

An overweight vehicle is generally any vehicle whose overall weight exceeds 80,000 lbs. However, road and bridge stress levels are determined by the distribution of the weight, so it is important that the weight per axle, or sets of tandem axles, be observed. Weight per tire also is considered. The total gross weight may be calculated by the following federal bridge formula and then compared to the established weight limits listed above.

$$W = 500\left\{\left[(LN) \div (N-1)\right] + 12N + 36\right\}$$

where:

W = The overall gross weight on any group of two or more consecutive axles, to the nearest 500 lbs,

L = The distance between the extreme of any group of two or more consecutive axles, and

N = The number of axles in the group under consideration, except that two consecutive sets of tandem axles may carry a gross load of 34,000 lbs each, providing the first and last axles of the consecutive sets of tandem axles are at least 36 ft or more apart.

Like most states, Indiana has some exceptions to their standard rules, however the gross vehicle weight, axle weight, tandem axle weight, and compliance with Formula B form the basis of the Indiana regulations.

Indiana considers permits exceeding the legal limits as "overweight" for loads up to a GVW of 120 kip. Permits exceeding 120 kip are given an extra designation as "superload" permits.

California Permit Regulations.   California follows the federal weight laws for legal limits. Federal Bridge Formula B is enforced for axle weight and spacing combinations. The single-axle weight limit is 20,000 lbs. Tandem axle group weights are limited to 34,000 lbs. Gross vehicle weights are limited to 80,000 lbs. One exception route (Port of Long Beach, Route 41) is present but it was not considered in this study.

California issues annual permits for vehicle weights exceeding 80,000 lbs. and less than 300,000 lbs. Permits for more than 300,000 lbs are only issued as single-trip permits. California requires that annual permits satisfy the Purple Weight Table that lists the maximum allowable permit weight on groups of axles as a function of axle spacing, without the gross vehicle weight limit. The maximum allowable weight on groups of axles is given as $1.50 \times 700 \, (L + 40)$ lbs, where L is the distance from first to last axle in feet. The Purple Weight

Table also limits the maximum tandem axle combination to 60,000 lbs. (Special, heavier, tandem axles with 8 tires per axle and 8 or 10 ft wide are allowed a bonus weight but this allowance is not considered in this study.)

California also limits the number of axles in tractor-trailer configurations with annual permits to six. Crane trucks are also issued annual permits and are allowed up to eight axles. However the maximum number of axles that can exceed permit weight is five.

Florida Permit Regulations.   The Florida *Commercial Motor Vehicle Manual,* 6th edition (FDOT 2006), defines legal and permit loads for the State of Florida.

Florida regulations mostly follow the federal legal load definitions. The legal single-axle weight is set at 22,000 lbs and the legal tandem-axle weight is 44,000 lbs. One difference between the typical federal legal load definitions and the Florida regulations is a grandfather exemption for short single-unit trucks. Florida allows short single-unit trucks as legal loads up to 70,000 lbs with the 22,000-lb axle weight requirement; these vehicles do not meet the Federal Bridge Formula B requirement. The Florida manual specifies legal loads using both the outer-bridge and inner-bridge distances. The inner-bridge distances allow the same checking as is done using Federal Bridge Formula B for tractor trailers. Tractor trailers meet the Federal Bridge Formula B requirements and have a maximum legal gross vehicle weight of 80,000 lbs.

Florida requires an overload permit for any vehicle that exceeds 80,000 lbs. Florida issues blanket (annual) permits based upon predefined routes shown on maps. These blanket permits are issued based on weight restriction charts matched to the maps for truck cranes and tractor trailers. The weight restriction charts use number of axles, minimum outer-bridge distance, and maximum axle group weights. Minimum distances between axle groups are also dictated. The outer-bridge distance is the length of the vehicle from front to rear axle.

From the Axle Weight Limitations Table, Florida also places a limit on special permit vehicles of 40,000 lbs for an axle with eight tires. For the typical blanket permits of greatest interest, the highest single-axle limit is 27,500 lbs and the highest gross vehicle weight limit is 199,000 lbs.

Review of Results

General Trends in Strength I Maximum r Values

Additional insight into the influence of truck sorting strategies on r values was gained by investigating the variations in r values based on the following:

1. Force effects such as simple-span moment, simple-span shear, and negative bending; and
2. Span length (20 ft, 60 ft, 120 ft).

The maximum moment or shear values of r for all span lengths considered (from 20-ft to 200-ft) have been tabulated in Table 60 for sorting variations P1 through P12 and the baseline sorting strategy.

1. As can be seen in the variations of r for Strength I in Table 60, the variation in number of axles does not have a large impact upon r values.
2. Increasing GVW for trucks in Strength I leads to a small increase in r values.
3. Configurations of the trucks as governed by state permit regulations (and weight regulations) have the greatest influence on r values when compared to either GVW or the number of axles.
4. Compared with P12 where all trucks are in Strength I, P8 and P9 see a big drop in Strength I r values. In P8 and P9, all illegal trucks and trip permits are moved to Strength II.
5. Comparing P8, P9, and P10 is instructive. The inclusion of annual permits in with legal trucks in P9 only resulted in a small increase in r values. However, when illegal trucks are added to legal trucks in P10, there is a significant increase in r values.
6. Comparing P11 to P12, the only difference is that trip permits are added to Strength I in P12. It is evident that adding trip permits causes no noticeable change in maximum r values. This shows that heavy permits, when they are legal and comply with permit regulations, do not induce significant load effects.

7. In P10 and P11 overloaded trucks not complying with permit or weight regulations were grouped into Strength I, which led to high r values.
8. Florida Site 9919 did not show a jump in r values between P9 and P10 as did the other sites. This may be explained by the low number of illegal trucks (only 24) at this site (see Table 63). With the exception of these 24 trucks, this site has only legal loads and annual permits that comply with all permit regulations. With this high level of compliance, the r values are predictably low. As the number of illegal loads increases for the other two Florida sites, the r values also show a big increase.
9. Most Strength II trucks in Indiana were classified as illegal (P9–P11). Most Strength II trucks in Florida were classified as annual permits (P10–P11). In California, the Strength II trucks were equally divided between illegal trucks and annual permits (P9 and P10).
10. There is a big drop in number of Strength II trucks with axles > 7 (baseline) and GVW > 100.
11. Baseline and P11 results provide a useful comparison. Both sorting cases seek to include all legal trucks, illegal overloads, and unanalyzed permits (all annual/routine permits) into Strength I, but execute this by different approaches as previously discussed. For Florida, the results are comparable. For Indiana, P11 is slightly higher. For California, it is about 30% higher. This means that California has more annual permits or illegal loads with number of axles greater than seven, which were being

Table 60. Summary of maximum Strength I r values for all WIM sites.

			Maximum r Values, Strength I								
Sorting Variation			IN WIM Sites			CA WIM Sites			FL WIM Sites		
			9544	9532	9512	Site 0003	Site 0059	Site 0072	9919	9926	9936
# Axles	Str. I: # Axles ≤ 5	P3	1.97	1.41	1.07	1.08	1.07	1.08	0.92	2.19	2.18
	Str. I: # Axles ≤ 6	(Baseline)	1.97	1.41	1.12	1.11	1.10	1.08	0.94	2.21	2.17
	Str. I: # Axles ≤ 7	P1	1.98	1.42	1.21	1.13	1.13	1.08	0.94	2.21	2.15
	Str. I: # Axles ≤ 8	P2	2.11	1.42	1.21	1.43	1.16	1.08	0.94	2.21	2.15
GVW	Str. I: GVW ≤ 84	P4	1.34	1.13	1.06	0.90	0.94	0.85	0.92	1.21	1.11
	Str. I: GVW ≤ 100	P5	1.51	1.29	1.07	1.08	0.96	0.89	0.93	1.35	1.22
	Str. I: GVW ≤ 120	P6	1.59	1.40	1.07	1.10	1.02	1.02	0.94	1.47	1.49
	Str. I: GVW ≤ 150	P7	1.82	1.41	1.18	1.13	1.11	1.08	0.95	1.87	2.03
State Permit Regulations	Str I: Legal	P8	0.76	0.71	0.68	0.64	0.71	0.67	0.83	0.92	0.80
	Str I: Legal & Annual	P9	0.85	0.71	0.72	0.99	0.95	0.95	0.95	1.33	1.42
	Str I: Legal & Illegal	P10	2.11	1.45	1.38	1.52	1.42	1.61	0.89	2.32	2.24
	Str I: All but Trip	P11	2.11	1.45	1.38	1.46	1.36	1.54	0.95	2.21	2.15
Non Sorted	All Trucks in Str I	P12	2.11	1.45	1.38	1.46	1.36	1.54	0.95	2.21	2.15

grouped into Strength II in the baseline case. Using a state's permit and weight regulations as in P11 to group trucks into Strength I and Strength II is considered more rational, whereas the axles-based approach used in the 12-76 protocols is considered simpler, yet less precise, when using national WIM data.

Sensitivity Analysis of Strength I Maximum r Values

The previous sections compared the maximum r values for the baseline and sorting variations P1 thru P12 by grouping them into the following:

Group I: Baseline, P1, P2, and P3 sorting based on number of axles;

Group II: P4, P5, P6 and P7 sorting based on GVW;

Group III: P8, P9, P10, and P11 sorting based on state permit regulations; and

Group IV: Non sorted—P12 used as a reference for sensitivity analysis.

Sensitivity Analysis Using r Differentials for Strength I

The key objective of this analysis is to investigate how sensitive the r values are to how the trucks are sorted. This section is comprised of the findings of a sensitivity analysis performed on r values by defining a new metric for Strength I termed the "r differential." This metric is defined as

$$r\ differential = \left[(r12 - rx)/r12\right] \times 100\%$$

Where:

r12 = r value for reference case P12, which includes all trucks in Strength I

rx = r value for sorting variation Px (could be any one of P1 through P11 or baseline)

It provides a quantification of how the r value changes in percentage terms as various trucks are removed from P12 (the reference case that was not sorted) and includes all trucks in Strength I. For example, to understand how sensitive the r values are when trucks that weigh more than 120 kips are excluded from Strength I, the following r differential is executed:

$$r\ differential\ for\ P6 = \left[(r12 - r6)/r12\right] \times 100\%$$

To understand how sensitive the r values are when trip permits are excluded from Strength I, the following r differential is executed:

$$r\ differential\ for\ P11 = \left[(r12 - r11)/r12\right] \times 100\%$$

Similarly, to understand how sensitive the r values are when all trucks but state legal loads are excluded from Strength I, the following r differential is executed:

$$r\ differential\ for\ P8 = \left[(r12 - r8)/r12\right] \times 100\%$$

General Trends in Strength I r Differential Results

The results of r differentials are summarized in Table 61. The average r differentials for the three WIM sites in each state are shown for the following force effects and span lengths:

- Force effects such as simple-span moment, simple-span shear, and negative bending; and
- Span lengths (20 ft, 60 ft, 120 ft).

The last three columns of Table 61 show the averages for all WIM sites by span length and load effect for easy comparison. A detailed review of r differential results for selected sites is included later in this chapter. Complete results for each WIM site are included in Appendix F.

The findings from Table 61 may be stated as follows:

1. Group III results (based on state permit regulations), particularly P8 and P9, are the most sensitive, followed by Group II (based on GVW), and then Group III (based on number of axles).
2. The r differential results for P8 were the highest. This signifies the biggest difference in r values occurs when only state legal loads are included in Strength I or when illegal loads, trip permits, and annual permits are excluded. The average drop was between 44% and 64%.
3. The r differential results for P10 and P11 were negligible. This indicates the minimal influence of removing annual permits or trip permits from Strength I.
4. The r differential results for P9 were the second highest in Group III. The average drop was between 32% and 40%. This signifies the sensitivity of the results to removing illegal loads and trip permits. P10 and P11 show that trip permits exert minimal influence on r values, which means that illegal trucks were essentially responsible for the drop in r values.
5. The Group III r differential results were not significantly sensitive to span length or load effect and remained relatively consistent for each state. Similar findings were identified in the previous discussions on r values for Group III.
6. P4 r differential results were the highest within Group II (based on GVW) and decrease gradually to the lowest values obtained for P7. This shows that as heavier trucks were included in Strength I the r differential is minimized as expected. This is in line with the previous discussions on Group II r values.

Table 61. Summary average r differentials.

Strength I Definition	Load Effect	Average for CA			Average for IN			Average for FL			Average for CA, IN,FL		
Average r Differential Values (percentage) for Strength I		20 ft	60 ft	120 ft	20 ft	60 ft	120 ft	20 ft	60 ft	120 ft	20 ft	60 ft	120 ft
Based on # Axles													
Baseline	M-simple	18	14	21	5	10	28	0	1	0	6	8	17
# Axles 6 or less	V-simple	18	13	29	4	16	29	0	0	3	5	10	20
	M-negative	26	40	44	11	29	37	1	15	9	8	28	30
P1	M-simple	15	11	11	3	6	20	0	0	0	5	6	11
# Axles 7 or less	V-simple	15	10	20	2	11	20	0	0	2	4	7	14
	M-negative	21	31	36	10	19	30	0	7	8	6	19	25
P2	M-simple	12	8	10	0	1	4	0	0	0	4	3	5
# Axles 8 or less	V-simple	12	8	17	0	2	6	0	0	0	4	3	8
	M-negative	15	24	33	3	7	14	0	0	4	3	10	17
P3	M-simple	22	28	33	5	13	32	4	1	6	7	14	24
# Axles 5 or less	V-simple	21	20	32	4	21	34	1	4	9	5	15	25
	M-negative	32	40	48	14	35	41	2	23	14	11	33	35
Based on GVW													
P4	M-simple	40	38	49	19	30	53	34	28	42	26	32	48
GVW 84 or less	V-simple	44	37	55	22	39	57	32	36	48	27	37	53
	M-negative	52	63	65	31	62	64	29	59	54	30	61	61
P5	M-simple	35	31	40	12	23	45	30	25	35	22	27	40
GVW 100 or less	V-simple	39	27	45	14	32	50	29	32	41	23	30	45
	M-negative	45	55	58	24	53	57	25	49	46	24	52	54
P6	M-simple	27	19	26	9	18	37	20	21	26	16	19	30
GVW 120 or less	V-simple	28	17	35	11	24	39	22	24	29	17	22	34
	M-negative	34	44	49	16	40	47	18	35	33	16	40	43
P7	M-simple	18	11	13	6	10	26	9	6	14	10	9	18
GVW 150 or less	V-simple	20	11	22	6	15	28	7	11	18	8	12	22
	M-negative	25	33	35	11	25	36	9	20	20	11	26	30
Based on State Permit Regulations													
P8	M-simple	52	53	55	50	52	62	46	40	52	47	48	56
Legal	V-simple	54	48	59	51	56	63	45	47	54	48	50	58
	M-negative	57	63	67	49	63	67	40	59	58	44	62	64
P9	M-simple	38	41	38	47	51	56	23	26	27	32	39	40
Legal & Annual	V-simple	37	33	35	49	54	55	25	29	23	34	39	38
	M-negative	34	33	30	49	51	55	23	17	14	35	34	33
P10	M-simple	0	0	-3	0	0	0	3	1	0	1	0	0
Legal & Illegal	V-simple	0	0	-4	0	0	1	1	0	2	0	0	0
	M-negative	1	-4	-3	0	0	0	2	12	7	0	3	1
P11	M-simple	0	0	0	0	0	0	0	0	3	0	0	1
All but Trip Permits	V-simple	1	0	0	0	0	0	0	2	4	0	1	1
	M-negative	1	0	0	0	0	0	1	7	6	0	2	2
P12	M-simple	0	0	0	0	0	0	0	0	0	0	0	0
All Trucks	V-simple	0	0	0	0	0	0	0	0	0	0	0	0
	M-negative	0	0	0	0	0	0	0	0	0	0	0	0

7. The r Differential results for Group II vary from under 10% for P7 to over 60% for P4. The r differential shows an increase with increasing span lengths, and generally the highest values were for the negative moments. This is likely due to the fact that the longer and heavier trucks could be dominating both the longer spans and the negative bending. The trends were similar for all three states, with the exception that Florida had a very low r differential for P7.

8. Group I r differential results were the lowest, particularly for Florida, where the results mostly were less than 10%. This shows that sorting trucks based on number of axles for Florida WIM sites is not particularly effective—at least when compared with Group II and Group III sorting strategies.

9. For California and Indiana, the Group I r differential results increase with increasing span lengths. The r differential also increases as trucks with a higher number of axles are removed from Strength I. The highest values were obtained for P3 and the lowest for P2. The general trends were similar for all load effects.

Sensitivity analysis of r values shows that Group III results (based on state permit regulations), particularly P8 and P9, are the most sensitive, followed by Group II (based on GVW), and then Group III (based on number of axles). In P10, when illegal trucks are added to state legal loads, the r differential disappears, which indicates that illegal trucks—not the permits that follow state permit regulations—are likely the biggest drivers of high r values.

Baseline and P11 results provide a useful comparison. Both sorting cases seek to include all legal trucks, illegal overloads, and unanalyzed permits (all annual/routine permits) into Strength I, but execute this by different approaches. For Florida, the results are comparable. But for Indiana and California P11 will give higher r values than the baseline case of using trucks with six or fewer axles to define all trucks other than heavy trip permits. **Using a state's permit and weight regulations (as in P11) to group trucks into Strength I and Strength II is considered more rational, and more precise,** when using national WIM data. The r differentials for a 60-ft span moment are given in Table 62.

Another helpful sensitivity index is the change in r values from P8 to P9 where annual permits are added to state legal loads and from P8 to P10 where illegal loads are added to state legal loads.

Table 63 also illustrates the influence of illegal trucks in driving high r values. For Indiana, adding annual permits to state legal loads did not result in a significant increase in r values. But this was very different when the illegal loads were included. To travel legally on any Indiana roads, trucks cannot exceed the federal weight limits and must comply with Federal Bridge Formula B. An overweight vehicle is generally any vehicle whose overall weight exceeds 80,000 lbs. However, the overweight truck must comply with Federal Bridge Formula B. Indiana considers permits exceeding the legal limits as annual permits for loads up to a GVW of 120 kips. The illegal trucks exceed the federal weight limits, and particularly the Formula B limits, resulting in high r values.

Table 62. Sorting variations showing r differential.

Sorting Variation	Trucks in Strength I	r Differential for 60-Ft Span Moment (CA, IN, FL)
P12	All trucks	(0,0,0)
GROUP I (Based on Number of Axles)		
P3	Trucks with 5 or fewer axles	(28, 13, 1)
Baseline	Trucks with 6 or fewer axles	(14, 10, 1)
P1	Trucks with 7 or fewer axles	(11, 6, 0)
P2	Trucks with 8 or fewer axles	(8, 1, 0)
GROUP II (Based on GVW)		
P4	Trucks with GVW ≤ 84 kips	(38, 30, 28)
P5	Trucks with GVW ≤ 100 kips	(31, 23, 25)
P6	Trucks with GVW ≤ 120 kips	(19, 18, 21)
P7	Trucks with GVW ≤ 150 kips	(11, 10, 6)
GROUP III (Based on State Permit Regulations)		
P8	State legal trucks only	(53, 52, 40)
P9	State legal trucks, annual (routine) permits	(41, 51, 26)
P10	State legal trucks, illegal trucks	(0, 0, 1)
P11	State legal trucks, illegal trucks, annual (routine) permits	(0, 0, 0)

Table 63. Percentage change in r values.

WIM Site	% Change in r values from P8 to P9 (number of added annual permits)	% Change in r values from P8 to P10 (number of added illegal trucks)
IN 9544	10.6 % (6685)	178 % (110,774)
IN 9532	0 % (433)	104 % (17,378)
IN 9512	0 % (17599)	103 % (140,098)
CA 0003	55 % (1118)	138 % (1576)
CA 0059	34 % (22,525)	100 % (26,487)
CA 0072	42 % (1411)	140 % (1200)
FL 9919	15 % (4389)	7 % (24)
FL 9926	45 % (219,378)	152 % (3259)
FL 9936	78 % (234,938)	180 % (2989)

Unlike the Indiana results, California and Florida show bigger increases when annual permits are added to state legal loads. California issues annual permits for vehicle weights up to 300,000 lbs. Florida requires an overload permit for any vehicle that exceeds 80,000 lbs. For the typical blanket permits, the highest gross vehicle weight limit is 199,000 lbs. Another difference between the typical federal legal load definitions and the Florida regulations is a grandfather exemption for short single-unit trucks. Florida allows short single-unit trucks as legal loads up to 70,000 lbs that do not meet the Federal Bridge Formula B requirement. For both California and Florida, the influence of illegal trucks on r values was far more significant than that of annual permits.

Detailed Review of Strength I r Differential Results

One WIM site from each state has been selected for a more in-depth review and discussion and will serve as representative examples of the other sites for each state. The sites to be discussed are Indiana Site 9544, California Site 0059, and Florida Site 9936.

A discussion of r differential results is provided following the sorting groups previously defined.

Group I: Sorting Variation Based on Number of Axles. The following sorting variations will be discussed under Group I:

- Baseline: Strength I = 6 axles or less,
- P1: Strength I = 7 axles or less,
- P2: Strength I = 8 axles or less, and
- P3: Strength I = 5 axles or less.

From Table 64 and Figure 40, sorting case P2 where trucks with nine axles or more are excluded from Strength I shows no noticeable r differential values. However, baseline, P1 and P2 show increasing r differential values with increasing span length. The trucks excluded in baseline, P1, and P3 are

- Baseline: 7 axles or more,
- P1: 8 axles or more, and
- P3: 6 axles or more.

Table 64. Indiana Site 9544 r differentials for Group I.

| Sorting Variation	Load Effect	Strength I r Values			r Differential = (r12 - rx) / r12 x 100%		
		Span Length (ft)			Span Length (ft)		
		20	60	120	20	60	120
Baseline	M-simple	1.77	1.45	1.28	7.22	12.86	30.99
	V-simple	1.97	1.54	1.38	5.56	27.14	34.27
	M-negative	1.45	1.12	0.74	21.24	29.24	35.18
P1	M-simple	1.78	1.50	1.34	6.52	9.94	27.72
	V-simple	1.98	1.64	1.46	4.77	21.96	30.21
	M-negative	1.47	1.15	0.78	20.39	27.92	31.66
P2	M-simple	1.91	1.66	1.86	-0.01	0.03	-0.04
	V-simple	2.08	2.11	2.10	0.00	-0.04	-0.07
	M-negative	1.84	1.58	1.14	-0.03	0.54	0.35
P3	M-simple	1.77	1.45	1.26	7.20	13.21	31.99
	V-simple	1.97	1.52	1.35	5.62	27.88	35.50
	M-negative	1.44	1.07	0.72	21.67	32.51	37.44
P12	M-simple	1.91	1.67	1.86	0.00	0.00	0.00
	V-simple	2.08	2.11	2.10	0.00	0.00	0.00
	M-negative	1.84	1.59	1.15	0.00	0.00	0.00
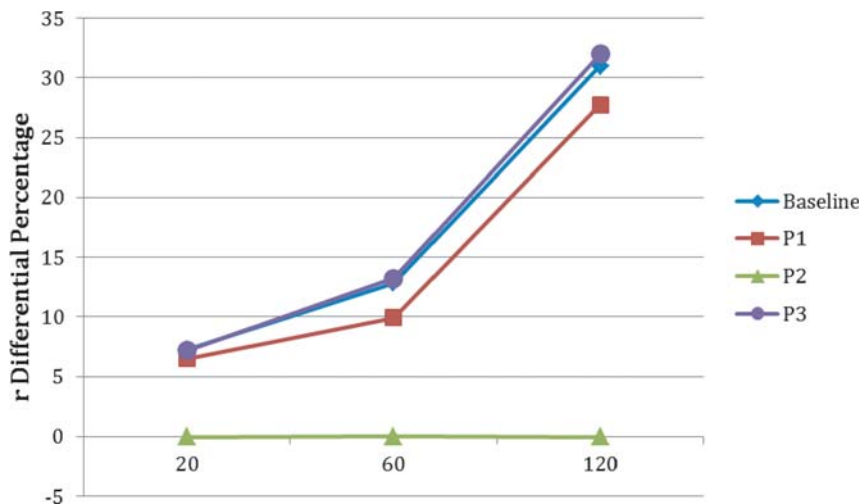
Figure 40. Strength I moment r differentials for Group I vs. span lengths (Indiana Site 9544).

P3, where trucks with six or more axles are excluded, has the highest r differential.

From Table 65 and Figure 41, all sorting cases show increasing r differential values with increasing span length. The trucks excluded in baseline, P1, P2, and P3 are

- Baseline: 7 axles or more,
- P1: 8 axles or more,
- P2: 9 axles or more, and
- P3: 6 axles or more.

P3, where trucks with six or more axles are excluded, has the highest r differential. Unlike the Indiana site, P2 values do vary with span length indicating that the California site has a population of trucks with 9 or more axles.

From Table 66 and Figure 42, all sorting cases show minimal r differential values with increasing span length for the Florida site.

Group II: Sorting Variation Based on GVW.   The following sorting variations will be discussed under Group II:

- P4: Strength I = GVW ≤ 84,
- P5: Strength I = GVW ≤ 100,
- P6: Strength I = GVW ≤ 120, and
- P7: Strength I = GVW ≤ 150.

In Table 67 and Figure 43 all sorting cases show increasing r differential values with increasing span length for the Indiana site. This shows that as increasingly heavier trucks are

Table 65. California Site 0059 r differentials for Group I.

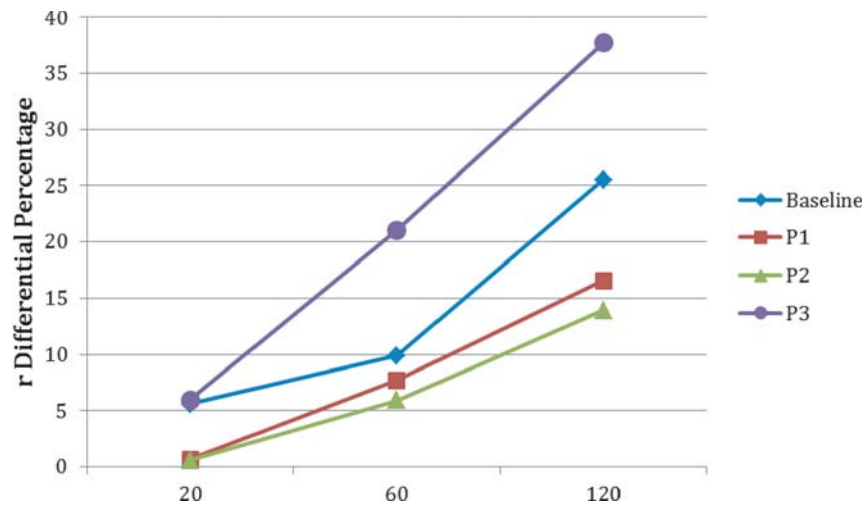| Sorting Variation	Load Effect	Strength I r Values			r Differential = (r12 - rx) / r12 x 100%		
		Span Length (ft)			Span Length (ft)		
		20	60	120	20	60	120
Baseline	M-simple	0.94	1.03	0.97	5.61	9.88	25.49
	V-simple	1.07	1.10	1.01	4.56	12.81	23.76
	M-negative	1.05	0.82	0.55	8.50	30.75	37.88
P1	M-simple	0.99	1.06	1.09	0.65	7.70	16.57
	V-simple	1.09	1.13	1.13	3.30	10.69	14.14
	M-negative	1.12	0.97	0.63	1.95	17.92	28.59
P2	M-simple	0.99	1.08	1.12	0.58	5.90	13.89
	V-simple	1.09	1.14	1.16	3.21	9.69	12.08
	M-negative	1.13	1.04	0.66	1.56	12.15	25.04
P3	M-simple	0.94	0.90	0.81	5.94	21.05	37.70
	V-simple	1.07	0.97	0.93	4.72	22.78	29.61
	M-negative	1.02	0.81	0.48	10.49	31.15	45.09
P12	M-simple	1.00	1.14	1.30	0.00	0.00	0.00
	V-simple	1.13	1.26	1.32	0.00	0.00	0.00
	M-negative	1.14	1.18	0.88	0.00	0.00	0.00

Figure 41. Strength I moment r differentials for Group I vs. span lengths (California Site 0059).

Table 66. Florida Site 9936 r differentials for Group I.

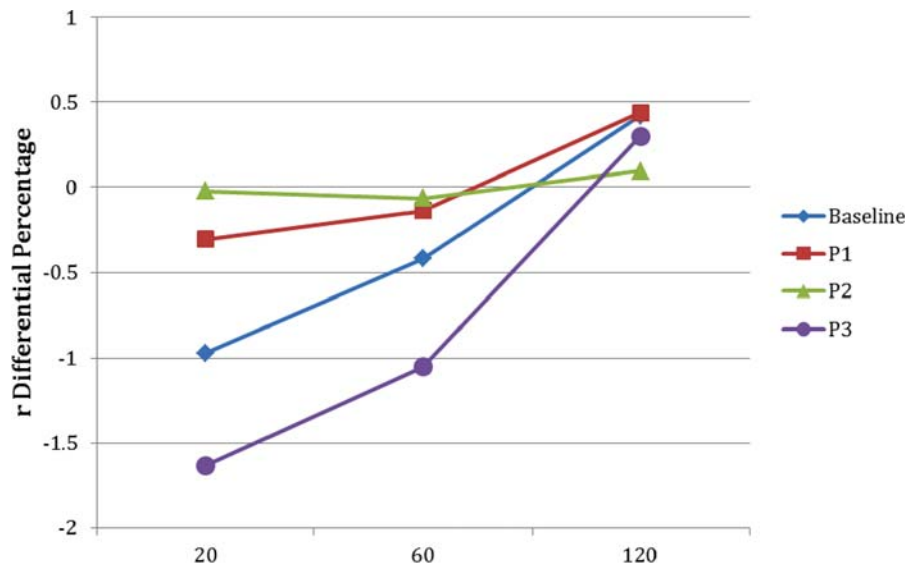| Sorting Variation	Load Effect	Strength I r Values			r Differential = (r12 - rx) / r12 x 100%		
		Span Length (ft)			Span Length (ft)		
		20	60	120	20	60	120
Baseline	M-simple	2.02	1.51	1.31	-0.97	-0.42	0.42
	V-simple	2.17	1.66	1.43	-0.91	-0.40	5.48
	M-negative	1.46	1.13	0.74	0.24	22.03	13.03
P1	M-simple	2.00	1.51	1.31	-0.30	-0.14	0.44
	V-simple	2.15	1.65	1.46	-0.31	-0.16	3.71
	M-negative	1.46	1.26	0.76	0.24	12.46	11.24
P2	M-simple	2.00	1.51	1.32	-0.02	-0.07	0.09
	V-simple	2.15	1.65	1.51	-0.02	-0.04	0.22
	M-negative	1.46	1.44	0.80	0.24	0.29	5.69
P3	M-simple	2.03	1.52	1.31	-1.63	-1.05	0.30
	V-simple	2.18	1.66	1.43	-1.50	-0.93	5.61
	M-negative	1.47	1.12	0.74	0.01	22.69	13.54
P12	M-simple	2.00	1.51	1.32	0.00	0.00	0.00
	V-simple	2.15	1.65	1.51	0.00	0.00	0.00
	M-negative	1.47	1.44	0.85	0.00	0.00	0.00

Figure 42. Strength I moment r differentials, Group I vs. span lengths (Florida Site 9936).

Table 67. Indiana Site 9544 r differentials, Group II.

Sorting Variation	Load Effect	Strength I r Values			r Differential = (r12 - rx) / r12 x 100%		
		Span Length (ft)			Span Length (ft)		
		20	60	120	20	60	120
P4	M-simple	1.34	0.92	0.67	29.56	44.80	63.93
	V-simple	1.31	0.91	0.68	37.06	56.86	67.48
	M-negative	0.92	0.51	0.35	50.10	67.76	69.51
P5	M-simple	1.51	1.08	0.81	21.14	35.38	56.55
	V-simple	1.50	1.08	0.84	27.93	48.97	60.00
	M-negative	1.09	0.65	0.43	40.74	59.25	62.42
P6	M-simple	1.59	1.13	0.92	16.88	32.13	50.48
	V-simple	1.59	1.19	1.00	23.76	43.59	52.20
	M-negative	1.24	0.80	0.53	32.53	49.53	54.14
P7	M-simple	1.64	1.37	1.14	14.25	17.43	38.71
	V-simple	1.82	1.46	1.23	12.80	30.85	41.49
	M-negative	1.43	0.97	0.65	22.30	38.72	43.60
P12	M-simple	1.91	1.67	1.86	0.00	0.00	0.00
	V-simple	2.08	2.11	2.10	0.00	0.00	0.00
	M-negative	1.84	1.59	1.15	0.00	0.00	0.00

included in Strength I, going from P4 to P7, the r differential is minimized as expected.

In Table 68 and Figure 44, all sorting cases show increasing r differential values with increasing span length for the California site. This shows that as increasingly heavier trucks are included in Strength I, going from P4 to P7, the r differential is minimized as expected.

In Table 69 and Figure 45, all sorting cases generally show increasing r differential values with increasing span length for the Florida site. This shows that as increasingly heavier trucks are included in Strength I, going from P4 to P7, the r differential is minimized as expected.

Group III: Sorting Variation Based on State Permit Regulations. The following sorting variations will be discussed under Group III:

- P8: Strength I = state legal trucks,
- P9: Strength I = state legal trucks and annual permits,
- P10: Strength I = state legal trucks and illegal trucks, and
- P11: Strength I = state legal trucks, illegal trucks, and annual permits.

In Table 70 and Figure 46, Group III results (based on state permit regulations), particularly P8 and P9, are the most sensitive. The r differential results for P8 were the highest. This signifies the biggest difference in r values occurs when only state legal loads are included in Strength I or illegal loads, trip permits, and annual permits are excluded.

The r differential results for P10 and P11 were negligible. This indicates the minimal influence of removing annual permits or trip permits from Strength I. The Group III r differential results were not significantly sensitive to span length or load effect.
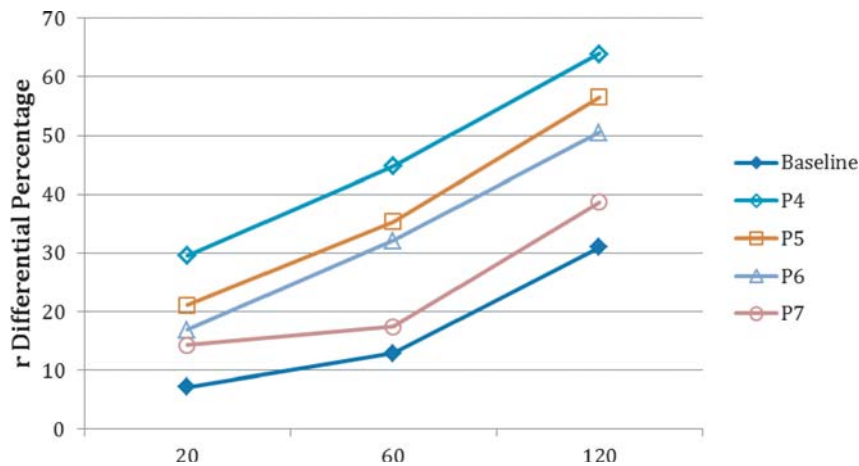

Figure 43. Strength I moment r differentials for Group II vs. span lengths (Indiana Site 9544).

Table 68. California Site 0059 r differentials for Group II.

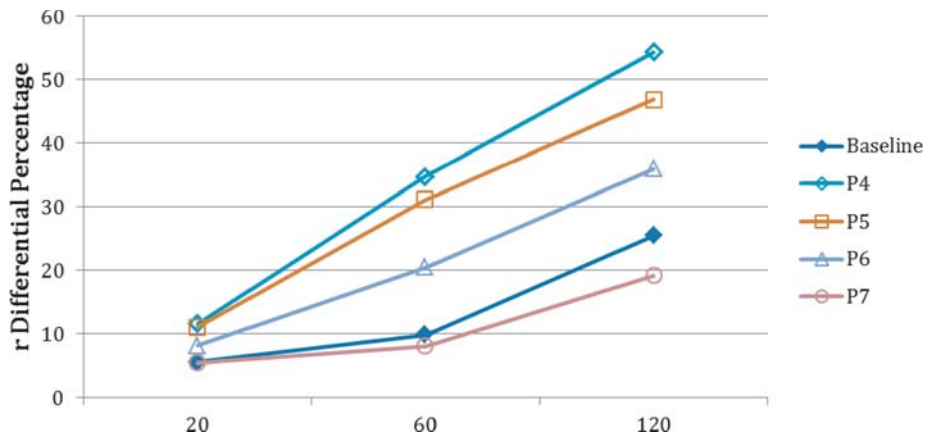| Sorting Variation	Load Effect	Strength I r Values			r Differential = (r12 - rx) / r12 x 100%		
		Span Length (ft)			Span Length (ft)		
		20	60	120	20	60	120
P4	M-simple	0.88	0.75	0.59	11.64	34.77	54.34
	V-simple	0.94	0.78	0.63	16.23	37.91	52.46
	M-negative	0.84	0.49	0.33	26.69	58.64	62.79
P5	M-simple	0.89	0.79	0.69	11.09	31.11	46.84
	V-simple	0.95	0.88	0.74	15.72	30.23	43.77
	M-negative	0.96	0.59	0.40	15.67	50.44	54.85
P6	M-simple	0.92	0.91	0.83	8.17	20.47	35.92
	V-simple	1.02	0.98	0.88	9.60	22.61	33.67
	M-negative	1.02	0.72	0.47	10.43	38.77	46.18
P7	M-simple	0.94	1.05	1.05	5.47	8.09	19.21
	V-simple	1.08	1.11	1.08	4.45	11.78	18.40
	M-negative	1.06	0.86	0.60	7.53	27.58	31.38
P12	M-simple	1.00	1.14	1.30	0.00	0.00	0.00
	V-simple	1.13	1.26	1.32	0.00	0.00	0.00
	M-negative	1.14	1.18	0.88	0.00	0.00	0.00

Figure 44. Strength I moment r differentials for Group II vs. span lengths (California Site 0059).

Table 69. Florida Site 9936 r differentials, Group II.

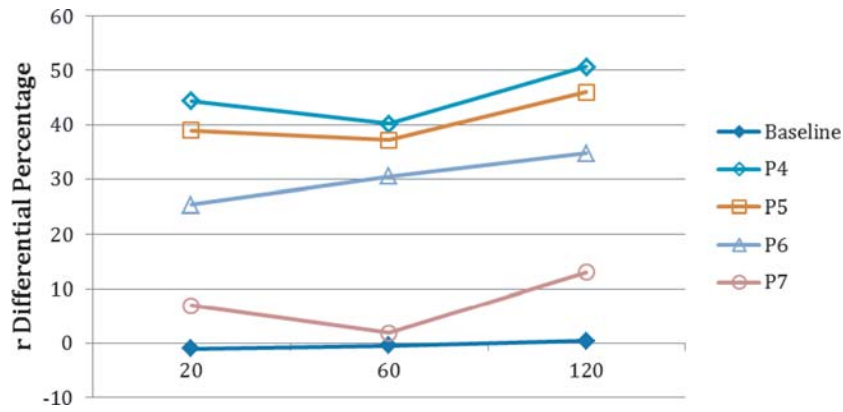| Sorting Variation	Load Effect	Strength I r Values			r Differential = (r12 - rx) / r12 x 100%		
		Span Length (ft)			Span Length (ft)		
		20	60	120	20	60	120
P4	M-simple	1.11	0.90	0.65	44	40.18	50.73
	V-simple	1.11	0.90	0.66	48	45.60	56.08
	M-negative	0.99	0.49	0.33	32.86	66.05	61.32
P5	M-simple	1.22	0.95	0.71	38.97	37.14	46.00
	V-simple	1.18	0.96	0.75	44.96	41.97	50.24
	M-negative	1.04	0.58	0.39	29.14	59.89	53.87
P6	M-simple	1.49	1.05	0.86	25.39	30.51	34.71
	V-simple	1.43	1.10	0.92	33.22	33.35	39.31
	M-negative	1.16	0.74	0.49	20.75	48.98	42.66
P7	M-simple	1.86	1.48	1.15	7.01	1.90	13.10
	V-simple	2.03	1.52	1.21	5.52	7.87	19.92
	M-negative	1.39	1.00	0.63	5.33	31.10	26.46
P12	M-simple	2.00	1.51	1.32	0.00	0.00	0.00
	V-simple	2.15	1.65	1.51	0.00	0.00	0.00
	M-negative	1.47	1.44	0.85	0.00	0.00	0.00

*Figure 45. Strength I moment r differentials for Group II vs. span
lengths (Florida Site 9936).*

Table 70. Indiana Site 9544 r differentials for Group III.

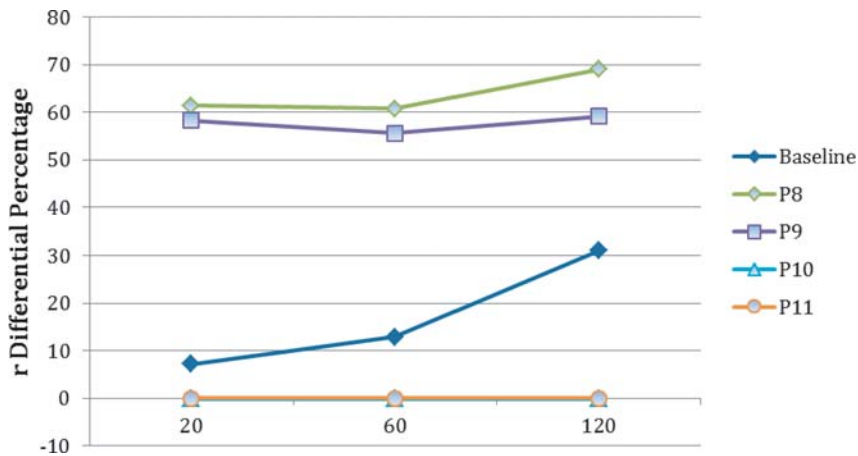| Sorting Variation	Load Effect	Strength I r Values			r Differential = (r12 - rx) / r12 x 100%		
		Span Length (ft)			Span Length (ft)		
		20	60	120	20	60	120
P8	M-simple	0.74	0.65	0.58	61.38	60.76	69.05
	V-simple	0.76	0.70	0.62	63.42	66.70	70.39
	M-negative	0.72	0.51	0.33	60.89	68.00	71.18
P9	M-simple	0.80	0.74	0.76	58.27	55.65	59.12
	V-simple	0.85	0.79	0.78	59.37	62.64	62.67
	M-negative	0.73	0.67	0.46	60.20	58.14	59.73
P10	M-simple	1.91	1.67	1.86	-0.04	-0.06	-0.07
	V-simple	2.09	2.11	2.10	-0.04	-0.04	-0.06
	M-negative	1.85	1.59	1.15	-0.04	-0.07	-0.07
P11	M-simple	1.91	1.67	1.86	0.00	0.00	0.00
	V-simple	2.08	2.11	2.10	0.00	0.00	0.00
	M-negative	1.84	1.59	1.15	0.00	0.00	0.00
P12	M-simple	1.91	1.67	1.86	0.00	0.00	0.00
	V-simple	2.08	2.11	2.10	0.00	0.00	0.00
	M-negative	1.84	1.59	1.15	0.00	0.00	0.00

*Figure 46. Strength I moment r differentials for Group III vs. span
lengths (Indiana Site 9544).*

Table 71. California Site 0059 r differentials for Group III.

Sorting Variation	Load Effect	Strength I r Values			r Differential = (r12 - rx) / r12 x 100%		
		Span Length (ft)			Span Length (ft)		
		20	60	120	20	60	120
P8	M-simple	0.65	0.57	0.52	35.09	50.16	60.07
	V-simple	0.69	0.66	0.59	38.83	48.03	55.40
	M-negative	0.71	0.48	0.31	38.03	59.14	64.58
P9	M-simple	0.87	0.70	0.68	12.92	39.22	48.06
	V-simple	0.95	0.79	0.86	15.52	37.26	34.89
	M-negative	0.81	0.85	0.62	29.31	28.24	29.84
P10	M-simple	1.00	1.14	1.34	-0.77	0.74	-3.02
	V-simple	1.14	1.26	1.37	-1.00	-0.13	-3.55
	M-negative	1.15	1.22	0.90	-0.32	-3.27	-2.73
P11	M-simple	1.00	1.14	1.30	0.00	0.00	0.00
	V-simple	1.13	1.26	1.32	0.00	0.00	0.00
	M-negative	1.14	1.18	0.88	0.00	0.00	0.00
P12	M-simple	1.00	1.14	1.30	0.00	0.00	0.00
	V-simple	1.13	1.26	1.32	0.00	0.00	0.00
	M-negative	1.14	1.18	0.88	0.00	0.00	0.00

In Table 71 and Figure 47, Group III results (based on state permit regulations) for the California site, particularly P8 and P9, are the most sensitive. The r differential results for P8 were the highest. This signifies that the biggest difference in r values occurs when only state legal loads are included in Strength I or illegal loads, trip permits, and annual permits are excluded.

The r differential results for P10 and P11 were negligible. This indicates the minimal influence of removing annual permits or trip permits from Strength I. The Group III r differential results for P8 and P9 were sensitive to span length.

From Table 72 and Figure 48, Group III results (based on state permit regulations) for the Florida site, particularly P8 and P9, are the most sensitive. The r differential results for P8 were the highest. This signifies that the biggest difference

in r values occurs when only state legal loads are included in Strength I or illegal loads, trip permits, and annual permits are excluded.

The r differential results for P10 and P11 were negligible. This indicates the minimal influence of removing annual permits or trip permits from Strength I. The Group III r differential results are not particularly sensitive to span length.

Findings and Recommendations

Some important findings from this study are

- Sorting based on the number of axles does not have a large impact upon r values.
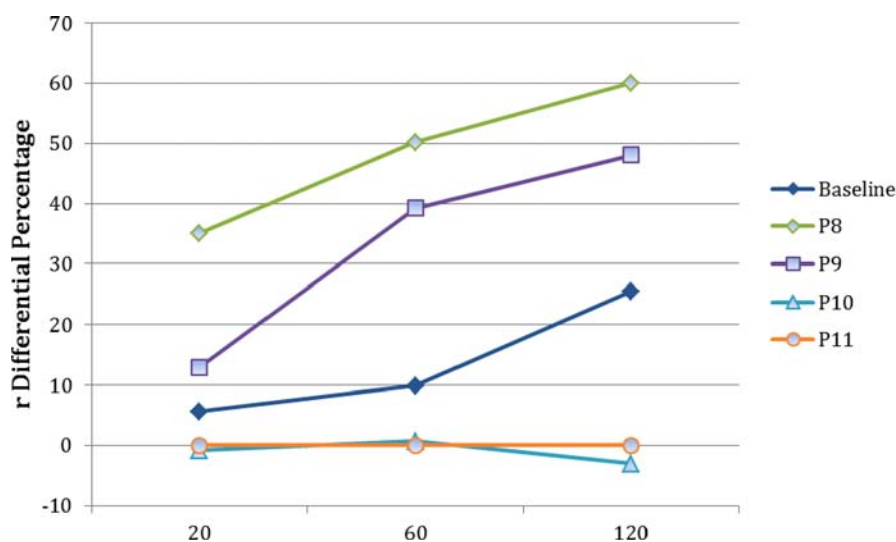

Figure 47. Strength I moment r differentials for Group III vs. span lengths (California Site 0059).

Table 72. Florida Site 9936 r Differentials for Group III.

Sorting Variation	Load Effect	Strength I r Values			r Differential = (r12 - rx) / r12 x 100%		
		Span Length (ft)			Span Length (ft)		
		20	60	120	20	60	120
P8	M-simple	0.76	0.68	0.52	61.70	54.83	60.19
	V-simple	0.80	0.68	0.59	62.70	58.74	61.24
	M-negative	0.71	0.48	0.31	51.61	66.53	64.18
P9	M-simple	1.42	0.95	0.90	28.61	37.02	31.95
	V-simple	1.37	1.03	1.08	36.27	37.44	28.50
	M-negative	1.07	1.08	0.73	27.33	25.43	14.47
P10	M-simple	2.09	1.58	1.38	-4.75	-4.59	-5.01
	V-simple	2.24	1.74	1.55	-4.32	-5.37	-2.50
	M-negative	1.55	1.48	0.83	-5.64	-2.29	2.23
P11	M-simple	2.00	1.51	1.31	-0.02	0.11	0.62
	V-simple	2.15	1.65	1.45	-0.01	0.06	3.79
	M-negative	1.46	1.33	0.78	0.21	8.08	8.39
P12	M-simple	2.00	1.51	1.32	0.00	0.00	0.00
	V-simple	2.15	1.65	1.51	0.00	0.00	0.00
	M-negative	1.47	1.44	0.85	0.00	0.00	0.00

- Increasing GVW for trucks in Strength I leads to a small increase in r values.
- Configurations of trucks as governed by state permit regulations (and weight regulations) have the greatest influence on r values than either GVW or the number of axles.
- The inclusion of annual permits in Strength I, along with legal trucks, only resulted in a small increase in r values. However, when illegal trucks are added to legal trucks, a significant increase in r values was observed. Adding trip permits to the vehicle mix causes no noticeable change in max r values.
- This shows that heavy permits, when they are legal and comply with permit regulations, do not significantly impact r values. However, overloaded trucks not complying with permit or weight regulations (illegal trucks), led to high r values.
- Baseline and P11 results provide a useful comparison. Both sorting cases seek to include all legal trucks, illegal overloads, and unanalyzed permits (all annual/routine permits) into Strength I, but execute this by different approaches. For Florida, the results are comparable. For Indiana, P11 is slightly higher. For California, P11 is about 30% higher. Using a state's permit and weight regulations as in P11 to group trucks into Strength I and Strength II is considered more rational, and more precise, when using national WIM data.
- A sensitivity analysis of r values shows that Group III results (based on state permit regulations), particularly P8 and P9, are the most sensitive, followed by Group II (based on GVW), and then Group III (based on number of axles).
- The biggest difference in r values occurs when only state legal loads are included in Strength I (P8). This highlights the influence of sorting trucks based on a state's weight and permit regulations (as opposed to an axle or GVW criterion).
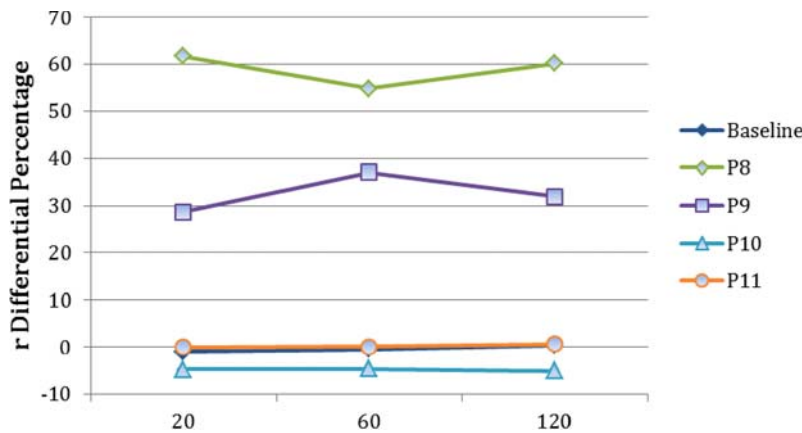

Figure 48. Strength I moment r differentials for Group III vs. span lengths (Florida Site 9936).

Recommendations for Sorting Traffic in the WIM Database into Strength I and Strength II

The NCHRP 12-76 study addressed the criteria for separating traffic data into Strength I and Strength II limit states by recommending that all uncontrolled traffic that constitutes normal traffic or service loads at a site be grouped into Strength I and all controlled or analyzed overload permits be grouped into Strength II. Strength I vehicles were taken to include state legal trucks, illegal overloads, and routine permits because they were considered to represent normal service traffic at bridge sites. Only the controlled trip permits or superloads were included in Strength II. Some questions on how to best implement this sorting criteria when using large WIM databases did arise in the 12-76 study. In the 12-76 study it was decided to use a simplified approach and group all trucks with six or fewer axles in the Strength I calibration as a reasonable though approximate way to capture all legal trucks, illegal overloads, and annual permits. Thus, trucks with seven or more axles were considered as controlled or trip permits.

More detailed recommendations for grouping trucks into Strength I and II, based on the additional research conducted in this phase on truck sorting strategies, are as follows:

1. Using a state's permit and weight regulations (as in variation P11) to group trucks into Strength I and Strength II is considered the **most precise and rational approach,** when using national WIM data. Variation P11 includes state legal trucks, illegal trucks, and annual (routine) permits in Strength I. P11 is best implemented using state permit and weight regulations as in Group III. Sensitivity analysis of r values shows that Group III results are the most sensitive. This demonstrates the effectiveness of this sorting approach for classifying trucks into Strength I and Strength II.

2. Using the number of axles as a means to separate the trip permits from the rest of the traffic is an **approximate** alternate sorting approach that may be easier to implement. Trucks with seven or more axles (or another suitable cutoff) could be grouped into Strength II as trip permits. It would be important that when setting the cutoff for the number of axles, the typical axle configurations for routine permits in a state are taken into account. In some states that have high GVW limits for routine permits, a cut off limit higher than seven axles for separating routine permits from trip permits would be appropriate.

3. Using GVW as a means to separate the trip permits from the rest of the traffic is also an **approximate** alternate sorting approach that can be implemented easily. Trucks with GVW = 150 kips or more could be grouped into Strength II as trip permits. For certain states this may need to be increased to 200 kips or higher depending on state permit regulations.

CHAPTER 4

Conclusions and Suggested Research

Conclusions

The present HL93 load model and the calibration of the AASHTO LRFD specifications are based on the top 20% of trucks in an Ontario truck weight database assembled in 1975 from a single site over only a 2-week period. The model reflects truck configurations and weights taken in the mid-1970s, which primarily consisted of 5-axle semi-trailer trucks. In the past 30 years, truck traffic has significantly increased in volume and weight. Therefore, current AASHTO specified live-load models that are based on past Canadian traffic data may not represent modern and future traffic conditions in some U.S. jurisdictions.

Bridge engineers often focus on enhancing the knowledge of member and system resistances with less effort expended on understanding the live-load demand on bridge elements and systems. Enhancement of bridge live-load models needs representative samples of unbiased truck weight data that meet accepted quality standards. It also requires information on the simultaneous presence of multiple trucks on bridges. Traditionally, the latter has been assembled from headway data, and has not been collected in a manner suitable for the development of design live loads. Due to the development of various weigh-in-motion (WIM) technologies, the quality and quantity of WIM data have greatly improved in recent years. Unbiased truckloads are now being collected at normal highway speeds, in large quantity, and without truck driver knowledge. Modern WIM data loggers have the capability to record and report truck arrival times to an accuracy of 0.01 second, sufficient for estimating multiple presence probabilities. This information, however, has not been used to update the bridge design loads. In this regard, the lack of nationally accepted protocols may have been a contributing factor.

The goal of this project, therefore, was to develop a set of protocols and methodologies for using available recent truck traffic data collected at different U.S. sites, and recommend a step-by-step procedure that can be followed to obtain live-load models for LRFD bridge design. The protocols are geared to address the collection, processing, and use of national WIM data to develop and calibrate vehicular loads for LRFD super-structure design, fatigue design, deck design and design for overload permits. The study also gives practical examples of implementing these protocols with recent national WIM data drawn from states/sites around the country with different traffic exposures, load spectra, and truck configurations.

Truck traffic data should be collected through WIM systems that simultaneously can collect headway information as well as truck weights and axle weights and axle configurations while remaining hidden from view and unnoticed by truck drivers. Truck data surveys collected at truck weigh stations and publicized locations are not reliable for use in live-load modeling because they are routinely avoided by illegal overweight vehicles that could control the maximum loads applied on bridge structures.

The selection of WIM system sites should focus on sites where the owners maintain a quality assurance program that regularly checks the data for quality and requires system repair or recalibration when suspect data are identified. Weighing accuracy is sensitive to roadway conditions. Roadway conditions at a WIM site can deteriorate after a system is installed and calibrated. Regular maintenance and recalibrations are essential for reliable WIM system performance. Quality information is more important than the quantity of traffic data collected. It is far better to collect small amounts of well-calibrated data than to collect large amounts of data from poorly calibrated scales. Even small errors in vehicle weight measurements caused by poorly calibrated sensors could result in significant errors in measured loads. For long-duration counts, the scale should be calibrated initially, the traffic characteristics at that site should be recorded, and the scale's performance should be monitored over time. The state should also perform additional, periodic, on-site calibration checks (at least two per year). These steps will ensure that the data being collected are accurate and reliable. Site-specific calibration is

the only way that the dynamic effects of the pavement leading to the scale can be accounted for in the WIM scale calibration. This calibration process should be executed for a whole range of truck and axle weight types and configurations.

In many spans, the maximum lifetime truck-loading event is the result of more than one vehicle on the bridge at a time. Obtaining reliable multiple presence statistics requires large quantities of continuous WIM data with refined time stamps, which may not be available at every site. Studies done using New York WIM data during this project show that there is a strong correlation between multiple presence and ADTT. The multiple presence statistics are mostly transportable from site to site with similar truck traffic volumes and traffic flow and need not be repeated for each site. The site ADTT could serve as a key variable for establishing a site multiple-presence value. The multiple-presence probabilities for permit trucks are significantly different from those used for normal traffic. Information on loads and multiple-presence probabilities for permits need to be obtained locally or regionally through WIM measurements and considered in the Strength II design process since the data used for calibration of national codes are unlikely to be representative of all jurisdictions.

Draft Recommended Protocols for Using Traffic Data in Bridge Design

An aim of these processes is to capture weight data appropriate for national use or data specific to a state or local jurisdiction where the truck weight regulations and/or traffic conditions may be significantly different from national standards. The objective is to use data from existing WIM sites to develop live-load models for bridge design. The models will be applicable for the strength, serviceability, and fatigue design of bridge members, including bridge decks and design vehicles for overload permitting. Based on the research findings of this project, step-by-step protocols for collecting and using traffic data in bridge design have been developed. The recommended protocols are summarized as follows.

Step 1. Define WIM Data Requirements for Live-Load Modeling

This step defines the types of traffic data and WIM sensor calibration statistics needed for live-load modeling of superstructure design load models (Strength I), overload permitting (Strength II), deck design, and calibration of fatigue load models.

Step 2. Selections of WIM Sites for Collecting Traffic Data for Bridge Design

This step defines the criteria to be used for selecting WIM sites for national, state-specific, route-specific, and site-specific design live-load modeling. National study of truck loads can be conveniently handled by dividing the country

into five regions. Representative states are selected from each region and the sites and routes for WIM data collection are selected based on roadway functional classifications. Some of the criteria for selecting WIM sites include remote WIM sites away from weigh stations with free-flowing traffic, sites that can provide a year's worth of continuous data, sites that have been recently calibrated and are subject to a regular maintenance and quality assurance program, and sites equipped with current sensor and equipment technologies (preferably able to capture and record truck arrival times to the nearest 1/100th of a second or better).

Step 3. Quantities of WIM Data Required for Load Modeling

There are several possible methods available to calculate the maximum load effect for a bridge design period from truck WIM data. The one implemented in these protocols is based on the assumption that the tail end of the histogram of the maximum load effect over a given return period approaches a Gumbel distribution as the return period increases. The method assumes that the WIM data are assembled over a sufficiently long period of time, preferably a year, to ensure that the data are representative of the tail end of the truck weight histograms and to factor in seasonal variations and other fluctuations in the traffic pattern. Sensitivity analyses have shown that the most important parameters for load modeling are those that describe the shape of the tail end of the truck load effects histogram. Step 3 provides recommendations for the quantity of WIM data to be collected from each site. Recommendations include the following:

1. A year's worth of recent continuous data at each site to observe seasonal changes of vehicle weights and volumes,
2. If continuous data for a year is unavailable, a minimum of one month of data for each season for each site, and
3. Data from all lanes in both directions of travel.

Step 4. WIM Calibration and Verification Tests

WIM devices used for collecting data for live-load modeling should be required to meet performance specifications for data accuracy and reliability. Field tests to verify that a WIM system is performing within the accuracy required is an important component of data quality assurance for bridge load modeling applications. Steps to ensure that the data being collected are accurate and reliable include the following:

1. Initial calibration of WIM equipment;
2. Periodic monitoring of the data reported by WIM systems as a means of detecting drift in the calibration of weight sensors; and
3. Periodic on-site calibration checks for long duration counts, where, in addition to Steps 1 and 2, the scale is

subjected to periodic on-site calibration checks at least twice per year, and the calibration statistics are retained for use in filtration of sensor errors.

Step 5. Protocols for Data Scrubbing, Data Quality Checks, and Statistical Adequacy of Traffic Data

High-speed WIM is prone to various errors that need to be recognized and considered in the data review process to edit out unreliable data and unlikely trucks to ensure that only quality data is made part of the load modeling process. It is also important to recognize that unusual data are not all bad data. The WIM data should therefore be scrubbed to include only the data that meet the quality checks. Filtering protocols provided in this step should be applied for screening WIM data prior to use in the live-load modeling and calibration processes. Adjustments to the data scrubbing rules may need to be made to accommodate changes in truck configurations from state to state. Reviewing a sampling of trucks that were eliminated during the data scrubbing process also is recommended to check if the process is performing as intended. Ongoing simple quality checks also are performed on the WIM data to detect any operational problems with the sensors.

Step 6. Generalized Multiple-Presence Statistics for Trucks as a Function of Traffic Volume

In many spans, the maximum lifetime truck-loading event is the result of more than one vehicle on the bridge at a time. Refined time stamps are critical to the accuracy of multiple-presence statistics for various truck loading cases including single, following, side-by-side, and staggered. However, multiple-presence statistics are mostly transportable from site to site with similar truck traffic volumes and traffic flow. A relationship between multiple presence and traffic volume could be developed to utilize the multiple presence values from national data to any given site without performing a site-specific analysis. In this step, the relationship between the trucks' weights in the drive lane and passing lanes must be established to determine whether passing trucks' characteristics are similar to those in the main traffic lane and if there is a correlation between the truck properties.

Step 7. Protocols for WIM Data Analysis for One-Lane Load Effects for Superstructure Design

In this step, single-lane load effects for single truck events and for following truck events for superstructure design are determined. Load effects for following trucks may be obtained directly from the WIM data where accurate time arrival stamps are collected. Generalized multiple-presence statistics obtained in Step 6 may be used for simulation of load effects where accurate truck arrival time stamps are not available. The trucks are grouped into bins by travel lane and run through moment and shear influence lines (or structural analysis program) for simple and two-span continuous spans. The results are normalized by dividing by the corresponding load effects for HL93.

Legal loads, illegal overloads, and routine permits are grouped under Strength I. These vehicles are considered to be enveloped by the HL93 load model. Heavy special permits/trip permits are grouped under Strength II. In most states, permit records are either not specific enough or detailed enough to allow separation of permit loads from non-permit loads in a large WIM database. Recommendations for grouping trucks into Strength I and II, based on the studies conducted on truck sorting strategies (Appendix F), are as follows:

1. Using a state's permit and weight regulations to group trucks into Strength I and Strength II is considered the most precise and rational approach, when using national WIM data.
2. Using number of axles as a means to separate the trip permits from the rest of the traffic is an acceptable approximate sorting approach that may be easier to implement. Typically, trucks with seven or more axles could be grouped into Strength II as trip permits. However, when setting the cutoff for the number of axles, it would be important to take into account the typical axle configurations for routine permits in a state. In some states that have high GVW limits for routine permits, a cut-off limit higher than seven axles for separating routine permits from trip permits would be appropriate.
3. Using GVW as a means to separate the trip permits from the rest of the traffic is also an acceptable approximate sorting approach that can be easily implemented. Trucks with GVW=150 kips or more could be grouped into Strength II as trip permits. For certain states this may need to be increased to 200 kips or higher depending on state permit regulations.

Step 8. Protocols for WIM Data Analysis for Two-Lane Load Effects for Superstructure Design

Determine the number of side-by-side or staggered truck multiple-presence events where trucks are in adjacent lanes in each direction. Run the combined truck with the trucks offset by their actual headway separation through moment and shear influence lines for simple and two-span continuous spans. Estimate the maximum daily load effects for two random trucks simultaneously crossing the bridge. The results are normalized by dividing by the corresponding load effects for HL93. Where accurate time arrival stamps are not available, generalized multiple-presence statistics obtained in Step 6 may be used for simulation of load effects.

Legal loads, illegal overloads, and routine permits are grouped under Strength I. These vehicles are considered to be enveloped by the HL93 load model. Heavy special permits/trip permits are grouped under Strength II. In most states, permit records are either not specific enough or detailed enough to allow separation of permit loads from non-permit loads in a large WIM database. As in Step 7, recommendations for grouping trucks into Strength I and II, based on the studies conducted on truck sorting strategies (Appendix F), are as follows:

1. Using a state's permit and weight regulations to group trucks into Strength I and Strength II is considered the most precise and rational approach, when using national WIM data.

2. Using number of axles as a means to separate the trip permits from the rest of the traffic is an acceptable approximate sorting approach that may be easier to implement. Typically, trucks with seven or more axles could be grouped into Strength II as trip permits. However, when setting the cutoff for the number of axles, it would be important to take the typical axle configurations for routine permits in a state into account. In some states that have high GVW limits for routine permits, a cut-off limit higher than seven axles for separating routine permits from trip permits would be appropriate.

3. Using GVW as a means to separate the trip permits from the rest of the traffic also is an acceptable approximate sorting approach that can be easily implemented. Trucks with GVW=150 kips or more could be grouped into Strength II as trip permits. For certain states, this may need to be increased to 200 kips or higher, depending on state permit regulations.

Step 9. Assemble Axle Load Histograms for Deck Design

As before, separate trucks into Strength I and Strength II groups for single events and for two-lane loaded cases. For each group, generate axle weight relative frequencies histograms for single, tandem, tridem, and quad axles. Multiple-presence probabilities are determined for side-by-side axle events.

Step 10. Filtering of WIM Sensor Errors/WIM Scatter from WIM Histograms

Current WIM systems are known to have certain levels of random measurement errors that may affect the accuracy of the load modeling results. This step proposes an approach to filter out WIM measurement errors from the collected WIM data histograms. To execute the filtering process, calibration data for the WIM system for a whole range of trucks should be obtained. The results of these sensor calibration tests will be the basis for filtering out WIM measurement errors for each WIM data site. The protocols present a procedure to filter out the WIM calibration errors from the measured WIM histograms of gross weights (or load effects) to obtain WIM data histograms that reflect the actual truck weights rather than the measured weights.

Step 11. Accumulated Fatigue Damage and Effective Gross Weight from WIM Data

Updating the LRFD fatigue load model using recent WIM data is described in this step. Damage accumulation laws such as Miner's Rule can then be used to estimate the fatigue damage for the whole design period for the truck population at a site. Cumulative fatigue damage from the WIM population is compared to the LRFD fatigue truck to determine the fatigue damage adjustment factor K. Based upon the results of the WIM study, changes may be proposed to the LRFD fatigue truck model, its axle configuration, and/or its effective weight.

Step 12. Lifetime Maximum Load Effect L_{max} for Superstructure Design

In order to check the calibration of load models and/or load factors for strength design, it is necessary to estimate the mean maximum lifetime loading or load effect L_{max}. There are several possible methods available to calculate the maximum load effect for a bridge design period from truck WIM data. Simplified analytical methods or simulations may be used to estimate the maximum loading over a longer period (75 years) from short-term WIM data. The approach implemented in these protocols is found to be one of the easiest methods that provides results comparable to many other computationally intensive methods, including Monte Carlo simulations. This statistical projection method is based on the assumption that the tail end of the histogram of the maximum load effect over a given return period approaches a Gumbel (extreme value) distribution as the return period increases.

Step 13. Develop and Calibrate Vehicular Load Models for Bridge Design

Various levels of complexity are available for utilizing the site-specific truck weight and traffic data to calibrate live-load models for bridge design. A simplified calibration approach (Method I) is proposed that focuses on the maximum live-load variable, L_{max} for updating the live-load model or the load factor for current traffic conditions, in a manner consistent with the LRFD calibration. The ratio, r (L_{max} WIM data, divided by L_{max} Ontario data) for one lane and for two lanes is used to adjust the live-load factor. This procedure assumes that the present LRFD calibration and safety indices are adequate for the load data and that the site-to-site variability (COV) of the present data and the data then available are consistent. A more robust reliability-based approach (Method II) also is presented that considers

both the recent load data and the site-to-site variations in WIM data in the calibration of live loads.

During the development of the step-by-step protocols, recent long-term WIM data collected at several New York WIM sites by NYSDOT were obtained and used to test the validity and applicability of the protocols. The testing process was very helpful in ensuring that the recommended draft protocols were practical and could be effectively implemented using already available national WIM data.

Demonstration of Protocols Using National WIM Data

The draft recommended protocols were implemented using recent traffic data for a whole year (either 2005 or 2006) from 26 WIM sites in 5 states across the country. The states were California, Texas, Florida, Indiana, and Mississippi. The states and WIM sites were chosen to capture a variety of geographic locations and functional classes, including urban interstates, rural interstates, and state routes. An aim of this task was to give practical examples of using these protocols with national WIM data drawn from sites around the country with different traffic exposures, load spectra, and truck configurations. Adjustments and enhancements were made to several protocol steps based on the experience gained from this demonstration task.

The lifetime maximum L_{max} and r values (ratio of L_{max} values) determined using Step 12 and Method I of Step 13 showed a significant, and consistent, difference between the r values for the one-lane and two-lane events. The r values for one lane events are significantly greater than those for two-lane events. Whereas the maximum r values for two-lane events had a maximum value of 1.184, the one-lane events had a maximum r value among all WIM sites of 2.402 (when sorted using all vehicles with six axles or less as belonging to Strength I). This seems to indicate that the live loading defined in the LRFD specification is fairly adequate in modeling the lifetime maximum loading on a span with two lanes loaded, but underestimates the lifetime maximum loading on a span with only one lane loaded. However, as discussed in Step 13, using a single maximum or characteristic value for L_{max} for a state would be acceptable if the scatter or variability in L_{max} from site to site for the state was equal to or less than the COV assumed in the LRFD calibration. The site-to-site scatter in the L_{max} values obtained from recent WIM data showed significant variability from span to span, state to state, and between one-lane and two-lane load effects—well above the overall 20% COV used during the LRFD calibration. For example, the data from Florida show a COV for the moments of simple-span bridges under one-lane loadings that varies from 32.5% for the 20-ft simple span to 22.3% for the 200-ft simple span. (On the other hand, the site-to-site COV statistics for California are lower.) Live-load modeling using Method II was then implemented to reflect the site-to-site variability.

The results show that for the California truck traffic conditions, the reliability index for one lane is, on average, equal to $\beta = 3.55$ which is close to the LRFD target $\beta = 3.50$. For two lanes of truck traffic, the average reliability index is $\beta = 4.63$. This indicates that for the two-lane loading of California bridges, the current AASHTO LRFD is conservative, producing higher reliability index values than the target $\beta = 3.50$ set by the AASHTO LRFD code writers. If the intent is to reduce the reliability index for the two-lane cases to the target $\beta = 3.5$, then an adjusted live-load factor $\gamma_L = 1.20$ would result, using the steps provided in the protocols. The reliability index for Florida for one-lane loading drops to an average of $\beta = 2.58$ (when sorted using all vehicles with six axles or less as belonging to Strength I). The two-lane L_{max} would lead to an average reliability index $\beta = 3.96$. The latter value is still higher than the target $\beta = 3.5$ while the one-lane reliability is lower than the target. If the live-load factor is raised to $\gamma_L = 2.37$ then the reliability indices for the Florida sites would increase to $\beta = 3.50$ for the one-lane cases. For Indiana, the reliability index for one lane of loading is, on average, equal to $\beta = 3.16$ for one-lane loading; the two-lane loading would lead to an average reliability index $\beta = 4.71$. The Indiana data show a site-to-site variability in COVs on the order of 11% to 15% for both one-lane and two-lane loadings.

Both calibration methods indicate that the live loading defined in the LRFD specification is generally adequate or even conservative in modeling the lifetime maximum loading on a span with two lanes loaded, but it underestimates the lifetime maximum loading for the one-lane loaded case. Studies on truck sorting methods indicate that illegal trucks—not the permits that follow state permit regulations—are likely the biggest drivers of high r values. The load limit enforcement environment in a state will have a more discernible influence on the maximum single-lane loading than the maximum two-lane loading, which results from the presence of two side-by-side trucks. Additionally, with more multiple-presence and WIM data currently available, the projections of L_{max} for two-lane events as undertaken in this study are based on actual side-by-side events rather than based on simulations using conservative, assumed side-by-side multiple-presence probabilities as done during the AASHTO LRFD code calibration. The WIM data collected as part of this study show that the actual percentage of side-by-side multiple truck event cases is significantly lower than assumed by the AASHTO LRFD code writers who had to develop their models based on a limited set of multiple-presence data.

Knowing the actual truck weight distribution in each lane allowed the determination of the relationship between the truck weights in the main traffic lane (drive lane) and adjacent

lanes, and if there is a correlation between the truck properties. This study seems to indicate that there is some negative correlation between the weights of side-by-side trucks. This means that when a heavy truck is in one lane, the other lane's truck is expected to be lighter. Here again, the conservative assumptions used during the LRFD calibration were not adequately supported by field measurements.

Recommendations for Sorting Traffic in the WIM Database into Strength I and Strength II

The NCHRP 12-76 study addressed the criteria for separating traffic data into Strength I and Strength II limit states by recommending that all uncontrolled traffic that constitutes normal traffic or service loads at a site be grouped into Strength I and all controlled or analyzed overload permits be grouped into Strength II. Strength I vehicles were taken to include state legal trucks, illegal overloads, and routine permits as they were considered to represent normal service traffic at bridge sites. Only the controlled trip permits or superloads were included in Strength II. In the initial NCHRP 12-76 study, the research team decided to use a simplified approach and group all trucks with six or fewer axles in the Strength I calibration as a reasonable, although approximate, way to capture all legal trucks, illegal overloads, and annual permits. Thus, trucks with seven or more axles were considered as controlled or trip permits and included in Strength II.

More detailed recommendations for grouping trucks into Strength I and II were developed based on additional research on truck sorting strategies performed under 12-76(01). The detailed recommendations are as follows:

1. Using a state's permit and weight regulations to group trucks into Strength I and Strength II is considered the most precise and rational approach, when using national WIM data.
2. Using number of axles as a means to separate the trip permits from the rest of the traffic is an acceptable approximate sorting approach that may be easier to implement. Trucks with seven or more axles could be grouped into Strength II as trip permits. When setting the cutoff for the number of axles, it would be important to take the typical axle configurations for routine permits in a state into account. In some states that have high GVW limits for routine permits, a cut-off limit higher than seven axles for separating routine permits from trip permits would be appropriate.
3. Using GVW as a means to separate the trip permits from the rest of the traffic also is an acceptable approximate sorting approach that can be easily implemented. Trucks with GVW=150 kips or more could be grouped into Strength II

as trip permits. For certain states this may need to be increased to 200 kips or higher depending on state permit regulations.

Suggested Research and Improvements in Data Collection

Developing and calibrating bridge live-load models requires large amounts of quality WIM data. Improvements in WIM data collection are needed to allow the effective implementation of these protocols. Suggested research on this topic for the future, and recommendations for improving WIM data collection, are as follows:

- States should evaluate their WIM data collection equipment to ascertain if it can provide the quantity and quality of data to implement these protocols. It may be necessary to upgrade the WIM technology and data collection system at specific sites selected for data collection.
- DOTs should carefully consider the locations of WIM sites within a state. Remote WIM sites away from weigh stations are needed to provide unbiased WIM data. Availability of WIM sites on heavy freight routes, hauling routes, or routes known to have significant permit traffic is important for live-load modeling purposes.
- WIM devices should be required to meet ASTM performance specifications for data accuracy and reliability. The WIM sites should be subject to a regular maintenance and quality assurance program. The system components should be reliable enough to be able to provide a year's worth of continuous data.
- The WIM system should be able to capture and record truck arrival times to the nearest 1/100th of a second or better to allow the determination of truck headway separations. Sensors should be placed in the drive lane and passing lanes at sites used for data collection.
- The WIM system should not cut off trucks having more than a certain number of axles or that are heavier than a certain upper weight limit. It is important to record the long heavy superloads that may have a dozen or more axles and weigh over 200 kips. These trucks populate the upper tail of the truck weight distribution and have a significant influence on bridge safety.
- WIM calibration and verification testing requirements defined in Step 4 should be implemented as part of an overall quality assurance program. Regular maintenance and periodic recalibration of any WIM system is critical for obtaining reliable traffic data. Initial calibration and periodic recalibration every 6 months are recommended for sites selected for data collection. Calibration of WIM equipment should follow LTPP calibration procedures or ASTM 1318 standards. Periodic monitoring and quality check of the

data reported by WIM systems should be performed as a means of detecting drift in the calibration of weight sensors. Calibration statistics should be maintained for each WIM site for use in the error filtration process during data analysis.

- Separating permit vehicles from non-permit traffic in large-scale WIM data requires the availability of a reliable electronic permits database/records of special permits authorized in a given period for a state. DOT surveys have indicated that such permit databases are not currently being maintained, at least in an electronic form. States should make necessary changes to their permit operations/management to create and maintain a comprehensive electronic database of overweight permits authorized that will allow these vehicles to be properly grouped as either Strength I or Strength II for live-load modeling.

Bibliography and References

AASHTO (2007), *LRFD Bridge Design Specifications,* 4th ed, with Interims, Washington, D.C.

AASHTO (1994), *AASHTO LRFD Bridge Design Specifications,* 1st ed, Washington, D.C.

AASHTO (1990), *Guide Specifications for Fatigue Evaluation of Existing Steel Bridges,* Washington, D.C.

AASHTO (1989), *Guide Specifications for Fatigue Design of Steel Bridges,* Washington, D.C.

AASHTO (1987), *Guide for Maximum Dimensions and Weights of Motor Vehicles and for the Operation of Non-Divisible Load Oversize and Overweight Vehicles,* Washington, D.C.

Agarwal, A. and M. S. Cheung (1987), "Development of Loading-Truck Model and Live-Load Factor for the Canadian Standards Association CSA-S6 Code," *Canadian Journal of Civil Engineering,* v 14, n 1, Feb 1987, 58–67.

Ang, A. H.-S. and W H. Tang (2007), *Probability Concepts in Engineering,* 2nd ed, Wiley, New York.

ARA Inc. (2004), NCHRP Project 1-37A Final Report: *Guide for Mechanistic-Empirical Design of New and Rehabilitated Pavement Structures, Parts I & II,* Transportation Research Board, Washington, D.C.

Au, A., C. Lam, A. C. Agarwal, and B. Tharmabala (2005), "Bridge Evaluation by Mean Load Method per the Canadian Highway Bridge Design Code," *Canadian Journal of Civil Engineering,* v 32, n 4, Aug 2005, 678–686.

Bakht, B. and L. G. Jaeger (1990), "Bridge Evaluation for Multipresence of Vehicles," *Journal of Structural Engineering,* v 116, n 3, Mar 1990, 603–618.

Bez, R., R. Cantieni, and J. Jacquemoud (1987), "Modeling of Highway Traffic Loads in Switzerland," *IABSE Proceedings P-117/87,* 153–168, International Association for Bridge and Structural Engineering.

Brameld, G. H. (1983), "Statistical Formulation of Highway Bridge Live Loads," *Pitagora Editrice,* v 2, 1983, 1073–1084.

Buckland, P. (1991), *North American and British Loan-Span Bridge Loads, ASCE Journal of Structural Engineering,* Oct 1991.

Buckland, P. G. and R. G. Sexsmith (1981), "Comparison of Design Loads for Highway Bridges," *Canadian Journal of Civil Engineering,* v 8, n 1, Mar 1981, 16–21.

Caprani, C. C., S. A. Grave, E. J. O'Brien, and A. J. O'Connor (2002), "Critical Loading Events for the Assessment of Medium Span Bridges," in B. H. V. Topping and Z. Bittnar, eds. *ICCST '02: Proceedings of the 6th International Conference on Computational Structures Technology,* Prague, Czech Republic, Sep 4–6 2002, 343–344 (abstract; paper on CD-ROM), Civil Comp Press.

Center for Transportation Research (1991), *Traffic-Load Forecasting Using Weigh-in-Motion Data,* University of Texas at Austin, Mar 1997.

Cheung, M. S. and W. C. Li (2002), "Reliability Assessment in Highway Bridge Design," *Canadian Journal of Civil Engineering,* v 29, n 5, Oct 2002, 799–805.

Chotickai, P. and M. D. Bowman (2006), "Truck Models for Improved Fatigue Life Predictions of Steel Bridges," *Journal of Bridge Engineering,* v 11, n 1, Jan 2006, 71–80.

Cohen, H., G. Fu, W. Dekelbab, and F. Moses (2003), "Predicting Truck Load Spectra Under Weigh Limit Changes and its Application to Steel Bridge Fatigue Assessment," *Journal of Bridge Engineering,* v 8, n 5, Sep 2003, 312–322.

Daniels, J. H., J. L. Wilson, B. T. Yen, L. Y. Lai, and R. Abbaszadeh (1986), "WIM Plus Response Study of Four In-Service Bridges," *Engineer's Society of Western Pennsylvania, Official Proceedings—3rd Annual International Bridge Conference,* Pittsburgh, PA, USA, 136–142.

FHWA Office of Transportation Policy Studies (2001), *Analysis of the Vehicle Inventory and Use Survey for Trucks with Five-Axles or More,* May 2001.

FHWA (1985), *Comprehensive Study of Bridge Loads and Reliability,* FHWA/OH-85/005.

FHWA, *Loading Spectrum Experienced by Bridge Structures in the United States,* FHWA/RD-85/012.

Florida Department of Transportation (2006), *Commercial Motor Vehicle Manual,* 6th ed, Tallahassee.

Frangopol, D. M., G. G. Goble, and N. Tan (1992), "Truck Loading Data for a Probabilistic Bridge Live Load Model," *Probabilistic Mechanics and Structural and Geotechnical Reliability, Proceedings of the 6th ASCE Specialty Conference,* Denver, CO, USA, Jul 8–10, 1992, 340–343.

Fu, G., J. Feng, W. Dekelbab, et al. (2003), *NCHRP Report 495, Effect of Truck Weight on Bridge Network Costs,* Transportation Research Board, Washington, D.C.

Fu, G. and O. Hag-Elsafi (2000), "Vehicular Overloads: Load Model, Bridge Safety, and Permit Checking," *Journal of Bridge Engineering,* v 5, n 1, Feb 2000, 49–57.

Fu, G. and O. Hag-Elsafi (1996), "New Safety-Based Checking Procedure for Overloads on Highway Bridges," *Transportation Research Record 1541,* Nov 1996, 22–28.

Fu, G. and O. Hag-Elsafi (1994), "Overweight Trucks and Safety of Bridges," *Proceedings of the ASCE Structures Congress '94,* Atlanta, GA, USA, Apr 24–28, 1994, 284–289.

Fujino, Y. and M. Ito (1979), "Probabilistic Analysis of Traffic Loading on Highway Bridges," *National Bureau of Standards,* Special Publication, v 2, 1979, 539–550.

Ghosn, M. and D. M. Frangopol (1996), "Site-Specific Live Load Models for Bridge Evaluation," *Probabilistic Mechanics and Structural and Geotechnical Reliability, Proceedings of the 7th ASCE Specialty Conference,* Worcester, MA, USA, Aug 7–9, 1996, 30–33.

Ghosn, M., F. Moses, and F. Gabriel (1990), "Truck Data for Bridge Load Modeling," *Second Workshop on Bridge Engineering Research in Progress,* Reno, NV, USA, Oct 29–30, 1990, 71–74.

Ghosn, M. and F. Moses (2000), "Effect of Changing Truck Weight Regulations on U.S. Bridge Network," *Journal of Bridge Engineering,* v 5, n 4, Nov 2000, 304–310.

Ghosn, M. and F. Moses (1986), "Reliability Calibration of a Bridge Design Code," *Journal of Structural Engineering,* v 112, n 4, Apr 1986, 745763.

Ghosn, M. and F. Moses (1985), "Markov Renewal Model for Maximum Bridge Loading," *ASCE Journal of Engineering Mechanics,* Sep 1985.

Gindy, M., and H. H. Nassif (2006a), "Comparison of Traffic Load Models Based on Simulation and Measured Data," *Joint International Conference on Computing and Decision Making in Civil Engineering,* Montreal, Canada, Jun 14–16, 2006.

Gindy, M. and H. Nassif (2006b), "Multiple Presence Statistics for Bridge Live Load Based on Weigh-in-Motion Data," Transportation Research Board, 86th Annual Meeting, Washington, D.C.

Grundy, P. and G. Boully (2004), "Fatigue Design in the New Australian Bridge Design Code," *Proceedings of the Austroads 5th Bridge Conference,* Hobart, Tasmania, May 19–21, 2004, 12 pages.

Hallenbeck, M. and H. Weinblatt (2004), *NCHRP Report 509: Equipment for Collecting Traffic Load Data,* Transportation Research Board, Washington, D.C.

Harman, D. J. and A. G. Davenport (1979), "Statistical Approach to Traffic Loading on Highway Bridges," *Canadian Journal of Civil Engineering,* v 6, n 4, Dec 1979, 494–513.

Harman, D. J., A. G. Davenport, and W. S. S. Wong (1984), "Traffic Loads on Medium and Long Span Bridges," *Canadian Journal of Civil Engineering,* v 11, n 3, Sep 1984, 556–573.

Heywood, R. J. (1992), "Multiple Presence Load Model for Bridges," *Probabilistic Mechanics and Structural and Geotechnical Reliability, Proceedings of the 6th ASCE Specialty Conference,* Denver, CO, USA, Jul 8–10, 1992, 579–582.

Heywood, R. J. and A. S. Nowak (1989), "Bridge Live Load Models," *Proceedings of ICOSSAR '89, the 5th International Conference on Structural Safety and Reliability,* San Francisco, CA, USA, Aug 7–11, 1989, 2147–2154.

Hwang, E.-S., H.-M. Koh, and D.-B. Bae (2001), "A Proposal for New Design Live Load Model in Korea," *Structural Safety and Reliability: Proceedings of the Eighth International Conference, ICOSSAR'01,* Newport Beach, CA, USA, Jun 17–22, 2001, abstract (paper on CD-ROM).

Hwang, E.-S. and H.-M. Koh (2000), "Simulation of Bridge Live Load Effects," *16th Congress of IABSE,* Lucerne, 2000, 8 pages.

Indiana Department of Revenue (no date), *Indiana Oversize/Overweight Vehicle Permitting Handbook,* Indianapolis, IN.

Jacobsohn, A. P. (1997), "Truck Weights: A Long and Winding Road," *Waste Age,* v 28, n 6, Jun 1997, 58–60, 62, 64–66, 68.

Jaeger, L. G. and B. Bakht (1987), "Multiple Presence Reduction Factors for Bridges," *Bridges and Transmission Line Structures, Proceedings of the Sessions at Structures Congress '87,* Orlando, FL, USA, 47–59.

Jamera, F. et al. (1997), "FHWA Study Tour for European Traffic-Monitoring Programs and Technologies," U.S. Department of Transportation, Federal Highway Administration, Aug 1997, 112 pages.

Jones, D. (2002), "Summary of U.S. National and Regional Trends in Truck Loading," *Proceedings of the Third International Conference on Weigh-in-Motion (ICWIM3),* Orlando, FL, USA, May 13–15, 2002, 277–280.

Kim, S., A. S. Nowak, and R. Till (1996), "Verification of Site-Specific Live Load on Bridges," *Probabilistic Mechanics and Structural and Geotechnical Reliability, Proceedings of the 7th ASCE Specialty Conference,* Worcester, MA, USA, Aug 7–9, 1996, 214–217.

Kim, S., A. F. Sokolik, and A. S. Nowak (1996), "Measurement of Truck Load on Bridges in Detroit, Michigan Area," *Transportation Research Record 1541,* 1996, 58–63.

Kulicki, J. M. (1982), "Rating Bridges for Special Permit Loadings with Considerations of Future Life—Case Studies," *Reports of the Working Commissions (International Association for Bridge and Structural Engineering),* v 38, 1982, 91–112.

Kulicki, J. M. and D. R. Mertz (1991), "New Live Load for Bridge Design," *Proceedings of the 8th Annual International Bridge Conference,* Pittsburgh, PA USA, Jun 10–12, 1991, 238.

Kulicki, J. M. (1994), "Development of Bridge Live Load Models," *Proceedings of the ASCE Structures Congress 1994,* Atlanta, GA, USA, Apr 24–28, 1994, 532–537.

Laman, J. A. and A. S. Nowak (1997), "Site-Specific Truck Loads on Bridges and Roads," *Proceedings of the Institution of Civil Engineers: Transport,* v 123, n 2, May 1997, 119–133.

Laman, J. A. and A. S. Nowak (1996), "Fatigue-Load Models for Girder Bridges," *Journal of Structural Engineering,* v 122, issue 7, Jul 1996, 726–733.

Laman, J. A. and A. S. Nowak (1995), "Verification of Truck Loads for Girder Bridges," *Proceedings of the 13th Structures Conference, Part 1 of 2,* Boston, MA, USA, Apr 3–5, 1995, 907–920.

Laman, J. A. and A. S. Nowak (1993), "Live Load Spectra for Bridge Evaluation," *Proceedings of the Symposium on Practical Solutions for Bridge Strengthening and Rehabilitation,* Des Moines, IA, USA, Apr 5–6, 1993, 13–22.

Lee, C. E. and N. Souny-Slitine (1998), "Final Research Findings on Traffic-Load Forecasting Using Weigh-In-Motion Data," *Research Report 987-7,* Sep 1998, 39 pages.

Lichtenstein Consulting Engineers, Inc. (2006), NCHRP Project 12-63 Final Report, *Legal Truck Loads and AASHTO Legal Loads for Posting,* Transportation Research Board, Washington, D.C.

Lichtenstein Consulting Engineers, Inc. (2001), *NCHRP Web Document 28 (NCHRP Project C12-46): Manual for Condition Evaluation and Load Rating of Highway Bridges Using Load and Resistance Factor Philosophy,* Contractor's Final Report, Transportation Research Board, Washington, D.C.

Lu, Q., J. Harvey, T. Le, J. Lea, R. Quinley, D. Redo, and J. Avis (2002), "Truck Traffic Analysis Using Weigh-In-Motion (WIM) Data in California," Jun 2002, 303 pages.

Lui, W. D., C. A. Cornell, and R. A. Imbsen (1988), "Analysis of Bridge Truck Loads," *Proceedings of the 5th ASCE Specialty Conference, Probabilistic Methods in Civil Engineering,* P. D. Spanos, ed, Blacksburg, VA, USA, May 25–27, 1988, 221224.

Miao, T. J. and T. H. T. Chan (2002), "Bridge Live Load Models from WIM Data," *Engineering Structures,* v 24, n 8, Jul 2002, 1071–1084.

Minervino, C. M., B. Sivakumar, F. Moses, D. Mertz, and W. Edberg (2004), "New AASHTO Guide Manual for Load and Resistance Factor Rating of Highway Bridges," *ASCE Journal of Bridge Engineering,* Jan 2004.

Moses, F. (2001), *NCHRP Report 454: Calibration of Load Factors for LRFR Bridge Evaluation,* Transportation Research Board, Washington, D.C.

Moses, F. (1999), "Calibration of Load Factors for Load and Resistance Factor Evaluation," *Proceedings of the 1999 Structures Congress*

"Structural Engineering in the 21st Century," New Orleans, LA, USA, Apr 18–21, 1999, 292–295.

Moses, F. (1982), "Probabilistic Load Modeling for Bridge Fatigue Studies," *International Association for Bridge and Structural Engineering,* 1982, 883–889.

Moses, F., M. Ghosn, and R. E. Snyder (1984), "Application of Load Spectra to Bridge Rating," *Transportation Research Record 950,* 1984, 45–53.

Moses, F., C. G. Schilling, and K. S. Raju (1987), *NCHRP Report 299: Fatigue Evaluation Procedures for Steel Bridges,* Transportation Research Board, Washington, D.C.

Najafi, F. T. and B. Blackadar (1998), "Analysis of Weigh-in-Motion Truck Traffic Data," *Proceedings of the 40th Annual Meeting of the Transportation Research Forum,* Philadelphia, PA, USA, Oct 29–31, 1998, 139–162.

Nichols, A. P. and D. M. Bullock (2004), "Quality Control Procedures for Weigh-in-Motion Data," FHWA/IN/JTRP-2004/12, Joint Transportation Research Program, Purdue University, West Lafayette, IN.

Nowak, A. S. (1999), *NCHRP Report 368: Calibration of LRFD Bridge Design Code,* Transportation Research Board, Washington, D.C.

Nowak, A. S. (1993a), "Development of Bridge Load Model for LRFD Code," *Structural Engineering in Natural Hazards Mitigation, Proceedings of the Symposium on Structural Engineering in Natural Hazards Mitigation,* Irvine, CA, USA, Apr 19–21, 1993, 1041–1046.

Nowak, A. S. (1993b), "Live Load Model for Highway Bridges," *Structural Safety,* v 13, n 1–2, Dec 1993, 53–66.

Nowak, A. S. and D. M. Ferrand (2004), "Truck Load Models for Bridges," *Proceedings of the 2004 Structures Congress—Building on the Past: Securing the Future,* Nashville, TN, USA, May 22–26, 2004, 1147–1156.

Nowak, A. S. and H. N. Grouni (1994), "Calibration of the Ontario Highway Bridge Design Code 1991 Edition," *Canadian Journal of Civil Engineering,* v 21, n 1, Feb 1994, 25–35.

Nowak, A. S. and Y.-K. Hong (1991), "Bridge Live-Load Models," *Journal of Structural Engineering,* v 117, n 9, Sep 1991, 2757–2767.

Nowak, A. S. and H. Nassif (1992), "Live Load Models Based on WIM Data," *Probabilistic Mechanics and Structural and Geotechnical Reliability, Proceedings of the 6th ASCE Specialty Conference,* Denver, CO, USA, Jul 8–10, 1992, 587–590.

Nowak, A. S. and M. M. Szerszen (1998), "Bridge Load and Resistance Models," *Engineering Structures,* v 20, n 11, Nov 1998, 985–990.

Nyman, W. E. (1985), "Calibration of Bridge Fatigue Design Model," *Journal of Structural Engineering,* v 111, n 6, Jun 1985, 1251–1266.

O'Brien, E. J. and C. C. Caprani (2005), "Headway Modeling for Traffic Load Assessment of Short to Medium Span Bridges," *Structural Engineer,* Aug 16, 2005, 33–36.

O'Brien, E. and A. Znidaric (2001), "Report of Work Package 1.2—Bridge WIM systems (B-WIM)," *Weighing In-Motion of Axles and Vehicles for Europe (WAVE),* Jun 2001, 100 pages.

O'Connor, A. and E. J. O'Brien (2005), "Traffic Load Modelling and Factors Influencing the Accuracy of Predicted Extremes," *Canadian Journal of Civil Engineering,* v 32, 2005, 270–278.

O'Connor, A. J., E. J. O'Brien, and B. Jacob (2002), "Use of WIM Data in Development of a Stochastic Flow Model for Highway Bridge Design and Assessment," *Proceedings of the 3rd International Conference on Weigh-In-Motion (ICWIM3),* Orlando, FL, USA, May 13–15, 2002, 315–324.

Qu, T., C. E. Lee, and L. Huang (1997), "Traffic-Load Forecasting Using Weigh-In-Motion Data," *Research Report 987-6,* Texas Department of Transportation, Austin, Mar 1997, 133 pages.

Sivakumar, B. (2006), *New AASHTO Load Models for Load Rating & Posting,* 23rd Annual International Bridge Conference, Pittsburgh, PA, Jun 2006.

Sivakumar, B. (2005a), *LRFR for More Uniform Safety in Bridge Load Ratings and Postings.* TRB Sixth International Bridge Engineering Conference, July 2005, Boston, MA.

Sivakumar, B. (2005b), "Recommendation of a New Truck Model for Bridge Evaluation," *Journal of Bridge Structures.*

Sivakumar, B. and C. M. Minervino, (1999a), *Bridge Evaluation using Load and Resistance Factor Philosophy,* 1999 ASCE Structures Congress, New Orleans, April, 1999.

Sivakumar, B. and C. M. Minervino (1999b), *Load Rating and Permit Review Using Load and Resistance Factor Philosophy,* Transportation Research Board 8th International Bridge Management Conference, Denver, CO, Apr 1999.

Sivakumar, B., F. Moses, G. Fu, and M. Ghosn (2007), *NCHRP Report 575: Legal Truck Loads and AASHTO Legal Loads for Posting,* Transportation Research Board, Washington, D.C.

Stamatiadis, N. and D. L. Allen (1997), "Seasonal Factors Using Vehicle Classification Data," *Transportation Research Record 1593,* 1997, 23–28.

Stone, J. R. (2002), "North Carolina Forecasts for Truck Traffic," North Carolina Department of Transportation, Raleigh, 19 pages.

Tallin, A. G. and T. Petreshock (2002), "Modeling Fatigue Loads for Steel Bridges," *Transportation Research Record 1275,* 23–26.

Transportation Research Board (2002), *Special Report 267: Regulating Weights, Lengths, and Widths of Commercial Motor Vehicles,* Washington, D.C.

Transportation Research Board (1997), *NCHRP Synthesis 241: Truck Operating Characteristics,* Washington, D.C.

Transportation Research Board (1990a), *Special Report 225: Truck Weight Limits: Issues and Options,* Washington, D.C.

Transportation Research Board (1990b) Special Report 227: *New Trucks for Greater Productivity and Less Road Wear: An Evaluation of the Turner Proposal,* Washington, D.C.

USDOT (2001), *Traffic Monitoring Guide,* Washington, D.C.

USDOT (2000), *Comprehensive Truck Size and Weight Study,* Vol I, II, and III, Washington, D.C.

van de Lindt, J. W., G. Fu, Y. Zhou, and R. M. Pablo Jr. (2005), "Locality of Truck Loads and Adequacy of Bridge Design Load," *Journal of Bridge Engineering,* v 10, issue 5, Sep 2005, 622–629.

van de Lindt, J. W., G. Fu, R. M. Pablo Jr., and Y. Zhou (2002), "Investigation of the Adequacy of Current Design Loads in the State of Michigan," *Research Report RC-1413,* Jul 2002, 60 pages.

Wang, T.-L., C. Liu, D. Huang, and M. Shahawy (2005), "Truck Loading and Fatigue Damage Analysis for Girder Bridges Based on Weigh-in-Motion Data," *Journal of Bridge Engineering,* v 10, issue 1, Jan 2005, 12–20.

Washington State University (1995), NCHRP Project 3-39(2) Final Report; *On-Site Evaluation and Calibration Procedures for Weigh-in-Motion Systems.*

Wu, S.-S. (1996), "Procedure to Estimate Loading from Weigh-in-Motion Data," *Transportation Research Record 1536,* 19–24, Transportation Research Board, Washington, D.C.

Protocols for Collecting and Using Traffic Data in Bridge Design

Unpublished Material

Appendices A through F as submitted by the researchers are not published herein. They are available on the TRB website at www.TRB.org by searching for NCHRP Report 683. Titles of Appendices A through F are as follows:

Appendix A   Survey Questionnaires & Responses
Appendix B   Main Features of Selected Studies
Appendix C   National WIM Data Analyses
Appendix D   Potential Processes to Develop and Calibrate Vehicular Design Loads
Appendix E   Implementation of WIM Error Filtering Algorithm
Appendix F   Truck Sorting Strategies & Influence on "r" Values

Abbreviations and acronyms used without definitions in TRB publications:

AAAE	American Association of Airport Executives
AASHO	American Association of State Highway Officials
AASHTO	American Association of State Highway and Transportation Officials
ACI–NA	Airports Council International–North America
ACRP	Airport Cooperative Research Program
ADA	Americans with Disabilities Act
APTA	American Public Transportation Association
ASCE	American Society of Civil Engineers
ASME	American Society of Mechanical Engineers
ASTM	American Society for Testing and Materials
ATA	Air Transport Association
ATA	American Trucking Associations
CTAA	Community Transportation Association of America
CTBSSP	Commercial Truck and Bus Safety Synthesis Program
DHS	Department of Homeland Security
DOE	Department of Energy
EPA	Environmental Protection Agency
FAA	Federal Aviation Administration
FHWA	Federal Highway Administration
FMCSA	Federal Motor Carrier Safety Administration
FRA	Federal Railroad Administration
FTA	Federal Transit Administration
HMCRP	Hazardous Materials Cooperative Research Program
IEEE	Institute of Electrical and Electronics Engineers
ISTEA	Intermodal Surface Transportation Efficiency Act of 1991
ITE	Institute of Transportation Engineers
NASA	National Aeronautics and Space Administration
NASAO	National Association of State Aviation Officials
NCFRP	National Cooperative Freight Research Program
NCHRP	National Cooperative Highway Research Program
NHTSA	National Highway Traffic Safety Administration
NTSB	National Transportation Safety Board
PHMSA	Pipeline and Hazardous Materials Safety Administration
RITA	Research and Innovative Technology Administration
SAE	Society of Automotive Engineers
SAFETEA-LU	Safe, Accountable, Flexible, Efficient Transportation Equity Act: A Legacy for Users (2005)
TCRP	Transit Cooperative Research Program
TEA-21	Transportation Equity Act for the 21st Century (1998)
TRB	Transportation Research Board
TSA	Transportation Security Administration
U.S.DOT	United States Department of Transportation